Ghita, Ryan (2021) *Adipose derived stromal vascular fraction: therapeutic potential of renal artery administration in renal ischaemia reperfusion injury.* PhD thesis, University of Glasgow.

http://theses.gla.ac.uk/82337/

ADIPOSE DERIVED STROMAL VASCULAR FRACTION: THERAPEUTIC POTENTIAL OF RENAL ARTERY ADMINISTRATION IN RENAL ISCHAEMIA REPERFUSION INJURY

By

Ryan Ghita

MBChB, MRCS (Glas.)

A thesis submitted in fulfilment of the requirements for the degree of Doctor of Philosophy (PhD)

Institute of Cardiovascular and Medical Sciences

College of Medicine, Veterinary & Life Sciences, University of Glasgow

April 2021

ABSTRACT

Shortages of kidneys for transplantation is a universal concern. Countries like the United Kingdom have had success improving the number of kidneys available notably through expanding their living donation program. However, trends indicate the discrepancy between supply and demand will never fully be met with current practise. Bioengineering of donor specific organs may provide the ultimate answer, but despite rapidly growing progress it will be many more years until complex organs, such as a kidney, are available for transplantation.

Utilising kidneys that traditionally would not be considered suitable for transplantation will drastically increase the donor pool of kidneys. To implant these 'marginal' kidneys we have to minimise the ischaemia reperfusion injury (IRI) they sustain during the transplantation process. Cellular therapies offer the greatest potential in ameliorating transplant related IRI and allowing these marginal kidneys to recover with acceptable long-term function.

The field of cellular therapies, in particular stem cell therapy, has expanded rapidly in the last ten years. Adipose tissue offers one of the most attractive sources of stem cells due to its relatively easy accessibility and high abundance of stem cells. The adipose derived stromal vascular fraction (ADSVF), which contains the adipose derived stem cells, can quickly be extracted from the adipose tissue with minimal technical expertise. Multiple animal studies of renal IRI have demonstrated significantly improved kidney function after treatment with ADSVF. However, administration of freshly isolated, uncultured ADSVF administered via the renal at the time of transplantation has never been attempted in human kidneys. Before considering clinical translation, we need to better understand the use of ADSVF in such settings.

In chapter one, experiments characterise the ADSVF obtained from inguinal and peri-renal adipose tissue of both rats and humans. Chapter two describes the development of a novel animal model which closely mimics the transplant recipient in order to accurately investigate the ADSVF. Chapter three demonstrates the biodistribution of the ADSVF administered via the renal artery and chapter four highlights some of the potential mechanisms of action of the ADSVF.

In summary, ADSVF from peri-renal and inguinal adipose tissue consist of a similar heterogenous cell population, although they differ in the proportions of each subset. When administered via the renal artery, ADSVF likely ameliorate IRI via multiple mechanisms,

by reducing the immediate injury, modulating the inflammatory response and reducing the progression to fibrosis. Administration via the renal artery is an effective means of reducing non-target biodistribution and deliver the majority of the ADSVF to the cortex of the kidney. The animal model developed as part of this research better mimics the transplant patient, compared to existing models, without increasing the risks to the animal.

The findings of this research combined with recently published data using mesenchymal stem cells in human kidney IRI, provides enough support to consider renal artery administration of uncultured ADSVF. Initially this translational research could be performed on declined kidney grafts.

TABLE OF CONTENTS

CHAPTER 1
INTRODUCTION

CHAPTER 2
GENERAL MATERIAL AND METHODS

CHAPTER 3
CHARACTERISATION OF ADIPOSE DERIVED STROMAL VASCULAR FRACTION

CHAPTER 4

DEVELOPMENT OF A NOVEL RAT MODEL OF RENAL TRANSPLANT ISCHAEMIA REPERFUSION INJURY

CHAPTER 5
BIODISTRIBUTION OF ADIPOSE DERIVED STROMAL VASCULAR FRACTION ADMINISTERED VIA RENAL ARTERY

CHAPTER 6
MECHANISM OF ACTION OF ADIPOSE DERIVED STROMAL VASCULAR FRACTION IN AMELIORATING RENAL ISCHAEMIA REPERFUSION INJURY

CHAPTER 7

GENERAL DISCUSSION

LIST OF TABLES

LIST OF FIGURES

LIST OF SUPPLEMENTARY MATERIAL

DEDICATION

To my wife Azlina – For your advice and encouragement throughout the challenging times over the last few years. I am grateful for the love you show, and the mother you are to our newborn son.

To my parents – For your unconditional support, and instilling knowledge and self-belief that has allowed me to pursue my ambitions.

ACKNOWLEDGEMENTS

DECLARATION

This work was undertaken during a period of research between 2016 and 2019 at the University of Glasgow's Institute of Cardiovascular & Medical Sciences.

I created and submitted an animal project license to carry out the work presented in this thesis. All tissue used in this thesis were obtained by me from animals under our approved project licence unless explicitly stated. The project licence has been approved by the Home Office until 2021 and will continue to be used by personal animal licence holders at the University of Glasgow until 2021.

Due to the sheer number of samples obtained, I received assistance in processing and analysing by Dr Rashida Lathan, Dr Rachanchai Chawangwongsanukun and Dr Dianne Hillyard. Many obtained samples have not been included in this thesis and may be the subject of future research.

I declare the work presented in this thesis was composed by myself except where indicated below:

Dr Rashida Lathan performed the single cell sequencing and data analysis.

Dr Rachanchai Chawangwongsanukun performed the immunohistochemistry of the histology slides.

Ryan Ghita
Glasgow, August 2020

PUBLICATIONS

Lathan, Rashida & Ghita, Ryan & Clancy, Marc. (2019). Stem Cells to Modulate IR: A Regenerative Medicine-Based Approach to Organ Preservation. Current Transplantation Reports. 10.1007/s40472-019-00240-7.

COMPLETED MANUSCRIPTS READY FOR SUBMISSION

Ghita R, Lathan R, Whalen H, Chawangwongsanukun R, Hillyard D, Touyz R, Mark P, Clancy M. (2020) Autologous adipose-derived cells transiently moderate inflammation and fibrogenesis in early renal ischemia reperfusion injury.

Ghita R, Lathan R, Whalen H, Mark P, Clancy M. (2020). A novel rat model of renal transplant ischaemia reperfusion injury.

NATIONAL AND INTERNATIONAL ORAL AND POSTER PRESENTATIONS

Adipose-derived regenerative cells: therapeutic potential in IRI, The Transplant Society, International Congress, Madrid, Spain, July 2018

Adipose-derived regenerative cells: therapeutic potential, British Transplant Society, Annual Meeting, Brighton, UK, March2018

Adipose-derived regenerative cells: therapeutic potential, UK Kidney Week, British Renal Society, Liverpool, UK, June 2017

Biodistribution of adipose derived regenerative cells administered via the renal artery in novel rat transplant model, American Transplant Congress, Chicago, USA, May 2017

Cell-subset diversity in adipose derived regenerative cells used in renal ischemic reperfusion injury treatment, American Transplant Congress, Chicago, USA, May 2017

Adipose-derived regenerative cells: therapeutic potential, The Scottish Renal Association, Dunblane, UK, Oct 2017

Biodistribution of adipose derived regenerative cells administered via the renal artery in novel rat transplant model, British Transplant Society, Annual Meeting, Harrogate, UK, March 2017

ADRC	adipose-derived regenerative cells
ADSVF	adipose derived stromal vascular fraction
A2AR	adenosine a2a receptor
ASC	adipose-derived mesenchymal stromal cells (which consist of adipose derived stem cells)
ASC	adipose-derived stem cell
BM MSC	bone marrow-derived mesenchymal stromal cells
BSC	biological safety cabinet
CAMKs	calcium/calmodulin-dependant protein kinases
CCL	c-c motif ligand
CCR	c-c motif chemokine receptor
CFDA-SE	carboxyfluorescein diacetate succinimidyl ester
CFSE	carboxyfluorescein succinimidyl ester
CIT	cold ischaemic time
CKD	chronic kidney disease
Col1	collagen type 1
Col4	collagen type 4
COX	cyclo-oxygenase
Cr	creatinine
CRF	chronic renal failure
Crry	complement receptor 1-related gene/protein ycrry
CSF	cytokine colony-stimulating factor
CTLA	cytotoxic t-lymphocyte-associated protein
CX3CR1	c-x3-c motif chemokine receptor 1
CXCL	c-x-c motif chemokine ligand
CXCR	c-x-c motif chemokine receptor
DAMP	danger-associated molecular patterns
DBD	donor/donation after brain stem death
DC	dendritic cells
DCD	donor/donation after circulatory-confirmed death
dCt	delta cycle threshold
DGF	delayed graft function
DiR	Lipophilic carbocyanine DiOC18
ECM	extracellular matrix
eGFR	estimated glomerular filtration rate
ESRD	end-stage renal disease
EV	extracellular vesicles
FGF	fibroblast growth factor
FITC	fluorescein isothiocyanate
FoxP3	forkhead box P3
GFR	glomerular filtration rate
GM-CSF	granulocyte macrophage colony-stimulating factor, also referred as CSF2
H2S	hydrogen sulphide
HGF	hepatocyte growth factor
HIF	hypoxia-inducible factor
HIF1A	hypoxia-inducible factor 1 subunit alfa
hiPSC- MSCs	human-induced pluripotent stem cell-derived MSCs

ICAM 1	intracellular adhesion molecule 1
IFN-y	interferon-gamma
IGF	insulin-like growth factor
IL	interleukin
IRI	ischemia reperfusion injury
ISCT	international society for cellular and gene therapies
IVIS	in vivo imaging system
KIM-1	kidney injury molecule-1
LLT	low-level laser therapy
MAPK	mitogen-activated protein kinases
MHC	major histocompatibility complex
MMPs	matrix metalloproteinases
MPT	mitochondria permeability transition
MSC	mesenchymal stem cells
MSC	mesenchymal stromal cells (which consist of mesenchymal stem cells)
NGAL	neutrophil gelatinase-associated lipocalin
NK	natural killer cells
NKT	natural killer T cells
NMP	normotensive machine perfusion
PBS	phosphate-buffered saline
PCR	polymerase chain reaction
PGE	prostaglandin
RIPK3	receptor-interacting serine/threonine kinase 3
RNS	reactive nitrogen species
ROI	region of interest
RONS	reactive oxygen nitrogen species
ROS	reactive oxygen species
RRT	renal replacement therapy
RT PCR	real-time polymerase chain reaction
S1P	sphingosine-1-phosphate
SCF	stem cell factor
SDF-1	stomal cell derived factor 1
SK1	sphingosine kinase-1
SP1	specificity protein 1
T-regs	T regulatory cells
TGFB1	transforming growth factor beta 1
TIMP	tissue inhibitor of metalloproteinases
TLR	toll-like receptors
TNF	tumour necrosis factor
Ur	urea
VCAM	vascular cell adhesion molecule
VEGF	vascular endothelial growth factor
VLA	very late antigen

CHAPTER 1:

INTRODUCTION

1.1 END STAGE RENAL DISEASE

When the kidneys can no longer adequately perform their vital functions, a state of end-stage renal disease (ESRD) is reached. Unlike acute kidney injury, which is often reversible, ESRD is of gradual onset and permanent. The most common causes are diabetes and hypertension, both of which are increasing worldwide and concernedly the highest rates of increase are in low middle-income countries (Mills et al. 2016; Saeedi et al. 2019). Autoimmune diseases, polycystic kidney disease and recurrent infection, make up most of the other aetiologies.

In 2017 there were 8001 people in the United Kingdom newly diagnosed with ESRD. There has been an overall upward trend of incidence since the United Kingdom renal registry was established (NHS BT 2019). Improved therapies and early diagnosis of kidney disease has not yet been enough to reverse this trend. Currently, there are no therapies that can reverse chronic renal damage and recuperate full renal function in the ESRD population. Early diagnosis of kidney damage allows making significant lifestyle changes or adding therapies that can slow down, halt or sometimes reverse some damage. Although this slows the progression and can prevent patients from developing ESRD, there is still a large proportion of patients in which therapies are ineffective, and often patients cannot achieve the drastic lifestyle changes required.

Kidneys play a significant role in the elimination of waste products, fluid balance, electrolyte balance, production of red blood cells, blood pressure control and vitamin D production. When any of these processes become disturbed, there is a knock-on detrimental effect on other bodily systems such as the cardiovascular, immune, and nervous system. Symptoms of decreasing renal function include nausea, lethargy, muscle cramps and shortness of breath. Left unchecked and unmanaged patients will ultimately succumb to their ESRD.

Once a patient develops ESRD, they will require some form of renal replacement therapy (RRT). This takes the form of kidney dialysis or kidney transplantation. The prevalence of patients on RRT in the United Kingdom in 2017 was 64,887. In 2013 there were almost 10,000 patients less on RRT.

Despite kidney dialysis being a lifesaving intervention, it is not without major drawbacks. Firstly, any type of dialysis requires a means of accessing the circulation or the peritoneal cavity. This involves an intervention that has risks associated with it. Secondly, these forms of access are not permanent and will eventually run into complications such as infection or decreased efficacy. At this point another procedure will be required to obtain access. In some circumstances the patient runs out of common access options and find themselves in a precarious situation, often requiring high-risk access procedures, when they are at their physiological weakest. In 2017 there were 28,433 adult patients in the United Kingdom on renal dialysis (NHS BT 2019). This is up from the previous year and is a trend that is increasing.

For patients that are suitable for transplantation, dialysis is a means of survival until such time an organ becomes available. Compared to patients that stay on dialysis, transplant patients live a longer life and have a significant reduction in cardiovascular events (Tonelli et al. 2011; Wolfe et al. 1999; Laupacis et al. 1996; Meier-Kriesche et al. 2001). Quality of life is also substantially better among transplant patients (Tonelli et al. 2011; Kontodimopoulos & Niakas 2008; Simmons et al. 1990; Laupacis et al. 1996). Transplantation does carry the risks of surgery, the need for lifelong immunosuppression and often the need for more than one transplant in their lifetime, however, it is still the preferred RRT of choice for patients. As a result, the number of patients on the transplant waiting list has always exceeded the supply of kidney grafts available. Unfortunately, time spent on dialysis is an independent predictor of poor transplant survival due to ESRD associated systemic physiological deterioration (Meier-Kriesche & Kaplan 2002).

As well as the health benefit of transplant over dialysis, there is also a significant cost-benefit. In the United Kingdom, haemodialysis costs £35,000 per annum per patient and peritoneal dialysis £17,500 per annum per patient. With 28,433 adults on dialysis, this is a high cost to the NHS, and in 2013 it accounted for 3% of the National Health Service budget. In comparison within dialysis, renal transplantation saves the NHS £25,800 annually per patient (Pruthi et al. 2013).With kidney transplants reported as lasting on average 8-15 years, they are extraordinarily cost-effective in addition to reducing morbidity and mortality of ESRD patients. Unsurprisingly, the discrepancy in the demand and supply of kidney grafts further increased as health service strategies pushed to increase transplant numbers.

1.2 TRENDS IN KIDNEY TRANSPLANTATION

Worldwide organ demand for transplantation has overwhelmed supply due to improved surgical safety, survival benefit over dialysis, improved immunosuppression regimes, increased ESRD patients and older and frailer patients being listed. On the supply side, there are reduced numbers of deceased donors due to factors such as improved road safety, advances in healthcare (such as interventional radiology to treat intracranial haemorrhage) and safer working environments.

Recent data from 2019 shows 4954 patients actively waiting for kidney transplantation in the United Kingdom and an additional 3147 patients suspended on the waiting list (Fig. 1.1). The number of patients on the waiting list has steadily declined over the last nine years. However, this rate of decline is slowing and could plateau especially as the number of transplants, for the first time in 2019, failed to be higher than the previous year (Fig. 1.3).
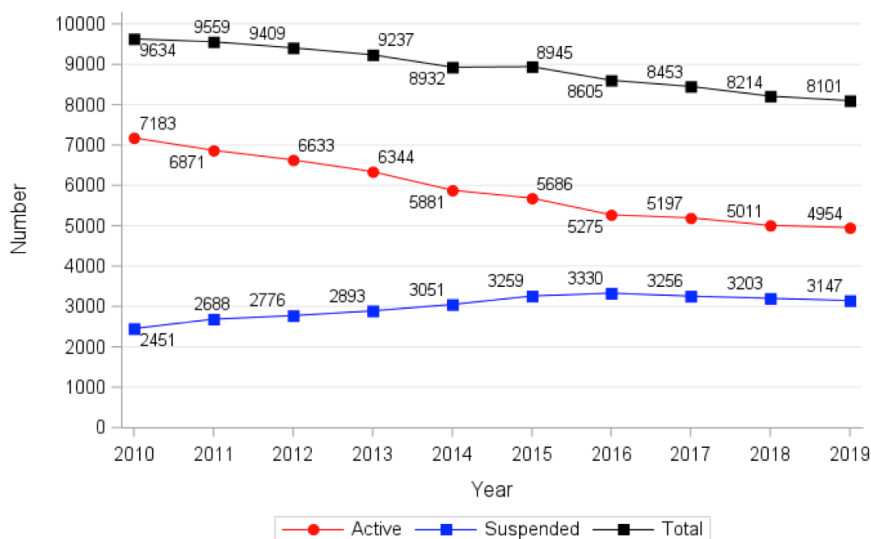
Figure 1.1 United Kingdom kidney transplant waiting list 2010 to March 2019. Taken from NHS Blood and Transplant annual report on kidney transplantation 2018/2019 (NHS BT 2019)

Delving deeper into the waiting list and transplantation data, it is crucial to understand the sources of renal allografts. Donor/donation after brain stem death (DBD), donor/donation after circulatory-confirmed death (DCD) and live donor are the three sources of kidney grafts.

Formerly known as "heart beating donors", DBD was traditionally the majority of all deceased donors. Donors who have suffered from irreversible brain injury and irreversible loss of central respiratory drive (ability to perform respiration). Once a donor has been pronounced brainstem dead, by two separate senior clinicians on two separate occasions, they remain on mechanical ventilation until all necessary pre-retrieval investigations, administration and consenting for donation has been completed. The donor remains on mechanical ventilation until the retrieval team has arrived and set up. Mechanical ventilation and organ perfusion persist as retrieval surgery begins. In contrast, with DCD donor's retrieval is performed after confirmation of death using cardio-respiratory criteria. This may be in a controlled environment where there is the withdrawal of life-sustaining treatments or in an unexpected cardiac arrest in which the patient cannot or should not be resuscitated. In the United Kingdom, there must be at least five minutes of monitored asystole before transfer to theatre and retrieval surgery can commence.

Physiological changes after brainstem death (a DBD donor) involve the cardiovascular, endocrine, and pulmonary systems. Core temperature changes and coagulopathies also add to the challenges of managing DBD donors. Many of these changes can be managed during the optimisation period; vasopressors can help maintain tissue perfusion after the loss of sympathetic tone, and administration of tri-iodothyronine can support pituitary failure. In DCD retrieval, the kidney is exposed to suboptimal perfusion after life-sustaining treatments are withdrawn. A kidney can be subjected to this hypotension and hypoxia for up to three hours (and potentially longer) in what is called the agonal phase (the time after the withdrawal of life support and the onset of cardiac arrest). After cardiac arrest, there is the further '5-minute mandatory wait' to ensure no further signs of life. These two periods expose the kidney to what is termed warm ischaemia. During the transportation of kidney grafts, they are perfused or preserved in cold preservation fluid. This is termed the cold ischaemic time (CIT) and lasts until the kidney is re-perfused by the recipient's blood at the time of implantation. The longer the ischaemia the higher the rates of primary non-function and delayed graft function (Singh et al. 2011; Renkens et al. 2005). Due to the addition of the warm ischaemia period – DCD kidneys often have a longer ischaemic time.

Nevertheless, DCD graft usage has grown every year to increase the donor pool. The Netherlands has some of the highest rates of DCD usage, and a study of 3611 DBD and 2711 DCD transplants reported long-term outcomes of DCD kidneys equivalent to that of DBD kidneys in terms of estimated glomerular filtration rate (eGFR) and graft survival (Schaapherder et al. 2018). In the short-term, DBD kidneys fared better in terms of graft

survival. This builds on similar outcomes from Huynh et al. and Weber et al. as long as cold ischaemic times are less than 24 hours (Huynh et al. 2015; Luan 2002). A survival benefit can still be demonstrated in recipients accepting a DCD kidney rather than waiting on dialysis for a DBD kidney to become available (Snoeijs et al. 2010).

Living donor transplants are either from family and friends or an unrelated altruistic donor in a directed or non-directed donation. Unlike deceased donations, retrieval and implant surgery are much more controlled with everything set up in advance and both donor and recipient optimised for surgery. Also, the donor is healthy with no significant co-morbidities, which is often not the case with deceased donors. The medical history of the donor is well known and, in most cases, both surgeries take place in the same hospital so cold ischaemic time for the kidney is significantly reduced. As would be expected, live donor kidney transplants give the best outcomes compared to age-matched deceased donor transplants (Meier-Kriesche & Kaplan 2002). Another advantage of living donor transplant is that they can be used as part of paired exchanges or a chain of donations making it possible for friends and family to donate even if they are not compatible (Fig. 1.2).

In 2013 there was a strategy set out by NHS Blood and Transplant division on how they would improve organ utilisation by 2020. Improving the number of grafts available has been a multi-strategic approach. Efforts included live donor awareness campaigns, chain donations, increased donor referral, ABO incompatibility transplants, opt-in donation, thereby improving decline rates of kidneys, improving consent rates for donation. From an administration point of view, a United Kingdom transplant HUB has been set up to effectively coordinate donations and collect data on transplant activity such as usage, declines and organ damage during retrieval. Real-time data sharing of donor parameters and medical history has helped surgeons accept marginal kidneys.
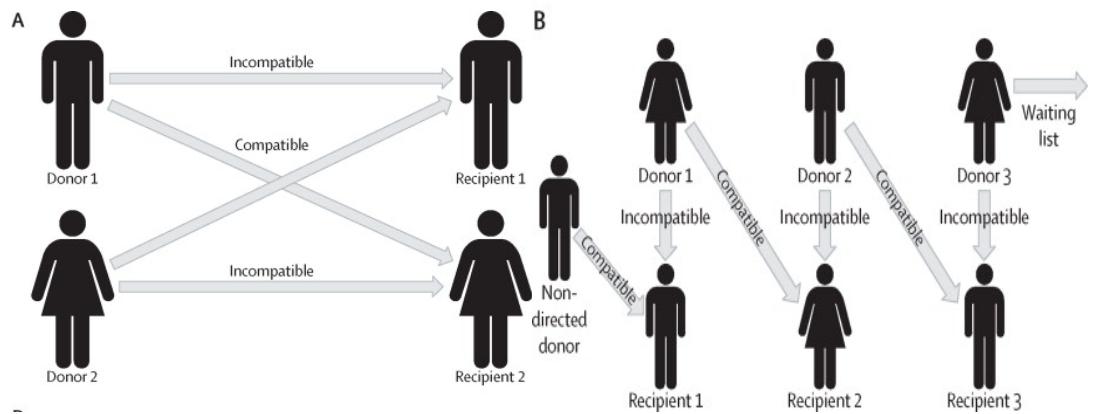
Figure 1.2 Live donor kidney donations can be used to trigger further donations. (A) Donation across two pairs and (B) open chain donation (Reese et al. 2015)

When scrutinising the data in 2019, we can see that most kidney donors remain DBD donors followed by DCD then living donors (Fig. 3). This has not always been the trend, and this is the first year in at least ten years in which the number of DCD transplanted kidneys is higher than living donors (NHS BT 2019). As knowledge, experience, strategies, and therapies have grown, so have the boundaries for accepting and implanting DCD kidneys. On the other hand, live donor transplant numbers seem to have plateaued (NHS BT 2019). Perhaps those who had a live donor have been transplanted, and we are nearing the maximum annual utilisation rate of live donors. If live donor transplant numbers continue to remain static, there will be further drive to use deceased donor kidneys.

Despite increasing DCD transplants, the number of patients on the kidney transplant waiting list remained at over 8000 people on the 31st of March 2019. It is encouraging that the number of patients on the waiting list has steadily declined since 2010, and continual innovations and strategies have the desired effect. The opt-out system introduced in the UK may help to further push deceased donor numbers. To fully utilise this increase in donors, we need to maximise acceptance rates of DCD grafts.
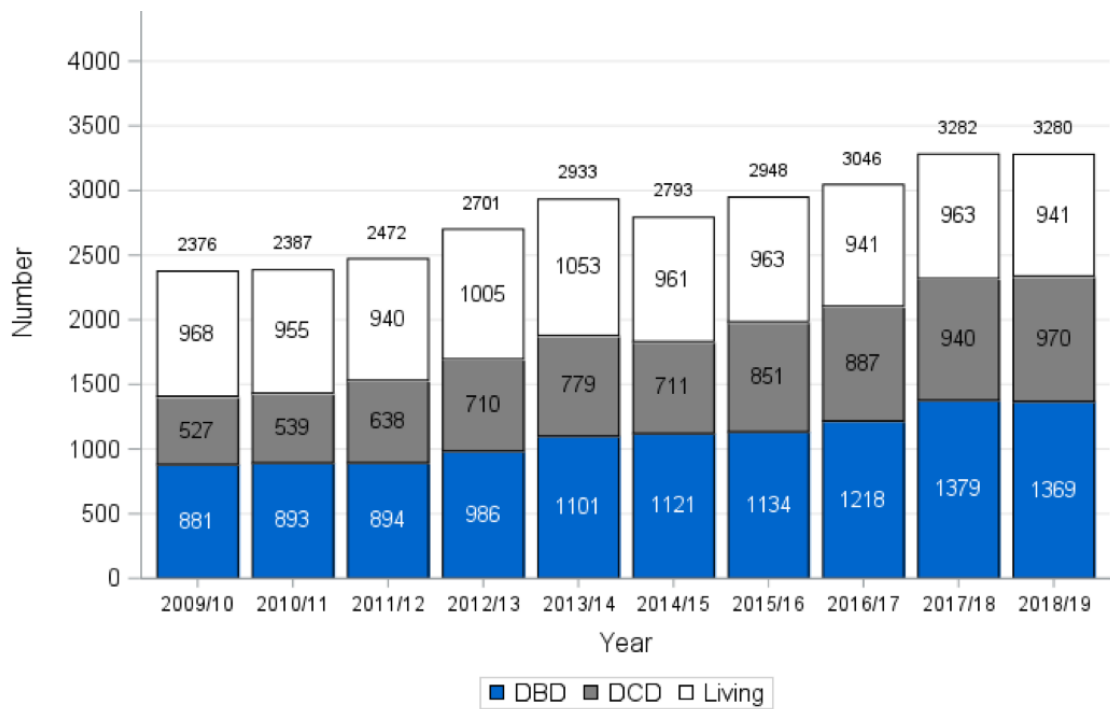
Figure 1.3 Type of adult only kidney transplants 2009 to 31st March 2019. Taken from NHS Blood and Transplant annual report on kidney transplantation 2018/2019 (NHS BT 2019)

From the early 2000s, most of the increase in donor numbers have come from DCD donors. An increase in DCD kidneys plus an increase in donor age and comorbidities have resulted in a surge in the use of "marginal" kidneys. With the fate of the waiting list relying on DCD and marginal kidneys, now more than ever do we require new therapies to improve graft function and survival.

1.3 STRATEGIES TO TACKLE THE KIDNEY TRANSPLANT WAITING LIST

To increase the number of transplanted kidneys, there are three main areas where intervention can be applied: the donor, the retrieval and peri-transplant period, and the recipient. Advances in one area which results in a seismic shift in practise and waiting times do not come around often. A combination of interventions is where progress has been made in the past, and it will likely be the same moving forward.

Donor strategies have aimed at increasing referrals for donation, improving consent rates and increasing the number of live donor transplants. Lowering the "minimal kidney criteria"

has also increased the number of kidneys available but we have now researched the point of diminishing returns. Improved optimisation of the donor before retrieval has extending graft survival and reduced the number of patients being relisted for another transplant.

The recipient can also play a role in tackling the waiting list times. If graft survival is prolonged, then the chance of requiring another transplant will reduce, and fewer patients will be re-listed. An effective method of achieving this is with pre-emptive transplants where it is known that both living and deceased transplant grafts last longer when the patient is transplanted preemptively or within six months after dialysis. Optimising the recipient before transplant by achieving and maintaining a healthy weight, improving cardiovascular health, positive lifestyle changes would seem to have obvious benefits. However, for dialysis patients, it is notoriously difficult to exercise, eat healthily, all the while battling lethargy (due to anaemia, medications, dialysis, poor sleep), having regular dialysis sessions, physiologically deteriorating and often under financial strain from not being able to work.

The 'obesity paradox' complicates issues with higher BMI associated with lower mortality risk in patients on maintenance haemodialysis (J.-L. Wang et al. 2012; Schmidt & Salahudeen 2007; Rhee et al. 2016). On the other hand, obese patients have higher peri-transplant complications and delayed graft function compared to non-obese patients. Considering these increased risks, obese patients receiving transplant still have better outcomes than those staying on dialysis (D. W. Johnson et al. 2002; W. M. Bennett et al. 2011; Gill et al. 2013). Therefore, the outcome for long term recipient and graft survival is not as clear with new evidence drawing doubt on the correlation between obesity and long-term graft and patient survival (Nicoletto et al. 2014). A carefully planned multidisciplinary approach to weight loss with minimal lean mass loss and protein-energy wasting will ensure optimisation for surgery, better graft survival and less chance of weight gain post-transplant. Evidence supporting recipients fasting peri-transplant has not been demonstrated clinically, but several animal models have shown the protective benefits against ischemia reperfusion injury (IRI) (Mitchell et al. 2010).

Post-transplant follow up, a healthy post-transplant adjusted lifestyle, adherence to immunosuppression should all be advocated, and the benefits of each can add up to significantly to improve graft function and longevity (Denhaerynck et al. 2005; Adams 2006). Nonadherence with immunosuppression is a particularly complex issues but is essential to address to maximise graft survival. First year after transplantation adherence is at its best but electronic monitoring has demonstrated a gradual increase in nonadherence

over time. However data on nonadherence is difficult to accurately collect and is often underpowered (Nevins et al. 2017). The strongest risk factor for nonadherence is being an adolescent. Tailored intervention, such as changing to a once daily regime in a patient with well-matched kidney, can help motivate and improve adherence. Immunosuppression regimes or tolerance inducing therapies could hold the key to the next seismic shift in transplantation with regards to the recipient interventions.

Strategies to improve the retrieval process have been successful not only in tackling the waiting list but by progressing in a timely manner – unlike other strategies such as live donor campaigns that may take years to come to fruition. A transplant hub to coordinate all donations with real-time donor data available for surgeons has helped to streamline the process of donation, retrieval, allocation, transportation, and implantation. The data collected by the hub has been used to audit practises such as refusal rates from different transplant centres, organ injury during retrieval and ischaemic times. Other approaches by NHS's Blood and Transplant division include disseminated activity reports, forwarding discarded organs for research, collation and analysis of decline data and support to clinicians who accept reasonable risk (NHS Blood and Transplant. 2019).

The 'Fasttrack' scheme which offer out kidneys which have already been retrieved but subsequently declined by the intentional implantation centre has further reduced the number of discarded kidneys. However, the risk of mistakes is inherent, such as the death of two young recipients who died of meningitis secondary to parasite infection transmitted from their transplant. Understandably transplant teams are now hesitant in accepting these higher risk organs. This case highlighted the dangers of pushing surgeons and the transplant teams to accept kidney offers that would conventionally be declined. Added to the further pressure that retrieval is now largely performed during the daytime and implantation at night. There is a growing issue of sustainability of delivering a service which involves making complex decisions and increased operating during the middle of the night.

Peri-transplant management, in particular induction immunosuppression, offers another vast area of research and potential. Tolerance inducing cellular therapies and other therapies administered peri-transplant have been widely studied over the last decade. Clinical trials of such therapies are taking place and if successful, could reduce the need for daily lifelong immunomodulatory drugs which eventually fail and have their associated risks. The field of tolerance inducing cellular therapies, although exciting and demonstrating huge potential, is out of the scope of this thesis.

This leaves us to one of the most widely researched fields of transplantation - ischaemia reperfusion injury (IRI). With many methods of intervention being investigated and already implemented, significant progress has been made. Ameliorating IRI will improve graft outcome, graft survival, and increase the kidney pool (as marginal kidney offers and acceptance will increase). A therapy that effectively treats or protects a kidney from IRI would drastically reduce waiting times.

1.4 KIDNEY ISCHAEMIA REPERFUSION INJURY AFTER TRANSPLANTATION

The degree of IRI a kidney sustains directly correlates to the long-term outcome in terms of overall graft function and survival. Over-simplifying it, renal IRI results in reduced nephron mass, increased allogenicity, a lower baseline for general decline, a predisposition to chronic fibrosis and tubular atrophy (Eltzschig & Eckle 2011; Mueller et al. 2011; Burns et al. 1998; Salahudeen et al. 2001).

The pathophysiology of IRI has been well studied, and many of the critical processes are well understood. Nevertheless, that should not take away from the complexity that is IRI with its array of interlinked cellular and molecular processes. The initial changes from the ischaemia trigger a switch to anaerobic metabolism, then the innate response begins to activate in response to cellular stress. The second wave of injury at reperfusion is mainly a result of the surge of reactive oxygen species. The limited capacity of repair and regeneration cannot return the kidneys to normal, but instead, the kidneys have remodelled vasculature with compromised flow, reduced nephron numbers and the beginning stages of fibrosis.

The ischaemic injury begins once the blood flow to the kidney does not meet the cellular demand for oxygen. When there is not enough oxygenated blood, the highly metabolically active renal cells convert to anaerobic metabolism. Following the brain and heart, the kidney is the third most susceptible organ to ischaemia. After 30 minutes, irreversible damage starts to develop, starting at the cortex, which has the highest oxygen requirements. Some of the critical and well-understood processes, of IRI, are described below.

Once the kidney converts to anaerobic respiration, via glycolysis to increase ATP, cellular lactate accumulates and is one of the primary reasons for the cellular pH to drop. H+ ions are exchanged for Na+ via the Na+/H+ exchanger in an attempt to counteract the drop in pH (Baines 2009; Murphy & Steenbergen 2008) The Na+ ions, in turn, are exchanged for

calcium by the Na+/Ca+ exchanger and this among other processes (such as impaired Ca+ uptake into the ER) causes a massive increase in intracellular calcium (Sanada et al. 2011; Szydlowska & Tymianski 2010; Talukder et al. 2009). This intracellular calcium initiates cell death through multiple pathways. Mitochondrial uptake of calcium, via the mitochondrial Ca+ uniporter, attempts to restore balance but once excessive levels of calcium are reached in the mitochondria, mitochondria permeability transition (MPT) ensues (Szydlowska & Tymianski 2010). Raised Cytosolic calcium also activates calpains and calcium/calmodulin-dependant protein kinases (CAMKs), which contributes to cell death(Kalogeris et al. 2012; Croall & Ersfeld 2007). Also, raised intracellular calcium and sodium lead to cell swelling and cell cycle arrest (Ponticelli 2015).

With the lack of oxygen, ATP production falls as does the intracellular pH, and the delicate balance within the mitochondria become disturbed. The mitochondria swell and allow the efflux of cytochrome c into the cytosol where it initiates apoptosis (Dorweiler et al. 2007; McCully et al. 2004). The fission and fusion cycles of the mitochondria become unbalanced, and excess fission causes fragmentation and damage to the mitochondria, which then leads to cell death. A study which inhibited mitochondrial fission demonstrated a reduction in IRI -induced mitochondria fragmentation (Ong et al. 2010). The MPT pore (a non-specific channel in the mitochondrial membrane) is opened in reaction to the increase of calcium and reactive oxygen species (ROS) causing further depletion of ATP as the permeability of the membrane dissipates the proton electrochemical gradient. Swelling, rupture and cell death is a high risk when the MPT pore remains open. Hence the MPT pore plays a vital role in necrosis (Baines 2009; Halestrap 2010; Kroemer et al. 2007).

When reperfusion ensues, essential ATP generation via aerobic respiration restarts; however, this critical reperfusion comes with its detrimental effects. The influx of oxygen and rapid production of ATP, from oxidative phosphorylation, results in an increased and overwhelming generation of the by-product ROS. ROS (precisely, a term for several reactive molecules and free radicals derived from oxygen) under normal circumstances can be handled and dealt with by the cell via several defence mechanisms, but when ROS levels become excessive the resultant damage is termed "oxidative stress". Reactive nitrogen species (RNS) which are nitrogen-containing oxidants, together with ROS are collectively termed RONS. The extent of injury from reperfusion is due to the individual and combined effects of ROS and RNS (Kvietys & Granger 2012). RONS affect cell signalling and directly damage DNA, protein, and lipids among other cell molecules. The damage can directly disrupt cell structure leading to cell death or can activate and propagate the inflammatory

cascade resulting in cytokine release, apoptosis, structural cell damage and again cell death (Kalogeris et al. 2012). Inflammatory cells such as macrophages and neutrophils also release a burst of ROS, typically reserved as a host defence against invading pathogens, but this is triggered in the immune response to IRI further adding to the overwhelming volume of ROS. (Kvietys & Granger 2012).

Cell death and injury activate the innate immune system with most of the insult from the immune system coming during the reperfusion stage in response to the injury caused by the RONS. The resultant inflammation is termed a sterile inflammation as there is no pathogen present, and its intensity relies on the pro and anti-inflammatory mediators released by resident renal cells and recruited inflammatory cells.

Initially thought to play a passive role, the epithelial cells are now considered to play a significant, initial role during the reperfusion phase. No reflow phenomenon, which is reduced or no blood flow, particularly in the outer medulla, without mechanical obstruction, is seen at reperfusion. It is a result of intense endothelial vasoconstriction, swelling of the endothelial cells (see above) and reduced production of vasodilators(Sutton et al. 2002; Flores et al. 1972). This causes patchy perfusion of the kidney, prolongation of the ischaemic insult and production of danger-associated molecular patterns (DAMPs) which in turn activate Toll-like receptors (TLR) (Beg 2002). These TLR are involved in the pathways associated with apoptosis and the production of many pro-inflammatory cytokines and chemokines such as tumour necrosis factor α (TNF- α), IL-1beta, IL-6, C-C motif ligand 2 (CCL2) which in turn can further cascade the increase of pro-inflammatory mediators (Wolfs et al. 2002; Huiling Wu et al. 2007). Animal studies looking at TLR2 and TLR4, in particular, found a dampened inflammatory response, better survival and reduced fibrosis when inhibited. (Huiling Wu et al. 2007; Leemans et al. 2005; L.-M. Zhang et al. 2016). The swollen injured tubular epithelial cells also activate the complement system through the alternative pathway as they produce less complement receptor 1-related gene/protein y (Crry). Crry is a complement inhibitor post-IRI (Thurman et al. 2006). Activated complement system enhances the attraction of immune cells like neutrophils and macrophages to the kidney. Macrophages and neutrophils are further attracted to the kidneys by many other immune effects after IRI such as the increased expression of intracellular adhesion molecule 1 (ICAM-1) and c-x-c motif chemokine ligand 1(CXCL1) within renal cells (Sutton 2009; Oh et al. 2008).

Neutrophils attracted to injured tubules have been found to have a negative effect. Studies looking at neutrophil depleted mice, and ICAM-1 knockout mice sustained less injury secondary to IRI (Kelly et al. 1996). Awad et al. suggested that among other detrimental effects, they create more ROS (Awad et al. 2009). After neutrophils, macrophages arrive attracted by the release of cytokine and chemokines such as C-X3-C motif chemokine receptor 1 (CX3CR1) and c-c motif chemokine receptor 2 (CCR 2). Along with dendritic cells, they propagate the immune-inflammatory response with the release of pro-inflammatory cytokines (X. Dong et al. 2007; Bajwa et al. 2009; L. Li et al. 2008) As the inflammatory process continues, dendritic cells make up the majority of the leukocytes in the kidney. However, not all leukocytes have a detrimental effect. Resident monocytes which are exposed to interleukin 4 (IL-4), IL-13, immune complexes, or IL-10 differentiate into resident anti-inflammatory or pro-repair macrophages also known as M2-type macrophages (Y. Wang et al. 2007; S. Lee et al. 2011). However, although the M2 phenotype may be initially beneficial, the longer-term effects are still uncertain, as they may drive renal fibrosis (Meng et al. 2014).

The full innate response is vast, complex, and out of the scope of this chapter; however, due to its translation in clinical trials, it is worth mentioning T cells. Natural killer cells (NK) and CD4+T cells seem to exacerbate IRI. Natural killer cells can be found in the kidney 30 minutes after IRI, and three hours later, its pro-inflammatory cytokines such as interferon-gamma (IFN-y) production is at its peak (X. Dong et al. 2007). Natural killer T cells (NKT) can also increase the dendritic cell response in IRI (X. Dong et al. 2007). CD4+T also act early in the IRI innate response with infiltration by one hour (Burne et al. 2001). Studies looking at blocking endothelial CD80 expression, which attracts CD4+T cells to migrate to the kidney, found reduced kidney injury and a reduction in pro-inflammatory cytokines (Burne et al. 2001; Z.-X. Zhang et al. 2008). However, not all T cells have a negative impact post-IRI on the kidney. T regulatory cells (T regs), which express the cell marker transcription factor forkhead box P3 (FoxP3) and CD25 have demonstrated promise in reducing the inflammatory response, graft rejection and even improving long term tolerance. Phase I clinical trials have shown their safety and feasibility (Romano et al. 2019). T regs interact with many other immune cells including CD4+ and CD8+ cells, NKT cells, B lymphocytes, dendritic cells (DC), neutrophils and monocytes suppressing their function either by direct interaction or indirectly through multiple mechanisms (Vignali et al. 2008). Tregs can produce anti-inflammatory cytokines such as (IL-10, IL-35) in addition to suppressing T lymphocyte proliferation and activity, both of which can ameliorate IRI(Romano et al. 2017). As mentioned earlier, the positive attributes of M2 macrophages

can be enhanced through Tregs ability to push monocytes toward the M2 phenotype (Tiemessen et al. 2007).

1.5 KIDNEY RECOVERY AFTER ISCHAEMIA REPERFUSION INJURY

The aftermath and long-term outcome for the kidney depend on the severity of the IRI and the kidney's capacity to repair itself. Recent studies have suggested that rodent adult kidneys can regenerate through unipotent precursor cells, but this has not been demonstrated in adult human kidneys. Human kidney regeneration potential and the exact source remains elusive. It could be through endogenous tubular epithelial cells, with the aid of bone marrow-derived stem cells and paracrine function, that divide and repair locally. Renal progenitor cells seem a more likely source of human kidney regeneration after injury (Lombardi et al. 2016; Rinkevich et al. 2014; Angelotti et al. 2012). Either way, there is no agreed conclusion. Unlike some human organs, the kidney, as far as we are aware, has a limited capacity to create new nephrons. The skin and intestine can completely self-renew within a few days, but even though limited studies exist, it is generally thought that human kidneys cease to create new nephrons after birth, with the majority of nephrons developing in the second half of gestation (Blanpain et al. 2007; Blanpain et al. 2004; Ryan et al. 2018). All is not doomed as the kidney can recover function after injury though not through regeneration, as described above, but through hypertrophy. Even if the patient is elderly or has some underlying comorbidities (Taner et al. 2015). The number of nephrons in the healthy human kidney can vary between 250,000 to two million, and it can be surmised that humans with high nephron count from birth are less susceptible to developing sequelae from nephron loss (Puelles et al. 2011).

1.6 THERAPIES TO MITIGATE TRANSPLANT RELATED KIDNEY ISCHAEMIA REPERFUSION INJURY

The degree of IRI, which is proportional to the CIT, harms graft function and survival (Quiroga et al. 2006; Sert et al. 2014; Barba et al. 2011). In addition to delaying graft function and reducing graft survival IRI triggers immune system activation subjecting the recipient to an increased risk of rejection which is associated with increased hospital admissions, monitoring and biopsies (Barba et al. 2011; Brennan et al. 2004). Conquering its complexity and developing an intervention will not only improve function but will open the door to more

DCD and marginal kidneys. Currently, many DCD and marginal kidneys are not accepted or offered for transplantation as the evidence tells us they will not have an acceptable function or longevity after sustaining an ischaemic reperfusion insult. Hoverer a therapy to ameliorate IRI will open the door to the kidneys which are not offered or declined.

IRI is associated with increased immunogenicity, chronic renal graft dysfunction, loss of renal mass, and fibrosis formation (H. Zhao et al. 2018). Multiple approaches are taken to address IRI, and the main areas of research and development include perfusion solutions and ex vivo perfusion rigs, pre and post graft conditioning, pharmacological interventions, and cellular therapies.

1.6.1 KIDNEY PERFUSION FLUID AND EX VIVO PERFUSION RIGS

Traditionally retrieved kidneys are preserved in static cold containers during transportation and the period spent there is termed the cold ischaemic time. Extreme efforts are made to keep this time as low as possible as CIT is directly related to delayed graft function (DGF) and graft survival and outcomes. To limit the damage caused during the CIT kidney storage solution was invented to perfuse and surround the kidney post retrieval and when being prepped for implantation. The most used are University of Wisconsin, Histidine-tryptophan-ketoglutarate and Celsior solution. These solutions aim to slow down the metabolic processes and preserve the grafts as long as possible. Key ingredients include colloids, buffers, nutrients and antioxidants (Yimeng Chen et al. 2019). Despite the three solutions mentioned above still widely used today, there have been many adaptations to these solutions.

Additives to the solutions have been investigated to target specific pathways of IRI such as the use of hydrogen sulphide (H2S) to slow O2 requirements and apoptosis, prostaglandin E1 to target oxidative stress, and various trophic factors (Lobb et al. 2015; McAnulty et al. 2002; Polyak et al. 1999). Novel gaseous additives such as xenon, argon, hydrogen sulphide and carbon monoxide, in addition, or as a replacement of traditional nitrogen gas saturation, have increased in popularity due to their favourable non-toxic characteristics at therapeutic doses, cheap cost and growing evidence in animal studies at ameliorating IR. Again, gasses target pathways of IRI such as H2S antiapoptotic and anti-inflammatory effects or the theory that CO will prevent a pro-inflammatory increase in haem content by inhibiting the degradation of cytochrome P450 (Nakao et al. 2008; Lobb et al. 2014; Hunter et al. 2012). Gases may also more easily permeate the cell membrane.

To improve on static cold storage, mobile rigs were created to constantly perfuse the kidney with cooled perfusion solution in an enclosed system under a specific pressure during transportation. This ex vivo hypothermic machine perfusion has significant evidence supporting it over cold static storage with a drop in delayed graft function, increase in 1-year survival and 3-year survival (Ray et al. 2009; Wszola et al. 2014; Treckmann et al. 2011; Tingle et al. 2020). With multiple temperatures, pressure and perfusion time combinations possible, there is likely to be further developments in this field with regards to optimal conditions (De Deken et al. 2016).

In 2011 the first renal transplant was performed using a kidney that underwent ex vivo normothermic perfusion (Hosgood & Nicholson 2011). This has the added advantages of limiting some of the effects of anoxic hypothermic preservation as the kidney is perfused with warm oxygenated red cell-based solutions. This not only preserves and resuscitates but allows observation of kidney perfusion, urine output monitoring and the option to perform biochemical or histological analysis. Phase II studies of 400 patients have already started recruitment (Hosgood et al. 2017). Again, this is likely only the beginning as there is a vast and growing combination of therapy time, pressure, and solutions.

Another significant advantage of ex vivo perfusion rigs is the opportunity to administer therapies while being perfused on the rig. Easy access to the kidney and its artery opens the door for several routes of administration. Administering therapies on the rig (ex vivo) reduces the risk of therapies passing onto patients and having undesirable side effects. Higher dosage regimes can then be tested, ethics approval for trials will be simpler, and kidneys that would otherwise be discarded can be given a chance to demonstrate if it has any acceptable residual function.

1.6.2 PRE AND POST ISCHAEMIC CONDITIONING

As with many therapies and techniques to counteract IRI, the renal transplant community attempted to adopt a technique which had shown much promise in cardiac surgery. Ischaemic preconditioning demonstrated significant amelioration in kidney dysfunction and damage in animal models of renal IRI (Jiang et al. 2015; van den Akker et al. 2013; Kadkhodaee et al. 2011). Popular regimes of pre-conditioning involve ischaemia and reperfusion of a limb for four cycles of 5 minutes either before transplant or post-implantation. Unfortunately, a multicentre prospective study between Sweden, Denmark and

Netherlands of 225 patients who underwent remote ischaemic pre-conditioning peri-implantation did not find any differences in their primary outcome of kidney function (serum Cr) (Krogstrup et al. 2017). Different combination of pre, post and remote ischemia for varying lengths of time in both live and deceased donors have been attempted, but none have shown significant long-term advantages(Jianyong Wu et al. 2014; Nicholson et al. 2015; Yeling Chen et al. 2013; van den Akker et al. 2014). A larger study of 406 live donors attempting late and early remote ischaemic preconditioning also found no change on glomerular filtration rate (GFR) or the inflammatory response to surgery (MacAllister et al. 2015). Clinical studies on remote ischaemic pre-conditioning for renal IRI seems to have largely fizzled out.

1.6.3 PHARMACOLOGICAL INTERVENTION

Pharmacological intervention has so far been disappointing. There is no widely used drug which convincingly ameliorations IRI and has made the transition to successful clinical application (despite promising animal studies). Two that made it to clinical studies (for acute kidney injury) were statins and erythropoietin. Statins were initially thought to improve contrast-induced kidney injury, but a prospective study failed to validate the improvement (Attallah et al. 2004; Khanal et al. 2005; S.-H. Jo et al. 2008). Erythropoietin administered peri transplantation again showed promising results both in animal models and in some clinical studies, but a metanalysis by Vlachopanos et al. found no significant difference when administered for deceased donor transplants in either DGF, mortality, rejection, DGF and 4-week kidney function (Xin et al. 2015; Vlachopanos et al. 2015). More novel pharmacological treatment has been promising in animal models such as CD47-blocking antibody (alphaCD47Ab). AlphaCD47Ab inhibits nitric oxide and oxidative stress by ameliorating thrombospondin mediated IRI signalling (Rogers et al. 2012). Helix B peptide surface peptide of erythropoietin reduced apoptosis and inflammation with subsequent increase in renal function in a rodent model of renal IRI (Yang et al. 2014). When added to reperfusion solution, the kidneys had improved urine output and decreased tissue damage – the helix B peptide seems to hold the protective abilities of erythropoietin (Yang et al. 2015). Pharmacological agents aimed at inhibiting the matrix metalloproteinases (MMPs) and ROS, both of which are heavily involved with the mechanism of injury, in theory could be a promising route of study and perfusion rigs could offer a means of administration. The scope of this research is enormous due to the thousands of interventions points possible in the complex IRI pathophysiology, more of which is described in chapter five. However,

currently, there have been no breakthroughs in terms of peri-transplant pharmacological intervention to reduce transplant-related IRI injury. Phase two clinical trials in 2009 of Diannexin were promising with improved GFR and urine output in recipients who received it intravenously post reperfusion of their marginal kidney (M et al. 2010). Diannexin is an agent that binds to phosphotidyl serine on the cell surface and inhibits mononuclear cell attachment attenuating IRI. No further research has been published regarding Diannexin in kidney transplant patients. Finally, the University of Edinburgh is currently recruiting for their randomised controlled clinical trial looking at the use of heme arginate to mitigate the inflammatory response of IRI. Heme arginate induces expression of the heme-oxygenase which is an enzyme that breaks down heme and reduces the inflammatory response. Recruitment is due to be completed by the end of 2020.

1.6.4 CELLULAR THERAPIES

Of all the interventions so far cellular therapies, in particular stem cell therapy, show the most promise. Therapies investigated to date have attempted to harness the protective and regenerative therapies not just of stem cell like cells but many cell types such as T cell, dendritic cells, and macrophages. The field is expanding rapidly, as is our understanding. It is a minefield of definitions, categories, disputes, and that was before the inclusion of stem cell-derived/associated mediators like stromal vascular fraction, extracellular vesicles, and stem cell-derived microRNA. So far, clinical trials of stem cells in renal transplantation have been low (Fig.1.4). However, with the popularisation of perfusion rigs and their unique ability to administer cellular therapies ex vivo, trials using cellular therapies in kidney grafts is undoubtedly going to surge.

1.7 STEM CELLS AND STROMAL CELLS WITH STEM CELL LIKE PROPERTIES

Within the scientific community, the first name that often comes to mind when discussing discoveries in stem cell research is Dr Yamanaka. In 2006 Dr Yamanaka reprogrammed adult (mature) human cells to become pluripotent by inserting four genes (retroviral transduction of Oct3/4, Sox2, c-Myc, and Klf4) (Takahashi et al. 2007). He later won the Nobel Prize for the work discovering the induced pluripotent stem cells. To the public, the most famous of all in the field of stem cell research is Dolly the sheep. A team from the

Roslin Institute, Edinburgh, led by Ian Wilmut, were the first to artificially clone an animal, by nucleus transfer, from a cultured embryonic cell line (Campbell et al. 1996). Although these breakthroughs were ground-breaking, there were many revolutionary discoveries that provided the foundations for stem cell research. 1969 saw the use of bone marrow transplants to treat immunodeficiency and there have been steady discoveries in animal and humans since then.

One of the earliest breakthroughs in terms of human stem cells for mass therapeutics was Dr Thomson and his team's achievement in creating the first human embryonic stem cell line (Thomson et al. 1998). A human stem cell line that still exists today and is one of the discoveries that has facilitated an explosion of research on stem cells as it negated the first (of many to come) stumbling block which was the need of repeated embryo retrieval from humans (not to mention the ethical issues associated with that). Since then, there has been a flow of discoveries such as new categories of stem cells, new sources, new stem cell lines. To add to all the discoveries, there are now thousands of ways they can be altered. Growing organs ex vivo, making organoids to test therapies and using animals to grow human organs are just a few ways in how they are now used but many of which will not see widespread clinical translation any time soon. However, the most likely approach that will see them widely used in the clinical setting is as an administered therapy for their regenerative, reparative, and protective effects.

With over 2000 publications per year and growing it can be overwhelming when trying to keep up with the field of stem cell research. Some of the directions of study has raised concern and beyond what is ethically acceptable not only to the scientific community but to donors, recipients, and society. Source selection, harvesting techniques, induction, the introduction of CRISPR gene editing and the crossover of humans and animals need to be regulated to safeguard the public but continue to allow research to progress. Laboratories, organisations, and governments have their regulations; however, as with many sectors, in recent times, the laws cannot keep up with the rate of research. Wading through the research, sparks new ideas but is also a rollercoaster of excitement, admiration, dubiety, and concern. Analysing the research from the late 90 into the 2000s, there is an impression that we were on the verge of changing medicine forever. Two things have since become apparent. Firstly, the field is more complex and challenging to implement than first anticipated, and secondly, despite point one, the future is cellular therapies.

1.7.1 DEFINITION AND CATEGORISATION

Within the scientific community, despite best efforts of organisations such as the International Society for Cellular and Gene Therapies (ISCT) and International Federation for Adipose Therapeutics and Science, there remains inconsistency in the categorising, phenotyping, and even what is considered a stem cell. Understandably, without careful reading of articles and understanding the retrieval and preparation process, it easy to get mislead if authors are referring to stem cells or stromal cells with some stem cell-like characteristics. The word "stem cells" is often inaccurately used as the authors have failed to stringently prove what they are referring to are stem cells and not stromal cells with stem cell-like characteristics. Bone marrow-derived mesenchymal stem cells and bone marrow-derived mesenchymal stromal cells being a prime example of two terms that are often interchanged but do not necessarily represent the same thing. Having the same acronym (MSC) does not help!

Mesenchymal stromal cells (MSC), as defined by The International Society for Cellular Therapy, are adherent to plastic, positive for CD105, CD73, and CD90 and negative for the expression of CD45, CD34, CD14 or CD11b, CD79 or CD19, and human leukocyte antigen class II, and should also be able to differentiate in vitro into osteoblasts, adipocytes, and chondroblasts (Horwitz et al. 2005). Cells were initially thought to be CD34- but processing and culturing techniques can alter their expression. This is the minimum criteria for MSC and all though very similar (and often argued to be the same population but just different due to their microenvironment, retrieval, and culturing techniques) there are some differences in cell surface markings from MSC of different sources. Table 1.1 displays some of the mild differences of surface cell markers from adipose-derived mesenchymal stromal cells (ASC) and bone marrow-derived mesenchymal stromal cells (BM MSC).

Source	Additional note	Positive cell surface markers	Negative cell surface markers
Minimal criteria to define multipotent MSCs	Mesenchymal stem cells refers to a stem cell population with demonstrable progenitor cell functionality of self-renewal and differentiation <u>whereas</u> MSC refers to a bulk population with notable secretory, immunomodulatory and homing properties and that is capable of in vitro differentiation into adipocyte, chondrocyte and osteoblast lineages.	CD73, CD090, CD105	Lacking the expression of hematopoietic and endothelial markers: CD11b, CD14, CD19, CD34, CD45, CD79a, HLA-DR
Bone marrow derived mesenchymal stromal cells (BM-MSC)	Method of isolation: Ficoll density gradient method Novel marrow filter device	CD73, CD90, CD105, STRO-1	CD14, CD34, CD45, HLA-DR
Adipose tissue derived mesenchymal stromal cells (ASC)	Method of isolation: Digestion method Membrane filtration method	CD73, CD090, CD29, CD44, CD71, CD105, CD13, CD166, STRO-1	CD14, CD31, CD34, CD45
	Other sources of MSCs include muscle, tendons, umbilical cord, synovial membrane, skin, nervous system, Wharton's jelly	There are other tissue specific MSC markers	

Table 1.1 Surface markers of bone marrow derived and adipose derived mesenchymal stromal cells.

According to the 2019 ISCT committee position statement the term "stem cell" should not be used unless they can be vigorously demonstrated to have more specific stem cell-like characteristics: 1) adherence to tissue plastic 2) multipotency and the maintenance of multipotency on in vitro expansion and 3) self-renewal capacity (Viswanathan et al. 2019). It can be said that MSC represents a bulk, unfractionated heterogeneous cell population that have secretory, immunomodulatory, and homing properties, of which a tiny population of the MSC will be true stem cells. As mass cytometry technology improves and the use of next-generation single-cell sequencing increases, these

population within MSC will likely become more defined (Viswanathan et al. 2019). The ISCT Mesenchymal Stromal Cell Committee made the following statement:

"Ultimately, the questions of whether mesenchymal stem versus stromal cells are functionally distinct subpopulations and whether the stem and stromal cells have overlapping paracrine and immunomodulatory functions are best answered based on single-cell sequencing experiments, statistical clustering and analyses of data. From a clinical translational perspective, the secretory and immunomodulatory functions associated with clinical benefits of MSC-based therapies are thought to reside in the bulk, heterogeneous stromal cell fraction." – 2019 ISCT position statement (Viswanathan et al. 2019)

BM MSCs, until recently, had been the most widely understood and studied. Friedenstein and colleagues first identified bone marrow-derived non-haemopoietic MSC in the 1970s (Friedenstein et al. 1970). Nowadays, MSCs have been isolated from almost every bodily tissue (Via et al. 2012). Bone marrow derived haemopoietic and MSCs may have had a head start in terms of research and clinical translation but in recent times focus and understanding of other tissues sources has dramatically increased as they offer different advantages and clinical potential.
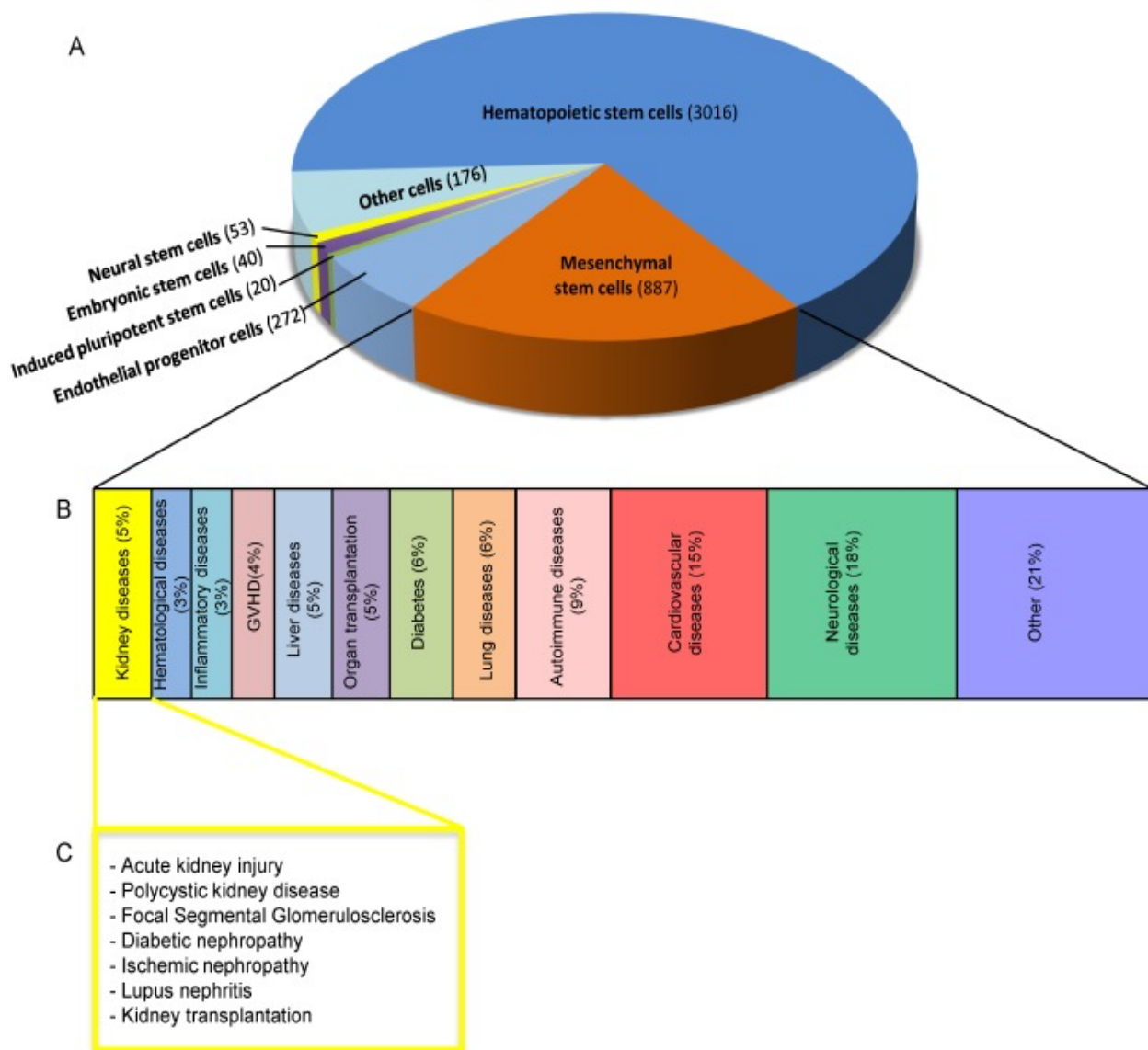
Figure 1.4 Clinical trials currently using embryonic and adult stem cells. (A) Pie chart showing the relative numbers of clinical trials using different types of stem cells as listed on the U.S. NIH website clinicaltrials.gov. (B) Percentage of MSC-based clinical trials classified by disease type. (C) MSC-based therapies in different kidney diseases. *Rota C, Morigi M, Imberti B. Stem Cell Therapies in Kidney Diseases: Progress and Challenges. Int J Mol Sci. 2019;20(11):2790. Published 2019 Jun 7. doi:10.3390/ijms20112790*

1.7.2 STEM CELLS IN ORGAN TRANSPLANTATION

Solid organ transplantation has revolutionized the treatment of organ failure. Immunological barriers have progressively reduced, but the challenge of inadequate donor organ supply has grown with increasing demand (Levitt 2015). This has led to escalating use of older/comorbid donor organs (Saidi et al. 2014). Aside from intrinsic increased cellular

senescence (Braun et al. 2012), such organs do not tolerate the injurious processes associated with removal, storage, and transplantation as well as traditionally used organs from younger donors {Port:2002in}. In particular, kidneys from older and co-morbid donors are more vulnerable to the ischemia reperfusion injury (IRI) (H. Zhao et al. 2018).

Regenerative medicine approaches to organ transplantation initially focused on the generation of functioning neo- tissue, highlighted widely as the main potential benefit of pluripotent stem cells. This approach spans artificial organ construction, the engineering of bioactive, organ-like tissue (Bantounas et al. 2018), and the use of infused stem cells (Raven et al. 2017). Examples of such tissue successfully generated for clinical use do exist (De Filippo et al. 2015) for relatively simpler tubular structures, but translation in solid organ transplantation has been slow and frequently remains at the preclinical stage (Taylor et al. 2018).

This has led to a switch in focus to addressing the regenerative capacity of organs already available — including those currently declined for solid organ transplantation because of predicted poor function post-transplantation. This approach focuses on protecting organs from peri-transplantation injury (principally IRI) and enhancing tissue regeneration after transplantation. Stem cells provide a promising source of protective and regenerative properties; however, there are many different forms of "stem cells" and accurate characterization and functionality can be complex. Pluripotency, multipotency, or oligopotency are clearly essential to form functioning neo-tissue but such characteristics may be less critical in stem cell's ability to influence other tissue to survive injury and regenerate. The wide variety of stem cell subtypes currently used in organ regeneration is illustrated in Table 1.2.

Class of stem cell	Potency	Clinical administration
Tissue-specific stem cells (Somatic-derived)		
Blood-derived stem cells	multipotent	Cultured expansion necessary
Adipose derived regenerative cells	pluripotent	Directly transplantable
Bone marrow derived cells	pluripotent	Cultured expansion necessary
Endometrial regenerative cells	pluripotent	Directly transplantable
Induced pluripotent stem cells (Somatic-engineered)	pluripotent	Cultured expansion necessary
Mesenchymal stem cells (Stroma-derived)		
Bone marrow derived mesenchymal stem cells	multipotent	Cultured expansion necessary
Adipose derived mesenchymal stem cells	multipotent	Cultured expansion necessary
Endothelial stem cells	multipotent	Cultured expansion necessary
Dental pulp stem cells	multipotent	Cultured expansion necessary
Embryonic stem cells (Embryo-derived)		
Morula derived stem cells	totipotent	Cultured expansion necessary
Blastocyst derived stem cells	pluripotent	Cultured expansion necessary
Umbilical derived stem cells	pluripotent	Cultured expansion necessary
Extraembryonic stem cells	multipotent	Cultured expansion necessary

Table 1.2 Stem cell diversity

1.7.3 UNDERSTANDING ANIMAL MODELS USED TO INVESTIGATE STEM CELLS IN RENAL TRANSPLANTATION

Most data which exist on stem cells in transplantation is based on animal models which attempt to mimic renal transplant IRI. Therefore, it important to understand the common models used and their limitations.

The aim of the animal model of renal IRI is to inflict a reproducible and significant insult that will develop into renal fibrosis. There needs to be a measurable and permanent reduction in renal function without unacceptable rates of animal mortality. Therefore, establishing a degree of renal failure. Animal models that achieve this can be used to test therapies aiming to ameliorate renal transplant related IRI along with other forms of renal IRI.

Animal models include bilateral ischaemia and unilateral ischaemia with contralateral nephrectomy (Fig. 1.6). Ischaemic times of 30 to 60 minutes have been shown to cause acute renal dysfunction. However, this length of ischaemia usually results in normal serum levels of urea and creatine within one week (Wei & Z. Dong 2012; Forbes et al. 2000; Ysebaert et al. 2000; Jablonski et al. 1983). In these models, more extended periods of ischaemia are associated with unacceptable rates of animal death from the acute kidney injury and in the majority of these model's serum creatinine (Cr), and urea (Ur) will return to normal within two weeks making it impossible to test the long term efficacy of therapies (Zager 1987; Zager 1991; Hörbelt et al. 2007; Basile et al. 2001). Therefore, to assess therapies more accurately, an animal model that causes a severe renal IRI injury that results in long term reduction in renal function (like the IRI associated with transplantation) is desired. Nevertheless, still adhering to the principles of the 3Rs as high mortality rates from an extreme IRI would not be acceptable.

Unilateral ischaemia, without nephrectomy, allows for more prolonged levels of ischaemia resulting in permanent renal injury. The untouched contralateral kidney ensures survival. Whalen et al. demonstrated that 120 minutes of ischaemia of the left kidney in adult Fischer 344 rats produced a significant loss of renal function that persisted after six weeks (Whalen et al. 2016). Histology at week six looking at hyaline casts and epithelial breaks confirmed chronic damage. Kidney function by Whalen et al. was measure by inulin clearance studies (Fig. 1.5).

Inulin is a fructose polymer that filtered via the glomerulus without being secreted, reabsorbed or metabolized in the renal tubules; therefore, an ideal molecule for GFR calculations (Aurell 1994). Determining the renal function of the injured kidney using inulin clearance is a terminal procedure. The inulin is injected systemically to create a constant plasma concentration then the ureters are cannulated, and urine and blood are serially collected to measure the inulin concentration. Inulin clearance and therefore, GFR can be calculated from the data. Plasma clearance studies such as this are considered the gold standard in determining renal function in the form of glomerular filtration rate and is significantly more accurate than serum Ur and Cr measurement. Cr and Ur are useful as surrogate markers of renal function but cannot be relied on for accurate renal function analysis, and they do not become elevated until 50-75% of kidney function is lost (Finco & Duncan 1976; Katayama et al. 2010). Even if there has been a severe long-standing injury to one kidney the normally functioning untouched contralateral kidney will be able to keep Ur and Cr serum levels within normal limits hence the additional need of inulin studies in the Whalen et al. model.
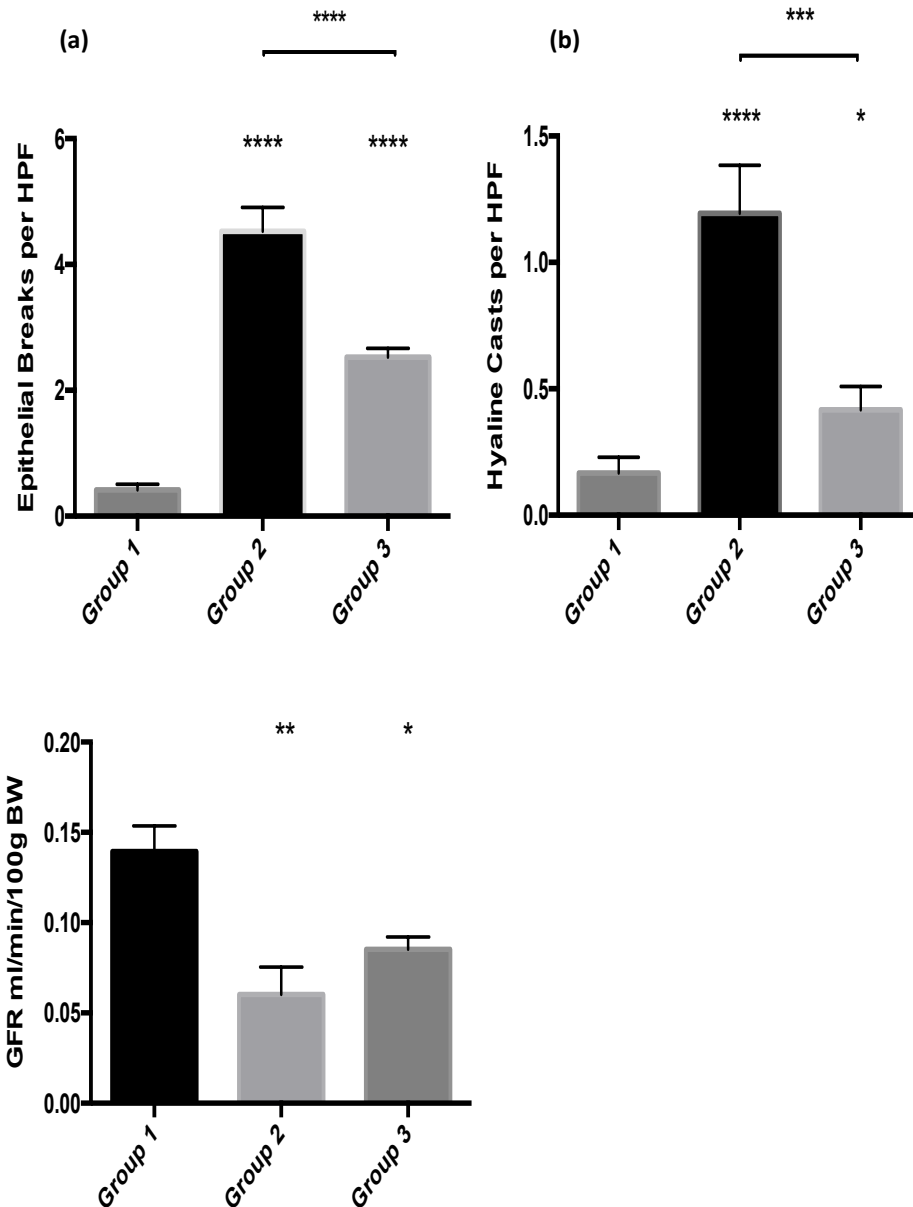
Figure 1.5 Functional and histological analysis performed by Whalen et al. demonstrating a significant and permanent reduction in renal function with correlating histological findings in kidneys that are exposed to 120 minutes of ischaemia and then reperfused. The left kidney of the rat was clamped for 120 minutes then reperfused. Kidneys were then retrieved two weeks and six weeks later, after functional analysis using inulin clearance studies, for histological analysis. Left kidney renal function in Group 1 (sham-operated), Group 2 (120 minutes IRI with two weeks recovery) and Group 3 (120 minutes IRI with six weeks recovery). (A) Renal histology shows that Group 2 animals exhibit significantly more epithelial breaks than Group 1 animals (p<0.0001). Similarly, more epithelial cell breaks are observed in Group 3 animals than Group 1 (p<0.0001). Group 2 animals had more epithelial breaks than Group 3 animals (p<0.0001). (C) Group 2 animal experience a severe reduction in GFR (~50%) compared to sham

operated animal (p=0.0022). GFR is typically ~65% of sham values after six weeks recovery (p=0.0013). Statistical analysis by one-way ANOVA with Turkey multiple comparisons test. Permission obtained from Whalen at al. to use figure. Published in Renal Failure 2016 Nov;38(10):1694-1701. doi: 10.3109/0886022X.2016.1144024. *A novel rodent model of severe renal ischemia reperfusion injury.* Whalen H, Shiels P, Clancy M.

Animal survival and well-being as assessed by weight gain in the Whalen et al. model was good and followed a similar trend to sham rats that underwent surgery with no IRI. Therefore, Whalen et al. produced an acceptable model of renal IRI which resulted in longstanding changes in renal function. With these long-term effects and the use of inulin clearance to measure renal function, it is a useful model to screen potential therapies before progressing on to technically more challenging and higher risk transplant models. Also, Whalen et al. would administer therapies directly into the renal artery at the time of the ischaemia by transecting the artery, cannulating it to administer the therapies then suture anastomosing the artery back together. With the renal artery easily accessible at the time of human transplantation, it could prove to be an efficient route for administration with improved retention, reduced extra-renal biodistribution (see chapter 4).

There were, however, some issues with the Whalen et al. model. Firstly, the fully functioning right kidney can effectively increase its functional capacity and meet the renal requirements of the rat including the "mopping up" of the metabolic disturbance, such as hyperkalaemia, uraemia, hypercalcaemia, hyperphosphatemia, that results from the IRI. Therefore, the environment in which the injured kidney is recovering is not representative of the transplant patient. Secondly, inulin studies in this model are time-consuming (taking up to 6 hours), surgically difficult and terminal therefore increasing the numbers or rats required as serial measurements are not possible. Thirdly, completely transecting the left renal artery was again time-consuming and technically challenging. To this end, an animal model that could provide the severe IRI but address some of the shortcomings would be optimal for testing therapies to ameliorate IRI in kidney transplantation.

BILATERAL IRI

- IRI NOT SEVERE ENOUGH
- NO ENVIRONMENT OF RENAL FAILURE

UNILATERAL IRI

WITH CONTRALATERAL NEPHRECTOMY

- IRI NOT SEVERE ENOUGH
- BLOOD ANALYSIS CAN GIVE SOME INDICATION OF RENAL FUNCTION

IDEAL RAT MODEL OF RENAL TRASPLANT IRI

- **SEVERE** IRI
- NOVEL NON TERMINAL MEASUREMENT OF GFR
- BETTER REPRESENTATION OF TRASPLANT PATIENT AS KINDEY RECOVERS IN ENVIRONMENT OF RENAL FAILUE

WITHOUT CONTRALATERAL NEPHRECTOMY

- IRI CAN BE SEVERE
- BLOOD ANALYSIS CAN NOT DETECT REDUCED RENAL FUNTION DUE TO COMPENSATING HEALTHY KIDNEY
- NO ENVIRONMENT OF RENAL FAILUE

WHALEN et al. MODEL

- VALIDATED **SEVERE** IRI
- GFR ACCURATELY MEASURED USING INULIN STUDIES
- NO ENVIRONMENT OF RENAL FAILUE

Figure 1.6 Commonly used rodent animal models of renal IRI. Animal models of IRI can be split into bilateral IRI models or unilateral IRI models. Figure highlights some of the limitations of each kind of model. Coloured box highlights the ideal model for testing therapies to ameliorate transplant related IRI. *Rat image obtained from Servier Medical Art, www.servier.com*

1.7.4 STEM CELLS AMELIORATE KIDNEY ISCHAEMIA REPERFUSION INJURY

The efficacy of infused MSCs, from various origins, in limiting IRI across multiple preclinical models is well established. Several such models have demonstrated this effect in rodent models of kidney IRI (Tögel et al. 2005; Lange et al. 2005; Asahara et al. 1996). A multicellular suspension of adipose-derived stromal vascular fraction cells (ADSVF) with a substantial MSC component has also exhibited similar properties (Z. Feng et al. 2010). Analogous observations have been described in liver models (X. Wang et al. 2018) and while less relevant to transplantation, similar cell types have been widely applied to the inhibition of ischemia reperfusion in myocardial infarction (Lim et al. 2018) and stroke (Nagahama et al. 2018).

While efficacy against IRI has been known for more than 10 years, the mechanism of stem cell action remains poorly understood (Morigi et al. 2008; Giordano et al. 2007). A consistent theme in recent studies suggests that stem cells exert a paracrine effect transferring cytokines and extracellular vesicles (EVs) to neighbouring cells, and in the context of IRI, initiate repair through the limitation of fibrotic progenitors, inhibition of cell death, and the reduction of inflammation. Zhu and colleagues show that injected EVs, exosomes, extracted from ASC in a renal IRI mouse model improved renal outcome by tubular epithelial cell activation of transcription factor, SRY (sex determining region Y)-box 9 (Sox9) (F. Zhu et al. 2017). Sox9 as a reparative factor is consistent with evidence that shows Sox9 promotion of tubular epithelial cell proliferation during embryonic development; and supports Zhu et al.'s additional studies which indicated an abrogation of tubular epithelial cell proliferation after administration of Sox9 inhibitors in the IRI model. ASC exosomal activation of Sox9 may also reduce progression to chronic kidney disease through simultaneous upregulation of Sox9 and downregulation of transforming growth factor (TGF)-β1 potentially avoiding upregulation of genes involved in building extracellular matrix and developing fibrosis (Meng et al. 2016). Sox9 may be a key regenerative mechanism in other organs as Sox9-dependant processes are also present during liver repair (A. Jo et al. 2014). However, whether the Sox9 gene can be administered as a therapeutic remains unclear, as a high Sox9 expression is correlated with glomerulosclerosis and liver fibrosis (M. R. Bennett et al. 2007). MSCs were also associated with elevated levels of transcription factors, AP-1, STAT3, and NF-kB. These factors may serve a reparative role by priming resident cells to enter the cell cycle, promoting proliferation and ultimately regeneration of injured tissue (W. Wang et al. 2014).

Stem cell extracellular vesicle transfer of specificity protein 1 (SP1) and its downstream regulators of necroptosis have been shown to be another paracrine mechanism in IRI inhibition. Necroptosis, like apoptosis, is a form of regulated cell death; however, unlike apoptosis, necroptosis is initiated by inflammation-related cellular damage that externally stimulates TNF receptors in the absence of active caspases (Belizário et al. 2015; Pasparakis & Vandenabeele 2015). SP1 is a transcription factor that upregulates sphingosine kinase-1 (SK1) which enzymatically catalyses the formation of sphingosine-1-phosphate (S1P). S1P is a bioactive sphingolipid metabolite that promotes cell growth and survival by acting on several G protein-coupled S1P receptors which upregulate anabolic and survival pathways (Jin et al. 2008; Maceyka et al. 2012). Delivering SP1-containing extracellular vesicles derived from human-induced pluripotent stem cell-derived MSCs (hiPSC- MSCs) to a rat IRI model improved renal function, histological features, and reduced kidney necroptosis as established by annexin V/PI positivity tests (Xiaodong Yuan et al. 2017). Co-administration of SP1 or SK1 inhibitors increased necroptosis and abolished the renoprotective effects in the animal model. Analogously, SK and S1P-dependant inhibition of necroptosis is also a demonstrated MSC mechanism in liver IRI treatment (Man et al. 2005).

In addition to inhibiting necroptosis, stem cells may also discourage cell death by inhibiting apoptosis. Stem cell pro- motion of mitogen-activated protein kinases (MAPK), which potentiate downstream signalling leading to apoptosis has been proposed as a potential stem cell induced pathway, especially given that bone marrow-derived stem cells have been shown to reduce the phosphorylation of ERK and p38, both vital signalling proteins in MAPK transduction(Qi & Dongcheng Wu 2013). However, further studies confirming stem cell downstream effects in inhibiting cell death, either through apoptosis or necroptosis are required.

Reducing regulated cell death may improve residual organ function but being able to modulate the immune systems' response to IRI may provide greater benefits on both retaining residual function and on long-term organ survival by disrupting positive feedback of sensitizing events. Stem cell immunomodulation has been extensively researched, in particular, stem cell-induced expansion of T-regs is proposed as a key therapeutic mechanism (Gonzalez-Rey et al. 2010). T-regs are known to suppress inflammatory functions of cells such as CD8+ T cells, macrophages, dendritic cells, natural killer cells, and B cells. In the context of renal IRI, it is reported that T-regs downregulate IFNγ production by local T cells, reducing the overall kidney inflammatory insult (Hu et al. 2016). In a recently studied IRI mouse model, endometrial regenerative cell treatment resulted in a

significant increase in splenic T-regs which is proposed to have improved the renal IRI outcome by potentiating a de- crease in CD4+ T cells, CD8+ T cells, and inflammatory-associated M1 macrophages levels while increasing levels of regulatory M2-type macrophages (P. Sun et al. 2016). Other potential mechanisms through which T-regs support organ preservation in IRI include metabolic interference, cytolysis, and targeting of antigen-presenting cells (Romano et al. 2017; Vignali et al. 2008). Multiple clinical studies modulating T-regs in the context of organ transplantation are on-going and while not the principal end-point, evidence of an improved preservation effect may emerge (Romano et al. 2017).

Another recent discovery implicating beneficial IRI immunomodulatory effects of stem cells was made by Shen et al. This group uncovered that mesenchymal stem cells and their exosomes contain particularly high levels of chemokine receptor proteins—CCR1 and CCR2 (Shen et al. 2016). These receptors actively bind and reduce the amounts of free CCL2. They went on to demonstrate that the decrease in available CCL2 resulted in reduced migration and activation of macrophages expressing the CCL2 cognate receptor, CCR2. Administration of MSC-derived exosomes rich in CCR2 to a mouse model of IRI conferred protection and was reversed by a knockdown of CCR2 on MSC-derived exosomes. This study thus provides a potentially novel target for therapeutic studies in IRI and suggests that stem cell-derived exosomes not only mediate cellular transfer of transcription factors and microRNAs but also of protein receptors.

Another recent study links stem cell IRI modulation of the complement pathway. C5a is a major regulator in inflammation and can potentiate NF-κB activation. NF-κB regulates the transcription of many inflammatory genes and can serve as an upstream activator of macrophages. Bone marrow derived MSCs administered in a mouse model of renal IRI significantly suppressed C5a in serum and C5aR in kidney tissue. The suppression of the C5a/C5aR-NF-κB pathway resulted in reduced macrophage activation and reduced secretion of macrophage pro-inflammatory cytokines, TNF-α and IL-6, with significant improvement in renal function (Tang et al. 2018).

Mechanistic data has paved the way for clinical trials in stem cell therapy in organ preservation and indicates important roles for reducing fibrosis, cell death, and inflammation. However, new discoveries of stem cell-derived regenerative factors and newly discovered stem cell targets of modulation still leaves us well short of understanding

the full scope of stem cell's potential beneficial effects including possible synergistic effects between multiple cell types.

Stem Cell Homing

Other factors that can affect the biodistribution of stem cells are the pathophysiological events taking place in the treated organ. During inflammation, hypoxia, repair and unregulated cell divisions, circulating chemokines, cytokines and integrins play a vital role in the homing ability of stem/stromal cells. Many factors are linked with the homing ability of both endogenous and exogenous stem/stromal cells. One of the most recognised pathways involved with stem cell homing is the SDF1/CXCR4 signalling pathway. SDF1 is thought to be the critical factor in attracting stem cells to repair damaged tissue (Rennert et al. 2012; Ko et al. 2013). Most studies involving this pathway were performed using bone marrow-derived stem cells, but there is research now supporting its vital role in adipose-derived stem cells and cells from other sources. Mi Jung Kim et al. previously demonstrated the efficacy of adipose-derived stem cells in the healing of ischaemic limbs. By transfecting stem cells with C-X-C motif chemokine receptor 4 (CXCR4), they were able to significantly demonstrate a correlation between CXCR4 expression levels and homing and engraftment rate of the adipose-derived stem cells. Also, they found the intra-arterial injection of stem cells to be just as effective as a direct intramuscular injection when comparing stem cell numbers within the ischaemic limb. They hypothesise that intravascular injection may be more effective as it protects the stem cells from being delivered directly into the severe environment induced by ischaemia.

It should also be noted that MSCs also express CCR1, CCR4, CCR7, CCR9, CCR10, CXCR5 and CXCR6 which play a role in migration (Lüttichau et al. 2005; Honczarenko et al. 2006). As well as these receptors, MSCs also express adhesion molecules – selectins and integrins. ASCs and BM MSCs are very similar when it comes to surface marker expression. These surface markers play essential roles in stem cell homing and mobilisation. However, it should not be presumed that research and factors on homing of certain types of stem cells like BM MSCs can be translated and relevant to other types of stem cells such as adipose-derived or embryonic. For example, ASCs unlike BM MSCs, express CD49d, CD54, but unlike BM MSCs, do not express CD106 (De Ugarte et al. 2003). These small differences could have vast effects on homing. CD106 plays a significant role in haemopoietic stem cell mobilisation and homing from bone marrow (De Ugarte et al. 2003). Likewise, CD54

(ICAM-1) was demonstrated by Kronenwett et al. to mediate the passage of haemopoietic stem cell across endothelium (Kronenwett et al. 2000).

Injury in organ systems can also affect biodistribution. Systemic injection of stem cells homes to injured heart, kidneys, liver, gut and brain (Yaojiong Wu & R. C. H. Zhao 2012; Morigi et al. 2004; S. Zhang et al. 2015; Parekkadan et al. 2011; Jiang Wu et al. 2007). As mentioned before the homing effect is often transient. Most of the research looking at stem cell chemo-attractants has been in the context of myocardial injury. Such chemo-attractants to the injured heart include monocyte chemotactic protein-3 but also the generic attractant found in other organs like SDF-1 (Schenk et al. 2007; Ghadge et al. 2011). What has still to be determined is if these chemo-attractants released during MI are released during other organ injury (not just MI) which again may alter the biodistribution of injected cells. Once the MSCs have reached areas of injury, adhesion molecules (selectins and integrins) seem to play a role in allowing the MSCs to migrate between the endothelial cells in a leukocyte type fashion by extending podia, rolling, then by manoeuvring between endothelial cells. Such adhesion molecules include very late antigen 4 (VLA-4) on the MSCs and vascular cell adhesion molecule 1 (VCAM-1) on the endothelial cells (Rüster et al. 2006). Christian Reiss et al. demonstrated that human-derived mesenchymal stem cells expressed proteolytic enzyme MMP-2 which allowed them to break down basement membranes and migrate between endothelial cells (Ries et al. 2007).

1.7.5 IMPROVING THE EFFICACY AND SURVIVAL OF STEM CELLS AGAINST ISCHAEMIA REPERFUSION INJURY

The lifespan of mesenchymal stem cells is short when administered to models of IRI, typically < 4% detectable by day 4 post-administration (Leibacher & Henschler 2016), potentially due to the harsh micro- environment created by IRI(Sosa et al. 2016). Improving stem cell resilience and survival could improve the efficacy and potency of the administered cells, perhaps reducing side effects related to cell dosage. Current techniques to fortify stem cells for clinical use include culture preconditioning and stem cell genetic transduction.

A recently devised method to precondition MSCs utilizes heat shock. Qiao et al. heated MSCs in a 42 °C water bath 2 h before treating rats suffering from hepatic IRI. They found that heat shock pre-treated MSCs experienced less apoptosis than non-treated MSCs and further discovered that pre-treated MSCs coped in a high oxidative stress environment of

hydrogen peroxide by increasing levels of autophagy. Furthermore, the authors demonstrated that an increase in autophagy was via the p38MAPK/mTOR signalling pathway, since a p38MAPK inhibitor removed the effect. Finally, it was demonstrated that MSCs pre-treated with heat shock before administration to hepatic IRI rats improved liver function, histological scores, and increased levels of proliferating cells compared to treatment with non-preconditioned MSCs, highlighting the importance of MSC resilience in the IRI microenvironment (Qiao et al. 2015).

3D (versus 2D) cultured stem cells have also been found to enhance stem cell survival and efficacy in IRI models of both hepatic and renal injury. 3D cultured cells exhibit an increased anti-inflammatory phenotype and exhibit a higher expression of angiogenesis genes. This anti-inflammatory effect may be explained by upregulated levels of ZC3H12A RNase, which destabilizes mRNAs of pro-inflammatory cytokines and chemokines like IL-6, CXCL1, CXCL2, and CXCL3 (Y. Xu et al. 2016). In addition, MSCs from a 3D culture were smaller in size which may allow them better penetration through the microvasculature of the lungs when administered intravenously, and in effect lower doses to be administered. In addition, multiple publications have documented improved angiogenic and anti- apoptotic effects of 3D versus 2D cultured cells and have demonstrated enhanced survival supporting the claim that they are less susceptible to the harsh IRI environment (Y. Xu et al. 2016; X. Zhao et al. 2016).

Since MSC-induced expansion of regulatory immune cells in IRI is believed to be an important component of their pro- regenerative effect, group Bai et al. pre-treated cultured MSCs in a regulatory cell attractant, cytokine IL-17A, before injection in a mouse model of renal IRI, demonstrating significantly reduced renal damage compared to non-treated MSC controls (Bai et al. 2018). The increase in splenic and renal T-regs demonstrated, occurred through a cyclooxygenase-2/prostaglandin E2 (COX- 2/PGE2)-dependent pathway, as blockage of COX-2 reversed the protective effect and reduced levels of T-regs. The involvement of COX-2 and of PGE2, (a hormone upregulated by COX- 2) in T-reg production is likely due to the PGE2 effect of inducing differentiation of T cells to regulatory T cells (Baratelli et al. 2005). A particularly interesting observation about IL-17A pre-treatment, not evident for other cytokine MSC pre-treatments such as IFNγ is that IL-17A enhanced downstream immunosuppressive effectors without inducing upregulation of histocompatibility molecules (MHC I and MHC II) and maintained normal MSC morphology—both of which could potentiate immunogenicity and harmful MSC properties (Sivanathan et al. 2015).

Genetic modification of pluripotent stem cells in humans has been possible and progressively refined since the 1990s (Thomson et al. 1998). More recently, this approach has been applied to improve stem cells' ability to ameliorate IRI. Administration of amniotic fluid stem cells expressing upregulated vascular endothelial growth factor (VEGF), via a lentiviral vector expressing VEGF, reduced tubular cell necrosis and improved renal function compared to treatment with non-transduced stem cells in a rat IRI model. Additionally, transduced stem cells had a mitogenic effect on tubular cells, increased the levels of T-regs and decreased pro-inflammatory M1 macrophage infiltration (Mori da Cunha et al. 2017). Similarly, bone marrow MSCs transduced to increase antioxidant, heme-oxygenase-1 expression, were more resilient to the IRI environment surviving longer, decreasing the number of tubular epithelial cells in the G0/G1 (resting/ interphase) stage, and significantly increasing proliferating cells (N. Liu et al. 2018). However, although gene modulation appears to be an attractive tool, safety issues remain a fundamental issue.

1.7.6 LIFESPAN AND ELIMINATION OF STEM CELLS

The fate of administered stem cells is still not fully understood. Very few living stem cells are detected 48-hour post-injection and almost none by one week (R. Zhang et al. 2015; Schmuck et al. 2016; Eggenhofer et al. 2013). These first hours are enough for the stem cells to exert their paracrine effect and reduce damage and increase repair. Many cells are thought to be destroyed during the turbulent administration process with their fragments being phagocytosed then cleared by the liver and spleen. The remaining cells may get trapped in the microvasculature where they exert their therapeutic effect and then die and eventually get phagocytosed.

Recent evidence moves away from the theory that stem cells integrate into the structure they home to and develop into the resident cell types. The fact that this is technically difficult to demonstrate contributes to the shift away from this theory. A small percentage of administered cells may home to the injured site and interact with the endothelial cells where they can reside long-term, but the numbers are small and perhaps under detected by imagining techniques.

With their low expression of major histocompatibility complex (MHC), one would think that the stem cells are not susceptible to NK cell detection and hence survive acute host rejection in the blood, but this theory is currently being debated and investigated (Leibacher &

Henschler 2016). There also does not seem to be a destructive T cell response to injected stem cells (Nauta & Fibbe 2007). That does not mean there is not some other form of interaction between stem cells and host cells in the bloodstream on administration such as that of the complement system (Leibacher & Henschler 2016). In summary, only a minority of injected cells can be traced once they have been administered, and the fate of stem cells cannot be confidently defined at present. The destiny of administered stem cells is dependent on many factors including route of administration, source and preparation, and the injury model in which they are administered.

During the kidney transplantation process, the surgeon has easy access to major recipient vessels, usually the internal, external, and common iliac arteries and veins and the kidney graft artery and vein. Therefore, clinical arterial administration of regenerative cell therapies at the time of transplantation would be straight-forward and would add little extra time to the procedure. As far as we are aware, there have been no studies tracking the biodistribution of uncultured MSCs delivered directly into the renal artery of the kidney graft just before reperfusion. The renal artery is a major medium-sized artery, but unlike other major intra-arterial injections, the artery is feeding directly into one organ (kidney) which will immediately face microvasculature and an evolving inflammatory response.

1.7.7 STEM CELL SOURCE AND PREPARATION AND ITS EFFECT ON BIODISTRIBUTION

Other major factors that can alter the biodistribution of stem cells are the methods in which they are prepared and their source. To be considered a MSC, the international society for cellular therapies proposed a standardised phenotype. Even after expressing this phenotype, there are still many variations, and this may affect the therapeutic potential and biodistribution. Furthermore, stem or stromal cells from the same source can have different biodistribution properties because of the method in which they are prepared. Rombouts et al. found that the percentage of MSC homing to the bone was drastically reduced when the MSC were cultured compared to primary non-cultured MSC. Many other studies have shown reduced homing and survival of cultured cells compared to freshly isolated cells with a resultant reduction in the therapeutic effect (Rombouts & Ploemacher 2003). Technique and environment, the stem cells are exposed to during culturing can also drastically change the phenotype like the loss of stromal cell derived factor 1 (SDF-1) (Wynn et al. 2004). However, this does not always have to be for the worse.

Altering the culture environment by adding cytokines, preconditioning the culturing process with heat shock or hypoxia can change the expression of the cultured cells to reverse the effects of the culturing process or even enhance the homing capacity beyond that of uncultured cells. Hypoxia can increase the expression of MMPs, which play a role in cell migration and adding cytokines such as stem cell factor (SCF) or IL-3 can re-establish the expression of SDF-1 (Shi et al. 2007; Annabi et al. 2003). 2D cultured stem cells are larger than uncultured stem cells of the same class; however, 3D culturing of cells can reduce this size discrepancy which theoretically would make them less susceptible to becoming entrapped in the microcirculation. Also, 3D cultured cells are more resilient to the harsh environment of IRI and have a stronger therapeutic effect. (Y. Xu et al. 2016; X. Zhao et al. 2016)

When discussing the biodistribution, we also must be mindful that studies do not always evaluate isolated stem cells. Whole stromal vascular fraction or extracellular vesicles, for example, have been used to treat many conditions and come under the umbrella term of "stem cells" or "cellular therapies" or "regenerative therapies". We discuss the nomenclature of regenerative cellular therapies in chapter three, but with regards to biodistribution, the results can be drastically altered depending on what specific cell population is utilised. For example, EV from stem cells or stromal cells are much smaller than whole stem cells; therefore, less affected by the capillary size and can cross the blood-brain barrier (Bang & E. H. Kim 2019). Also, EV may not possess the ligands to respond to chemo-attractants of injured cells. Therefore, the biodistribution of stem cell therapy made up of EV could differ than from complete stem cells from the same source.

1.7.8 MOBILIZING ENDOGENOUS STEM CELLS IN TRANSPLANT RECIPIENTS

Exogenous administration of cells carries the risk of infection, immune-sensitivity, teratogenicity, microvascular thrombosis as well as the possible logistical and cost issues associated with administration. To address some of these concerns, several groups have investigated methods to increase the production and mobilization of stem cells from one's own resident stem cell populations. Rats treated with SCF and granulocyte macrophage colony-stimulating factor (GM-CSF) in renal models of IRI were found to have increased mobilization of endogenous stem cells, which homed to the injured kidney and ameliorated IR through mechanisms associated with up- regulation of angiogenic factor, VEGF and anti-

oxidant factor, hypoxia-inducible factor (HIF)-1alpha. Treated rats displayed reduced kidney apoptosis and increased tubular repair (Bi et al. 2015). However, as an IRI treatment, there is concern with systemic administration of growth factors related to high bioactive effects which can lead to deleterious side-effects including tumorigenesis (Carragee et al. 2011). Additionally, evidence indicates that resident stem cells become depleted or dysfunctional with in- creasing age, limiting this approach in older patients (Woolthuis et al. 2014). There may however be potential for this approach if stem cell mobilization therapies can be rendered organ and/or signalling pathway specific.

In a novel attempt to reduce injury from IRI by recruitment of endogenous stem cells, Tan et al. investigated postconditioning kidneys with supplementary mechanical injury insult in their rat model (X. Tan et al. 2015). The postconditioning model consisted of 3 cycles of 30 s of ischemia followed by 30 s of reperfusion in a kidney which previously sustained 45 min of ischemia followed by 7 min of reperfusion. Postconditioning markedly reduced features of renal injury including kidney necrosis, neutrophil infiltration, and cellular vacuolization, and significantly reduced creatinine levels compared to non- preconditioned rats (X. Tan et al. 2015). Importantly, the Tan et al. group illustrated that this technique mobilized endogenous stem cells as blood from preconditioned rats had increased levels of CXCR4+ and CD34+ (haemopoietic) bone-derived stem cells. They concluded that preconditioning regulated oxidative stress and increased HIF-1alpha levels which then in- creased stromal cell-derived factor expression, a stem cell attractant, resulting in stem cell migration and homing to ischemic tissues (L. Liu et al. 2011; Ceradini et al. 2004). MacAllister et al. performed a similar preconditioning technique in a trial of 406 live donor kidney transplants. Though there was only mild improvement in glomerular filtration rate when compared to control, the trend of graft functional improvement appeared promising and may be greater in deceased donor transplantation where IRI is more significant (MacAllister et al. 2015).

In an innovative attempt to mobilize resident stem cells, Wang et al. used low-level laser therapy (LLT) treatment of bone marrow in rats before renal IRI. By exposing both tibiae to two episodes of 100 s each of LLT they significantly in- creased bone marrow-derived stem cell infiltrates in the glomerulus and renal tubules but not in the peripheral blood. Interestingly, rats undergoing LLT without IRI had elevated levels of bone marrow-derived stem cells in the peripheral blood, indicating that injury status affected migration. Notably, LLT-treated rats had significantly improved renal function and kidney histology indicating the potential value of LLT mobilized stem cells as an IRI therapy. They hypothesized that LLT induces proliferation of bone marrow-derived mesenchymal stem cells, which home to

injured kidney tissue and elicit repair (Oron et al. 2014). Promising as this seems, further studies are required to understand if enough ameliorative endogenous stem cells can be mobilized to influence larger human organs that have sustained clinically significant tissue injury. There is also a potential limit in elderly or physiologically unfit patients where the capacity of endogenous stem cells to replicate may be significantly impaired.

1.7.9 ROUTE, DOSAGE, AND TIMING OF ADMINISTRATION OF STEM CELLS

Clinical considerations also include, but are not limited to the route, dosage, and timing of administration. Injecting ADSVF before ischemia in a rat model of renal IRI demonstrated more ameliorative properties and significantly reduced tubulointerstitial fibrosis than when injected post-ischemia (Zhou et al. 2016). However, the clinical nature of transplantation may provide greater freedom in choosing exactly when to administer the regenerative therapy compared to other indications.

The route of administration should also not be overlooked, as many studies have shown that MSCs injected into the venous system often become trapped in the microvasculature of the lungs (Leibacher & Henschler 2016). Compared to systemic arterial or venous injection of stem cell therapies, studies have found that direct MSC injection (in this case into the renal artery in a renal model of IRI) has the most profound effect on the injured organ and also required much lower doses (Cai et al. 2014). Direct intraparenchymal or intra/subcapsular routes have also been utilized in stem cell renal IRI research as direct renal artery injection can be associated with renal microvasculature occlusion at higher therapeutic doses. The nature of solid organ transplantation, however, may allow beneficial flexibility in the choice of administration route since the organ's vessels are at least transiently accessible. Lam et al. also tested the topical route of application to the liver in a rat hepatic IRI model. with promising effects (Lam et al. 2017). Lastly, the clinical setting of administration may also be important. MSCs may be altered by commonly used anaesthetic agents as highlighted in a recent rat model of hepatic IRI. Intravenously administered dexmedetomidine and midazolam enhanced the protective effects of MSC during liver IRI more effectively than propofol by binding to MSC receptors and regulating a downstream paracrine effect (J. Feng et al. 2018). Collectively, this is a reminder that other manipulations during organ repair could also have an opposing effect on MSC regenerative properties, thus reducing their potential benefits.

In the future, the increasing accessibility of ex vivo perfusion technologies may provide an ideal setting to address the many remaining questions around stem cell therapy's role in preventing peri-transplant injury and provide the bridge to translating its potential into real patient benefit.

1.8 INTRODUCING STEM CELL THERAPY TO CLINICAL PRACTISE

For over six years, our group have been studying the application of stem cells in renal IRI, with animal models at the core of our research. Moving forward towards clinical translation, we envisage the use of adipose derived stromal vascular fraction (ADSVF) as our choice source of stem cells. In brief, ADSVF is the heterogenous cell population that persists when the adipocytes are removed from adipose tissue. Within this heterogenous population are the ASC. ADSVF possess favourable therapeutic stem cell criteria: safe, effective, ethically acceptable, easily sourced and require minimal preparation. For clinical translation we aim to focus efforts particularly on uncultured ADSVF administered via the renal artery at the time of transplantation for the following reasons:

1.   Adipose tissue is easily accessible throughout the body. At the time of transplantation, subcutaneous adipose tissue can be easily obtained within minutes after making the skin incision. There is also easily accessible preperitoneal adipose tissue during the traditional right iliac fossa approach of a kidney transplant procedure. Also, the kidney graft arrives at the implanting centre wrapped in donor adipose tissue.

2.   The whole adipose derived stromal vascular fraction is key to minimal preparation. ADSVF can be obtained within an hour from a batch of adipose tissue. ADSVF is discussed in detail in chapter three but in essence this is what remains from adipose tissue once all the adipocytes and connective tissue are removed. This heterogeneous solution, among other cells, contains the adipose-derived stem cells adipose derived mesenchymal stromal cells. In some studies, the ADSVF is more effective than isolated stem cells at ameliorating IRI. With no culturing, isolation of stem cells or pre-treatment/conditioning, the ADSVF is ready immediately.

3.   As the adipose tissue is coming from the recipient or the graft, there will be no additional immunogenicity issues. In addition, ADSVF do not express HLA-DR. Using the recipients own adipose tissue reduces regulatory criteria.

4. Culturing, gene modification and pre-conditioning donor stem cells could all drastically alter the outcome and would require extensive safety studies in addition to a preparation room or facility which would further complicate implementation. Therefore, we focus on fresh uncultured ADSVF that can be extracted from the adipose tissue in the same theatre suite as the transplant operation or perfusion rig.

4. Administering the ADSVF via the renal artery reduces systemic interactions and ensures maximum delivery to the kidney. In addition, the renal artery is easily accessible at the time of transplantation. They could also be administered via the renal artery while on an ex vivo organ perfusion rig.

5. Clinical trials using ADSVF have not identified any significant contraindications. However, the mechanism of action of ADSVF administered via the renal artery to treat IRI has not been studied – although it is likely to be like other routes of administration of stem cells.

In 2020 Thompson et al. performed the first administration of cultured bone marrow-derived adult stem cells into a human kidney on an ex vivo kidney perfusion rig. The kidneys that received the stem cells demonstrated improved urine output, reduced injury markers and reduced microvascular injury (Thompson et al. 2020). Before we can replicate a similar model on human kidneys using uncultured ADSVF, further research is required to add to the safety profile and understanding of ADSVF especially once administered via the renal artery.

1.9 HYPOTHESES

Uncultured adipose derived stromal vascular fraction demonstrates favourable characteristics which make them an effective therapy in ameliorating renal transplant induced ischaemia reperfusion injury.

1.10 AIMS

The main emphasis of this thesis is to bridge the void between promising preclinical models and utilization in the clinical setting; specifically, administration of uncultured ADSVF via the renal artery around the time of transplantation.

We need to establish whether there are significant differences in rodent ADSVF, which has shown promise in animal models, and human peri-renal or subcutaneous ADSVF, which will be the likely sources in clinical translation. Furthermore, most current studies look at cultured stem cells as opposed to the whole fresh uncultured ADSVF in which the stem cells reside. Therefore prior to clinical translation we need to determine the biodistribution and potential mechanism of action of uncultured ADSVF administered via the renal artery into an environment of renal IRI.

To achieve this, I focussed on three main aims:

1. To further characterise the ADSVF and demonstrate similarities between rat ADSVF, used in the animal models, and human ADSVF, which will be used in the clinical setting.
2. To demonstrate the biodistribution of uncultured ADSVF when it is administered via the renal artery
3. To identify some of the mechanisms of action of the fresh uncultured ADSVF in ameliorating IRI

In addition, I aim to develop a novel animal model which more closely mimics the transplant recipient. This will facilitate accurate investigation of the ADSVF when accomplishing the proposed aims.

This thesis is split into five main chapters. Chapter two details all methods used. Chapter three aims to characterise the ADSVF obtained from inguinal and peri-renal adipose tissue. Chapter four describes a novel rat model of renal transplant related IRI to accurately assess the ADSVF. Chapter five demonstrates the biodistribution of ADSVF when administered via the renal artery, and chapter six attempts to delineate some of the mechanisms of actions of ADSVF.

The effectiveness of ADSVF in ameliorating IRI and improving kidney function has previously been demonstrated by our group and others and is therefore not a focus of this research. The final chapter aims to summarise all the findings and bring together a proposal for moving forward and predict where the field of transplantation is heading.

In 2019 a proportion of this introduction was published in Current Transplantation Reports. Permission has been granted by the Editor, Dr Lockhart, for it to be included in this thesis and be available in Glasgow University's online theses repository.

CHAPTER 2:
GENERAL MATERIAL AND METHODS

The materials and methods described apply to all results chapters. The animal model of renal IRI used is described separately and in detail in chapter 4. Additional materials and methods specific to individual chapters are detailed within that chapter

2.1 ANIMAL HOUSING AND HUSBANDRY

Fischer 344 rat strain was used for all surgical experiments reported in this thesis. Rats were either purchased from Charles River (Kent, United Kingdom) or bred in the Joint Research Facility at the University of Glasgow. Rats transferred from Charles River were housed for at least two weeks before any procedure. All rats were a minimum of 12 weeks old at the time of the first procedure. Rodents were house in plastic metal cages with a maximum of two adult rats per cage. They were fed a standard diet of rodent chow and had free access to tap water. Room temperatures were kept a 22°C +/- 2°C, humidity 55%+/-5% and light-dark-cycling of 12/12 hours.

2.2 RETRIEVAL OF RAT ADIPOSE TISSUE

All rat adipose tissue was obtained from Fischer 344 adult rats. Rats were terminated using CO_2. Once terminated, the rats were immediately transferred to a sterilised operating bay. Chlorhexidine was used to sterilise thoracic region, abdominal midline and both groin regions. Once dry, blood was taken via a cardiac puncture. An incision was made over both inguinal regions. Using toothed forceps to hold skin edge, scissor dissection of the inguinal fat pad was performed taking care not to take any connective tissue off the skin or the underlying muscle tissue. The inguinal lymph nodes were not dissected out. Care was taken to avoid transecting blood vessels as this would contaminate the fat tissue. Once the inguinal fat pad was dissected out, it was placed in a tube with cold phosphate-buffered saline (PBS), weighed and then placed on ice. The same technique was used for the inguinal fat pad on the contralateral side. A midline laparotomy incision was then made, and the peritoneum opened. The perirenal fats were excised from both kidneys and put in a separate tube with PBS. The tube was weighed, labelled, and put on ice.

Adipose tissue was then immediately taken for isolation of the ADSVF. Blood taken was spun down for eight minutes (800x g at 4ºC) and the serum extracted and stored in a-20ºC freezer. The rat was then placed in two cadaveric sealed bags and disposed of as per animal unit protocol.

2.3 RETRIEVAL OF HUMAN ADIPOSE TISSUE

Human peri-renal adipose tissue was obtained from patients undergoing hand-assisted donor nephrectomy at the Queen Elizabeth University Hospital of Glasgow, United Kingdom. Once retrieved, the kidney was transferred to a sterile bench in theatre for preparation for implantation. Peri-renal adipose tissue was removed from the kidney by the operating surgeon and placed in a sterile tube containing cold PBS then placed on ice. The sample was then immediately taken to the onsite Greater Glasgow and Clyde biorepository unit. An arrangement was made with the biorepository department, through the appropriate regulatory channels and approval, for this adipose tissue to be returned for research. Returned samples were anonymised and available for collection almost immediately. Samples were then transported on ice to our laboratory at the University of Glasgow for processing (see section below).

2.4 ISOLATION OF ADIPOSE DERIVED STROMAL VASCULAR FRACTION

Adipose tissue is excised from either the inguinal, peri renal or subcutaneous region of Fischer 344 rats or humans as described above. The adipose tissue is homogenised with scissors. Homogenised adipose tissue is processed with Celase and Intravase (Cytori Therapeutics Inc., San Diego, USA) and then filtered to separate the ADSVF from the rest of the adipose tissue. A detailed SOP is provided in Appendix 1.

2.5 QUANTIFICATION, STORAGE AND PREPARATION OF ADSVF FOR ANALYSIS

ADSVF cells were counted using the ChemoMetec NC-100 Mamillian NucleoCounter (Allerod, Denmark, Product number 900-0004) and its associated Reagent A100 (lysis buffer) & Reagent B (stabilizing buffer) and Nucleocounter cassettes.

Once counted, the ADSVF was prepared for storage if they were not going to be used immediately. For storage they were suspended with Dulbecco's Modified Eagle Medium (DMEM) (Life Technologies Corporation. Paisley, UK), Dimethyl sulfoxide (Fisher Scientific UK Ltd. Loughborough, UK) and rat serum. They were then stored in liquid nitrogen until required.

When required the ADSVF were thawed from the liquid nitrogen, washed, and resuspended with PBS. They were counted prior to administration or interrogation.

A detailed SOP of quantification, storage and preparation is provided in Appendix 2.

2.6 RODENT ORGAN RETRIEVAL AND PROCESSING AFTER IRI

Carbon dioxide euthanasia was performed on the rats at the desired time points post-IRI surgery (1 hour, 24 hours, 48hours and one week). Once the rat was confirmed dead, cardiac puncture was performed to collect a blood sample. The serous fraction of the blood was stored in minus 20°C freezer and used in microparticle measurement, which is described in chapter 5.3.6.

Immediately after cardiac puncture, the incision sites were prepped with chlorhexidine. A midline laparotomy and bilateral thoracotomy were performed, and in the following order, the organs are removed: left kidney, right kidney, spleen, liver, lungs, heart, and brain.

Depending on the planned investigation for each organ it was processed accordingly and described within each results chapter.

CHAPTER 3:
CHARACTERISATION OF ADIPOSE DERIVED STROMAL VASCULAR FRACTION

3.1 INTRODUCTION

Adipose Tissue as a Source of Stromal and Stem Cells

ASCs have several characteristics which make them stand out. Firstly, adipose tissue is easily accessible and abundant when compared to other sources of stem cells. Tissue can be obtained at the time of open surgery or from liposuction procedures which can be performed under local anaesthetic. From the same weight of tissue, there are tenfold as many mesenchymal stem cells in adipose tissue than bone marrow. Plus, humans have considerably more adipose tissue than bone marrow (X. Zhu et al. 2012). Compared to embryonic stem cells, adult stem cells also evade much of the ethical issues around retrieval and subsequent research.

The ADSVF, which contains the ASC, can be extracted from the adipose tissue in less than an hour. Currently, there are several different techniques in use for extracting the ADSVF. Through a process of enzymatic digestion and centrifugation (see chapter 2 and Appendix 1), adipocytes and connective tissue are removed from the adipose tissue to leave a solution termed the ADSVF. Even after the ADSVF has been extracted from the adipose tissue, cellular viability remains high. This solution consists of a heterogeneous cell population. MSCs can then be isolated from the ADSVF, which are termed ASC (Fig. 3.1). If any subpopulation of the ASC can stringently be shown to have more specific stem cell-like characteristics (as described above), then they could be termed stem cells, or in this case, adipose-derived stem cells (Horwitz et al. 2005).

With adipose tissue relatively easy to access, quick and straightforward extraction of their ADSVF, a high return of ASC and surrounded by less ethical controversy, they make an attractive source of stromal/stem cells. Unlike most other stromal or stem cell populations, they have the most potential for extraction and administration in the clinical setting.
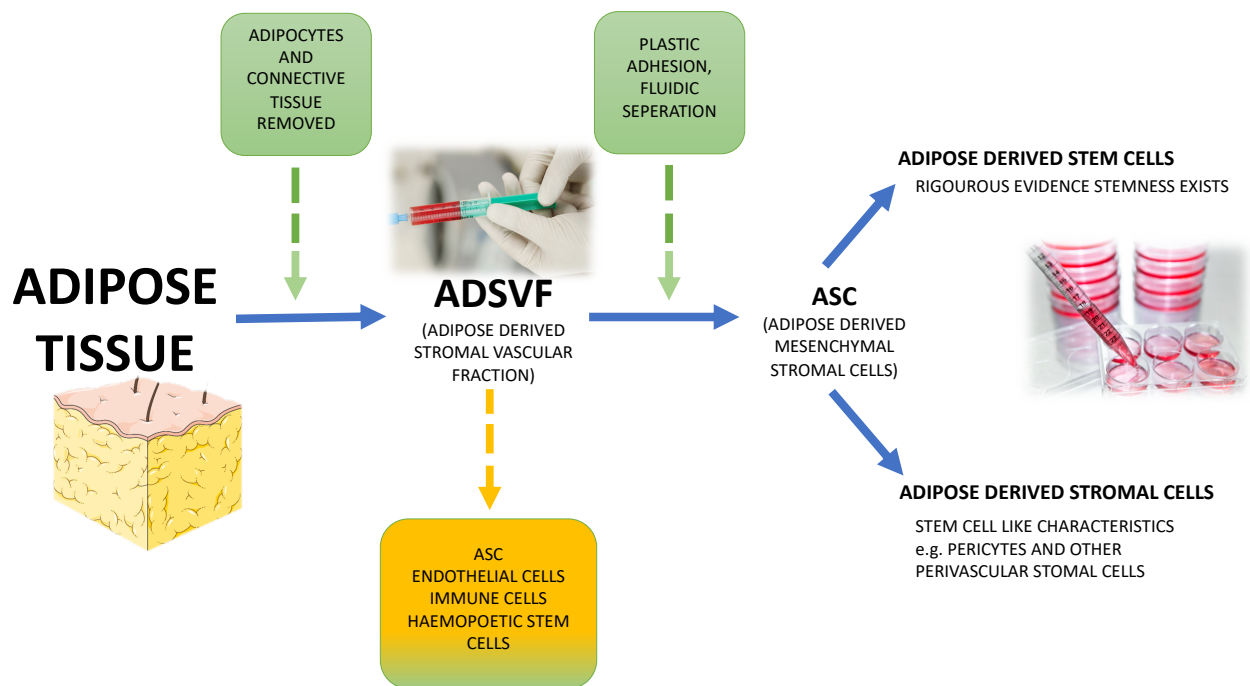
Figure 3.1 The heterogenous subpopulations extracted from adipose tissue. Adipose tissue can be obtained from many regions of the body. After removing the connective tissue and adipocytes from the adipose tissue you are left with the ADSVF. ADSVF consists of multiple cell populations. Through further preparation more of these subpopulations can be extracted - in particular, the ASC.

Adipose Derived Stem and Stromal Cells

Another substantial advantage of ASC (compared to an embryonic stem cell line), is the absence of (MHC) HLA-class II antigens on the cell surface. Therefore, they can evade the host immune surveillance and be used for xenogenic transplantation (Lin et al. 2012). Also, human ASC have been shown to have a lower susceptibility to natural killer cells compared to BM MSC cells, further supporting the consensus that ASC can evade the host immune system (delaRosa et al. 2012). Initially, adipose-derived stem cells demonstrated mesodermal multipotency, but they have since been expanded into ectodermal and endodermal lineages and therefore potentially possess trigerm lineage and pluripotency capacity like embryonic stem cells(Zuk 2013). Although in vitro differentiation into the three germ layers has been demonstrated, differentiation into different germ lineage and being functional when they are implanted in vivo has not been

confidently demonstrated unlike induced adipose-derived stem cells (Harn et al. 2012). Conflicting evidence also exists if adipose-derived stem cells express embryonic stem cell-like pluripotent markers (A. S. Lee et al. 2011; Tat et al. 2010; Gu et al. 2012). Induced pluripotent adipose stem cells do, however, carry the burden of an increased risk of teratoma formation.

Other (minor and disputed) differences between BM MSC and ASC exist not just in their immunophenotype but in their ability to develop into certain lineages. ASC have less robust chondrogenic and osteogenic properties, although this may be secondary to the microenvironment where these cells reside (Choi et al. 2012) (Im et al. 2005). It should also be noted that mesenchymal heterogenicity may exist not only between different tissues but even within the same tissues (Hardy et al. 2017). CD34+ subpopulations of adventitial MSC and CD34- pericyte MSC are both found to reside in adipose tissue. Differences are also seen in their functional ability, such as CD34-ve MSCs greater angiogenic influence. (Esteves et al. 2017).

With much of the research, especially when adult stem cell research was in its infancy, it is often not entirely clear if the author is referring to ASC or specifically adipose-derived stem cells. Again, like bone marrow stromal fraction, the ADSVF consists of cells which show multipotency but do not meet the exact criteria to be classified as a stem cell. For that reason, the International Federation of Adipose Therapeutics and Science and the International Society for Cellular Therapy have set out criteria that the population should be referred to as adipose-derived stromal cells (ASC). The umbrella term covers all the cell types with stem cell-like characteristics, including adipose-derived stem cells themselves (Bourin et al. 2013). Adipose-derived stem cells should only be used if the cells have stringently been demonstrated to be stem cells.

Adipose Derived Stromal Vascular Fraction

For many proposes the ADSVF may be more advantageous than isolated ASC. Other cells within the ADSVF other than ASC include immune cells and endothelial cells. Studies comparing ASC and ADSVF in myocardial infarction and ischaemia reperfusion injury found the therapeutic effect, fibrosis formation and expression of favourable markers (like anti-inflammation, anti-apoptosis, angiogenesis) to be superior in the stromal vascular fraction group (Sheu et al. 2019; Zhou et al. 2017). Using fresh ADSVF

versus ASC has a significant advantage in that it does not need to go through further isolation or culturing and can be ready for administration within one hour of retrieving the adipose tissue. With minimal expertise, ADSVF can be prepared quickly for clinical use onsite. Using requires more technically demanding isolation and likely culturing, which would take weeks and have the added risk of human and microbial contamination. Pre-prepared ASC that are thawed at the time of administration is also an attractive option but again would be more complicated with storage, transportation and preparation factors compared to using fresh uncultured ADSVF. Also, depending on the culturing environment, there is the risk of unintentionally immortalising the ASC. Although some groups intentionally attempt to immortalise the cells in order to prolong their life span and therapeutic potential (Balducci et al. 2014).

Details on how we envisage the use of the regenerative potential of adipose tissue is described in chapter one. In brief, the fresh, uncultured ADSVF isolated from either donor peri-renal adipose tissue or recipient adipose tissue is administered via the renal artery at the time of transplantation. For this reason, we are focussing our research on the ADSVF.

Our research uses an animal model of renal ischaemia reperfusion injury (IRI) to investigate the therapeutic effects of ADSVF on Fischer 344 rats. The animal model utilises ADSVF from the inguinal and peri-renal adipose tissue of Fischer 344 rats; therefore, we need first to confirm we have a viable cell population after the extraction of the ADSVF from the adipose tissue. Secondly, we need to characterise the ADSVF to establish if its phenotype is in keeping with current evidence and is like the ADSVF from human adipose tissue. To help guide future mechanistic studies of ADSVF, it will also be valuable to determine their gene expression profile.

In keeping with the positions of the International Federation of Adipose Therapeutics and Science and the International Society for Cellular Therapy, the heterogeneous collection of cells obtained from adipose tissue will be referred to as ADSVF. In the literature, it has been referred to as processed lipoaspirate and adipose-derived regenerative cells. At the time of writing, those nomenclatures were perhaps not inappropriate, but as our knowledge has grown, so has our need and ability to classify better and sub-classify. Likewise, cells extracted from the ADSVF, which are stem cells or demonstrate stem cell-like characteristics will collectively be termed ASC. In the literature, they have also been referred to as adipose-derived adult stem cells, adipose-derived mesenchymal stem cells, adipose-derived regenerative cells (ADRC) and processed lipoaspirate cells.

3.2 HYPOTHESIS

1. ADSVF from inguinal and peri-renal adipose tissue of Fischer 344 rats will consist of a heterogeneous population of viable cells including stem/stromal cells

2. ADSVF from human peri-renal adipose tissue will consist of a heterogeneous population of viable cells including stem/stromal cells

3. Adipose SVF from inguinal adipose tissue of Fischer 344 rats will express markers of regeneration and anti-inflammation.

3.3 METHODS

3.3.1 ANIMAL HOUSING AND HUSBANDRY

Animal housing and husbandry was standard throughout all procedures and is described in chapter 2.1.

3.3.2 RETRIEVAL OF RAT ADIPOSE TISSUE

Retrieval of rat adipose tissue was standard throughout all procedures and is described in chapter 2.2.

3.3.3 RETRIEVAL OF HUMAN ADIPOSE TISSUE

Retrieval of rat adipose tissue was standard throughout all procedures and is described in chapter 2.3.

3.3.4 ISOLATION OF ADIPOSE DERIVED STROMAL VASCULAR FRACTION

Isolation of adipose derived stromal vascular fraction was standard throughout all procedures and is described in chapter 2.4.

3.3.5 QUANTIFICATION, STORAGE AND PREPARATION OF SVF FOR ANALYSIS

Quantification, storage, and preparation of ADSVF for analysis was standard throughout all procedures and is described in chapter 2.5.

3.3.6 MAGNETIC BEAD SEPERATION

Quantification and preparation of ADSVF for administration was conducted in standard fashion, as described above. Magnetic bead separation was used to separate the cell population into leukocyte (CD45+) and non-leukocyte (CD45-) fractions by antibody based magnetic bead separation protocol (Miltenyi Biotech, UK). Fractions were washed in buffer before use.

3.3.7 FLOW CYTOMETRY ANALYSIS

Cells were incubated with the rat 2.4G2 Fcyll blocker (BD Biosciences, San Jose, CA) and surface markers for 60 minutes. Cells were then fixed in 4% solution and resuspended in 2% albumin (PAN-Biotech, Aidenbach, Germany) in PBS. For intracellular staining, cells were treated with a permeabilization buffer (eBioscience, San Diego, CA). Antibodies used for staining are listed in Table 3.1. Leukocytes were classified as CD45+; t-cells as CD3+: CD45+ CD3+; killer t-cells as CD45+ CD3+CD8+; mesenchymal stem cells as CD45-CD90+CD34-; pericyte-like cells as CD146+: CD45- CD146+; macrophages as CD45+ CD11b+ CD11c-; cytotoxic T-cells as CD45+ CD3e+ CD8+; helper T-cells as CD45+ CD3e+ CD4+; and conventional dendritic cells (DCs) as CD45+, CD1b+, CD11c+. Fluorescence was measured using a Fortessa flow cytometry (BD Biosciences). Each sample contained at least 200,000 viable cells using FSC x SSC gating and viability (e780) negative. Typical gating scheme is shown in the results section. Gating was determined by both single-stained control and fluorescence minus one control (Table 3.1). FlowJo software version 10 (Ashland, OR) was used for data analysis.

Antigen	Clone	Fluorochrome
CD90	5E10.	FITC
CD3	SK7	PerCP-Cy55
CD11c	S-HCL-3	PE
CD11b	ICRF44	BD Horizon PE-CF594
CD146	P1H12	PE-Cy7
CD73	AD2	APC
CD34	581	Alexa Fluor 700
CD105	266	BD Horizon BV421
CD14	MoP9	BD Horizon V500
CD45	HI30	BD Horizon BV605
CD31	WM59	BD Horizon BV650
CD8	RPA-T8	BD Horizon BV711
CD19	SJ25C1	BD Horizon BV786
CD4	SK3	BD Horizon BUV395

Table 3.1 Rat flow cytometric markers used to assess ADSVF

3.3.8 SINGLE-CELL RNA-SEQUENCING PREPARATION AND ANALYSIS

A frozen aliquot of pooled ADSVF was thawed and acclimated in PBS with 10% rat serum. Cells were stained with DAPI and flow assisted cytometry sorted by DAPI exclusion (removing dead cells). Ten thousand cells were loaded on a droplet-based Chromium Next GEM Single Cell 3' v3 kit (10X Genomics) and cDNA was low depth pair-end sequenced on a NextSeq500 (Illumina). Demultiplexing and alignment to rat genome (build Rnor_6.0.97) was performed on Cell Ranger and STAR (Glasgow Polyomics) before downstream analysis in R using the Seurat method. Since clustering identity can be inferred as a property of cell number sequenced and depth, gene transcript signatures were utilized for unbiased clustering and cell identification, but not function due to the low depth. Cell cluster transcript/read averages and comprehensive signature genes of each cluster provided in figure 2.5. Data files are accessible at NCBI GEO database (GSE139318). *ADSVF preparation for single-cell sequencing and analysis of single-cell sequencing data performed by scientist Dr R Lathan who is a member of our research group.*

3.3.9 QUANTITATIVE REAL-TIME POLYMERASE CHAIN REACTION (PCR) ARRAY

Total RNA was isolated from samples using QIAzol® RNA Lysis reagent (QIAGEN, Hilden, Germany). Centrifugation and chloroform were used to separate the aqueous and organic phases. The RNA was recovered from the aqueous phase by precipitation with isopropyl alcohol and resuspended in nuclease-free water. RNA was counted using Nanodrop (Nanodrop 2000, Thermoscientific), and RNA was purified by removing DNA with DNAs I, Amplification Grade (ThermoFischer/Invitrogen). A Nanodrop Spectrophotometer (Thermo scientific) was used to ensure the quality of the RNA and a 260/280 ratio of around 2 was used as our threshold of acceptably pure RNA. Reverse transcriptase (ThermoFischer/Invitrogen) was used, following the protocol to create complement DNA (cDNA) from the RNA. The cDNA and fast master mix (ThermoFischer) were then prepared for the Taqman Array card and added to the custom Taqman array plates as per instructions. The custom made Taqman array plates assay candidate genes and housekeeping controls (Table 3.2) and was ran on a QuantStudio PCR cycler (Applied Biosystems, Foster City, CA, USA). Relative Ct levels were normalised by housekeeping controls (average of the same three housekeeping genes) and represented as dCt. Data are represented as mean ± SEM. Differences in average means between two groups determined by Mann-Whitney U test, differences between three groups by One-way ANOVA. $*p<0.05$, $**p < 0.01$.

Protein of interest	Representative gene	Gene Symbol
Markers of kidney injury		
IL-18	interleukin 18	Il18
Atxn3	ataxin 3	Atxn3
kidney injury molecule-1 (KIM-1)	hepatitis A virus cellular receptor 1	Havcr1
neutrophil gelatinase-associated lipocalin (NGAL)	lipocalin 2	Lcn2
B2-microglobulin (B2M)	beta-2 microglobulin	B2m
retinol binding protein (RBP)	retinol binding protein 7, cellular	Rbp7
HIF-1a	hypoxia-inducible factor 1, alpha subunit	Hif1a
HO-1	heme oxygenase (decycling) 1	Hmox1
Nox1	NADPH oxidase 1	Nox1
Nox4	NADPH oxidase 4	Nox4
Slc7a11	solute carrier family 7 (anionic amino acid transporter light cha	Slc7a11
Immune Regulation		
IL-4	interleukin 4	Il4
IL-10	interleukin 10	Il10
TGFb	transforming growth factor, beta 1	Tgfb1
IL-1a	interleukin 1 alpha	Il1a
IL-1b	interleukin 1 beta	Il1b
IFNg	interferon gamma	Ifng
IL-6	interleukin 6	Il6
CCL2	chemokine (C-C motif) ligand 2	Ccl2
CXCL2	chemokine (C-X-C motif) ligand 2	Cxcl2
G-CSF	colony stimulating factor 3 (granulocyte)	Csf3
GM-CSF	colony stimulating factor 2 (granulocyte-macrophage)	Csf2
KC	chemokine (C-X-C motif) ligand 1	Cxcl1
MIP3a	chemokine (C-C motif) ligand 20	Ccl20
CTL-A4	cytotoxic T-lymphocyte-associated protein 4	Ctla4
indoleamine 2,3-dioxygenase	indoleamine 2,3-dioxygenase 1	Ido1
Markers of growth and repair		
EPO-1	erythropoietin	Epo
FGF-2	fibroblast growth factor 2	Fgf2
IGF-1	insulin-like growth factor 1	Igf1
VEGF	vascular endothelial growth factor A	Vegfa
HGF	hepatocyte growth factor	Hgf
Met receptor	MET proto-oncogene, receptor tyrosine kinase	Met
SDF-1	chemokine (C-X-C motif) ligand 12	Cxcl12
LIF	leukemia inhibitory factor	Lif
EGF	epidermal growth factor	Egf
TIMP-1	TIMP metallopeptidase inhibitor 1	Timp1
MMP-2	matrix metallopeptidase 2	Mmp2
adiponectin	adiponectin, C1Q and collagen domain containing	Adipoq
ADAM-19	ADAM metallopeptidase domain 19	Adam19
Col4a1	collagen, type IV, alpha 1	Col4a1
Collagen I	collagen, type I, alpha 2	Col1a2
Wnt5a	wingless-type MMTV integration site family, member 5A	Wnt5a
Tie-2	TEK tyrosine kinase, endothelial	Tek
Ang2	angiogenin, ribonuclease A family, member 2	Ang
RT-PCR housekeeping gene controls		
Actb	Actin beta	Actb
Ring1	ring finger protein 1	Ring1
Mapk14	mitogen activated protein kinase 14	Mapk14

Table 3.2 RNA taqman array probes

Statistics. A 2-way student's t-test was carried out to determine the differences in the mean average for sample sizes >5 of equal variance. Mann-Whitney U test was used to analyse smaller sample sizes. One-way ANOVA and a Tukey post hoc test was used to detect

differences between the means of the three groups. Analyses was performed with Prism 6.02 (GraphPad, San Diego, CA). Mean and standard error of mean (SEM) are displayed. Significance was considered for p values <0.05 (*) but included p values <0.01 (**), and <0.001 (***) as indicated.

3.4 RESULTS

3.4.1 FLOW CYTOMETRIC PROFILING AND SINGLE CELL SEQUENCING OF ADSVF

Adipose tissue was collected from the inguinal region and peri-renal region of Fischer 344 rats. Frozen and thawed ADSVF were used in experimentation since fresh and frozen ASC have been shown to maintain comparable phenotypes (Z. Feng et al. 2010). Peri-renal adipose tissue was also obtained from healthy human living kidney donors. There was limited availability of subcutaneous human fat. No red blood cell lysis was used on the ADSVF before flow cytometric analysis. This was deemed unnecessary as the adipose tissue was minimally contaminated with blood vessels. Also, as cells are destroyed when lysis buffer is used, it was felt not worth the potential advantages. Being small, the red blood cells were gated out as debris.

A high level of heterogenicity was seen in flow cytometric profiling of ADSVF from all sources investigated. Cell types identified include leukocytes (defined as CD45+), in particular CD8+ T cells (CD45+CD8+) and CD3+ T cells (CD45+CD3+), mesenchymal stem cell-like cells (CD45-CD90+CD34-) and pericyte like cells (CD45-CD146+). Further analysis of rat inguinal ADSVF established evidence of other leukocytes such as macrophages and dendritic cells (Fig. 3.2).

Cell viability remained high from all sources. Rat peri-renal and inguinal and human peri-renal viability was around 60% after going through retrieval, extraction from adipose tissue, freezing in liquid nitrogen, thawing and then processing for analysis (Fig. 3.3 and 3.4).

Mesenchymal stem cell-like cells (CD45-CD90+CD34-) were found in ADSVF from all sources. Rat inguinal fat contained the highest percentage followed by rat peri-renal (mean 22.71%, SEM +/- 3.45% and 10.39% SEM +/- 3.95%) then human peri-renal (Fig. 3.3 and 3.4). Human peri-renal and inguinal fat appear to have the same numbers of mesenchymal stem cell-like cells, but we only have an n of 1 for human inguinal fat. Rat inguinal ADSVF single-cell sequencing confirmed transcript signatures representative of mesenchymal stem cells (Fig. 3.5).

Rat inguinal adipose tissue appear to have a lower composition of pericyte like cells, identified as CD45-CD146+, compared to rat peri-renal adipose tissue (mean inguinal = 3.21%, perirenal = 15.02%, SEM +/- 1.46 and 3.77 % respectively, **p=0.0047). From the 1 sample of human inguinal adipose tissue tested the opposite is the case with human inguinal fat having more pericyte like cells compared to the human peri-renal fat. Their concentration is likely determined by the location in which the subcutaneous fat is retrieved, with adipose tissue with more capillaries running through it containing more pericytes. Either way, a pericyte population is likely to be present.

Rat inguinal tissue contains a significantly higher percentage of leukocytes, as defined as CD45+cells, compared to rat peri-renal fat (mean inguinal = 72.35%, perirenal = 16.21%, SEM +/- 6.89 and 4.70 respectively, **p=0.0026). This may be due to the presence of lymph nodes within the inguinal tissue (Fig. 3.3). Human and rat peri-renal tissue had similar levels of CD45+ cells of around 20%. Within the leukocytes, there was a robust T cell population. Flow analysis suggests the presence of CD8+ T cell and CD3+ T cells in both humans and rats. Single-cell sequencing confirms the presence of a strong T cell population, in particular a CD4+ T cell population (Fig. 3.5). The inguinal depot had a significantly greater percentage of killer T cells (CD3+CD8+) compared to the perirenal depot (34.05%, SEM +/- 3.50% versus 11.33% SEM +/- 3.20%). Despite human and rats having similar levels of leukocytes, human fat reservoirs have a significantly higher percentage of CD3+ T cells and CD8+ T cells (Fig. 3.4).

Single-cell sequencing added a few new cell populations not tested for by flow cytometry with the majority being immune-related. Many of the leukocytes are B lymphocytes/lymphoblasts with NK cells and macrophages decently represented. Interestingly there was quite a high proportion of T regulator cells which may play a significant role in the therapeutic potential of ADSVF. The rest of the population is largely as expected and confirmed the heterogeneous nature of ADSVF.
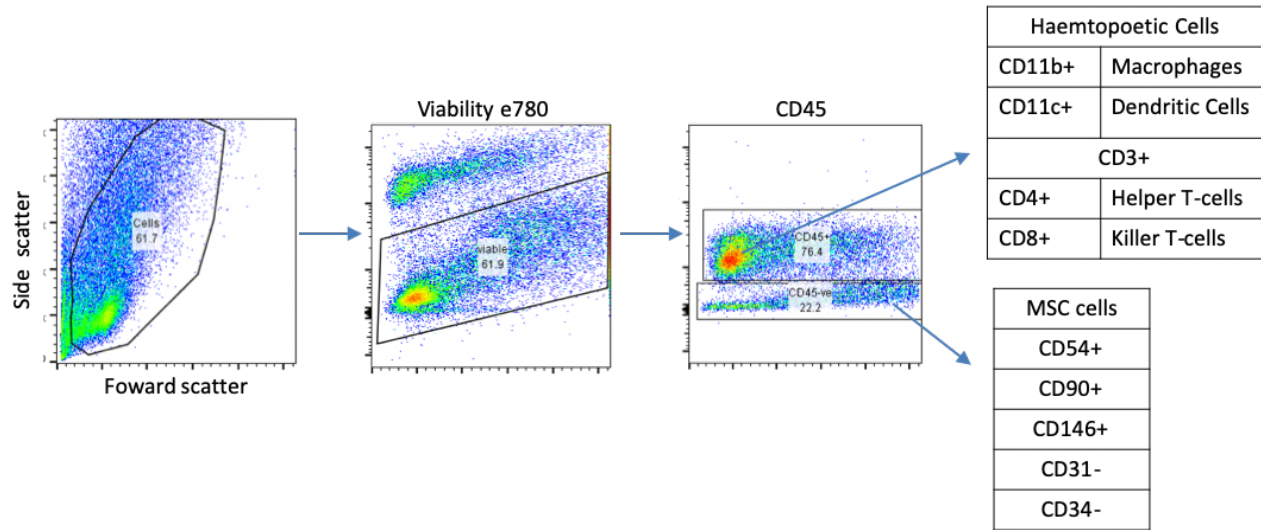
Figure 3.2 Gating strategy for cell subsets representative of the ADSVF from rat inguinal tissue. Typical gating scheme used to identify immune and stromal cell populations. Example of leukocytes (CD45+) that were positive taken from adipose tissue of a F344 rat. Each sample consisted of at least 200,000 viable cells (FSC × SSC gated and viability e780 negative). Gating was determined by both single-stained control, and fluorescence minus one control.
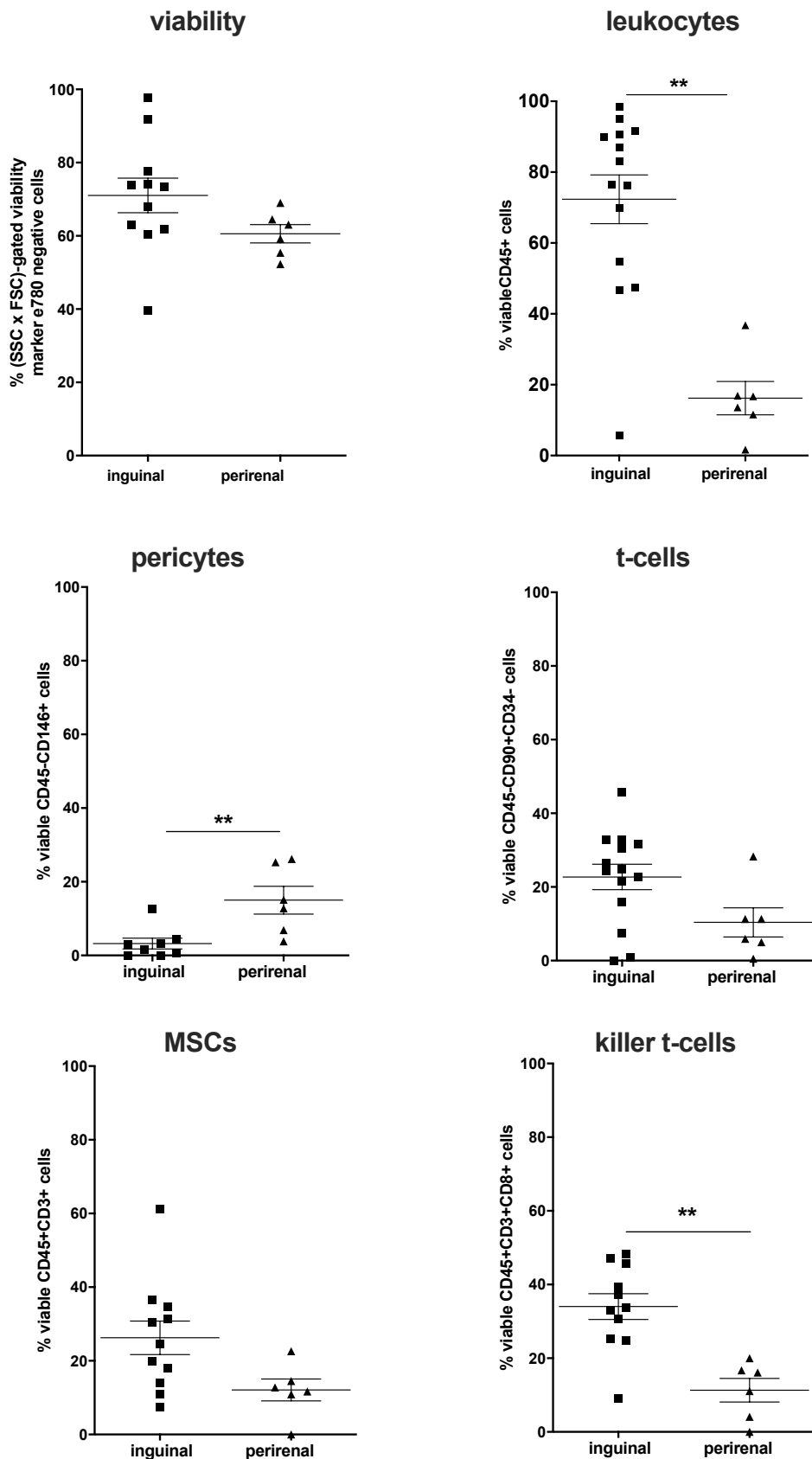
Figure 3.3 ADSVF from inguinal and perirenal adipose tissue have diverse and similar cell subsets but vary in the proportion of some of the cell subsets. Flow cytometric profiling of ADSVF extracted from rat inguinal and peri-renal adipose tissue was performed. A diverse cell subset was seen in ADSVF from both inguinal (n=14) and peri-renal (n=6)

adipose tissue. Profiling of the ADSVF leukocytes (CD45+), t-cells (CD3+: CD45+ CD3+), killer t-cells (CD45+ CD3+ CD8+), mesenchymal stem cells (CD45-CD90+CD34-) and pericyte-like cells (CD146+: CD45-, CD146+) confirms diverse cell subsets. Over 60% of cells remain viable in ADSVF from both regions. Both regions contained similar proportions of MSCs. Inguinal ADSVF consisted of a higher percentage of leukocytes and killer T cells. Significance was considered for p values <0.05 (*) but included p values <0.01 (**), and <0.001 (***) as indicated.
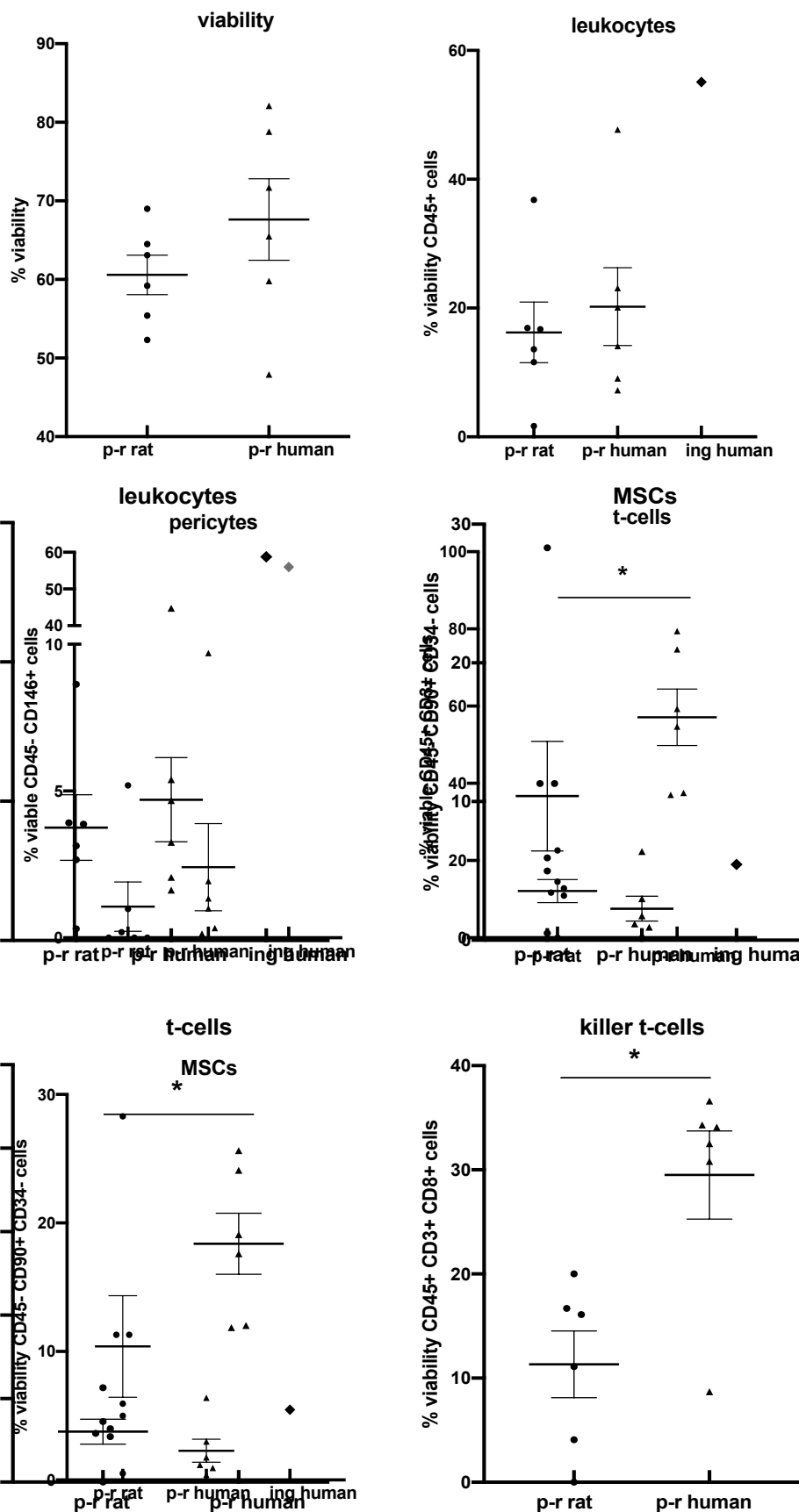
Figure 3.4 ADSVF from human peri-renal and rat peri-renal adipose tissue have diverse and similar cell subsets but vary in the proportion of some of the cell subsets. Flow cytometric profiling of ADSVF extracted from rat peri-renal, human peri-renal and human inguinal adipose tissue was performed. A diverse cell subset was seen in ADSVF

84

from rat peri-renal (n=6), human peri-renal (n=6) and human inguinal (n=1) adipose tissue. Profiling of the ADSVF leukocytes (CD45+), t-cells (CD3+: CD45+ CD3+), killer t-cells (CD45+ CD3+ CD8+), mesenchymal stem cells (CD45-CD90+CD34-) and pericyte-like cells (CD146+: CD45-, CD146+) confirms diverse cell subsets. Over 60% of cells remain viable from both human and rat peri-renal ADSVF. There is a significantly higher proportion of t-cells and killer t-cells in the human peri-renal ADSVF. Significance was considered for p values <0.05 (*) but included p values <0.01 (**), and <0.001 (***) as indicated.
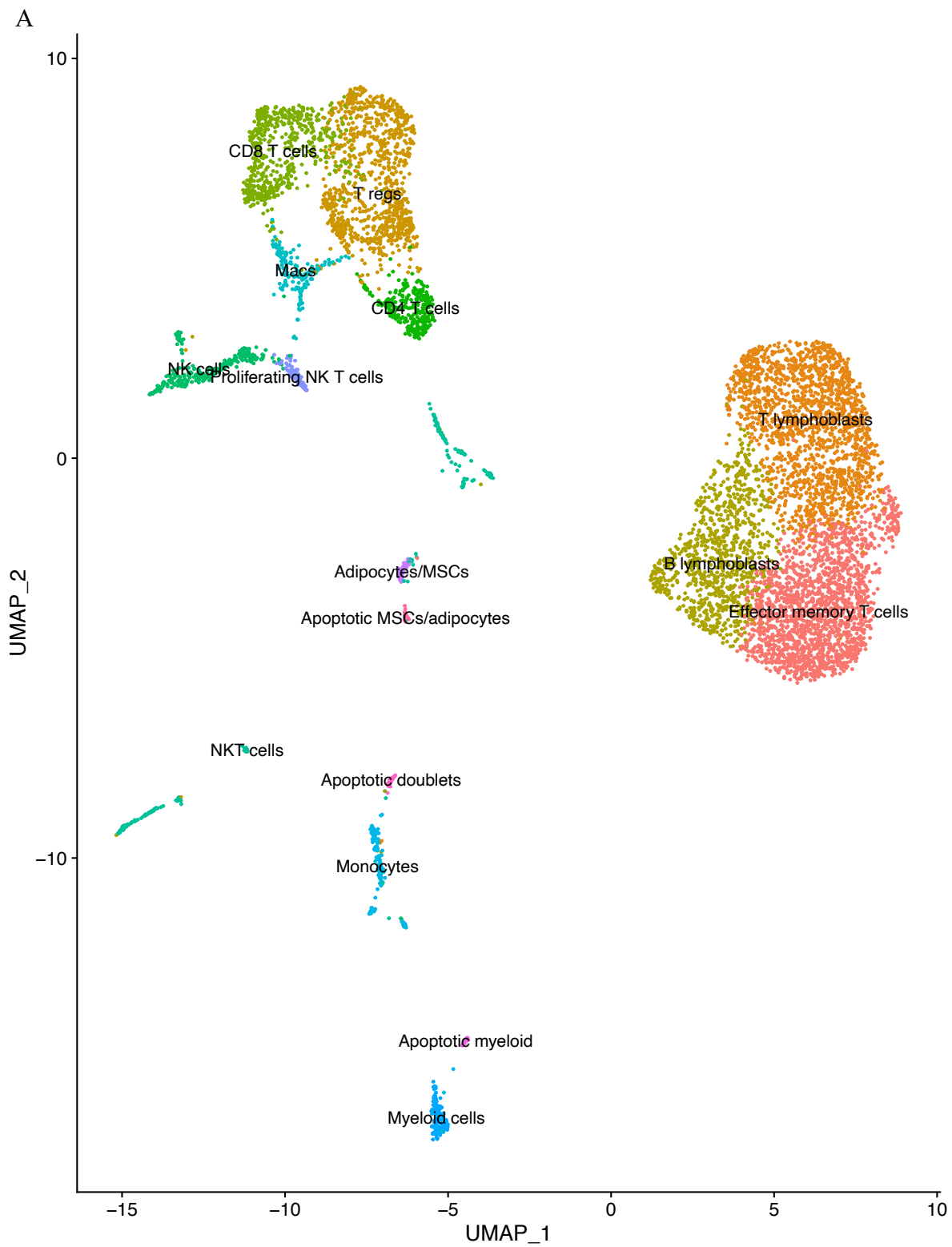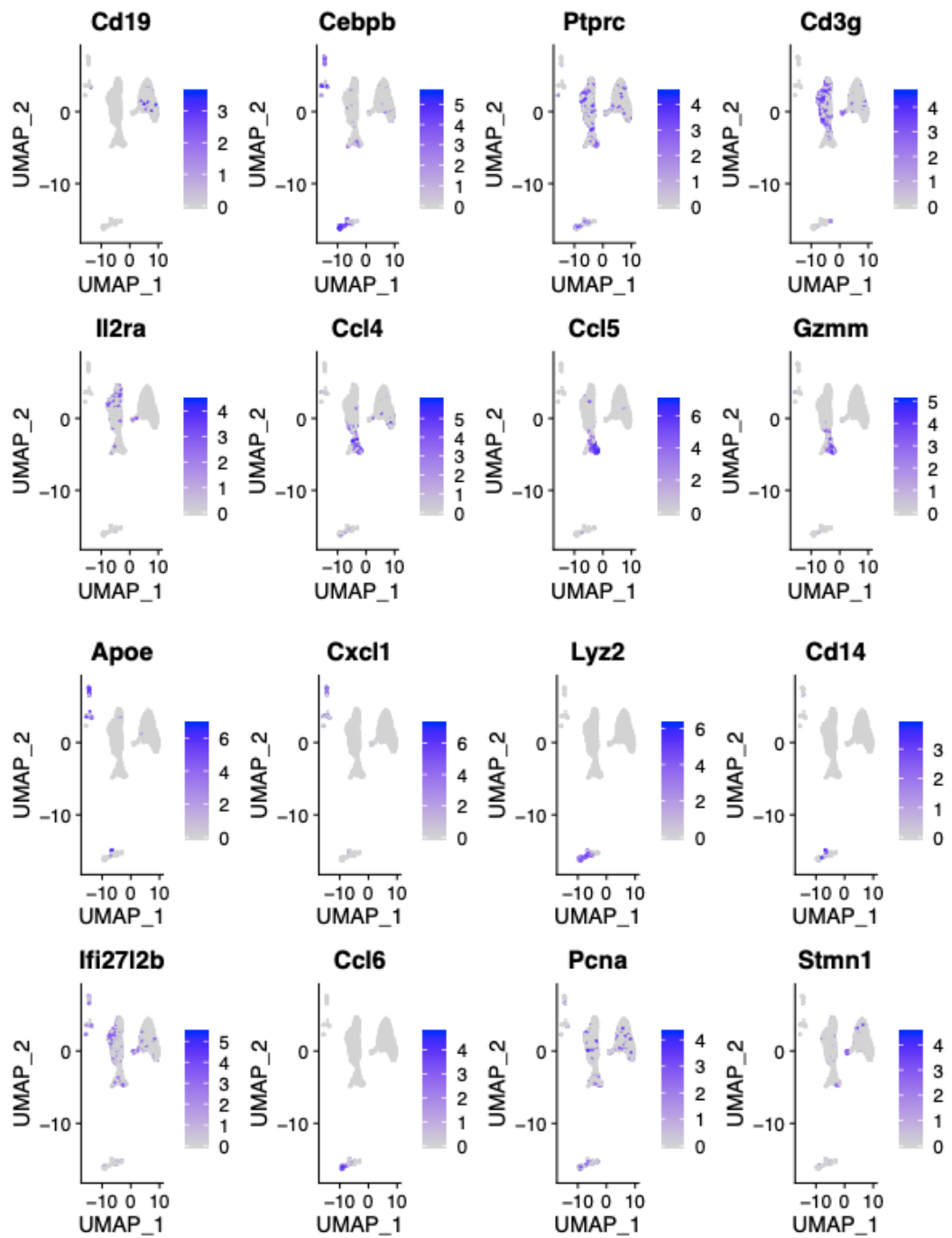
Lymphoblast

C

Cluster	C1 # cells	C2 # cells	Signature Genes	Cell type
0	1595	380	Cd19, Pkib, Marcks , Ms4a1, Ighm, Ccr7	B-lymphoblasts
1	1253	247	CD19, Ms4a1, Ighm	B-cells
2	982	264	CD3g/e/d, IL2ra, Cd99, Icos, some Foxp3, Cd2	CD4 T cells
3	891	236	Cd19, Pkib, Marcks , Ms4a1, Ighm, Ccr7	B-lymphoblasts
4	770	185	CD19, Cebpb, Marcks, Ms4a1, Ighm	B-cell lymphoblasts
5	567	256	Cd3d/e, Ifi27l2b, Fgl2, Ccr7, Cd8a, Lef1	Naive CD8 T-cell
6	372	70	CD3g/e/d, Gzmm, CCL5, Nkg7, Icos, Cd2, Tyrobp, Xcl1	NK cells
7	286	53	CD3g/e/d, IL2ra, Cd99, Icos	CD4 T cells
8	160	40	Cd34, Fgl2, Ccl2, Cst3, Cd14, Cd44, Thy1, Ms4a7, Ccl6, Lgals3, Tyrobp, Flt3	MSCs
9	140	32	CD3g/e/d, Cd8a, Ccl4	CD8 T-cells
10	127	13	Cd14, Cd59, G0s2, Lyz2, Cd40, Lgals3, Tyrobp	Macs
11	104	17	Ccl2, Fabp4, ~Apoe, Lgals3, Tpm1	Adipocyte
12	80	41	Ccl2, Apoe, Pdgfrb, Cebpb, Col3a1, Lgals3, Pdgfrb	Adipocyte
13	36	26	Krt18, Apoe, Lgals3	Epithelial cells
14	18	27	Ccl2, Apoe, Pdgfrb, Cebpb, Pdgfrb, Tpm1, Acta2	Adipocyte MSCs Myofibroblasts
15	30	14	Cd8a CD3g, Cd3e, Cd3d, Nkg7 Gzmm	NKT cells
16	39	4	Ccl6, G0s2, Lyz2, Tyrobp	Neutrophils
17	33	5	Cst3, Tyrobp, Siglech	pDC
18	2	34	Ccl2, Apoe, Tpm1, Plk3	Cycling Adipocyte/Macs

Figure 3.5 Single cell sequencing of ADSVF from rat inguinal adipose tissue confirms a diverse cell population. Single cell sequencing performed on ADSVF from rat inguinal adipose tissue. 3 runs performed in total. (A) Inguinal ADRC yielded 4,251 cell transcriptomes through scRNA-seq that by unsupervised clustering identified 10 distinct populations. Umap indicates a diverse population of cells, abundant in leukocytes including robust T-cell and myeloid populations, but also included cells with transcript signatures representative of adipocytes and mesenchymal cells. (B) Umap plot showing expression of selected genes among single cells. (C) cell populations identified from the first two runs starting with the most abundant cells.

3.4.2 RAT INGUINAL ADSVF REAL TIME PCR

As peri-renal adipose tissue yielded a significantly lower number of total cells compared to inguinal adipose tissue (223,997 cells/gram versus 1,626,164 cells/gram, respectively) and rat inguinal tissue is analogous to subcutaneous fat tissue in humans, we conducted all following experiments with inguinal-derived ADSVF.

The list of genes of interest tested for by real-time PCR can be found in Table 3.2 and included genes involved in immune regulation, growth and repair. ADSVF from rat inguinal adipose tissue had mRNA expression for over 50% of the tested genes (Fig. 3.6). Real-time PCR results are represented as the delta cycle threshold (dCt). The Ct of the gene of interest was subtracted from the Ct of the housekeeping genes giving a representation of gene expression from the standard number of RNA in each sample. Emphasis is on the amount of mRNA present relative to other genes and tissue subsets than the absolute amount of mRNA.

After testing for mRNA expression of whole ADSVF population, the ADSVF was separated into ADSVF leukocytes (CD45+) and ADSVF stomal (CD45-) subsets, by magnetic bead separation, to help understand if any particular subset played a more significant role in the therapeutic effects.

For most genes, there were no significant differences identified between the two subsets in the loosely divided categories of immune regulation, protection, growth and repair. There was a statistically significant difference between groups expressing TGFB1 as determined by one-way ANOVA ($F(2,14) = 6.504$, p = .0101). A Tukey post hoc test revealed that expression was statistically significantly lower in the CD45-ve subsets (-6.196 ±0.19, p = .0151) compared to the CD45+ve subsets (-3.885 ± 0.53). There was also a difference between groups expressing collagen type 1 alpha 2 chain (Col1a2) as determined by one-way ANOVA ($F(2,14) = 8.168$, p = .0045). A Tukey post hoc test revealed that expression was statistically significantly lower in the CD45+ve subsets (-4.782 ±1.27, p =.0033) compared to the CD45-ve subsets (-0.5271 ± 0.4974). Finally, a difference between groups expressing CXCL 12 was identified by one-way ANOVA ($F(2,14) = 10.23$, p = .0018). A Tukey post hoc test revealed that expression was statistically significantly lower in the CD45+ve subsets (-5.302 ±0.5813, p =.003) compared to the CD45-ve subsets (-2.022 ±0.5929).
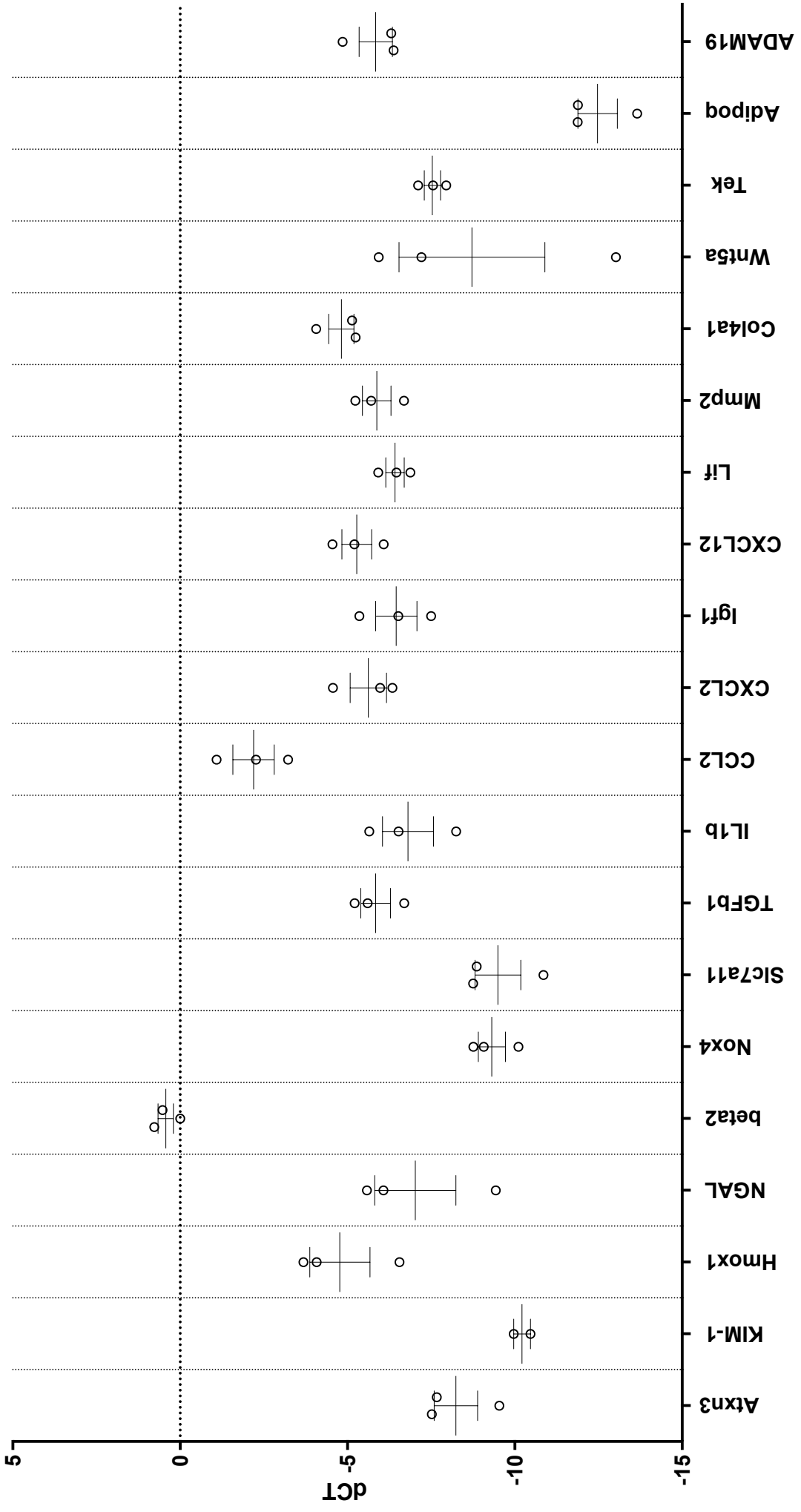
Atxn3	KIM-1	Hmox-1	NGAL	beta2	Nox4	Slc7a11	TGFb1	IL1
+	+	++	++	+++	+	+	++	++
CCL2	CXCL2	Lif	Mmp2	Col4a1	Wnt5a	Tek	Adipoq	ADAM19
+++	++	++	++	++	++	++	+	++

Figure 3.6 ADSVF from rat inguinal adipose tissue express a diverse array of genes involved in immune regulation, protection, growth and repair. Gene expression of ADSVF, derived from rat inguinal adipose tissue, using RT-PCR analysis. 26 of the 44 genes (Table 3.2) tested within the Taqman array panel were expressed and 20 of those 26 are shown in this figure (the remaining 6 are covered in more detail in the following figures). These were expressed over all the broad categories of injury, immune regulation and growth and repair. Table summarises expression.Represented as their delta CT (housekeeping genes Ct minus gene of interest Ct) after 40 cycles (n=3).

immune regulation
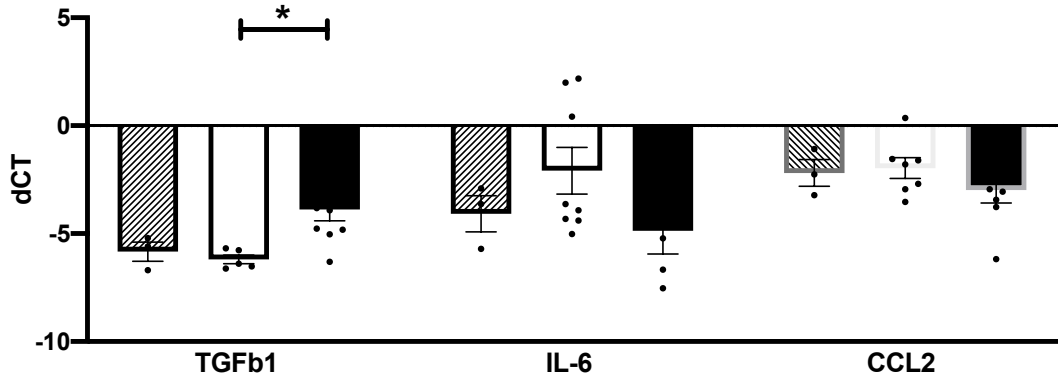
growth and repair

growth and repair

The table embedded in the figure:
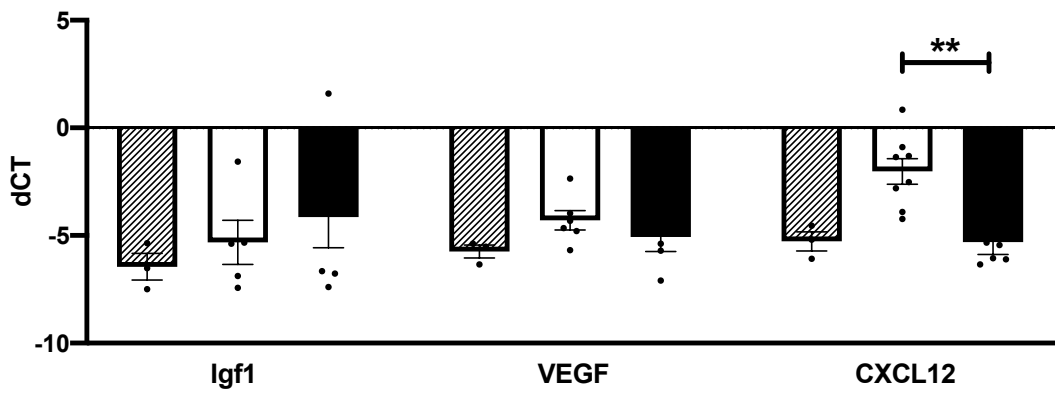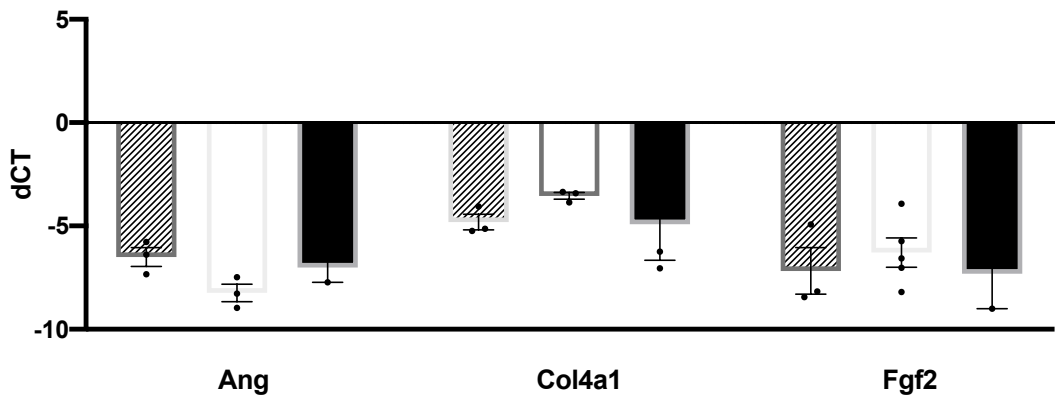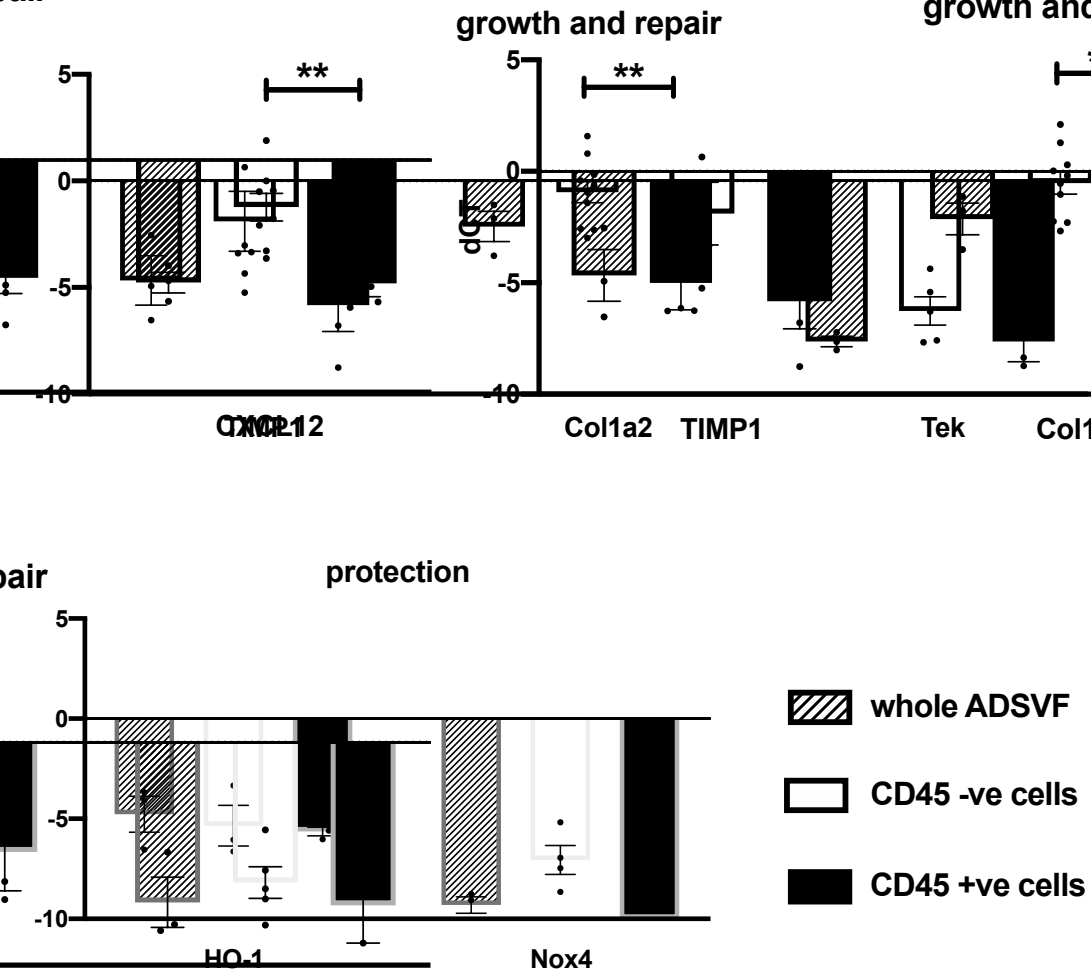
	Whole ADSVF	CD45-ve	CD45+ve
TGFb1			+ (p=0.015)
CXCL12		++ (p=0.0018)	
Col1a2		++ (p=0.0045)	

Figure 3.7 The leukocyte and stromal subsets of ADSVF have significant differences in gene expression. ADSVF was divided into CD45+ (leukocytes) and CD45-ve (stromal) subsets. RT-PCR analysis of the subsets was then performed looking at selected genes described in Table 3.2 represented as their delta CT (housekeeping genes Ct minus gene of interest Ct) after 40 cycles (n=8 for CD45+ and CD45-ve subsets and n=3 for whole ADSVF).Results after 40 cycles. There was a statistically significant difference between groups expressing TGFB1as determined by one-way ANOVA ($F_{(2,14)}$ = 6.504, p = .0101). A Tukey post hoc test revealed that expression was statistically significantly lower in the CD45-ve subsets (-6.196 ±0.19, p = .0151) compared to the CD45+ve subsets (-3.885 ± 0.53). There was also a difference between groups expressing collagen type 1 alpha 2 chain (Col1a2) as determined by one-way ANOVA ($F_{(2,14)}$ = 8.168, p = .0045). A Tukey post

93

hoc test revealed that expression was statistically significantly lower in the CD45+ve subsets (-4.782 ±1.27, p =.0033) compared to the CD45-ve subsets (-0.5271 ± 0.4974). Finally, a difference between groups expressing C-X-C motif chemokine ligand 12 (CxCL12) was identified by one-way ANOVA ($F_{(2,14)}$ = 10.23, p = .0018). A Tukey post hoc test revealed that expression was statistically significantly lower in the CD45+ve subsets (-5.302 ±0.5813, p =.003) compared to the CD45-ve subsets (-2.022 ±0.5929).

3.5 DISCUSSION

This chapter aimed to characterise ADSVF that have previously been demonstrated to ameliorate transplant related renal IRI. Going forward, this data will be used in studies looking at its biodistribution and mechanisms of action. Although articles exist on the characterisation of ADSVF, including from rat inguinal fat, this chapter focuses on Fischer 344 rats. We looked at both inguinal and peri-renal fat sources. Looking to the future clinical translation, we were also able to study human peri-renal adipose tissue and compare that to the rat peri-renal tissue. Any significant discrepancies between the characteristics of human and rat ADSVF would add a layer of doubt over the translation from rat studies to clinical use of ADSVF.

One of the first steps was to ensure after the retrieval process that there remains a viable population. After going through a standard process, ADSVF cell viability from Fischer 344 rat inguinal adipose tissue was over 60%. Viability from human and rat peri-renal adipose tissue was similar. This is particularly reassuring as viability was not only after retrieval of adipose tissue and processing to extract the ADSVF but also after the cryogenically freezing then subsequent thawing. The human adipose tissue had a particularly long time between retrieval and processing as it had to be taken to the biorepository for processing before then being transferred from the hospital to the science laboratories. This added one hour before processing on the human adipose tissue could begin. Respectable viability partnered with adipose tissue's high concentration of MSC and easy accessibility, compounds its position as one of the more favourable sources of adult stem cells. More than any other source adipose tissue offers the highest potential of obtaining therapeutic concentrations of fresh (uncultured) MSC for point of care use.

Rat inguinal ADSVF had a significantly higher leukocyte population as defined as CD45+ when compared to both rat and human peri renal ADSVF. 73% of rat inguinal ADSVF cells expressed CD45 which was higher than previously published. In our case, this was likely due to the inguinal lymph node not been excised from the adipose tissue, which is often the case. The inguinal lymph node of the Fischer 344 rats was small and could not always be confidently excised. Therefore, in a bid to maintain consistency, it was left in all samples. Even with the inguinal lymph node excised we would still expect the CD45+ population to be higher from the inguinal ADSVF compared to the peri-renal ADSVF as major vessels and lymphatics draining the limbs will run close or even through the inguinal fat. The

inguinal area is more susceptible to infections spreading from the groin area than sterile intra-abdominal peri-renal fat. There was no significant difference in human and rat peri-renal CD45+ ADSVF. The one sample of human inguinal tissue that we did manage to test unsurprisingly had a higher percentage of leukocytes compared to human peri-renal and was consistent with the normal range of CD45+ve cells of around 60% (Bourin et al. 2013). This is in keeping with another study which found 63% of the ADSVF from subcutaneous adipose tissue to be CD45+ve (Acosta et al. 2016). Similar reasons to rats likely explain why subcutaneous adipose tissue has higher leukocyte count than peri-renal tissue.

Within the leukocyte population, a robust T cell population was seen in all tested adipose tissue. Human peri-renal tissue had a significantly higher T cell (CD3+) and killer T cell (CD8+) population compared to the rat peri-renal tissue. Inguinal tissue has a higher percentage of killer T cells compared to the peri-renal tissue, which is not surprising due to the higher number of leukocytes. Single-cell sequencing added B cells, T regulator cells, other CD4 T cells, NK cells, dendritic cells, monocytes, and neutrophils to the immune cell population which made up the most substantial representation within the ADSVF of rat inguinal depot. The single-cell sequencing is a non-biased approach using expression signatures to identify cell types. It is not as representative in composition as flow cytometric data. Low expressed cell groups may not be captured, and the single-cell sequencing interrogates 2000 cells compared to the 200,000 cells in flow cytometry analysis. Flow cytometric data was, therefore, more helpful in drawing quantitative conclusions compared to the single-cell sequencing data.

With ADSVF showing to be as effective in ameliorating injury as isolated ASC in multiple animal models the leukocyte population at the very least are not detrimental to the therapeutic potential of ADSVF (with some studies finding the ADSVF more effective than ASC alone). To the best of our knowledge, no study has looked at the efficacy of ADSVF minus the ASC in renal IRI animal models. ADFSVF have the added advantage of being much quicker and simpler to obtain than isolated ASC and therefore carries fewer risks. The leukocyte population are likely contributors to the paracrine actions of ADSVF. Being extracted and expanded, ASC will lack many of the exosomes present within the ADSVF. The identification of a strong representation of T regs cells is interesting as many clinical studies are currently in phase II looking at their role in inducing and maintaining immunological tolerance in solid organ transplantation. So far, they have found to be safe when expanded and administered peri and post-transplant. With their potent anti-inflammatory and suppressive properties, their role within ADSVF at ameliorating renal

transplant-related IRI has not been thoroughly investigated (Alessandrini & Turka 2017; van der Veeken et al. 2016; Feuerer et al. 2009). T regs may be the tip of the iceberg when it comes to other cell populations within the leukocyte population with therapeutic potential against IRI.

The mesenchymal stem cell-like cell fraction was identified as CD90+ CD45- and CD34-. CD34 expression can vary depending on the retrieval process and in culturing expansion of ASC, and it tends to be present at the beginning and less frequent at the end phases. As true mesenchymal stem cells are CD34- we went with that in our criteria for ASC. Also, angiogenesis was an essential part of recovery post-IRI and CD34-ve MSCs promote greater angiogenicity. As there will be mesenchymal stem cell-like cells which are CD34+ve, they are likely underrepresented in our flow cytometric studies of the ADSVF. Despite that, there was mesenchymal stem cell-like cell population in all inguinal and peri-renal adipose tissue of humans and rats. The inguinal region may have a higher concentration of ASC but going to clinical translation, it is not just the ASC that hold the therapeutic benefit. If higher concentrations of ASC were deemed necessary, then the plentiful supply of adipose tissue will make the need for culturing unnecessary. MSC were identified in the single-cell sequencing. The majority identified as mesenchymal stem cells but a small population of adipocyte specific MSC. As further single-cell sequencing data becomes available on uncultured ASC, we will develop a better understanding of the stromal and stem cell population. Undoubtedly it will be complex and dynamic with retrieval techniques, processing and depot sites all effecting the phenotype of stem cells and stromal cells present.

Deeper interrogation of ADSVF from human subcutaneous adipose tissue was planned. Unfortunately, obtaining significant human sample sizes was not possible. However, recently a laboratory in Montreal performed single cells analysis of visceral ADSVF (represented by omental fat) and subcutaneous fat of both diabetic and non-diabetic patients. They characterised the similarities and differences in the populations, in particular, the unique adipocyte progenitors found in visceral adipose tissue (Vijay et al. 2020). Data on the human peri-renal ADSVF overall in the literature is limited and there has been no single-cell sequencing on uncultured human peri-renal ADSVF. With the samples we have this could be performed by our group moving forward and would add to conclusions generated from flow cytometric and gene expression data.

The real-time PCR studies, as predicted given the heterogeneous cell population of the ADSVF, demonstrated gene expression for proteins that cover an array of functions. Given

they have shown to improve the functional status in models of ischaemia reperfusion injury, it is not surprising that genes expressed are related to growth, repair and immune regulation. Markers of injury were also included on the array panel, which will be valuable when analysing kidney that has undergone IRI and treated with ADSVF and controls.

The panel represents an array of genes that in literature have been demonstrated to play a role in the recovery after IRI. Other proteins were chosen as their role in likely mechanisms of recovery and the limitations of the array card. From the custom selected array panel over half of the proteins, we looked at tested positive. These proteins covered all the loosely grouped functions. Results indicated expression of angiogenic genes, VEGF-a and anabolic genes such as insulin growth factor-1 (IGF-1). Also, genes involved in fibrogenesis (TGFB1 and Collagen type 1a2) and inflammation (IL-6 and chemokine, CXCL12) were expressed.

Specific proteins were singled out for having notably higher levels relative to the others. These were then tested again in CD45+ve and CD45-ve subgroups. In the majority, there was no significant difference between the groups. The leukocyte population expressed higher levels of the immunomodulatory protein TGFB1. The mesenchymal stem cell-like population expressed higher levels of CXCL12 and collagen type 1a2 (Col1a2). As leukocyte and stromal fractions contributed differentially in transcript expression relative to each other and with the whole ADSVF, it is possible cell-subset synergism may be responsible for the overall ADSVF expression effect.

To speculate the potential mechanism each protein may play in IRI would be a laborious task. Gene expression of tissues treated with ADSVF could help narrow down key pathways.

Although we were only able to test gene expression studies on rat ADSVF recent data has been published on human ADSVF by Baer et al. (Baer et al. 2019). They demonstrated the similar immunomodulatory potential of human peri-renal adipose tissue through PCR studies; however, their work was performed on cultured adipose-derived stem cells and not on the whole ADSVF. Another publication by Na Eun Lee et al. found that cultured MSC from subcutaneous tissue vs retroperitoneal adipose tissue (peri-renal adipose tissue is retroperitoneal) had a faster growth rate and was more angiogenic (Lee NE 2019).. This would be favourable in pathologies with underlying vascular disease (they propose this is due to their high CD146 positivity). They also showed their morphology and immunophenotype to be similar. All of which confirms our work on the demonstrated benefits of each source but also on their general overall similarity. More specific

characterisation of the peri-renal adipose tissue may support future uses of peri-renal-derived ADSVF.

In summary, the ADSVF from the inguinal depot of Fischer 344 rats consist of a heterogeneous population of viable cells. In particular, there is a strong B lymphocyte and T cell representation within the leukocytes. Human peri-renal tissue consists of a similarly heterogeneous population but with a reduced proportion of leukocytes. Single-cell sequencing supports the presence of MSC within the ADSVF. Having less mesenchymal stromal like cells from the human tissues is not necessarily a problem as humans have large depots of adipose tissue.

From this data and the literature, it seems overall different sources of adipose tissue have differing proportions of a similar cell population. Further complex and expensive research on the exact composition of ADSVF from different human sources would be an interesting intellectual exercise. However, perhaps not a priority from a translational perspective if the intention is to use the whole population of ADSVF. When moving to clinical trials, both subcutaneous and peri-renal adipose tissue should be considered.

The rat inguinal ADSVF express an array of transcripts that are related to repair, growth and immune regulation which are adventitious traits to have when faced with IRI. Some transcripts are differentially contributed by the leukocyte and stromal fraction, suggesting a synergistic contribution of repair factors. Mechanistic studies could focus on where these proteins interact within the pathways of IRI. Other future studies could concentrate on administering only the leukocyte population to see if it still has the desired or potentially enhanced ameliorative action against renal IRI.

CHAPTER 4:
DEVELOPMENT OF A NOVEL RAT MODEL OF RENAL TRANSPLANT ISCHAEMIA REPERFUSION INJURY

4.1 INTRODUCTION

Animal models have been a vital tool in the research of many human and animal conditions. They will remain for the foreseeable future until such time that we have the technology or in vitro experiments that can accurately replicate the human physiology and interconnected environment between organs and systems. Animal models have been vital in the discovery of therapies that have saved millions of human and animal lives. The complexity of the human body currently makes animal models indispensable if research is to continue to develop therapies. The similarities between human and animal anatomy and physiology make animal models an applicable method to guide therapies. However, no animal model can accurately mimic human disease and along with animal research come the ethical and political debate on its existence.

Opinion polls have shown acceptance to animal testing if it practises a strict code of conduct (the 3Rs: Refine, Reduce, Replace). The United Kingdom has some of the most stringent laws in the world, protecting animals and is covered in the UK Animals (Scientific Procedures) Act 1986. Many of the principles of this Act was replicated in the European Directive 2010/63/EU. Animal licence applicants must demonstrate the cost (non-financial) benefit assessment of requesting permission of animal testing. Any project plan must demonstrate strict adherence to the 3R principles – Replace, Reduce, Refine. Avoiding the use of animals where possible and reducing the number of animals required by carefully planned projects. Refinement of the research at conception and throughout the project licence term that reduces suffering and improves welfare. This can be achieved by applying new technologies, methods, and research. Before the animal licence is granted, the person, project and place or establishment must also satisfy the strict criteria of training, competency, regulation, and facilities. An animal ethics committee that includes members concerned with animal protection and not involved in animal research shall decide if the licence application can be submitted to the home office for approval.

As described in the introduction section the widely used models of kidney IRI is short bilateral ischaemia or a longer unilateral ischaemia. Bilateral ischaemia has the major drawback in that it does not inflict a severe enough ischaemia representative of a transplant related IRI. Longer ischaemic times in a unilateral ischaemia model are possible and inflict a severe and permanent injury to the kidney, but the contralateral untouched kidney can effectively increase its functional capacity and meet the renal requirements of the rat including the "mopping up" of metabolic disturbances. A summary of current popular animal models is shown in figure 1.6.

To address the issue of having an untouched fully functioning contralateral kidney a hybridization of a severe unilateral renal ischaemia model and the traditional 5/6 nephrectomy model may provide a solution. Since the 1970s, the 5/6 nephrectomy model has been used as a way of inducing chronic renal failure in rodents. This animal model involves the removal of one kidney and ligation of 2/3 of the blood supply or 2/3 resection of the remaining kidney. After an initial period of hypertrophy and hyperplasia of the remnant kidney tissue there is progressive tubulointerstitial injury and glomerulosclerosis (Chanutin & Ferris 1932; Olivetti et al. 1977; Shea et al. 1978; Olson et al. 1982; Purkerson et al. 1976). Features of chronic renal failure can be seen with increased blood pressure, urea, creatinine, sodium and potassium (Baracho et al. 2016; R.-Z. Tan et al. 2019). Significant changes are also seen in calcium, magnesium and phosphate (R.-Z. Tan et al. 2019). The homeostasis of uremic toxins, metabolites, peptides, proteins, and electrolyte are all disturbed in CKD.

Therefore, the potential interference the renal failure environment may have on a kidney recovering for IR should not be ignored. Metabolite changes following the 5/6 nephrectomy are involved in many pathways including ROS, acid-base balance, energy metabolism and the gut-kidney axis (Hanifa et al. 2019). Disturbances in uremic toxins, metabolites and electrolytes affect the recovery of transplanted grafts (Duranton et al. 2012; K. Wang & Kestenbaum 2018; Y.-Y. Zhao 2013). Hyperuricemia may itself have direct involvement in the development of chronic kidney disease and increases the risk of cardiovascular disease (Grassi et al. 2013; Dousdampanis et al. 2014; R. J. Johnson et al. 2013). High blood pressure and increased renal flow, because of chronic renal failure, exert a pressure on the kidneys that would be present in the transplant recipient but not replicated in current animal models.

The 5/6 model has excellent translation to human disease as it represents a significant decrease in renal function due to loss of functional nephrons, glomerulosclerosis,

tubulointerstitial fibrosis and proteinuria (Platt 1952; Shimamura & Morrison 1975; Kwon et al. 1998). Other models of chronic kidney disease exist such as glomerulonephritis induced, radiation-induced and ureter occlusion (R.-Z. Tan et al. 2019). However, in these models, it is difficult to accurately reduce the function of just one of the kidneys.

One drawback of the 5/6 nephrectomy model is the inconsistency in achieving exactly 2/3 nephrectomy, which results in varying degrees of uraemia and creatine clearance (Z. C. Liu et al. 2003). Surgical ligation of the kidney tissue can offer a more precise nephrectomy over renal artery branch ligation but does carry an increased risk of haemorrhage and infection.

Rodent allograft kidney transplantation into a nephrectomised animal would most closely represent clinical transplantation. However, this is technically very challenging with a long learning curve, high risk of stenosis, thrombosis, and bleeding. Plus, removal of the kidneys at the time of transplantation will result in unacceptable numbers of animal deaths as there is no capacity to perform rodent dialysis. It also requires a further sacrificial rodent for the kidney graft and is more time-consuming.

To refine the measurement of GFR, novel methods have been developed that removes some of the drawbacks of inulin clearance studies (time-consuming, technically challenging, often terminal, serial blood or urine measurements). One such technique is the administration of a florescent labelled polysaccharide (FITC-sinistrin, Fresenius Kabi, Linz, Austria) then measuring the light emitted transcutaneously with a fluorescent imager once it has been excited. This method progressed to using a small device attached to the rat for a few hours, in a jacket. The device which would transcutaneously excite the FITC-sinistrin at 480nm and detect the emitted light at 520nm (Schock-Kusch et al. 2011). This allows longitudinal detection of emitted light in freely moving rats. Thousands of data points are taken over the 120minutes, and the elimination half-life is determined using an established one-compartment model (Schock-Kusch et al. 2009; Pill et al. 2006; Pill et al. 2005). The GFR can then be derived from the half-life as a linear relationship is expected between GFR and half-life. A deduced conversion factor to calculate the GFR was obtained from enzymatically measuring Sinistrin clearance (Schock-Kusch et al. 2009). GFR results using this method are highly comparable to the gold standard plasma clearance studies (Schock-Kusch et al. 2009). Also, temporarily attaching a small transcutaneous device, with a jacket, to the rodent versus anaesthetising the rodent to go under a fluorescent imager reduces the need for anaesthesia which can alter GFR.

A modified Whalen et al. animal model which better mimics the transplant patient and technically easier to perform without long, laborious terminal renal function testing could potentially be the optimal model for testing therapies against transplant-related IR.

Fischer 344 rats are well suited to renal IRI as they are large enough to allow for dissection, cannulation, and anastomosis of the renal artery. In addition, they are robust and recover well from major surgery.

4.2 HYPOTHESIS

The severe unilateral ischaemia reperfusion injury model can be further modified to better mimic the renal transplant recipient.

4.3 METHODS

Ethics: All animal procedures were performed in accordance with the Animals (Scientific Procedures) Act 1986 (ASPA) and approved by the Home Office (England, Scotland, and Wales) and University of Glasgow Animal Welfare and Ethical Review Body. *Methods of sterility, intraoperative monitoring and positioning, anaesthesia, surgery and peri-operative care were all observed and approved by the Home Office veterinary surgeon.*

4.3.1 ANIMAL HOUSING AND HUSBANDRY

Animal housing and husbandry was standard throughout all procedures and is described in chapter 2.1.

4.3.2 EQUIPMENT

Microsurgical equipment:

- Wild Heerbrugg Ltd operating microscope – zoom 10-30x 60mm LED light ring (Microscope Systems Scotland)
- Far infrared heating pad and infrared thermometer (Kent Scientific: DCT-15)
- Operating board (30x30cm). Covered with disposable plastic sheeting, held in place with adhesive tape.
- The following microsurgical instruments were obtained from Mercian® (Mercian Surgical Supply Co Ltd, Worcestershire, United Kingdom)
  - – Microsurgical vessel dilators with 0.1mm tips. (D-5a.1)
  - – Microsurgical vessel dilators with 0.2mm tips. (D-5a.2)
  - – Microsurgical vessel dilators with 0.3mm tips. (D-5a.3)
  - – Angulated forceps with 0.3mm tips. (JFA-5b)
  - – Dissecting microsurgical scissors with curved tips (SDC-15)
  - – Adventitia microsurgical scissors with sharp tips (SAS-15)
  - – Microsurgical needle holder without a lock, curved tips 0.4mm. (B-15-8)
  - – Tubing introducing forceps, tips 0.35mm. (TIF02)
  - – Clamp applying forceps. (CAF-4)

- o – Atraumatic vascular clamps. (B1-V and B2-V))
- Electric hair clippers
- 15G Scalpel
- Sterile Dressing packs (Nu-care Products Ltd, Bedfordshire, United Kingdom: DP10025)
- Sterile Cautery (John Weiss & Son Ltd, Milton Keynes, United Kingdom: 0111122)
- 30G Rycroft Cannula (0108003)
- Blunt retractors (18200-12) and elastomers (18200-07) (Fine Science Tools, Heidelberg)
- Sterile cotton tip applicators (Nu-care Products Ltd, Bedfordshire, United Kingdom: M982S)
- 10/0 nylon sutures. (Schuco Ltd, ZX-AK-0105, DR4 needle) or Ethilon® Suture, 10/0 non absorbable, monofilament, 13cm, 3.8mm, 3/8 circle taper point needle (Ethicon, Inc. W2870)
- Vicryl® Suture, 4/0 undyed, 19mm, 45cm, circle reverse cutting (Ethicon, Inc. W9925)
- Prestige Latex Sterile Gloves (Nu-care Products Ltd, Bedfordshire, United Kingdom: GS33LE)
- 365 Standard Sterile Gowns (Nu-care Products Ltd, Bedfordshire, United Kingdom: D20304)

Non-terminal / non-invasive renal function measurement equipment:
- Electric hair clippers
- Depilatory cream
- Double sided adhesive patch
- Transcutaneous optical device (MediBeacon, Mannheim, Germany *formerly known as Mannheim Pharma & Diagnostic GmbH, Mannheim, Germany prior to acquisition*)
- Fluorescein isothiocyanate (FITC)-sinistrin (MediBeacon, Mannheim, Germany)
- FITC-Sinistrin reading software (Sensor_ctrl_app.exe. MediBeacon, Mannheim, Germany)

4.3.3 RODENT ANAESTHESIA

Animals were weight before surgery. Surgical induction was performed in the animal operating suite using an anaesthetic chamber. 5% isoflurane was used for induction, and anaesthesia was maintained using an inhaled mix of 5% isoflurane and 1litre/minute oxygen via a face mask. According to the animal's respiratory rate and pain withdrawal reflexes, the flow could be adjusted by the surgical assistant.

4.3.4 INTRA-OPERATIVE MONITORING AND POSITIONING

Rats placed supine under a sterile drape on a board which has heating mat incorporated into it—placing the rodent on a board allowed for easy mobilization of the rodent while being able to maintain sterility. The temperature was monitored using an infrared thermometer and maintained between 36.9°C-37.3°C. The far-infrared heating mat and built-in procedural table heater were used to control rodent body temperature.

4.3.5 SURGICAL STERILITY

Surgery was performed in a dedicated animal surgical suite. Only the surgeon and assistants present in the operating suite. Green scrubs and dedicated surgical footwear were required throughout the facility. Before any procedure, the operating table, microscope, and surrounding areas were sprayed down with chlorhexidine. After surgical scrubbing of forearms and hands with chlorhexidine surgical scrub, sterile gown and gloves were worn. Sterile drapes were placed on the surgical field, over a microscope and on top of the rodent (Fig 4.1). Rodents were then prepped with 2% chlorhexidine solution which was left to dry before starting procedure. Surgical instruments are autoclaved 30 minutes before the start of operation (30minutes at 134°C). Any consumables were opened from their sterile pack and dropped onto the sterile field. Postoperatively, surgical instruments were washed with warm soapy water, dried, cleaned with chlorhexidine then autoclaved and stored in their custom storage trays.

4.3.6 PERI-OPERATIVE ANALGESIA AND POST-OPERATIVE MANAGEMENT

At induction of general anaesthesia for any operation, the rodent is administered buprenorphine (0.005mg per 100g) subcutaneously. Viscotears was applied to both eyes. Before wakening, 4ml of sterile saline was administered subcutaneously but can be increased if the procedure took longer than usual or if there was slightly more blood loss than average. Immediately post-operative the rodent is recovered and monitored closely in a heated recovery cage with free access to food and water. Once the rat has fully recovered from the anaesthetic, they are placed back into their home cage. Buprenorphine (100ug) is given orally on days one and two post-operative. Daily weights for at least seven days post-surgery plus the NC3Rs grimace scales were used to make sure rodent pain was controlled and to identify any complications as early as possible (National Centre for the Replacement, Refinement and Reduction of Animals in Research, London, United Kingdom). The operating surgeon, project licence holder or the named veterinary officer were available 24 hours a day if there were any concerns with operated rats.

4.3.7 STAGE 1 – 2/3 NEPHRECTOMY OF RIGHT KIDNEY

Young adult male Fisher 344 rats were anaesthetised with isoflurane. Abdominal hair was shaved, and the rat was placed on a heating mat. The skin was prepped with chlorhexidine and draped to obtain a sterile field. A two-centimetre upper midline incision was made using a fully aseptic technique. Using scissors, the peritoneum was opened. Bowel contents were gently retracted to the left to reveal the right kidney. The fascia surrounding the renal hilum was opened and the renal artery identified. Due to varying anatomy, non-traumatic micro-forceps were used to briefly (3 seconds) clamp branches of the renal artery in order to determine blood distribution form that particular artery. Using 10-0 Nylon one or two or three branches of the renal artery were ligated to leave only 1/3 of the kidney perfused with arterial blood (Fig 4.2). Bowel retraction was then removed to return the normal positioning of the bowel. Peritoneum and skin were closed individually using a continuous 4-0 polyglactin suture (Vicryl®). Total surgical time ranged from 15-30minutes. Post-surgical care: The animal was injected with 4ml of subcutaneous 0.9% saline postoperatively and placed alone in the warmed recovery cage with free access to food and water. Buprenorphine analgesia was injected subcutaneously, at 0.005mg per 100g of body weight. The animal was returned to its home cage once fully recovered from the anaesthesia.

4.3.8 STAGE 2 – ISCHAEMIA REPERFUSION INJURY OF LEFT KIDNEY AND CANNULATION OF RENAL ARTERY

Once recovered from the right partial nephrectomy procedure for at least two weeks the rats were anaesthetised with isoflurane (Fig 4.3). Abdominal hair was shaved, and the rat was placed on a heating mat. The temperature was adjusted to maintain the core temperature of 36.5-37°C. The skin was prepped with chlorhexidine and draped to obtain a sterile field. Using a fully aseptic technique, the previous midline incision was reopened and extended to around five centimetres. Bowels were gently retracted to expose the left kidney. The fascia surrounding the renal hilum was opened, and the left renal artery was identified. A segment of the renal artery was carefully cleared of fascia and its attachment to the renal vein with blunt dissection using cotton tips and forceps. Two non-traumatic vascular micro clamps were placed on the renal artery to induce renal ischaemia and the time noted (Fig 4.4). The kidney was inspected to make sure the clamps have entirely occluded perfusion. If the animal is to receive an intervention via the renal artery (as in our research) then 20 minutes before the end of the ischaemia (minute 100) an incision large enough to fit a 30-gauge catheter was made to the anterior wall of the renal artery between the clamps. 7×10^5 ADSVF cells in 0.3ml PBS was administered with a 1ml syringe and a 30-gauge catheter through the incision. The distal clamp was momentarily released to allow the infusion to travel through the renal artery and into the kidney. Perfusion of the kidney with the ADSVF/PBS was confirmed by the visualisation of the kidney changing colour. The distal clamp was re-applied to prevent back bleeding from the kidney. The renal artery incision was repaired longitudinally with interrupted 10-0 Nylon. Clamps were removed after 120 minutes of warm ischaemia. Bowel retraction was removed to allow the normal positioning of the bowel. Peritoneum and skin were closed individually using a continuous 4-0 polyglactin suture (Vicryl®). Total surgical time ranged from 140-160minutes. Post-surgical care: The animal was injected with 2.5ml of subcutaneous 0.9% saline postoperatively and placed alone in the warmed recovery cage with free access to food and water. Buprenorphine analgesia was injected subcutaneously, at 0.005mg per 100g of body weight. The animal was returned to its home cage once fully recovered from the anaesthesia.

4.3.9 NON-INVASIVE MEASUREMENT OF RENAL FUNCTION

Preparation of FITC-sinistrin Injection Solution

1. FITC-sinistrin (MediBeacon, Mannheim, Germany) was dissolved in physiological saline to prepare a stock solution. The recommended dose in in rats is 5 mg/100 g BW FITC-sinistrin.

Animal Preparation

2. Induction and maintenance of general anaesthesia if rat not already under general anaesthesia for another procedure. The level of anaesthesia should be sufficient so as to prevent the animal experiencing any discomfort or distress.

3. Fur is removed from the back of the animal using an electric shaver. An area slightly bigger than the area that will be occupied by the double-sided adhesive patch, which has dimensions of 3cm x 6cm will be shaved.

4. Depilatory cream will be applied for a short period (2-3 min) to remove the remaining fur.

5. The cream will be thoroughly washed off.

Fixation of the Device on the Animal

6. The optical device is placed onto one side of the adhesive patch and device and patch are then placed onto the shaved area on the back of the animal.

7. For animal comfort, and to secure the device, tubular elastic gauze bandage is stretched over the abdomen of the animal, ensuring that the limbs can move freely (Fig 4.5).

FITC-sinistrin Administration and Measurement Procedure

8. FITC-sinistrin stock solution is injected into the tail vein.

9. The animal is returned to its home cage and is recovered from the short anaesthetic. The animal is left in its cage with the device attached for 2 hours. **Note:** During the recording period the animal will be individually housed in a cage with no protruding structures, such as wire lids, to avoid damaging of the electronic device and movement artefacts due to impacts with objects.

Device Removal

10. Once the recording period is over, the tubular bandage and adhesive tape with the device is gently removed without the need of anaesthesia and the animal is returned to its normal home cage.

11. The device is then connected to a PC via a micro USB for data analysis.

Data Analysis

12. FITC-sinistrin reading software (Sensor_ctrl_app.exe. MediBeacon, Mannheim, Germany) is used to extract the data from the device.

13. The shape of the graph displaying time versus signal can be visualised to ensure FITC-sinistrin was administered adequately and detected by the optical device.

14. The software will calculate the half-life of the FITC-sinistrin. The following formula is then used to calculate the GFR:

$$_t\text{GFR [ml/min/100 g } BW] = \frac{21.33[\text{ml}/100 \text{ g } BW]}{t_{1/2}(\text{FITC} - S)[\text{min}]}$$

4.3.10 DEVELOPED STANDARD OPERATING SURGICAL PROCEDURE

Operating personal licensees underwent an approved animal microsurgery training course or were trained by a personal licence holder with vast experience in this type of microsurgery.

When learning either the 2/3 nephrectomy procedure or the IRI with renal artery cannulation procedure, there is initially a period of training on humanely killed rats. The number varies as per trainee but is approximately five. Then, under supervision, the trainee will commence a period of training on several live animals which will be humanely killed before recovery (5 to 10 depending on trainee progress). The trainee will commence to operate, supervised, on experimental rats that will be recovered. Once a success rate of >80% is achieved, then they are approved for independent practice.

To reduce animal numbers during training, the 2/3 nephrectomy procedure can be performed on both the left and right kidneys of the cadaveric and non-recovered rats. Similarly, the IR with renal artery cannulation training can be performed on both the right and left kidney of the cadaveric and non-recovered rats.

The Named Veterinary Officer was informed and observed multiple stages of the training. Only once deemed competent by the trainer and the Named Veterinary Officer was the personal licence holder then able to perform the procedures independently.
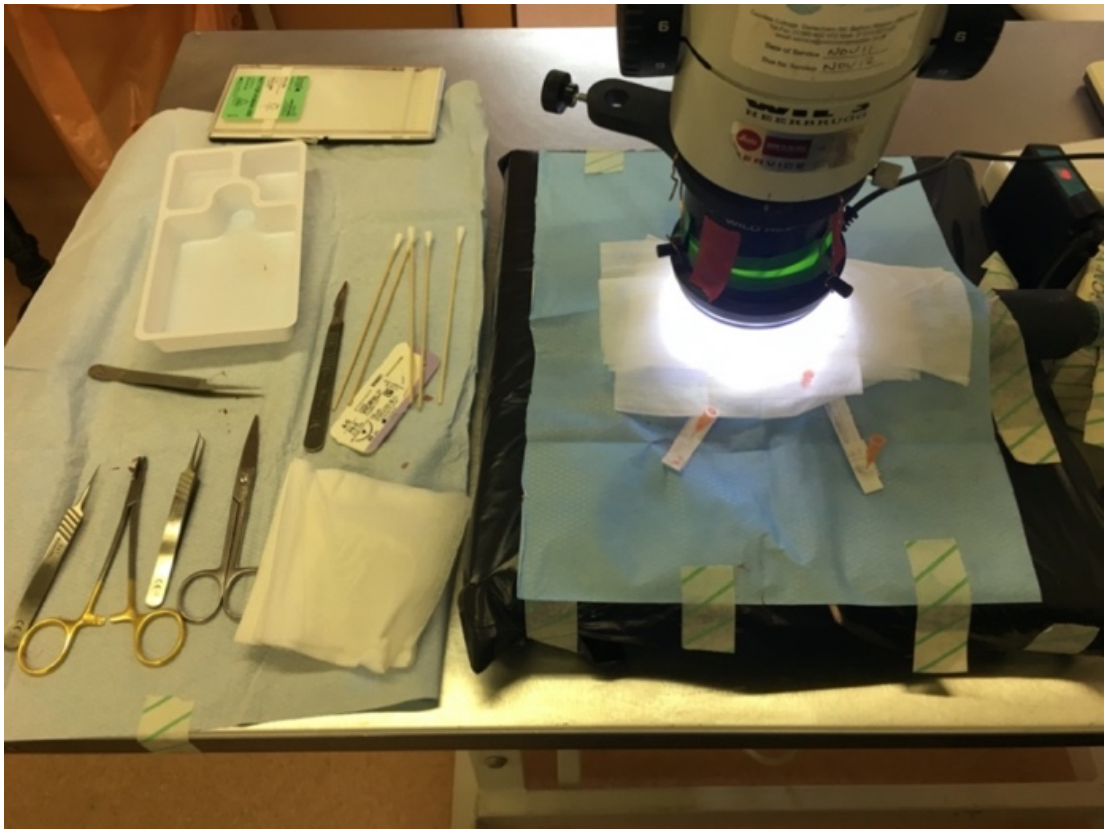
Figure 4.1 Surgical field set up for microsurgery.

A
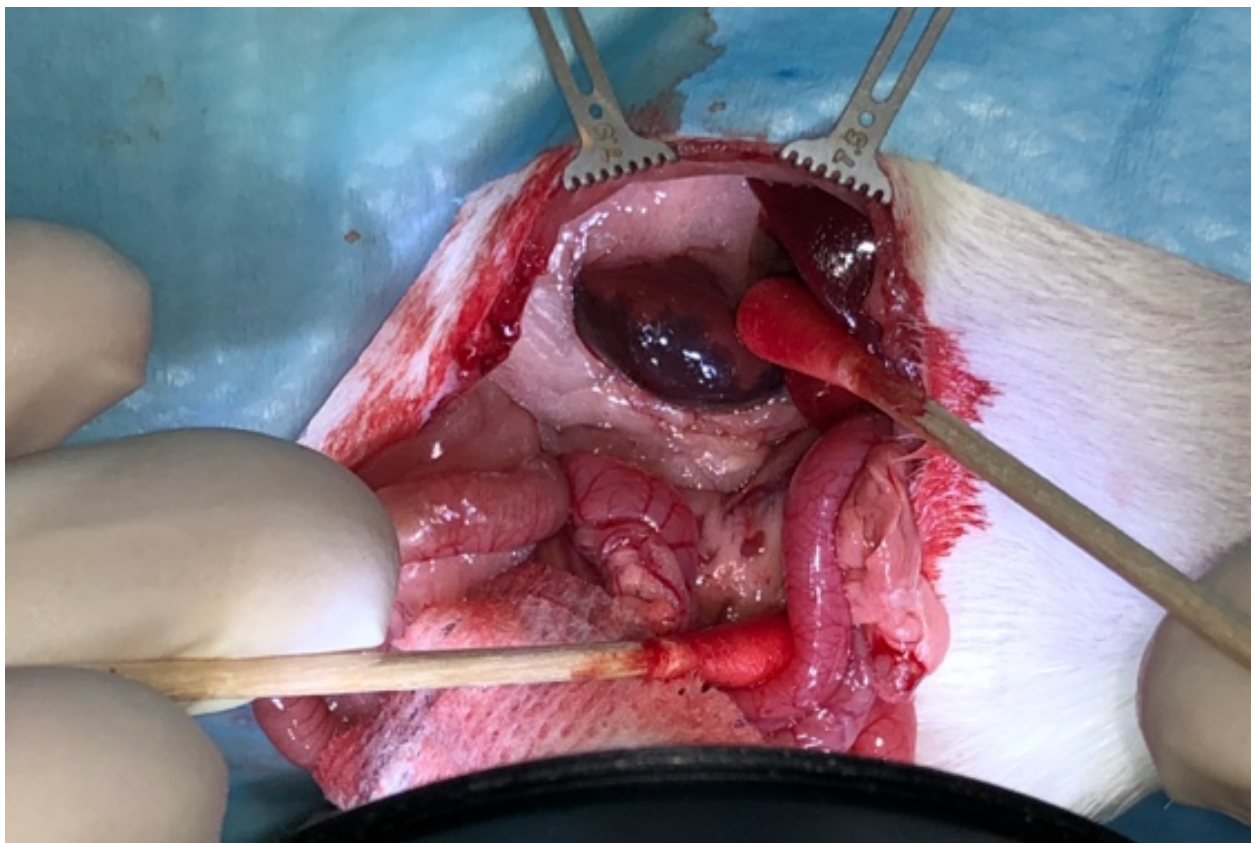
B

Figure 4.2 Images of 2/3 nephrectomy surgery. (A)Discolouration of the right kidney after ligation of renal artery branches. (B) Wound 2 weeks post 2/3 nephrectomy heals well.

Stage 1:
2/3 nephrectomy of
RIGHT kidney

Minimum 2 week interval

Stage 2:
120 minutes Ischaemia
and reperfusion surgery
of the LEFT kidney

Stage 3:
Transcutaneous
measurement of renal
function at desired time
points

Termination timepoint as per project plan

Stage 4:
Termination of rat and
tissue retrieval
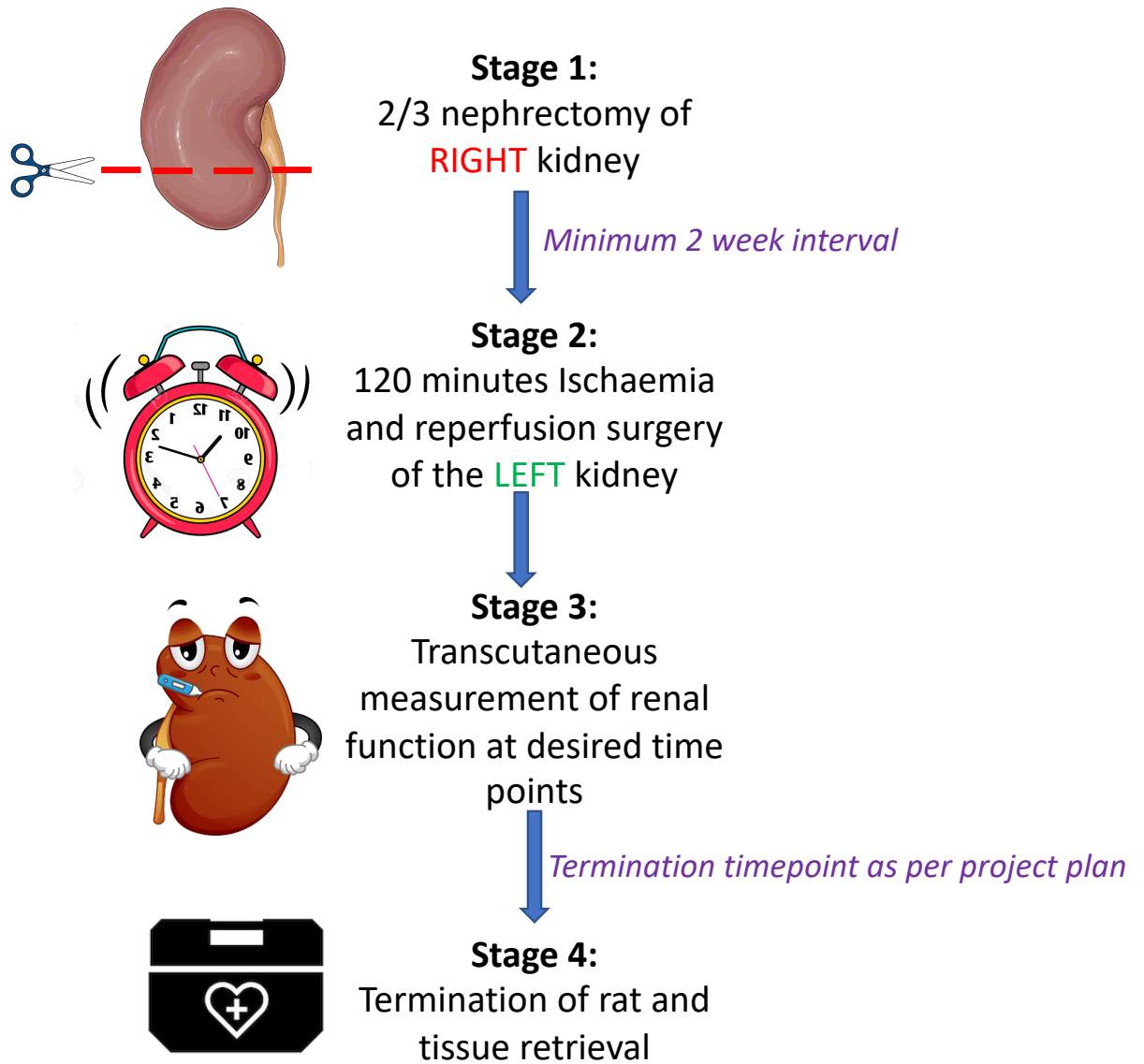
Figure 4.3 Stages of our animal model of renal transplant IRI.
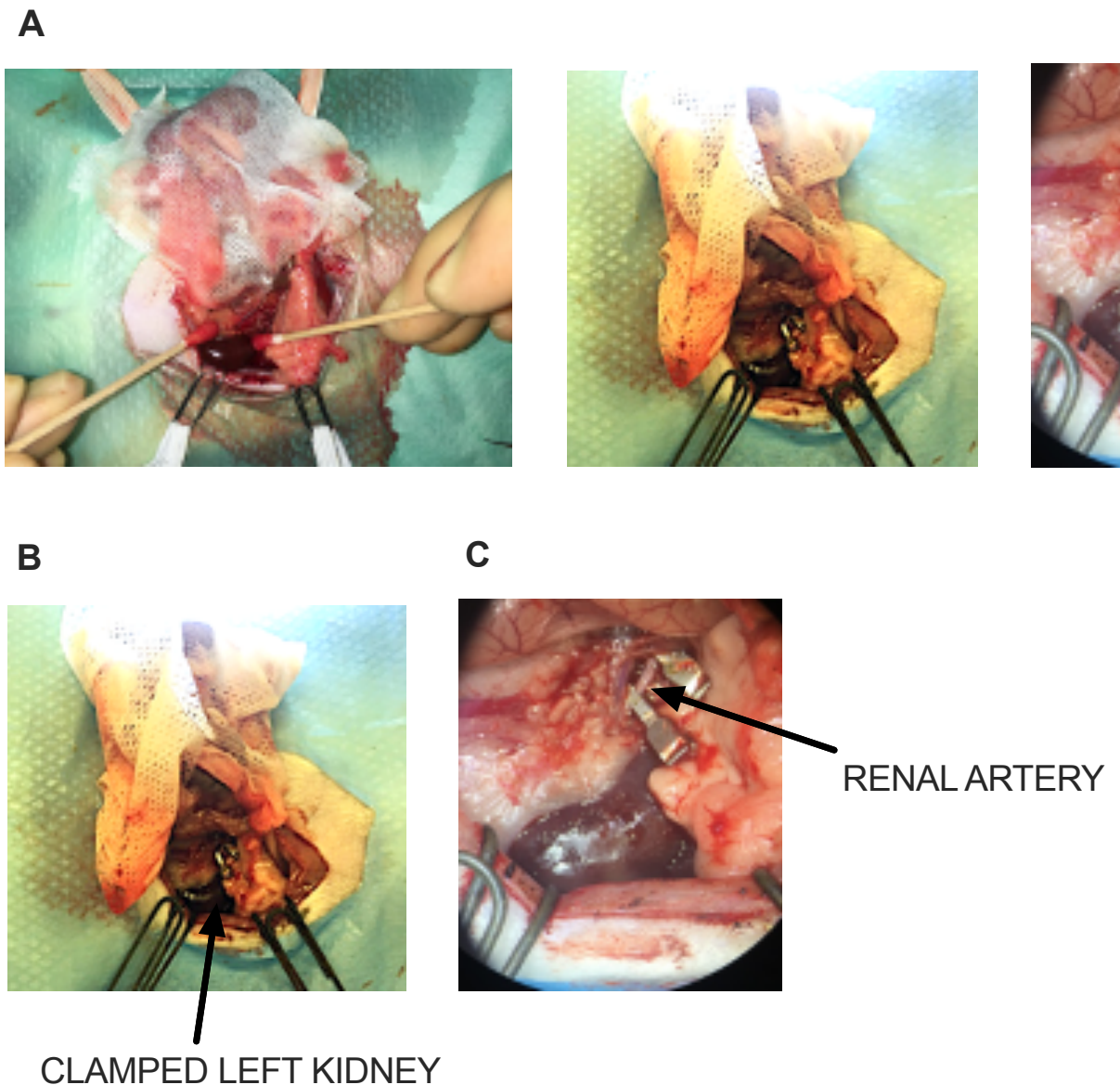
Figure 4.4 Left kidney IRI surgery and renal artery cannulisation. (A) Bowel retracted and protected in swab soaked in sterile water. Surgical exposure with retractors. Sterile cotton tip applicators ideal for retracting tissue and displaying the planes for dissection. (B) Macroscopic view of claps on renal artery within 15minutes of starting operation. Note discoloration of kidney confirms occlusion of renal artery and 120-minute countdown can commence. (C) Microscope view of clamps on renal artery which can now be dissected further to create more renal artery length for cannulation.
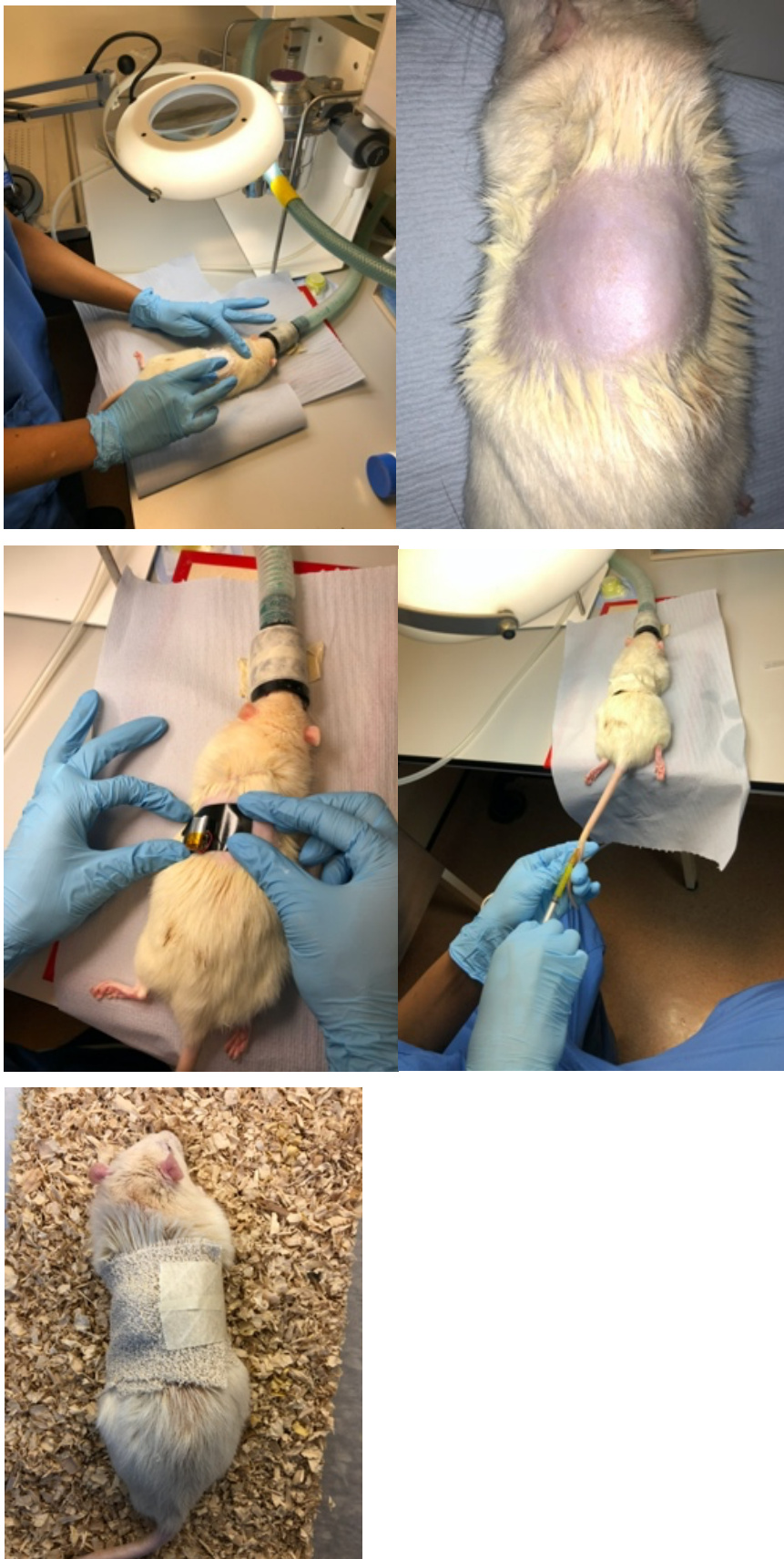
Figure 4.5 Transcutaneous GFR measurement. Rat is briefly anaesthetised, and the skin is shaved, and depilatory cream is applied. Transcutaneous device attached to back. FITC-sinistrin injected via tail vein then rat is recovered and allowed to roam free with transcutaneous measuring device attached.

4.4 RESULTS

4.4.1 HISTOLOGY

Whalen et al. eloquently demonstrated the long-term reduction of renal function with correlating histological findings such as epithelial breaks and hyaline cast formation. At six weeks post-IRI surgery there is a persistent, significant reduction in renal function compared to sham-operated rats (Fig. 1.5). When looking at the rat kidneys that underwent 2/3 nephrectomy, it is clear to see the degree of necrosis and remaining functional mass (Fig. 4.6). In our model, we identified features of tubular injury, at 48 hours post 120-minute ischaemia and reperfusion, which is expected and like the results seen by Whalen et al.
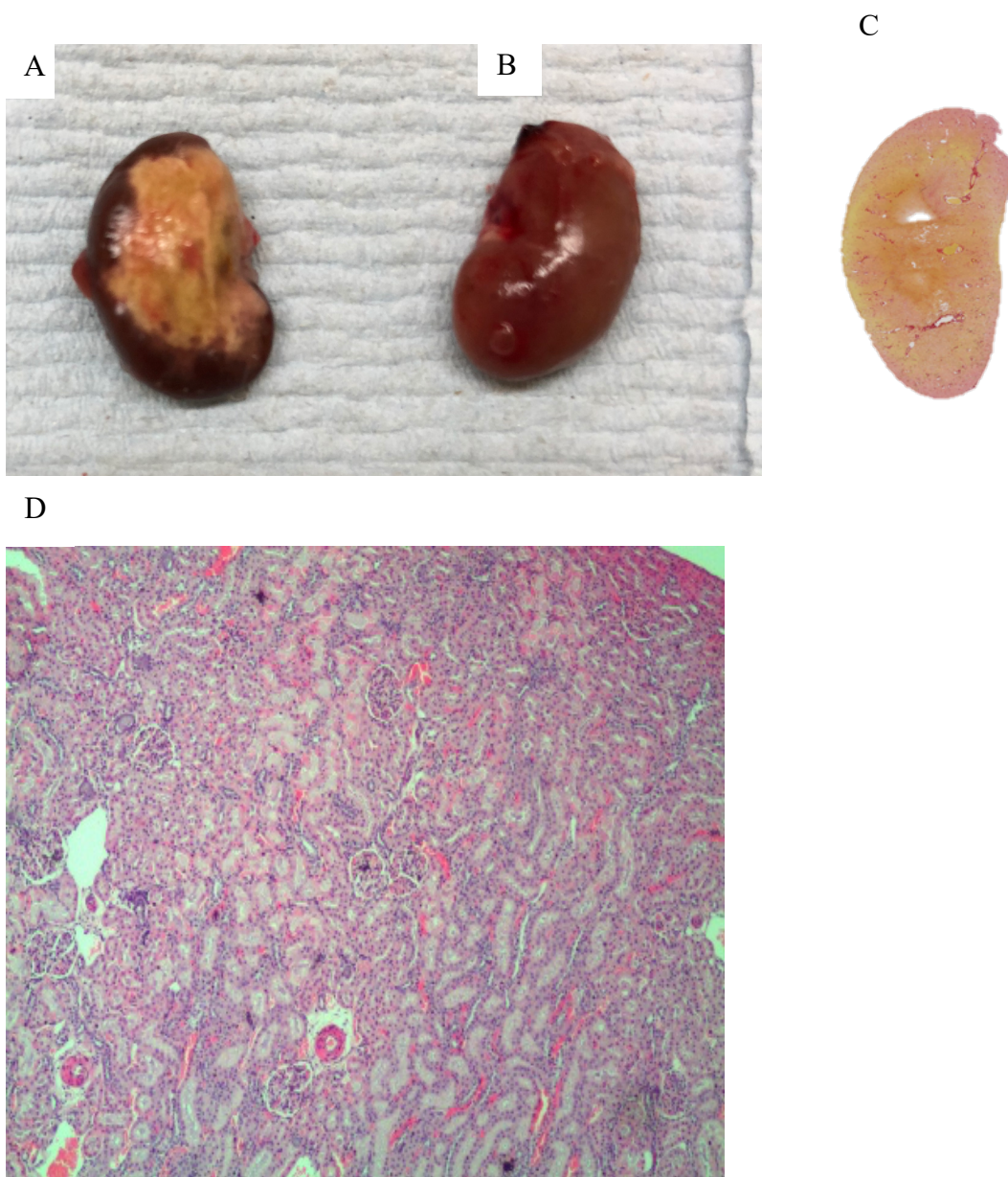
E
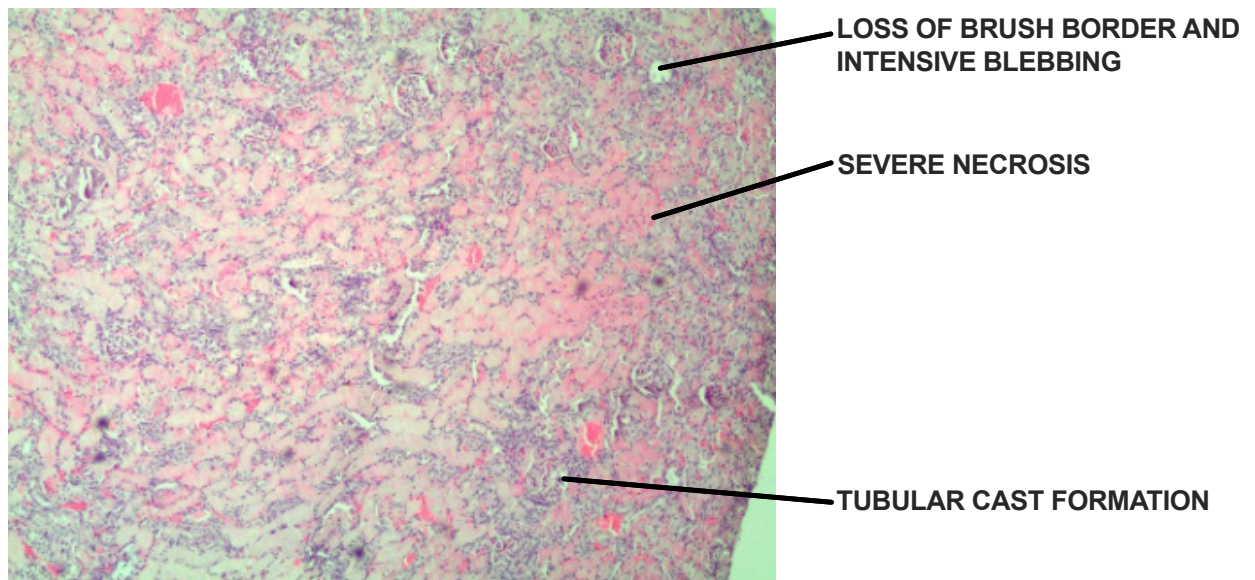
Figure 4.6 Kidneys retrieved 48 hours post IRI surgery confirm injury secondary to 2/3 nephrectomy surgery and IRI surgery. Left and right kidneys retrieved 48 hours post IRI surgery which is 2 weeks and 48 hours post 2/3 nephrectomy surgery. (A) Macroscopic picture of 2/3 necrosis of right kidney. (B) Left kidney recovering from severe IRI with no evidence of macroscopic necrosis. (C) Typical histological slide of left kidney. (D) 4x magnification of naïve left kidney for reference (E) 4x magnification of left kidney that underwent 120 minutes ischaemia with histological features of injury. Not possible to perform histological analysis on the necrosed right kidney

4.4.2 OPERATING TIME

The 2/3 nephrectomy operating time from the skin to skin varied between 15 and 30 minutes, depending on how quickly it took to identify the relevant vessels that supply two-thirds of the kidney. This does not include the time to get the equipment ready and to prep and drape the animal. The rats recover fast as the anaesthesia time is short, and the incision is small compared to other major abdominal surgeries. Three 2/3 nephrectomy procedures were comfortably achievable in a three-hour morning session.

The modified IRI of the left kidney operating time varied between 140 minutes and 160 minutes. Much of this time is waiting for the 120minutes of ischaemia to be reached. In this modified version, a puncture was made in the renal artery instead of completely transecting it. The puncture was large enough to allow the 30G Reycroft cannula to cannulate the vessel.

The first advantage of this was that there was a tighter seal around the cannula; therefore, no need for a rubber sloop and less spillage and more accurate delivery of the therapies. Secondly, repair of this puncture is quicker, less intensive and uses less suture material. On average, two interrupted sutures were required to close the defect compared to 12 interrupted sutures when the artery is completely transected. We had no instances of catching the back wall when closing the defect, but there is likely a higher chance of this happening compared to repairing a completely transected artery in the frame clamp. To test the artery is patent post suture repair the proximal clamp can be released to ensure there is no haemorrhage from the anastomosis and to see the vessel distal to the anastomosis expand. The distal clamp will stop any premature reperfusion of the kidney during this test.

The non-invasive renal function measurement takes around 15minutes to instigate once the rat has been anaesthetised. Once the device is attached, and the FITC-sinistrin has been administered data collection from the device begins and last for two hours. During this period the rat is placed back in its home cage where it can recover from the anaesthetic and roam freely. The rat does not have to be supervised, but regular checks can ensure the device remains in the right position. Removing the device does not require an anaesthetic and takes just a couple of minutes.

4.4.3 NON-INVASIVE RENAL FUNTION MEASUREMENT

The transcutaneous renal function measurement (Fig. 4.7) detects a significant reduction in renal function in our full model (stage 1 and 2) compared to naive rats at 48 hours.
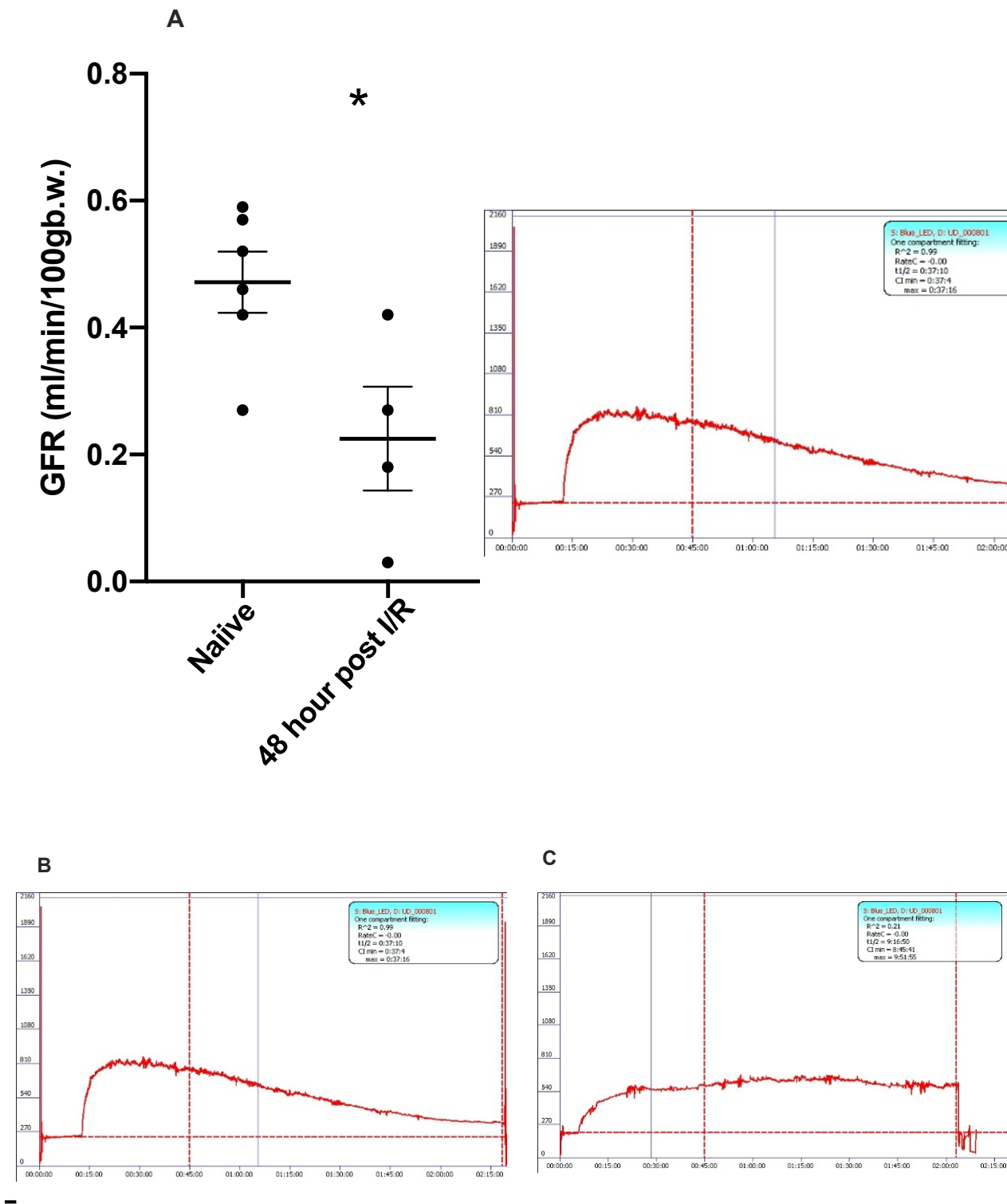
Figure 4.7 48 hour post IRI surgery there is a detectable reduction in renal function using the transcutaneous non-terminal renal function measurement device. A) Renal function 48 hours post full animal model (n=4) vs naïve rats (n=6) B) Typical FITC-sinistrin clearance post injection in a healthy rat taken from data collected from transcutaneous device. C) Typical clearance in a rat with reduced renal function. Significance was

considered for p values <0.05 (*) but included p values <0.01 (**), and <0.001 (***) as indicated.

4.4.4 MORBIDITY AND MORTALITY

On average weight dropped 5% by day five post-op then consistently increases after that back towards pre-operative weight and continues to increase (Fig. 4.8). Pre IR surgery weight was higher than pre 2/3 nephrectomy weight. A steady increase in weight in post 2/3 nephrectomy surgery (after the initial post-operative weight drop) supports the notion that rats recover well from the brief operation and suffer no significant sequelae from the 2/3 nephrectomy alone. During the two weeks between procedures, the healthy untouched left kidney ensures that the rat is not suffering from renal impairment. Weight and no concerning scoring on the grimace scales suggest the rats have minimal suffering and physiological upset postoperatively and has likely made a full recovery by the time of the second surgery.

There was an incisional hernia identified in the recovery of one rat that underwent the IRI surgery. The rat was taken back to theatre, and the suture was taken out and the abdomen re-closed. The animal made a full uneventful recovery afterwards.

There were two rat deaths after 2/3 nephrectomy procedure within a short period. The deaths were reviewed by the chief veterinary officer who also performed a post-mortem on both rats. The chief veterinary officer concluded that the deaths were not the result of the 2/3 nephrectomy surgery as there was no evidence of bleeding, wound infection, thrombosis or injury to surrounding structures. All other organs looked unremarkable except an enlarged spleen. It was concluded that an unknown infection was the cause and measures were taken to investigate the unit, but nothing was identified. Out of 47 2/3 nephrectomy procedures, there were no other deaths.

One rat died after IR surgery. The cause was intra-abdominal sepsis. During surgery (likely when retracting the bowel) there was what appeared to be a small serosal tear of the large bowel. As there was no visible contamination at the time a suture repair of the tear was performed, and the animal was closed as usual. The rat was kept under intensive observation postoperatively, but it was clear he was not recovering, and the decision was made to kill the rat humanely.

Due to the lower-than-expected morbidity and mortality, the named veterinary officer downgraded the severity of the 2/3 nephrectomy and IRI protocol from severe to moderate.
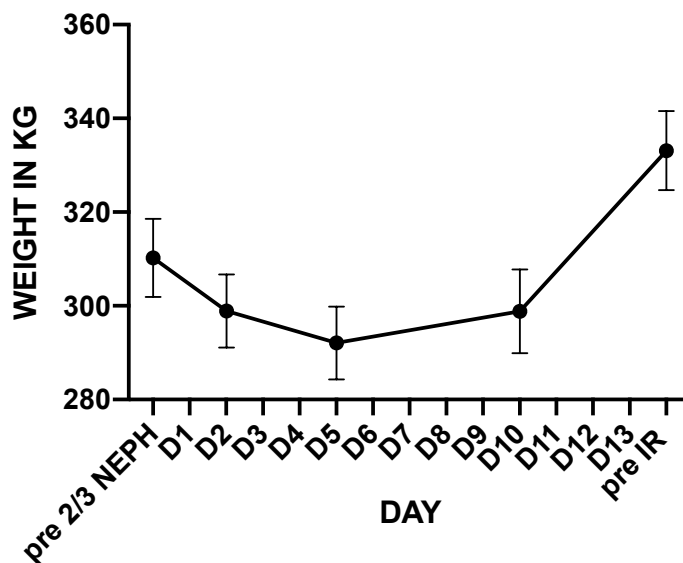
Figure 4.8 Rats recover well from 2/3 nephrectomy surgery. Mean rat weights pre and post 2/3 nephrectomy and pre IRI surgery measured in grams. (n=47). Rat surpass their pre 2/3 nephrectomy weight by the time there are scheduled for IRI of the contralateral (left) kidney.

4.4.5 DEVELOPED SURGICAL GUIDELINES

After performing over 200 microsurgical procedures, we have found the following tips to be helpful:

- 10-0 monofilament suture is expensive and was not always straightforward to source. After using it use the remaining suture was soaked in chlorhexidine, rinsed and stored. Before the next operation, the suture was then autoclaved in autoclave approved box. The same suture could be used to perform multiple procedures. We had no issue with infection or suture fracture, causing the breakdown of the anastomosis.
- Closing peritoneum with a continuous suture (3-0 Vicryl®), locking it then running the stitch back to close the skin allows for a two-layer closure with one stitch. We had no hernia postoperatively using this method.

- Having two sets of microsurgical instruments makes it possible to perform multiple 2/3 nephrectomy surgeries in a morning session. One set can be sterilised as the other is in use.

- Precise, sharp and undamaged microsurgical scissors are essential to make a small clean hole in the renal artery. We had our scissors refurbished and realigned if they were dropped or not cutting cleanly.

- Surgery should be stopped, and rat terminated if any bowel injury occurs. Suture repair of the bowel, washout of abdomen and antibiotics postoperatively is unlikely to be successful and can lead to unnecessary distress to the rat postoperatively.

- When performing IR surgery, a 1cm x 1cm cutting of a sterile swab rolled up can be placed in the abdomen to gently wedge the spleen up into the left upper quadrant out of the operating field. Good surgical exposure is essential for efficient and safe operation. Make sure to remove at the end of the operation.

- Opening the avascular tissue between the kidney hilum and peri-renal fat and then following this plane up the medial edge of the kidney is a quick route to get behind the fat covering the renal artery. Once making this incision, the fat medial to the kidney can be lifted, and the renal artery can be easily identified and traced back to the aorta. Not only is this route quick and causes minimal bleeding it also avoids the need to tie off the suprarenal vein.

- During IRI surgery locating the renal artery should be the priority after creating adequate exposure. Once the artery has been located, it should be clamped. This will start the 120 minutes of ischaemia. Then skeletonising the rest of the renal artery can begin, so it is ready for cannulation. Skeletonising the artery may take up to 30 minutes, and if this is done before clamping it is essentially adding 30 minutes on to the operation. From knife to skin to clamping the renal artery takes around 15 minutes. After the 120 minutes ischaemia, it takes around 10 minutes for a final inspection to ensure no bleeding, placement of organs back into their anatomical position and closure of peritoneum and skin. Total operative time can, therefore, be as little as 2hour 30minutes. Two per day is feasible.

- Cannulating the renal artery with the 30G Rycroft cannula in the right hand and using not traumatic forceps in the left hand to gently clamp around the artery cannulated by the catheter allows administration of therapy in a more controlled manner with minimal spillage and minimal damage to the artery.

- Opening the proximal renal artery clamp but leaving the distal clamp can allow testing of renal artery suture repair without reperfusion of the kidneys. Patency and haemostasis of the repair are assessed. Once the repair is proven to be adequate, the

distal clamp remains on until the desired 120minutes of ischaemia has been achieved then the distal clamp can be removed at exactly 120minutes.

- Some bleeding after suture closure of the renal artery defect does not necessarily mean a further suture is required. Some very light pressure with a cotton tip applicator (just enough pressure to stop bleeding but not occlude the vessel - often the weight of the applicator alone is enough) for one full minute can often be enough to stop the bleeding. If it is still bleeding, another suture can be added.

4.5 DISCUSSION

The transplant recipient often has little to no residual renal function at the time of transplantation. If the kidney graft does not recover quick enough, the patient can survive on dialysis until the graft kidney function picks up. This means the transplanted kidney graft recovers in an environment of renal failure. As far as we are aware, there is no rodent model of IRI in which the injured kidney recovers in and environment of renal failure. In the rat model of renal IRI described in this chapter, the 2/3 nephrectomy of the right kidney before the severe ischaemia reperfusion injury (IRI) of the left kidney creates an environment of reduced renal function. Therefore, the left kidney is recovering in an environment closer to mimicking renal failure and better representing the transplant patient.

One reason this had not been tested before is the fear of increased rat deaths. Whalen et al. severe rat model of IR results in kidney nephropathology seen in transplanted human kidney grafts (Whalen et al. 2016; Salahudeen 2004). The untouched contralateral kidney in that model protects the rat from acute kidney injury and death (Zager et al. 2011). If we then look at the 5/6 nephrectomy model of chronic renal failure (CRF) the rat is left with only 1/6th of its renal function. Despite this survival rates are high, and due to its excellent translation to human diseases, it has commonly been used in models of CRF over the last 50 years. Therefore, a hybrid Whalen et al. model and 5/6 nephrectomy animal model would leave the rat with 1/6th of its renal function and a recovering kidney. In theory, this type of model should not carry a significant risk of animal death and proving this was one of the main focuses of this chapter.

Performing a 2/3 nephrectomy on the right kidney prior to the severe IR of the left kidney, we can see that the survival was excellent and did not change compared to when the contralateral (right) kidney was untouched. Renal function tests confirmed that the IR kidney is recovering in an environment of reduced renal function. We can presume Ur, Cr, Mg, P, urea, uremic toxins will be increased, as this has been proven in 5/6 nephrectomy models; however, this was not tested on this occasion. There is an argument that the effects of a 5/6 nephrectomy have been well studied and documented so it will likely not add to the existing data and is not worth further animal studies. It remains unknown what effect the renal failure environment will have on a recovering kidney but the potential of the renal failure environment to interact with the many hundreds of pathways that are taking place after IRI cannot be ignored. It should be noted that this model represents a kidney recovering in a new environment of renal failure, not a longstanding "chronic" renal failure environment.

Therefore, although not fully representative of the transplant recipient, performing the 2/3 nephrectomy is a worthy addition as it does take the animal model one step closer without sacrificing animal welfare or research time and resources.

Tying a suture around the top and lower 1/3 of the right kidney instead of locating branches of the renal artery which supply 2/3 of the kidney would simplify the procedure even further. Not only would it be quicker but likely more accurate as some of the nephrectomised kidneys had slightly more than 2/3 nephrectomy and some slightly less – all depending on the renal artery branches which were tied.

As it has been proven to be safe, considering the 2/3 nephrectomy at the same time of IRI surgery is now also a possibility. Especially as a 2/3 nephrectomy will not create an immediate environment of renal failure as the untouched left kidney is enough to maintain sufficient renal function (until it undergoes the IRI). The argument against performing the 2/3 nephrectomy at the same time as the IRI surgery is that the inflammation and necrosis from the 2/3 nephrectomy may affect data analysis – especially if research is focusing on inflammation or immune response. The ischaemia of the right kidney at the time of IRI on the left kidney may also alter left kidney recovery like the distal ischaemia preconditioning discussed in chapter one.

This animal model has pushed the boundaries in terms of mimicking the transplant patient, and there is likely no further reduction of renal function that will be survivable (Craddock 1976). It may be possible to increase the 120minutes of IR, as 190minutes has been observed, but with 120 minutes already achieving a severe, longstanding injury there may not be much more to be gained versus the associated increased risks. The only animal model that would be more representative of the transplant patient would be to implant a kidney graft into a rat that has had a 5/6 nephrectomy. However, such a transplant model will be more time consuming, require a donor rat, be technically more challenging and carry more risks of surgery such as thrombosis and stenosis. A transplant model like that could still have its place in testing promising therapies developed on lesser severe models like the one described in this chapter.

The 2/3 nephrectomy surgery is an additional step to the Whalen et al. model. Once competent in the procedure, skin to skin operating time was quick and through a small midline laparotomy incision. All rats recovered swiftly apart from the two deaths that were concluded as not being a direct surgical complication by a post-mortem performed by the

chief veterinary officer for the University of Glasgow. After the 2/3 nephrectomy surgery, the rat does not suffer from any sequelae of CRF as they still have a healthy contralateral kidney. Weights did not take any continuous unexpected drop supporting the notion that there was minimal suffering and physiological stress after the surgery. Two weeks recovery before embarking on IRI surgery ensures the rat is fully recovered and there is no ongoing post-operative inflammatory response which could interfere with the IRI and therapies being tested. The IRI surgery was not any more difficult because of the 2/3 nephrectomy surgery two weeks prior. There were no adhesions, altered anatomy or difficulty dissecting out the left kidney and the midline laparotomy wound healed the same as it did after the first operation. Two methods which could potentially reduce the operative time further are cauterisation of the renal artery branches or ligation of the top and lower poles of the kidney. Ligation of the kidney itself has been reported to be quicker with less associated complications of bleeding and infection compared to kidney pole excision (R.-Z. Tan et al. 2019)

Whalen et al. successfully transected the renal artery, and eloquently demonstrated how it was possible to administer therapies via the renal artery in the animal model of severe IRI. Human transplantation gives unique easy access to the renal artery at the time of transplantation and could be the optimum route for many therapies with less biodistribution, avoidance of first-pass metabolism and optimal dosing. However, completely transecting the renal artery to administer the therapies is technically very challenging as two ends need to be anastomosed together using multiple interrupted sutures. The learning process is also long, and the risks of complications are not insignificant. To address these issues, an alternative method of renal artery cannulisation was attempted. Instead of transecting the renal artery completely, a puncture was made in the artery, with the microsurgical scissors, big enough to allow the 30G cannula to pass. Cannulation via this puncture was straight forward with 100% success and perfusion of the kidney was confirmed by colour changes of the kidney on the administration of vehicle control or therapy. There was also no need to sloop the artery. Closing of the hole was achieved with 1 to 3 interrupted sutures. This is significantly easier, less intensive and less time consuming than anastomosing two completely transected ends together. Although Whalen et al. did not experience any unacceptable levels of complications, in theory, this newer technique would reduce the risk of thrombosis or stenosis as there is fewer sutures, scarring and no chance of the vessels becoming twisted when brought together all of which could cause bleeding, stenosis or thrombosis. No kidney was ischaemic when retrieved at a later date and being more comfortable to perform made it is easier to teach and learn.

Another shortcoming of the Whalen et al. model was the time consuming, terminal and technically challenging inulin plasma clearance studies. Although inulin clearance studies are considered the gold standard in measuring the glomerular filtration rate the FITC-sinistrin transcutaneous clearance measurement method offers a means of measuring renal function that is still significantly more sensitive than serum Ur and Cr. GFR results using this method are highly comparable to the gold standard plasma inulin clearance studies (Schock-Kusch et al. 2009). The novel transdermal transducer which measures FITC-sinistrin is a much easier alternative. Administration of the FITC-sinistrin and application of the device is straightforward and can be completed under a brief general anaesthetic. The device is then left on the rat for two hours in an unmonitored cage. Removal of the device is straight forward and did not require a further anaesthetic. The animal is free to roam the cage with the device attached, and the light device stuck to the back does not seem to cause much discomfort. If multiple devices are available, it is possible to measure the renal function of multiple rats in a short period. This is not possible with inulin plasma clearance studies as the whole procedure takes around 6 hours; therefore, limited to one per day. Being able to measure the renal function at multiple time point on the same rat reduces rat numbers compared to the terminal inulin studies and satisfies 2 of the 3R principles - reduce and refine. In chapter five, FITC-sinistrin transcutaneous measurement is used to compare rats treated with vehicle control and adipose-derived stromal vascular fraction. Serum Ur and Cr measurement would not be sensitive enough to detect differences between the two groups.

Replacing the inulin clearance studies and modifying the renal artery cannulation technique has made the Whalen et al. model less technically challenging, less time consuming and quicker to learn. An experienced rodent microsurgeon or human surgeon can competently perform the procedures after a short period of training, especially as the complex inulin studies have been replaced. Non-experienced surgeons will likely take longer, but careful planning can reduce the number of rats required for training and ensure maximum usage of the rat (such as removing the inguinal fat pad beforehand for extraction of stem cells). Early involvement of the named veterinary officer during training and subsequent experiments is essential for animal welfare, training, and experimental support and to ensure the principles of 3Rs are being upheld.

In conclusion, this animal model better mimics the transplant patient, is less technically challenging and is less time-consuming. It has pushed the boundaries of the severe renal IRI rodent model. By reducing rat numbers required for training and experiments and reducing the potential risks of surgery, this model adheres to and promotes the 3R principles.

However, it has yet to be demonstrated if these renal failure changes caused by the 2/3 nephrectomy have a significant impact on the kidney recovering from IRI or the therapies being investigated.

CHAPTER 5:
BIODISTRIBUTION OF ADIPOSE DERIVED STROMAL VASCULAR FRACTION ADMINISTERED VIA RENAL ARTERY

5.1 INTRODUCTION

A vast array of factors can alter the biodistribution of administered regenerative cells such as route of administration, cell source, method of cell preparation. Recipient inflammation, hypoxia, repair, and malignancy can also modify their movements. To our knowledge little data exists on the biodistribution of ADSVF administered via the renal artery in a bid to ameliorate renal IRI.

It is essential that we better understand the biodistribution of administered cells to ensure safety, effectiveness, and aid mechanistic understanding. Furthermore, biodistribution knowledge is crucial when it comes to dosage regimes as we know from some safety studies that thromboembolic events are a potential risk from high dosage regenerative cell therapies.

Stem Cell Labelling and Tracking

To acquire biodistribution data, a variety of labelling and imaging techniques are available. Popular methods of imaging include bioluminescence, fluorescent, MRI, CT, ultrasound, and nuclear imaging. Each has its advantages and limitations. Considerations when choosing the right modality include resources, experience, available expertise, the size of the animal or tissue and the length of time tracking is required. Often a combination of modalities is used, and with each modality, there is an ever-expanding repository of labelling techniques and molecules.

The PerkinElmer In Vivo Imaging System® (IVIS) (PerkinElmer, Massachusetts, USA) is an optical imager that can perform either trans-illumination or epi-illumination with its range of 28 high-efficiency filters. It can detect bioluminescent and fluorescent reporters from the blue to near-infrared wavelength {PerkinElmer:va}. Its high sensitivity and resolution make it suited to in vivo small animal imaging or ex vivo imaging of harvested organs for higher sensitivity. In vivo, imaging also allows for longitudinal imaging if required, and the lack of

radiation makes it a safer alternative to modalities such as Computed Tomography and positron emission tomography.

Unlike pharmacological agents, regenerative cells may not merely be metabolised and excreted. They can migrate, proliferate, and integrate. To track administered cells with a fluorescent imaging modality like the IVIS, the administered cells of interest need to be labelled. An ideal label will be non-toxic, stable, highly fluorescent, have minimal cross-contamination and have a cost-effective and straight-forward labelling process. Widely used cell tracking labels include carboxyfluorescein diacetate succinimidyl ester (CFDA-SE), carboxyfluorescein succinimidyl ester (CFSE) and PKH26. Lipophilic dyes in the far-red spectrum, such as carbocyanine DiOC18 (DiR), have excellent fluorescent properties and make them an attractive label, particularly with whole-body imaging. However, like all dyes, contamination of dye to the microenvironment can be an issue; therefore, cross-validation with another dye or modality is necessary (Lassailly et al. 2010).

Routes of Administration of Regenerative Cells

There are multiple routes in which stem cells can be administered for therapeutic use. Intra-arterial and intra-venous administrations via major arteries and veins such as those in the neck provide an easily accessible route of administration. High doses can be given in a short period, and the risk of clogging up vessels is reduced compared to using smaller vessels, and in many clinical studies, this route is safe. Other research has looked at more targeted administration to aid the therapeutic intent, such as into the supplying artery of a particular organ of interest. However, the technical difficulties and risks can diminish the advantage of direct injection to the organ. Non-intravascular routes like intraperitoneally, subcutaneously, intramuscularly, and direct injection into organs such, as the liver or heart, have also been researched.

Stem cells delivered into major veins, such as the external jugular, appear to get trapped in the microvasculature of the lungs as described since 2003 by Barbas et al. and has subsequently been reproduced in several other studies (Barbash et al. 2003). Initially, what was not clear was whether the trapped cells in the lung were living and continue to have the pluripotent capacity. However, in more recent studies of cells injected into the lung, it seems that the cells remain living for the first 24hr and soon after disappear (Eggenhofer et al. 2013). The majority of the signal seen 24 hours post-administration via a major vein, is

within the liver but on analysis, these cells are not living, and the signal represents cell debris or phagocytosed labelled cells (Eggenhofer et al. 2012).

To get around the microvasculature of the lung, intra-arterial administration or direct organ arterial administration has been attempted. There has been a particularly abundant volume of research in using intra-arterial administration in cardiology and the management of ischaemia of the heart. Intracoronary and intracardiac administration of stem cells has advanced to clinical trials with favourable outcomes on ventricular function (Brehm & Strauer 2006; Strauer et al. 2005). Many studies have demonstrated the administration of cells intra-arterially significantly reduces the incidence of stem cells becoming trapped within the lung microvasculature (Mäkelä et al. 2015) and have increased uptake at target organs (Toupet et al. 2015). There have also been studies looking at direct renal artery injections as we propose. Previously concern was raised that intra-arterial administration caused entrapment and occlusion in the microvasculature of first-pass organs. However, a study found that bone marrow-derived stem cells injected directly into the renal artery of cats with IRI did not have a detrimental clogging effect. Similar to the rodent models, the stem cell recipient cats had fewer degenerative changes on histology and less apoptotic renal tubular epithelial cells (L.-J. Wang et al. 2019). A multicentre randomised control trial involving 21 cases found umbilical cord-derived stem cells delivered directly into the renal artery at the time of transplantation to be safe and feasible (Q. Sun et al. 2017). Nevertheless, there is evidence that once a threshold concentration is reached there can be occlusion of the microvessels when administered intra-arterially, especially into arteries directed to single organs with microvasculature such as the kidney or brain. Li-li A Tan et al. also found that velocity of administration can enhance the micro-embolic complication; however, these effects as far as we can see have not been seen in human-sized organs (Cui et al. 2015).

5.2 HYPOTHESIS

Administration of adipose-derived stromal vascular fraction, via the renal artery in an animal model of renal ischaemia reperfusion injury, is an effective method of delivery and reduces off-target biodistribution.

5.3 METHODS

Adipose tissue was retrieved from the inguinal fat pad of adult Fischer 344 rats. The stromal vascular fraction (containing the adipose-derived stem cells) was isolated from the adipose tissue, and the cells were labelled. The labelled ADSVF was then administered via the renal artery in our model of rat renal ischaemia reperfusion injury. The rats were sacrificed at 1 hour, 24 hours, 48 hours, and 1-week post-administration of ADSVF. Organs were retrieved, directly imaged in the IVIS, and processed for histological analysis to determine the location of labelled cells in the major organs or processed for flow cytometric analysis.

Total radiance efficiency was used to measure the fluorescence of each organ. Weights of animals were recorded at multiple time points, including at termination. All rats used were adult Fischer 344 of similar ages and size. Organs were imaged ex-vivo.

5.3.1 ANIMAL HOUSING AND HUSBANDRY

Animal housing and husbandry were standard throughout all procedures, as described in section 2.1.

5.3.2 ISOLATION OF ADIPOSE DERIVED STOMAL VASCULAR FRACTION FROM ADIPOSE TISSUE

Adipose tissue was obtained from the inguinal region of adult Fischer 344 rats. The retrieval of rat adipose tissue is described in chapter 2.2. Isolation of adipose-derived stromal vascular fraction were conducted in a standard fashion, as previously described in section 2.4.

5.3.3 QUANTIFICATION, STORAGE AND PREPARATION OF ADSVF FOR ADMINISTRATION

Quantification, storage, and then subsequent preparation of ADSVF for administration was conducted in standard fashion, as previously described in section 2.5.

5.3.4 LABELLING OF ADIPOSE DERIVED STOMAL VASCULAR FRACTION FOR ADMINISTRATION

For IVIS imaging and flow cytometric analysis, ADSVF were labelled with the near-infrared fluorescent lipophilic DIR (ThermoFisher Scientific). The cellular membranes were labelled according to the manufacturer's protocol. For rats that would undergo fluorescent imaging of organ sections, PKH26 (Sigma-Aldrich, UK) lipophilic dye was used. Cells were labelled as per recommended Sigma-Aldrich protocol.

5.3.5 GROUP SELECTION

Adult male Fischer 344 rats were randomly assigned to either a control group or treatment group. Control group received PBS with 10% rat serum, and the treatment group received 7E+5 to 1E+6 labelled ADSVF. The different time points at which the rats were terminated are 1 hour, 24 hours, 48 hours and one week.

5.3.6 RENAL ISCHAEMIA REPERFUSION INJURY MODEL, ADMINISTRATION OF THERAPIES AND PERIOPERATIVE CARE

The ischaemia reperfusion injury model is described in detail in chapter 4. In brief, male adult Fischer 344 rats undergo a 2/3 nephrectomy of the right kidney. The rat is recovered for at least two weeks before undergoing surgery in which the left renal artery is clamped for 120 minutes. Prior to releasing the clamp, the labelled ADSVF or control is administered via the left renal artery. At 120 minutes the clamp is removed, and reperfusion of the left kidney ensues. The animal is then recovered, and its post-operative care is given as described in chapter 4.3.6. Rats were then terminated at specific timepoints and organs analysed for biodistribution of ADSVF.

5.3.7 ORGAN RETRIEVAL AND PROCESSING

Organ retrieval and processing was standard throughout all procedures, as described in section 2.6.

5.3.8 WHOLE ORGAN FLUORESCENT IMAGING

As each organ was retrieved, it was individually placed in a Petri dish containing PBS to rid surface blood then placed in another Petri dish with PBS. The organs were stored at 4°C in darkness as the rest of the organs are being retrieved. Time for all organs to be retrieved averaged less than 10 minutes. The organs were then immediately taken to the IVIS scanner (covered from light) for imaging located in the same facility.
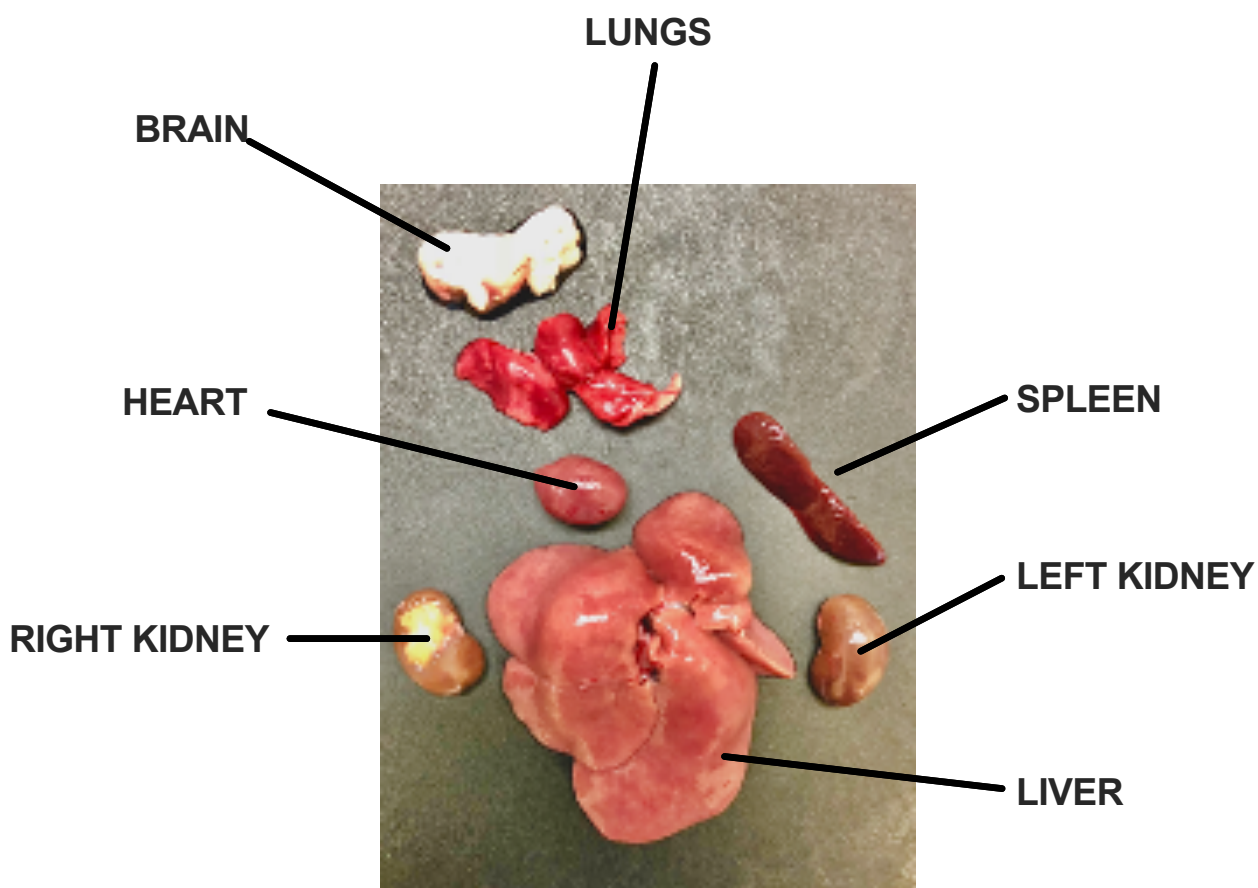
Figure 5.1. Retrieved rat organs in standard position ready of IVIS imaging.

The PerkinElmer In Vivo Imaging System® (IVIS) is a non-invasive imaging device that uses a set of filters which allow detection of bioluminescent and fluorescent reporters across the blue to near infrared wavelength region {PerkinElmer:va}. Organs were laid out in the IVIS in a standard layout mimicking in vivo positioning (Fig. 4.1) and scanned using the following settings:

- Epi-illumination
- 2D imaging only
- Fluorescence is measured in Radiant efficiency (total)
- Exposure 0.5 seconds

- Binning: small (see IVIS tips and trick at CTAC.mbi.ufl.edu)

- Excitation filter 680 for DiR and 551 for PKH26

- Emission filter 700 for DiR and 567 for PKH26

- The aperture (f/stop) was set at 2

Images were saved and analysed using the PerkinElmer In Vivo Imaging Software for the IVIS imaging systems®. The software was used to identify regions of interest, label organs and measure the radiant efficiency so that organ fluorescence could be analysed.

5.3.9 RENAL HISTOLOGY PREPARATION

Organ retrieval was described in chapter 2.6 and organs were imaged as described in chapter 5.3.8. After imaging in the PerkinElmer In Vivo Imaging System® they were immediately removed two thirds of the organ was stored in 10% formalin. The remaining third was used for flow cytometry described below. After three to seven days of being fixed in 10% formalin the organs were then transferred to 70% ethanol for a further 48 hours before being subjected to a tissue dehydration and paraffin embedding process. All tissues were then sectioned at 5 micrometres. During storage and transportation, the tissues were kept in darkness.

5.3.10 SECTIONED TISSUE FLUORESCENT IMAGING

Paraffin embedded organs were sectioned into a thickness of 5 micrometres then transferred to histological glass slides. Unstained sections were imaged using the Odyssey CLx, LI-COR® (Biosciences Ltd.) fluorescent imager. Scanning was performed using the 700 Channel Laser Sources (which is the lowest and has a wavelength of 685 nm nanometres) for detecting PHK26 labelled ADSVF. Program was set at 42 μm resolution and 0 mm offset with the lowest quality. Scan setting were the same throughout all section imaging. A freehand region of interest (ROI) was created to define the outline of the organ using Odyssey software. To determine the organ biodistribution of ADSVF within the kidney, ROI were measured in two areas, renal cortex, and renal medulla. Signal intensity was measured by Image Studio (version 5.2) software.

5.3.11 FLOW CYTOMETRIC ANALYSIS

Once the rat was terminated at the designated time point, the organs were retrieved as described in section 4.3.7. One third of each organ was immediately stored in 20mM HEPES PBS (Sigma Aldrich) at 4°C. The organ was then mechanically homogenised to 1mmx1mm then incubated with a digestive enzyme solution (hyaluarinase 1.33mg/ml, collagenase 1S 18.36 mg/ml, collagenase X1 1.56mg/ml, Sigma Aldrich). After red blood cell lysis buffer (Miltenyi Biotec SAS) was added to the suspension it was washed in PBS and diluted 1-8 million cells/ml. Cells were incubated with the rat 2.4G2 Fcyll blocker (BD Biosciences, San Jose, CA) and surface markers for 60 minutes. Cells were then fixed in 4% solution, and resuspended in 2% albumin (PAN-Biotech, Aidenbach, Germany) in PBS. Fluorescence was measured using a Fortessa flow cytometry (BD Biosciences). Each sample contained at least 200,000 viable cells using FSC x SSC gating and viability (e780) negative. Gating was determined by both single-stained control and fluorescence minus one control. FlowJo software version 10 (Ashland, OR) was used for data analysis. Table 3.1 describe the markers used to interrogate ADSVF.

Statistics. A 2-way student's t-test was carried out to determine the differences in the mean average for sample sizes >5 of equal variance. Mann-Whitney U test was used to analyse smaller sample sizes. One-way ANOVA and a Tukey post hoc test was used to detect differences between the means of two or more groups. Analyses was performed with Prism 6.02 (GraphPad, San Diego, CA). Mean and standard error of mean (SEM) are displayed. Significance was considered for p values <0.05 (*) but included p values <0.01 (**), and <0.001 (***) as indicated.

5.4 RESULTS

5.4.1 EX-VIVO FLUORESCENT IMAGING OF ORGANS

In each rat after 24 hours, the highest signal, on IVIS scanning, is seen in the liver, followed by both kidneys then spleen and lungs (Fig. 5.2a). Due to scale settings, fluorescence in the lungs of rat 2 is likely autofluorescence. Focal hot spots can be seen in the left kidney in rat two even under IVIS scanning. In comparison to other organs within the rat, there is no signal in the brain. Imaged sections of the left kidney better demonstrated the focal signal spots seen on whole organ IVIS imaging (Fig. 5.2b). In particular, the signal is around the edges likely representing the renal cortex. No such focal spots of DiR labelled cells were seen in any other slides under LI-COR imaging, including the liver.

In F344 rats 48 hours post-ADSVF injection, intense focal signal points are seen within the left kidney (Fig. 5.3). Again, the liver had a diffuse signal. The spleen after 48 hours appears to fluoresce brighter when compared to 24 hours. No evidence of signal in the remaining organs relative to the kidneys, liver, and spleen. The picture was similar after one week (Fig. 5.4). However, this time signal was now more prominent in the spleen and liver compared to the other organs. The left kidney still showed some focal spots of signal.

IVIS images of rats treated with PBS and 10% rat serum did not have any of the focal hotspots seen in rats that received labelled ADSVF (Fig. 5.5). The liver did not overly emit signal compared to other organs. The organs with the highest radiant efficiency were the kidneys. Nevertheless, imaging sections of these control kidney did not identify any signal confirming that the signal seen in IVIS was likely autofluorescence (Fig. 5.5c).

A

ROI 5[31%]=4.327e+08
ROI 7=1.970e+08
ROI 6=6.309e+08
ROI 2[31%]=8.508e+08
ROI 3[31%]=8.056e+08
ROI 1[31%]=9.246e+09
ROI 4=5.226e+08

Rat 1

ROI 7[28%]=7.571e+08
ROI 4[28%]=2.729e+09
ROI 6=3.675e+08
ROI 3[28%]=2.604e+09
ROI 2[28%]=9.041e+10
ROI 5[28%]=1.035e+09
ROI 1=1.915e+09
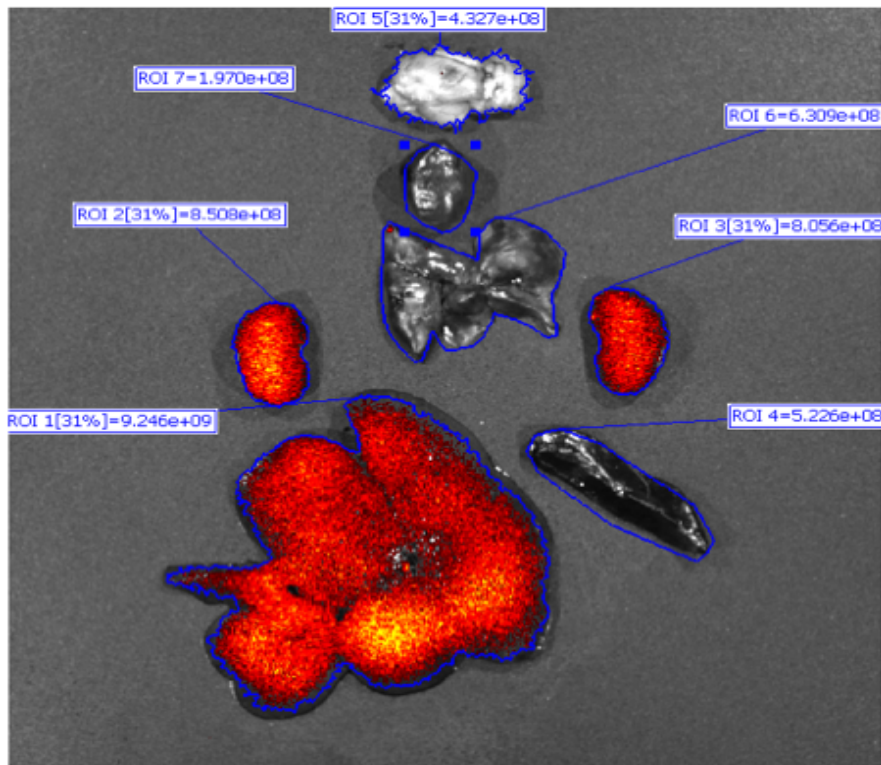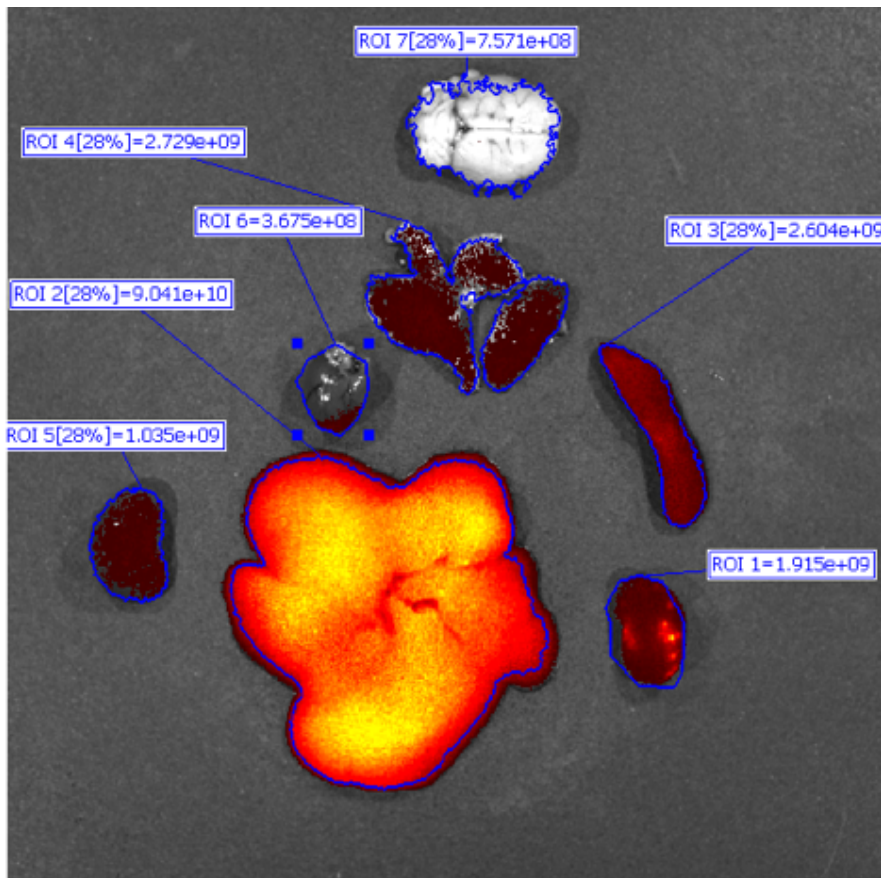
Rat 2

B
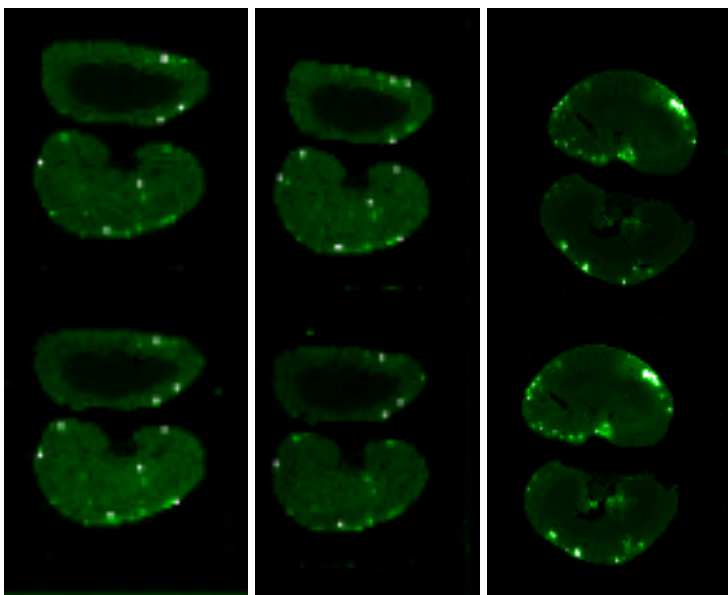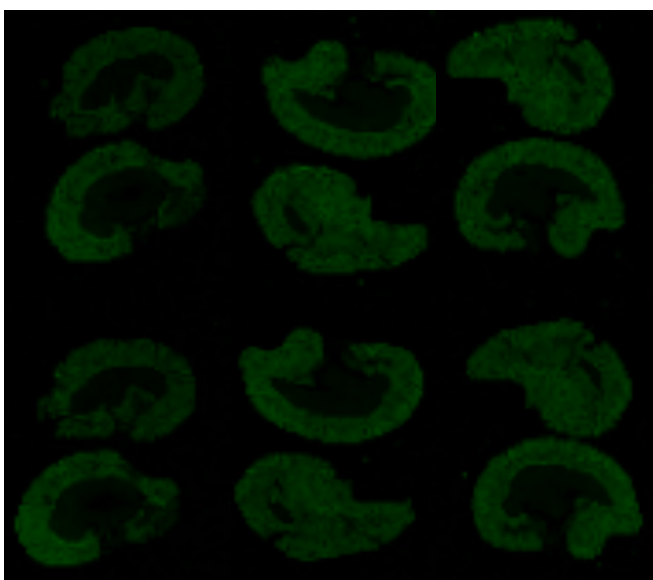
Left kidney

Right kidney
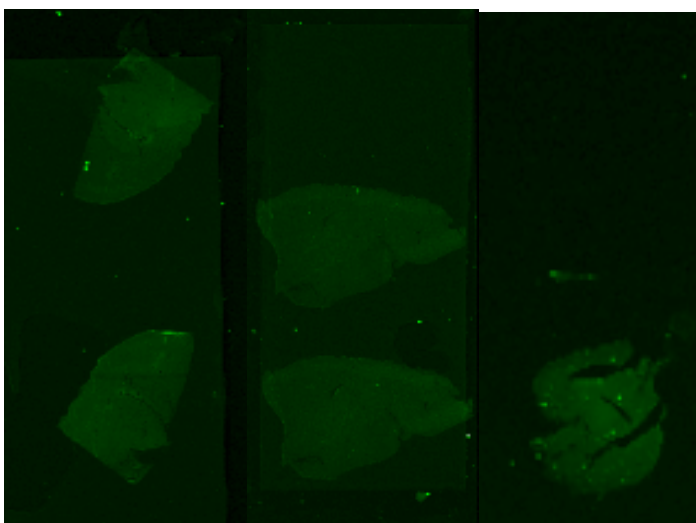
Liver
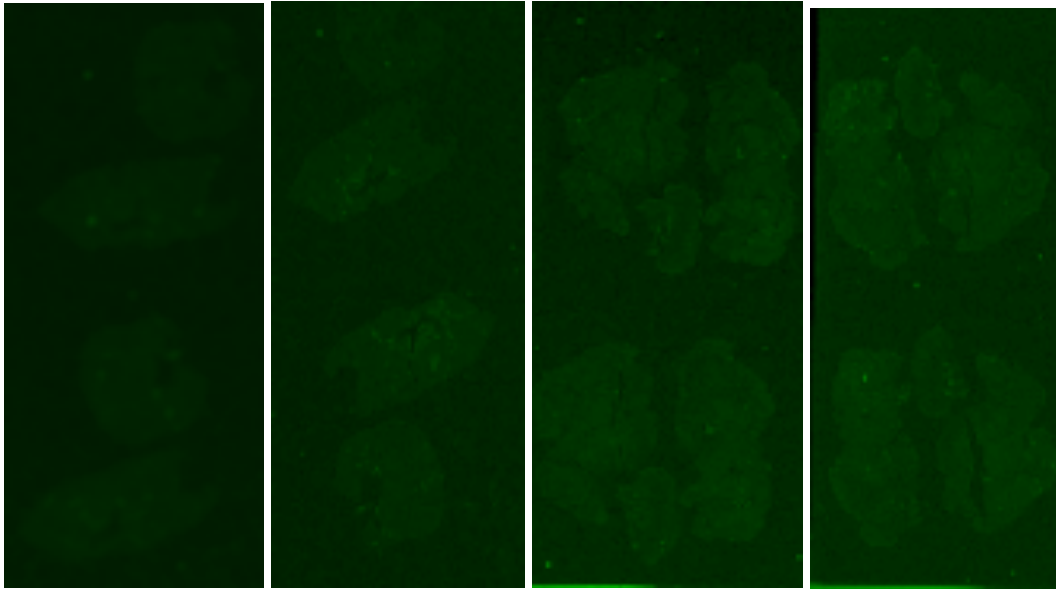
Lung   Brain

Figure 5.2 DiR labelled ADSVF can be seen in the left kidney 24 hours post administration via the left renal artery. Fluorescent images of experimental rats which underwent severe renal IRI of the left kidney, as described in chapter 4, then received DiR labelled ADSVF via the renal artery and terminated 24 hours later. (**A**) Ex vivo IVIS imaging of organs from 2 rats demonstrated the appearance of increased signal within both kidneys and the liver with intense hotspots within the left kidney. (**B**) LI-COR® images of organ sections from the same 2 experimental rats confirms signal within the left kidney but no other convincing evidence of signal in any other organ.
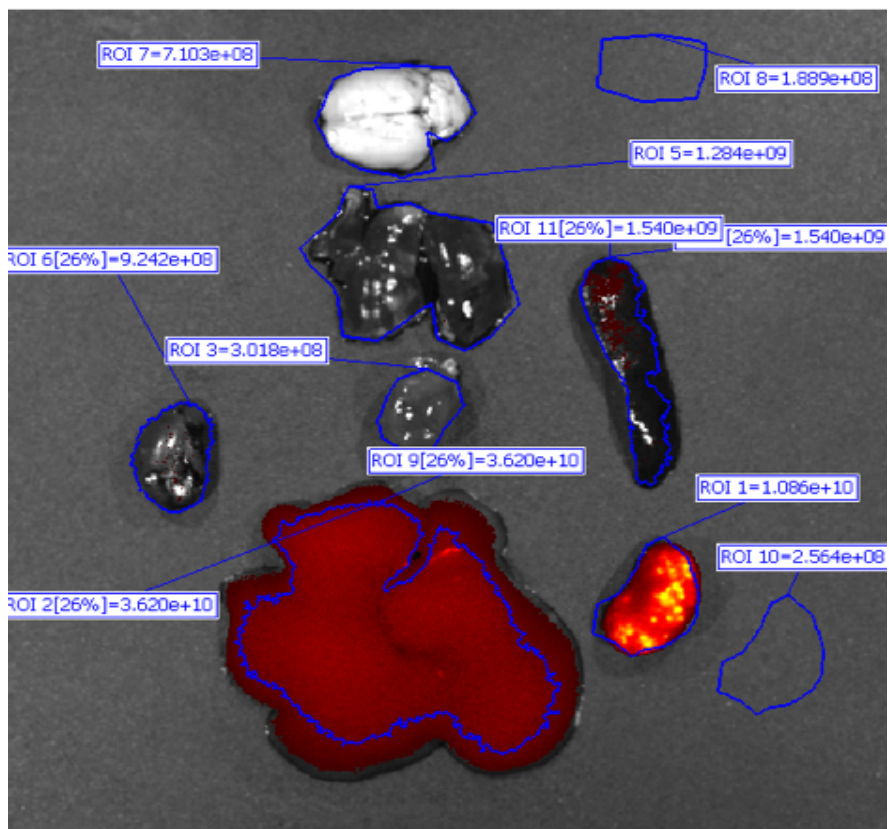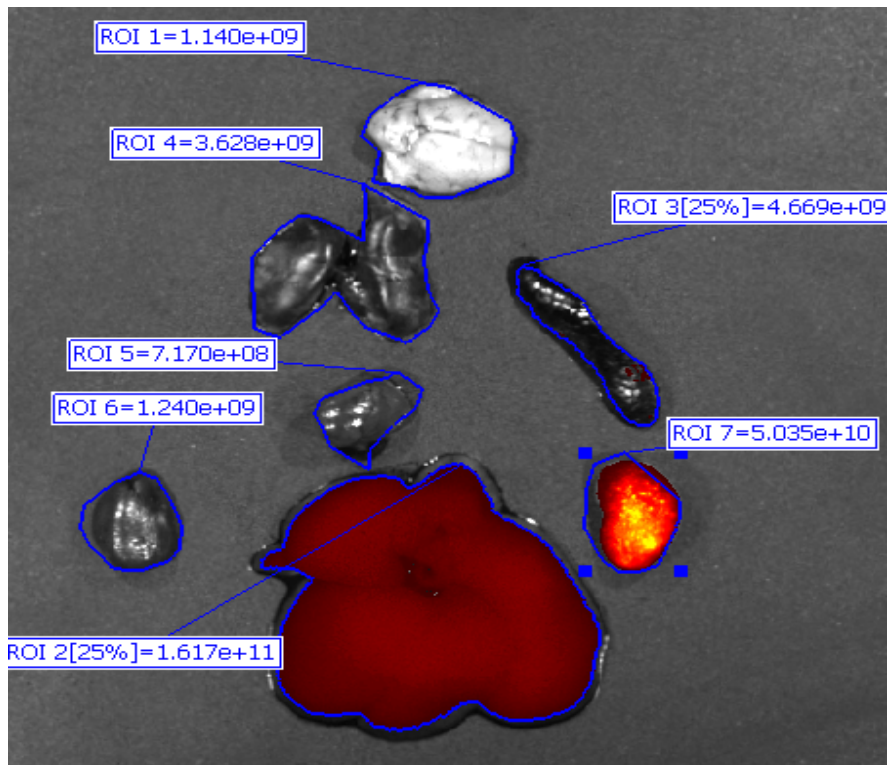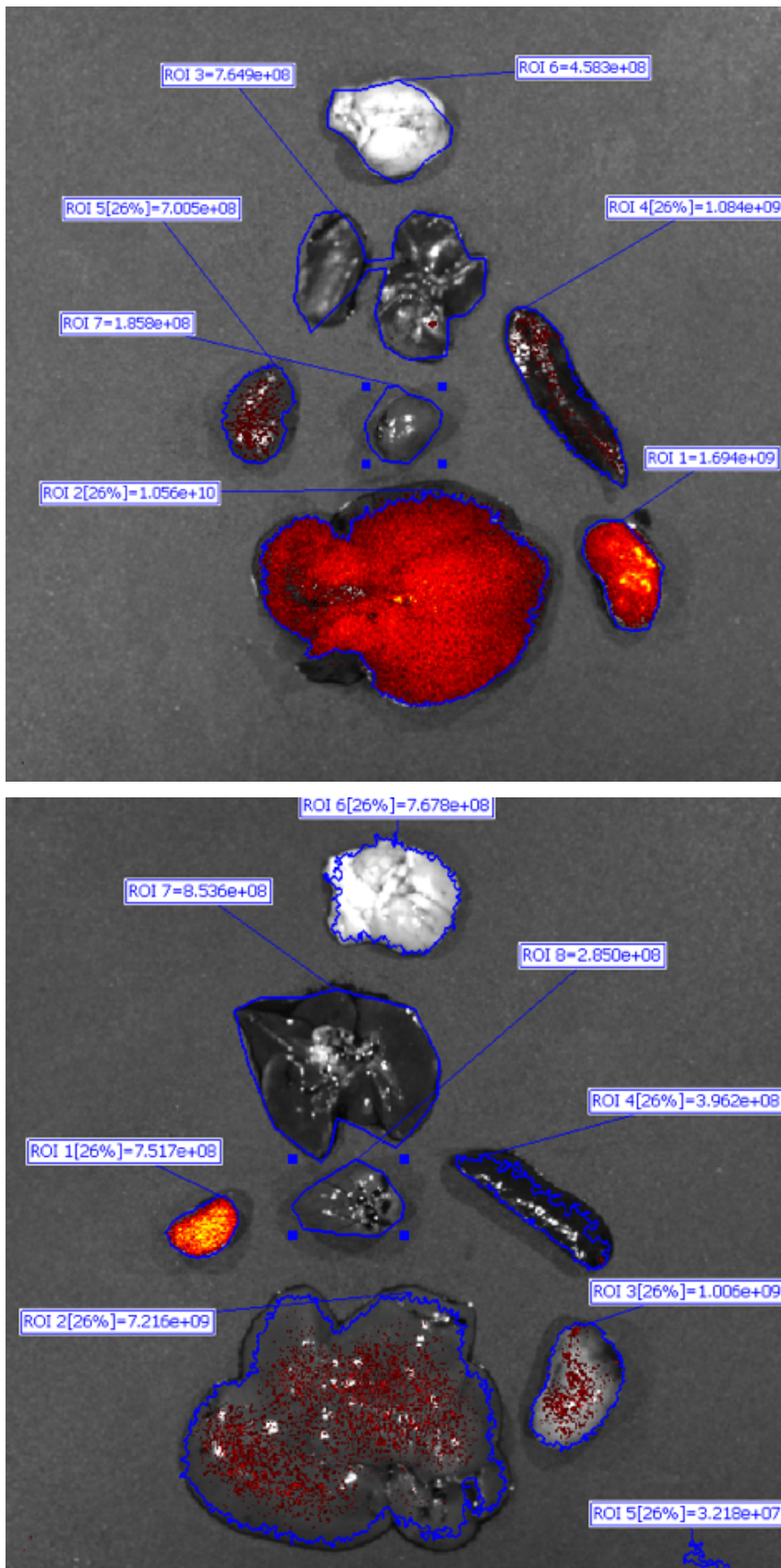
Figure 5.3 DiR labelled ADSVF can be seen in the left kidney 48 hours post administration via the left renal artery. Fluorescent images of experimental rats which underwent severe renal IRI of the left kidney, as described in chapter 4, then received DiR

labelled ADSVF via the renal artery and terminated 48 hours later. Ex vivo IVIS imaging of organs from 4 rats demonstrated the appearance of strong signal hotspots within the left kidneys only of 3 out of the 4 rats. There is the appearance of some increased signal to a lesser degree from the liver. No signal emitted from lungs, heart, and brain in comparison to liver and kidney.
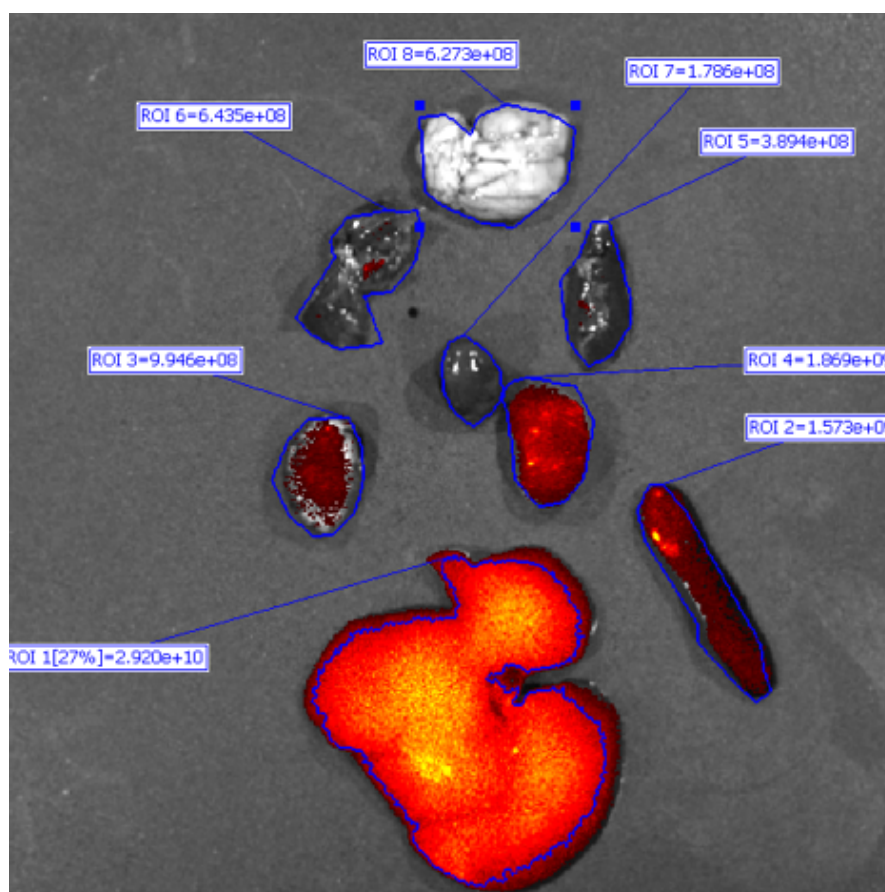
Figure 5.4 DiR labelled ADSVF can be seen in the left kidney 1 week post administration via the left renal artery. Fluorescent image of the experimental rat which underwent severe renal IRI of the left kidney, as described in chapter 4, then received DiR labelled ADSVF via the renal artery and terminated 1 week later. Ex vivo IVIS imaging of the rat demonstrated the appearance of strong signal hotspots within the left kidney, liver, and spleen.

A
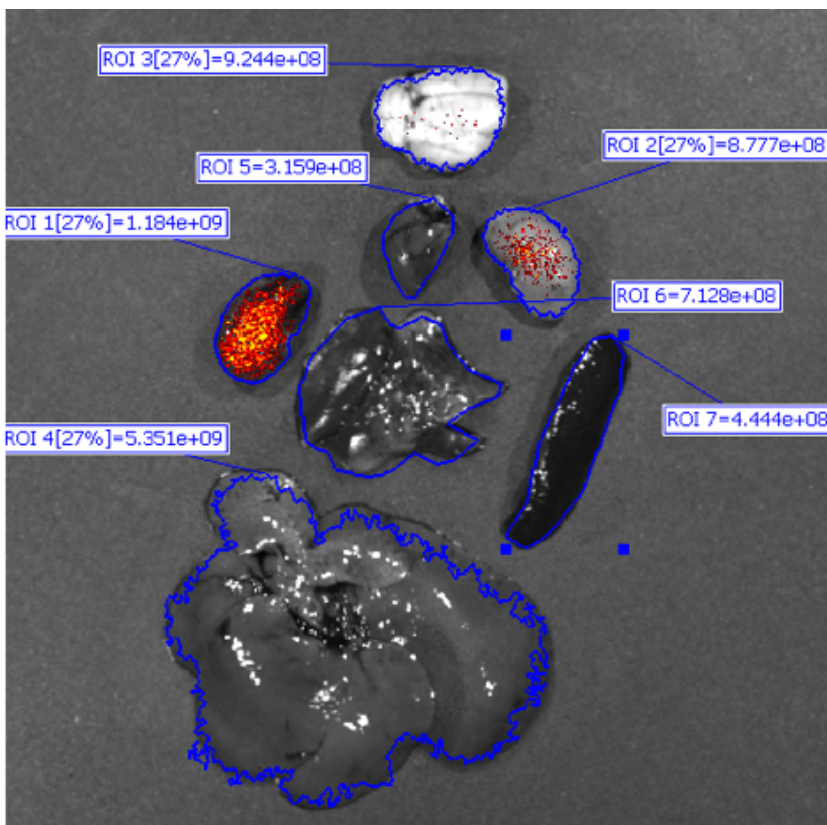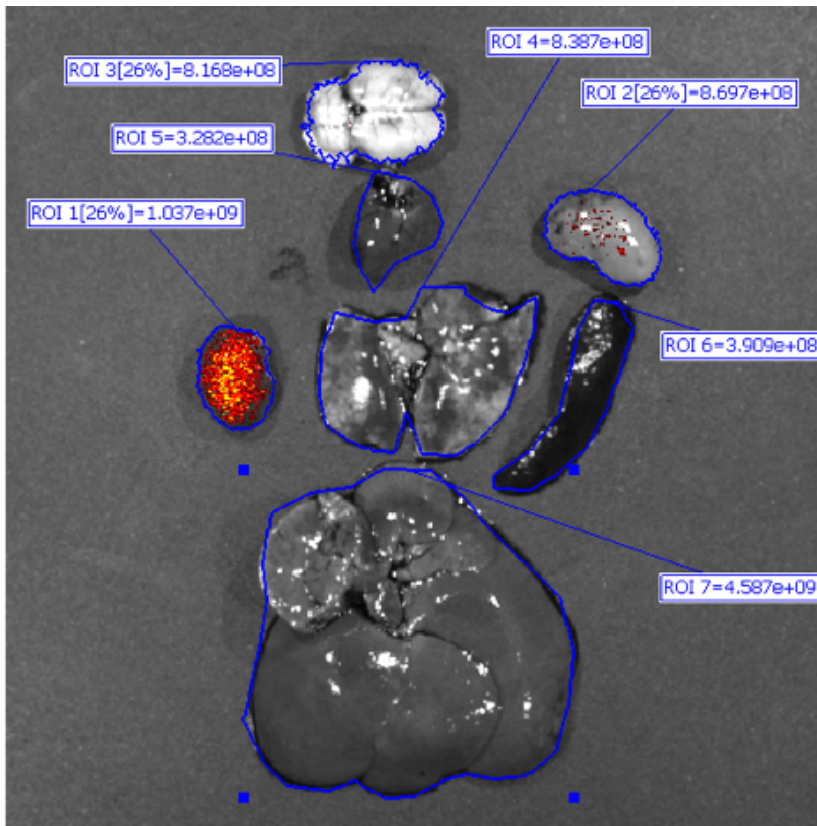
B
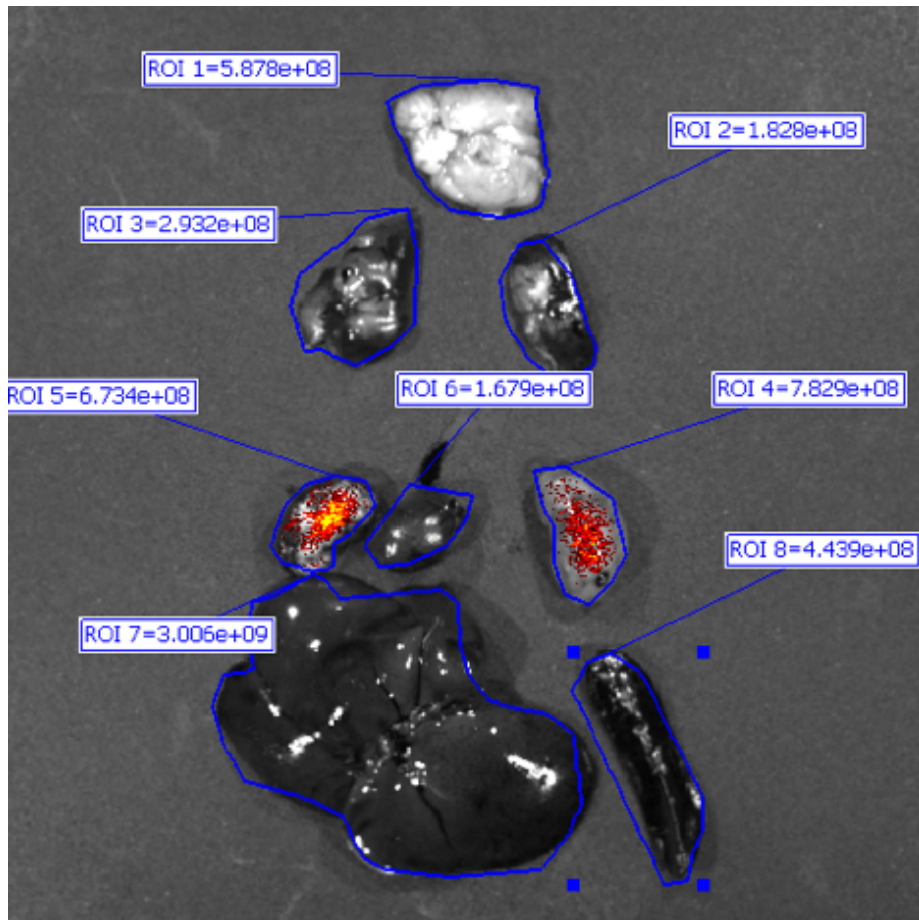
C
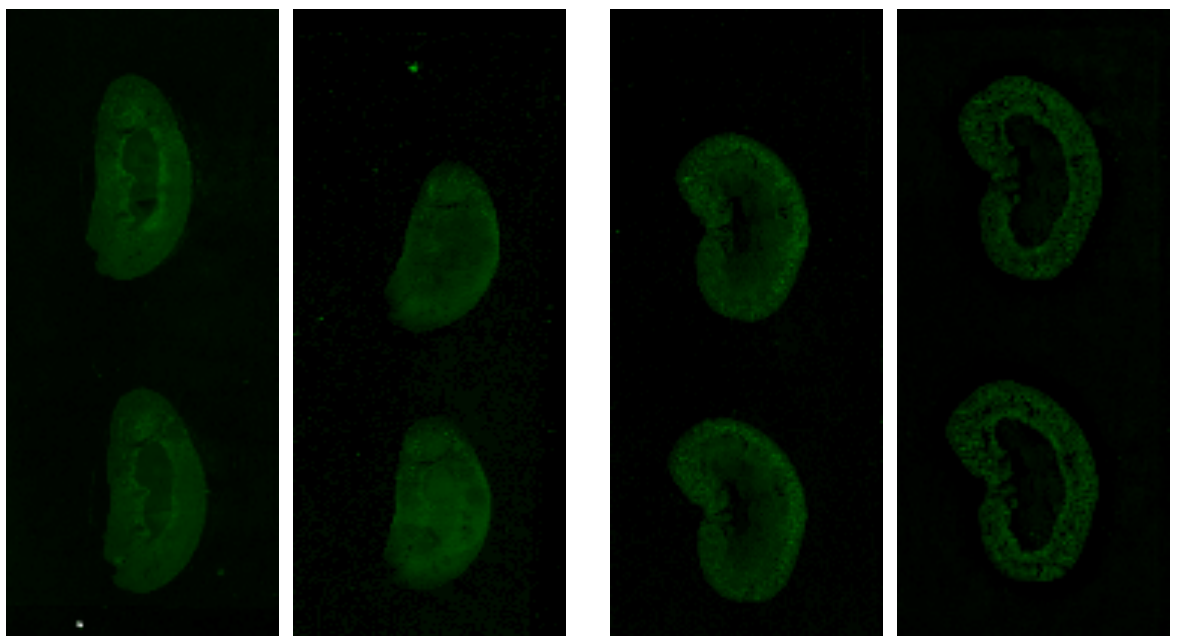
Left Kidney   **Right kidney**

Figure 5.5 Rats which receive unlabelled ADSVF demonstrate no signal hotspots in the left kidneys. Fluorescent images of experimental rats which underwent severe renal IRI of the left kidney, as described in chapter 4, then received unlabelled ADSVF via the renal

artery and terminated at various time points. (**A**) Ex vivo IVIS imaging of organs from 2 rats terminated after 48 hours have no increased signal within the left kidney. Although no hotspots are seen there is the appearance of increased signal in the right kidney compared to other organs. (**B**) Similar appearances are seen after 1 week. (C) LI-COR® images of organ sections from rats terminated after 24 hours demonstrates no signal within either right or left kidney.

5.4.2 SECTIONED TISSUE FLUORESCENT IMAGING

Comparisons were made between left kidney sections of rats that were given vehicle control, labelled ADSVF but no IRI or labelled ADSVF in a rat model of renal IRI. For the following analysis, cells were labelled with PKH26 as the LI-COR® fluorescent imager has the optimal filters for its excitation and emission range. Although DiR emitted a strong signal detectable in the IVIS animal scanner, the LI-COR fluorescent imager available, used for imaging sections, did not have the optimal filters for the DiR excitation and emission range.

Four rats were in each group and four sections, each containing two slices of the kidney, were imaged from each rat. The left kidney of rats that received labelled ADSVF had higher signal than the vehicle control-treated rats (Fig. 5.6). A statistically significant difference between groups was determined by one-way ANOVA (F $(2,9) = 8.738$, p $=0.0078$). A Tukey post hoc test revealed that vehicle control group had statistically significantly lower signal intensity (56963 ± 22421, p $= 0.0061$) compared to the labelled ADSVF, no IRI, group (252000 ± 42994).

Looking at the labelled ADSVF treated kidneys in more detail, regions of interest were drawn round the medulla and cortex regions of the kidney. The medullary regions of vehicle control and labelled ADSVF treated kidneys did not seem to have any difference in signal intensity. However, in the cortex of the kidney there was an increase in signal in the labelled ADSVF treated kidneys (Fig. 5.7). Referring to the preliminary LICOR images (Fig 5.2b) in which the cells were labelled with DiR, the labelled cells again appear to be collecting within the cortex.

Only the left kidney had a significant increase in signal intensity after injection of labelled ADSVF. No increase was seen in the lungs. There is an increase in signal, above autofluorescence, seen in the liver sections after the administration of labelled ADSVF but

it did not quite reach significance as determined by one-way ANOVA ($F_{(2,7)}$ =2.09, p=0.1942).
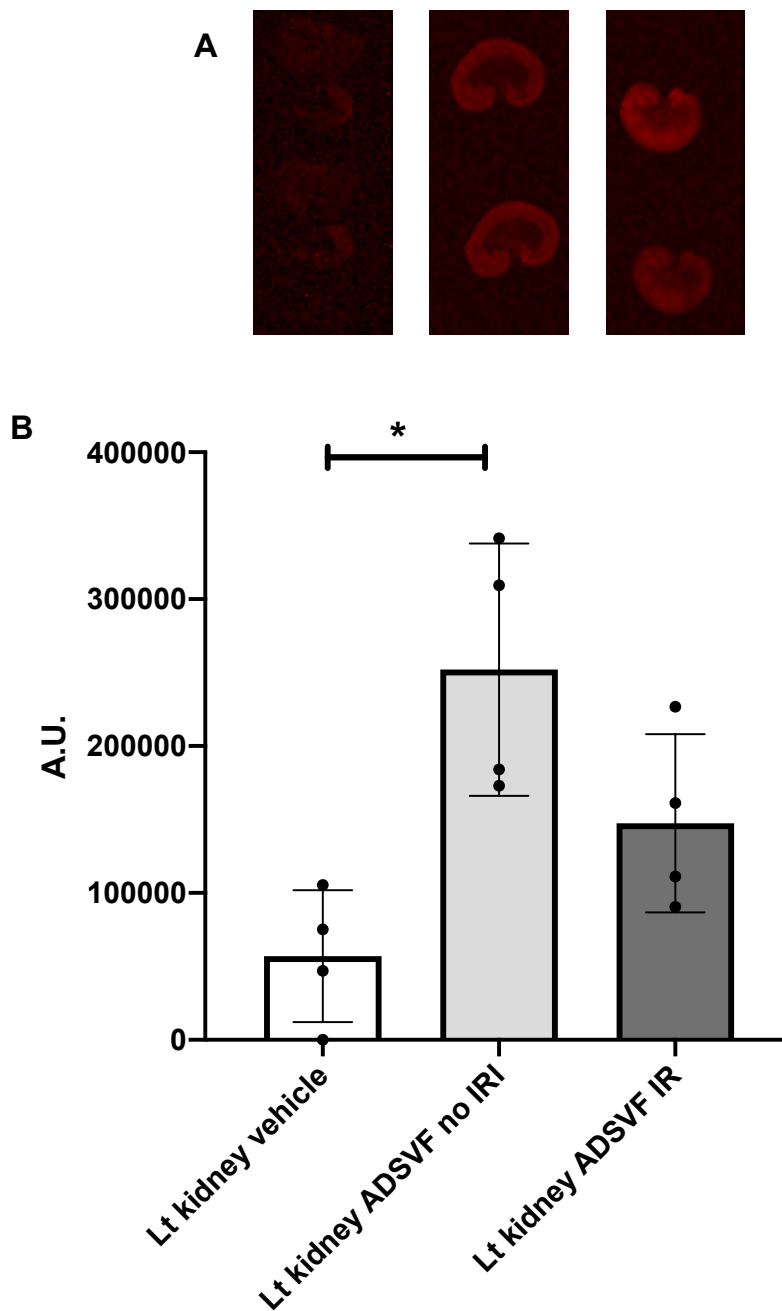
Figure 5.6. Kidneys which receive fluorescently labelled ADSVF via their renal artery have significantly higher signal compared to kidneys which receive non-labelled vehicle control. Fluorescent imaging of sections performed on left kidneys post treatment with PKH26 labelled ADSVF or vehicle control in rats terminated 48 hours post administration. Labelled ADSVF no IRI, n=4, labelled ADSVF with IRI, n=4, vehicle control with IRI, n=4. 4 sections taken of each kidney. (A) LI-COR® images of corresponding kidney section (B) Quantification of LI-COR® scans of left kidney tissue sections. Kidneys treated with PKH26

labelled cells have increased fluorescence. There is a significant increase in signal between left kidneys which received labelled ADSVF and had no IRI and kidneys that underwent IRI and received vehicle control. Significance was considered for p values <0.05 (*) but included p values <0.01 (**), and <0.001 (***) as indicated.
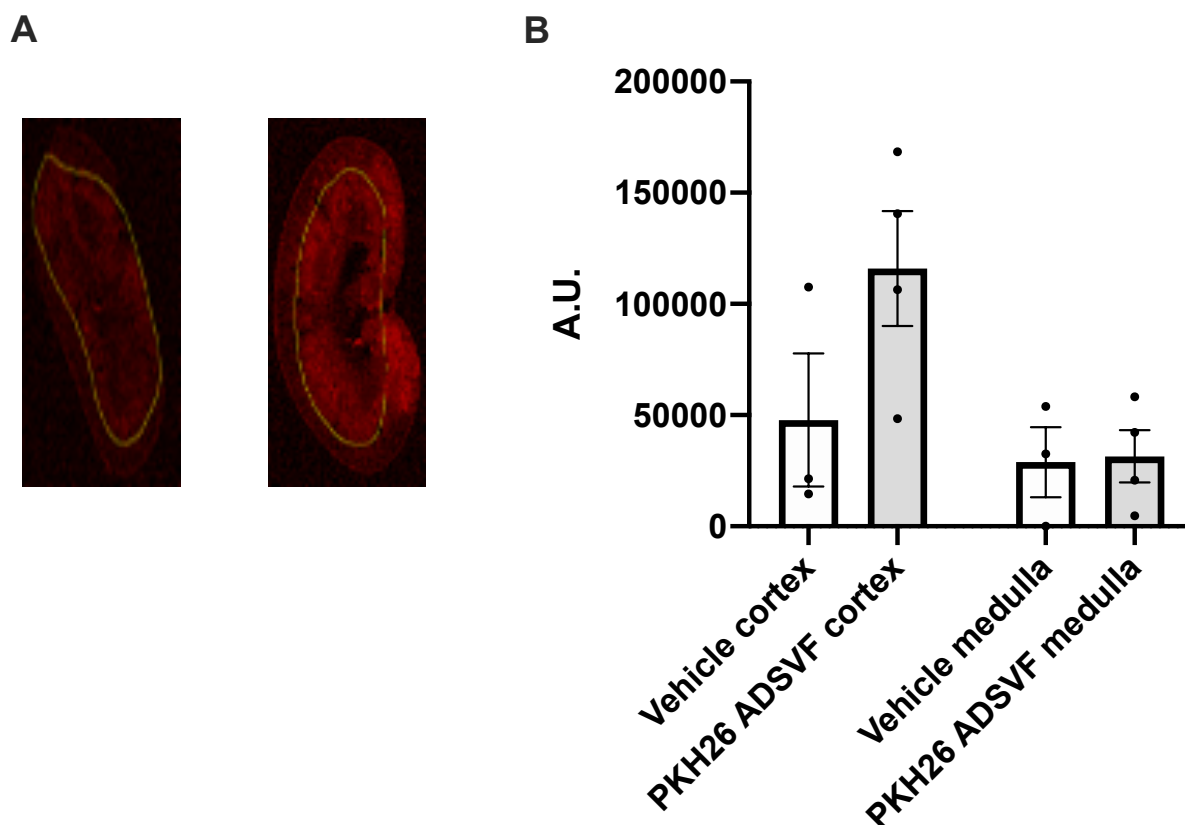
Figure 5.7. The cortex of kidneys which receive labelled ADSVF via the renal artery has higher signal intensity compared to the medulla. Signal intensity measured from fluorescent imaging of sections of left kidneys, divided into medullary and cortex regions, post treatment with PKH26 labelled ADSVF or vehicle control in rats that undergo IRI. Rats terminated 48 hours post IRI/administration of cells. PKH26 labelled ADSVF, n=4, vehicle control, n=3 4 sections were measured for each organ. **(A)** LI-COR® images with marking separating cortex region and medullary region. **(B)** Quantification of LI-COR® scans of cortex and medullary region of left kidney tissue sections. In the labelled ADRC group, sections demonstrate an increase in signal intensity in the cortex compared to the medulla. Comparing the cortex of kidneys which received labelled and unlabelled cells there is an increase in signal in the cortex of the labelled cells group compared to the cortex of the unlabelled cells group. Significance was considered for p values <0.05 (*) but included p values <0.01 (**), and <0.001 (***) as indicated.
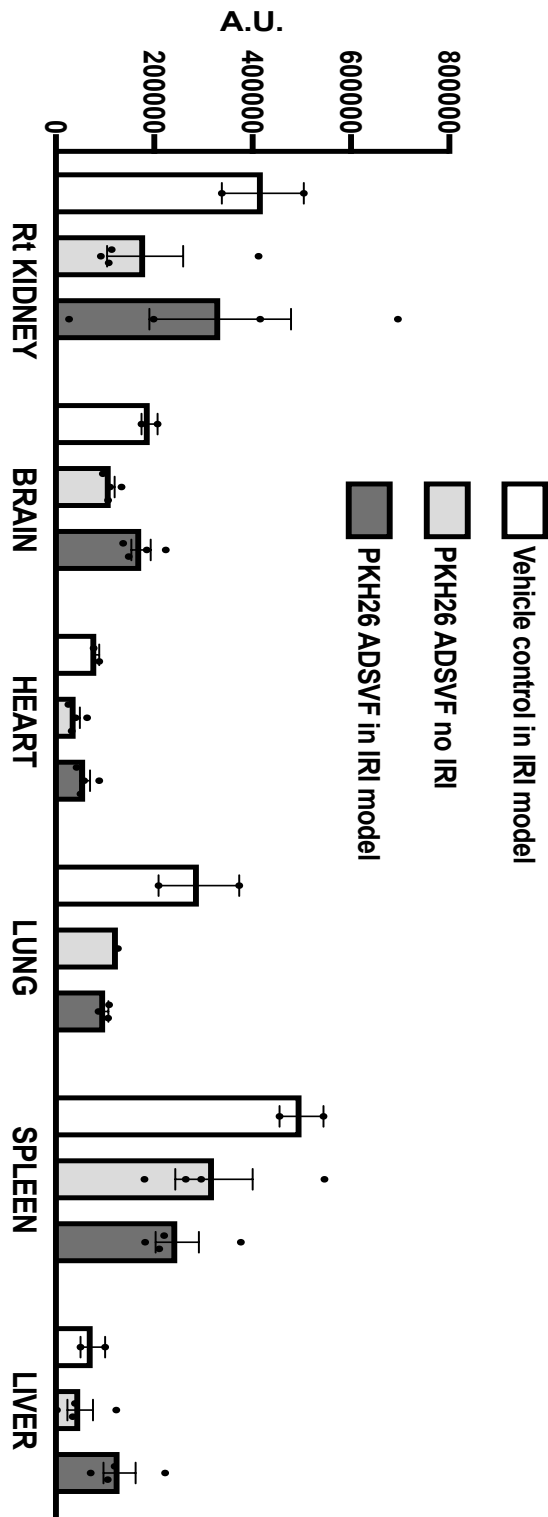
Figure 5.8. In rats that receive labelled ADSVF, apart from the liver, no organs have increased signal intensity when compared to rats that receive vehicle control. Fluorescent imaging of sections of organs (except left kidney which is described in figures 5.6 and 5.7) from rats administered, via the renal artery, with PKH26 labelled ADSVF with IRI (n=4), PKH26 labelled ADSVF no IRI (n=4) or vehicle control with IRI (n=2). All rats

terminated 48 hours post IRI and administration of ADSVF/vehicle. Summary of quantification of LI-COR® scans. The liver in rats that receive labelled ADSVF have increased signal intensity compared to the liver of rats that receive vehicle control. However, the increase was not significant. There is no increase in signal intensity in any organ that receives labelled ADSVF compared to organs which received vehicle control. Significance was considered for p values <0.05 (*) but included p values <0.01 (**), and <0.001 (***) as indicated.

5.4.3 FLOW CYTOMETRIC ANALYSIS

To confirm that administered ADSVF are present within the kidney, as demonstrated by fluorescent imaging, flow cytometric analysis of the left kidney was performed. After gating for the viable cell population, over 1000 viable labelled ADSVF were detected after interrogating 2 million kidney cells (Fig. 4.9). Unpublished work by Dr Chawangwongsanukun, on organs retrieved from the rats used in this thesis, nicely demonstrates PKH26 cells within the glomerulus under fluorescent confocal microscopy at 40x magnification (Fig. 5.9).

Further analysing demonstrates an almost 50:50 distribution of CD45+ and CD45- cells. Almost all the CD45+ cells were CD8 T cells. The majority of the CD45- cells were pericyte like cells. There was also a respectable mesenchymal stem cell-like population identified (Fig. 5.10). Comparing this to the ADSVF population prior to injection via the renal artery we can see that the CD8 T cells and pericyte like cells are overrepresented within the kidney (Fig. 5.10b)

A
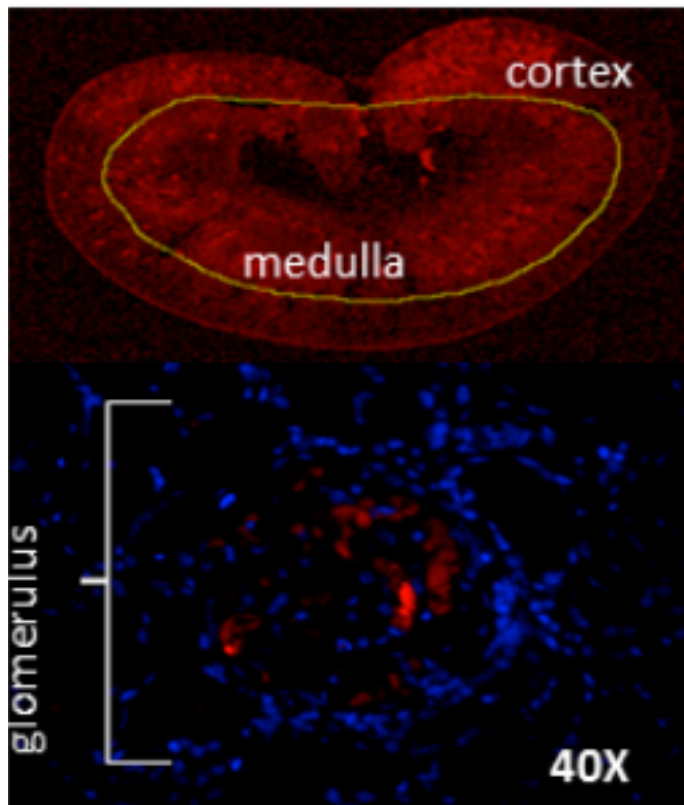
B
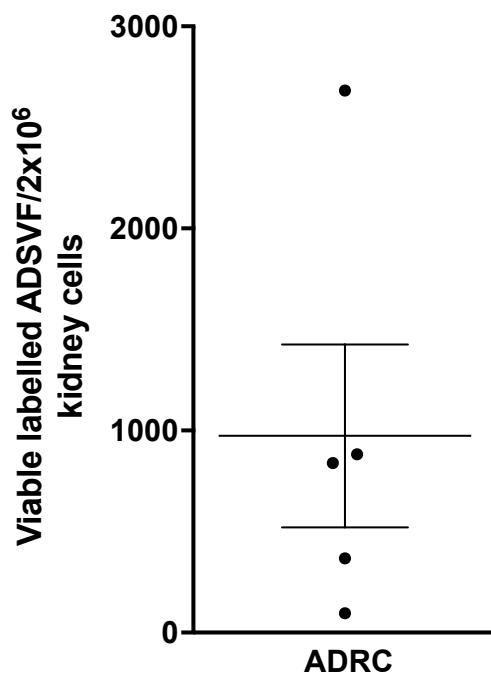
Figure 5.9. ADSVF administered via the renal artery collect within the cortex and strongly associate with the capillary bed of the glomeruli. Rats underwent renal IRI and received PKH26 labelled ADSVF via the renal artery. 48 hours later rats were terminated, and injured kidney retrieved. DAPI stained kidney sections interrogated by fluorescent

microscopy and homogenated kidney analysed by flow cytometry to look for viable labelled cells. **(**A) ADSVF are seen in the injured kidney collecting within the cortex and strongly associated with the capillary bed of the glomeruli. (B) Interrogating 2 million events with flow cytometry approximately 1000 viable DiR labelled cells could be recovered from the injured kidney. Picture taken from unpublished work from our group (Dr Chawangwongsanukun)

B

CD8 T cells

pericyte like cells
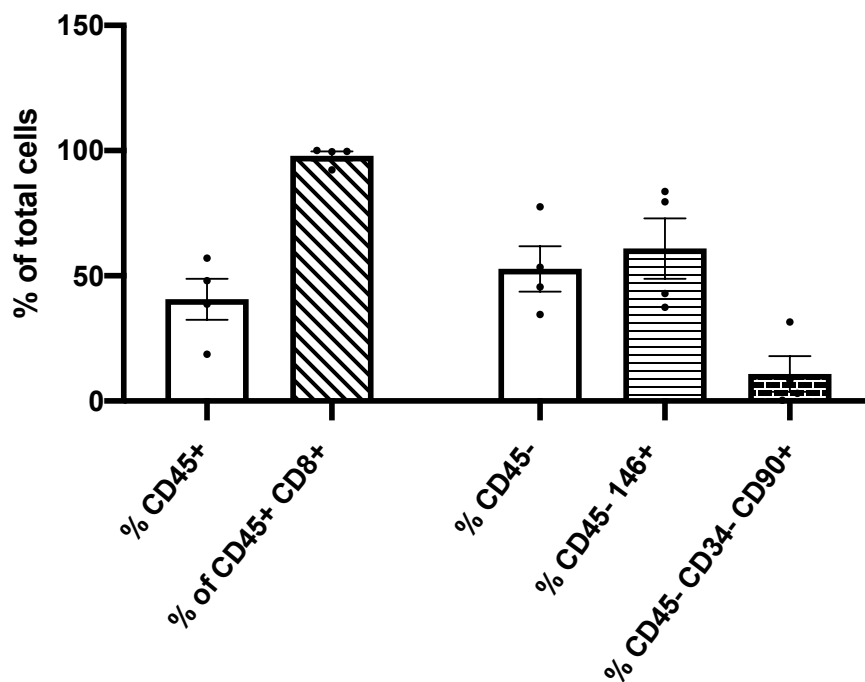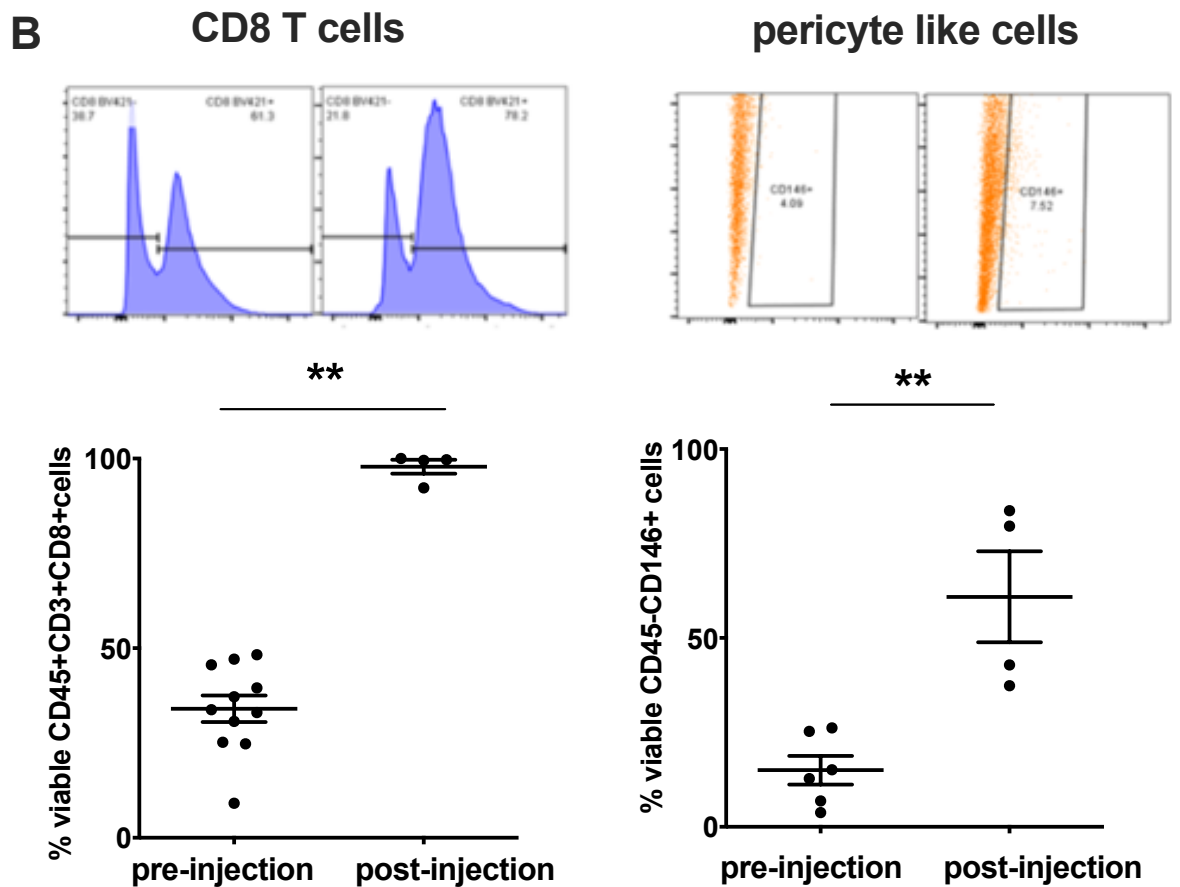
Figure 5.10 Of the ADSVF detected in the kidney after renal artery injection, there is an equal split of leukocyte and stomal cells. Flow cytometric extraction of DiR labelled cells from left kidney 48 hours post administration of DiR labelled ADSVF, via the renal artery, in rat model of IRI (n=4). Extracted cells interrogated further using flow cytometry. (A) The majority of CD45+ cell found to be CD8 T cells. The majority of CD45- cells found to be pericyte like cells (CD146+) with some mesenchymal stromal cells also identified (CD90+ CD34-). (B) Comparing the CD8 T cell and pericyte like cell population of ADSVF prior to administration and from recovered ADSVF post administration demonstrates that the CD8T cells and pericyte like cells now make up a far larger proportion of the ADFSVF population once extracted from the injured kidney. Significance was considered for p values <0.05 (*) but included p values <0.01 (**), and <0.001 (***) as indicated.

5.5 DISCUSSION

From published studies and our groups own work, most injected ADSVF are not detectable after one week and likely have their ameliorative effect within the first 48 hours; therefore, we concentrated on 24- and 48-hours post-injection and limited operations on rats at one week. For this section of the analysis, ADSVF was labelled with DiR as this gave a much better signal on IVIS scanning of ex vivo organs compared to PKH26 labelled cells. PKH26 was used for the fluorescent imaging of tissue sections, therefore, using two different modalities to label the administered ADSVF. Particular attention was given to the kidneys and liver as they had the most prominent signal on IVIS imaging. The lung was also of particular importance as evidence suggests that systemic intravenous administration of stem/stromal cells get trapped in the lung.

Many variables make it difficult to quantify and directly compare different organs, including the same organs from different rats using a fluorescent optical imager. Fluorescence can be affected by the size of the organ and composition, the volume and efficacy of administration, the labelling process and efficacy, the retrieval of the organs and the regions of interest created for analysis. Many of these factors could be counteracted by high sample numbers, but in keeping with the principles of the 3Rs and due to the complex surgery and long recovery, this was not an attractive option. However, analysis comparing organs taken from the same rat and viewed under identical parameters can allow for some qualitative analysis and indication of distribution.

The ex-vivo fluorescent imaging provides an initial overall indication of any hotspots or increased uptake in a particular organ. Imaging settings for each rat is identical, but the scale used when producing the visual pictures were adjusted to fully represent as best as possible the fluorescence of the organs. Autofluorescence is a significant limitation, making small quantities of labelled ADSVF within the tissue undetectable. Therefore, the IVIS images were not used to quantify fluorescence. However, the images were used to gauge changes in the distribution of fluorescence between organs at different time points. IVIS imaging was also able to pick up focal signal hotspots in the left kidney, which persisted for up to 1 week. We then focused on sectioned imaging to get more accurate analysis and validate the signal increase found from the IVIS images.

IVIS images taken 24 hours post-injection of the ADSVF (Fig. 5.2) show high fluorescence within the liver. This most likely represents autofluorescence, cell debris containing the dye

or dye itself. From other studies, we know cell debris and dye can be phagocytosed and end up in the liver where it is likely metabolised (Schmuck et al. 2016; Leibacher & Henschler 2016; Eggenhofer et al. 2013). Therefore, we cannot evaluate the liver the same way we would other organs which may have had increased signal due to ADSVF homing or entrapment within that organ. When looking at imaged histological sections of liver, there are no focal hotspots, unlike the section of the left kidney, further supporting the fluorescence of the liver as autofluorescence or diffuse infiltration of dye/cell debris. The liver is the largest organ imaged and sectioning it did not detect a significant increase in fluorescence, but perhaps if experimental rat numbers were higher, it might detect an increase. Alternatively, the IVIS images were perhaps able to detect potentials differences as it looks at the whole liver which will contain an increased number of total labelled cells, but when divided into thin sections, the concentration of fluorescence per section is only modestly increased.

After 48 hours and one week, the liver remains one of the most fluorescent images for likely the same reasons and not dissimilar to other studies. Following on from this it would be worth testing for any viable ADSVF within the liver at different the time points (as we did with the left kidney). If a viable ADSVF cell population is present, like the flow cytometry findings of the injected kidney, then monitoring of liver function should be a consideration if ever using ADSVF in a clinical setting.

In addition to the liver, the left kidney was found to have very high signal intensity. The left kidney, which is the kidney that undergoes IRI and injection of labelled ADSVF, appears to have very high focal areas of signal intensity which differs from the liver's diffuse signal. When the left kidney is sectioned and imaged, there are hotspots throughout the kidney which is not seen in any other organ. Whole organ IVIS imaging and kidney sectioning imaging highly suggests that DiR labelled ADSVF remain in the kidney for at least 24 hours (Fig. 5.2). From the whole organ IVIS images taken at 48 hours (Fig. 5.3) the picture is similar with robust focal hotspots remaining. Fluorescent imaging of the left kidney sections looking for PKH26 labelled ADSVF (Fig. 5.6) confirmed a significant increase in the signal intensity of rats that received ADSVF labelled with PKH26 compared to the control. It was initially surprising that there was a significant increase in the ADSVF no IRI group compared to the control and not between the ADSVF IRI and control group (Fig. 5.6). If anything, the addition of IRI would have further increased the signal intensity of the ADSVF IRI group. Qualitatively there looked to be more signal intensity within the ADSVF IRI group compared to control. Perhaps if the number of samples in each group was increased,

reducing the effect of the many variables described before, then this increase in the signal would have reached significance.

When these sections are analysed further, we can see that the signal intensity of the renal cortex of PKH26 labelled ADSVF treated kidneys has a significantly higher signal compared to the medulla. The medulla signal intensity from labelled ADSVF treated kidneys and vehicle control-treated kidneys remain similar (Fig.5.7) indicating that by 48 hours, the majority of ADSVF within the kidney are residing within the cortex. No increased uptake in the medulla suggests that administered cells or associated EV are not being filtered out. The labelled cells are potentially being trapped by the microvasculature of the glomerulus which resides in the renal corpuscle and cortex. Nevertheless, we know form histological and functional studies if this is the case then it is not detrimental to organ function up to a particular concentration of cell therapy. Fluorescent confocal microscopy confirms the presence of PKH26 labelled cells within the glomerulus of the renal corpuscle (Fig. 5.9).

Within a specific concentration range, the administered ADSVF improves renal function (chapter 1 Fig. 1.5). This clogging effect of high dosages will likely be less of an issue on larger human-sized organs, and will likely allow for higher concentrations of ADSVF, but further studies or porcine kidneys may be necessary to safely titrate up to find a maximum dose with no occlusive effect. An alternative theory is that the ADSVF may have a strong affinity to remain within the damaged renal cells due to chemo-attractants released by the damaged renal cells and adhesion molecules of the ASC. From here within the renal cortex, and likely the renal corpuscle, the ADRCs can exert their paracrine effect. Kidneys that received ADSVF but did not undergo IRI continue to have an increase signal intensity within the cortex. This does not rule out the chemo-attractant effect of the injured renal cells. Even in the non-IRI model, there is still a period of ischaemia when the renal artery is transected for ADSVF injection (around 20 minutes ischaemia compared to 120 minutes ischaemia in the full IRI model). Flow cytometry of ADSVF injected left kidneys (Fig. 5.9) further confirms the presence of viable ADSVF within the kidney at 48 hours; likely secondary to a combination of being trapped in the microvasculature and the chemo-attractant/homing properties of injured kidney cells.

In some imaging, the right kidney displayed high signal intensity; however, this is unlikely due to the presence of labelled ADSVF. For labelled ADSVF to get trapped in the right kidney, they would need to pass through the left kidney microvasculature then into the inferior vena cava, through the heart and lungs before potentially entering the right kidney.

From previous studies in which labelled, stromal cells have been injected into major veins they are detected in the lung microvasculature and not in any significant numbers within the kidneys (Eggenhofer et al. 2012; Gao et al. 2001; Schrepfer et al. 2007).Therefore high signal intensity is likely due to necrosis of the right kidney as a result of 2/3 nephrectomy. The nephrectomy causes 2/3 of the kidney to become necrosed and hard, almost crystal-like, (Fig. 4.2). This could explain the appearances seen on IVIS imaging. It is not possible to create histological slides of the hard necrosed tissue, but slides created from the remaining healthy 1/3 of the kidney did not demonstrate any evidence of labelled cells.

Lungs, heart, and brain did not show any fluctuance of fluorescence compared to the other organs in the same rat when imaged as whole organs under the IVIS. When these organs were prepared into histology slides and analysed under the LI-COR, there were no significant changes in fluorescence like seen in the left kidney. That does not necessarily mean there are no ADSVF in theses organs but just not a detectable concentration. It is unlikely that any cells that do manage to travel to any of these organs will be in any significant quantity to have any detrimental effect. Particular attention was given to the lungs due to reason described in the introduction, but there is no convincing evidence of any viable ADSVF trapped within the microvasculature. Therefore, it is likely that the highest concentration of ADSVF is in the left kidney compared to any other organ and the concern of ADRCs getting trapped in the lungs may be bypassed by administration via the renal artery. Also, we had no unexplained deaths in control or treatment group despite over 70 operation, further supporting no significant occlusion of the lungs. To further emphasise this point we could in the future perform flow cytometric analysis on the lungs to look for any viable ADSVF and 40x magnification of lung microvasculature to look for any vessel "clogging" as seen in intravenous administration.

The spleen at 24 and 48 hours seem to show some increased fluorescence compared to lung, heart, and brain, but this was likely due to autofluorescence as sectioned images did not show increased fluorescence. At one week, there was strong signal intensity with some hotspot's matching that of the left kidney. The spleen was not sectioned at one week and it would be sensible to consider doing this in the future. Currently, it would not be unreasonable to suggest that this increase in splenic signal represents diffuse infiltration of non-viable ADSVF, ADSVF debris or dye being collected by the splenic macrophages or ADSVF leukocytes homing as they filter the blood (Bronte & Pittet 2013).

The majority of the biodistribution studies concentrated on the first 48 hours. PKH26 is not ideal for long term tracing. Peng Li et al. found that debris from PKH26 labelled ADRCs when injected without ADRCs can be detected by immunofluorescence microscopy at day 7 post-injection in the liver, spleen, kidney and brain (P. Li et al. 2013). In our mechanistic studies, described in chapter 5, a major therapeutic effect of the ADSVF was detected within the first 48 hours. In addition, studies have failed to detect any living stem cells long-term reliably; hence the biodistribution study here concentrate 48 hours post-injection.

From initial clinical trials using ADSVF, the leading potential causes of concern are thromboembolic events, tumorigenesis, and immune activation. From injecting the kidney via the renal artery, up to a particular therapeutic dose, we have not seen any evidence that ADSVF collects in high enough volumes to cause detrimental occlusion of the blood supply of the left kidney. Despite their presence confirmed within the kidney. Therefore, it is unlikely for ADSVF to pass through the microvasculature of the left kidney and cause occlusion in distant organs.

Many factors affect the biodistribution of ADSVF and mesenchymal stromal cells other than the route of administration. Even studies investigating biodistribution after being administered via the same route have had different results. Schmuck E et al. found the highest retention of stem cells within the liver after labelling them with Qdots, injecting them into the jugular vein and using three-dimensional cryo-imaging (Schmuck et al. 2016). Contradicting many studies that found the majority of the labelled cells administered via a central vein end up in the lung – Fischer et al. found 99% of administered MSCs in the lung (Fischer et al. 2009). These differences are likely contributable to the animal model, cell source and preparation, labelling and detection techniques and time intervals at which they are injected. All studies failed to find viable stem cells mid to long term. Like our flow cytometry results looking for viable ADSVF population after 48 hours, Eric Scmuck et al. detected less than 0.6% of the total cells infused by day 2, 4 and 8 (Schmuck et al. 2016).

Superparamagnetic iron oxide nanoparticle (SPION) labelling of ADSVF and MRI scanning of the kidney in vivo was also attempted. Excellent MRI images of the kidney were obtained, but detection of the SPIONS were not demonstrated. Due to IVIS being more successful, technically easier, and more accessible compared to the MRI scanning, we continued with IVIS scanning. However, the MRI images could certainly be revisited in the future especially for longitudinal analysis of kidney injury over time within the same animal.

In conclusion, ADSVF injected via the renal artery in a model of renal IRI can be detected in the injected kidney up to 48 hours post-injection. They can be seen within the cortex of the kidney where they have potentially become entrapped in the microvasculature of the glomerulus or are encouraged to stay by the chemoattract of the injured kidney. In the glomerulus, the ADSVF exert their paracrine ameliorative effects against IRI. By 24 and 48 hours, there does not seem to be any ADRCs in any other organ at a significant concentration. The brutality of the injection process, the harsh environment in which they enter, the microvasculature that they need to pass through, and their short life span make it unlikely that many living cells pass through the kidney into generic circulation and have any additional clinical significance. Renal artery injection prevents the immediate entrapment of cells in the lung. Therefore, administration of ADSVF via the renal artery in an animal model of renal ischaemia reperfusion injury is an effective method of delivery and reduces non-targeted biodistribution.

During human kidney transplantation, administration of ADSVF via the renal artery could allow for maximal delivery of ADSVF to the kidney with reduced risk of adverse or toxic effects of ADSVF in other organs and open the door to higher therapeutic dosage regimes. However, discrepancies between the calibre of rat and human renal microcirculation need to be further investigated. Porcine animal models or kidney perfusion rigs using human ADSVF are two potential methods that could be considered. Determining the therapeutic window for ADSVF is also vital to reduce the risks to kidney grafts during translational studies.

CHAPTER 6:

MECHANISM OF ACTION OF ADIPOSE DERIVED STROMAL VASCULAR FRACTION IN AMELIORATING RENAL ISCHAEMIC REPERFUSION INJURY

6.1 INTRODUCTION

Currently, there is no method to retrieve, store, transport and implant a kidney without it succumbing to injury from the ischaemia, which is initiated the moment the arterial blood supply to the kidney is reduced. This begins when the renal artery is clamped for resection or during suboptimal perfusion of retrieval from DBD and DCD donors. Ischaemia persists during the cold storage and transportation time and as the kidney is prepared and then implanted. The injury does not stop when the kidney has finally been implanted in the recipient. The arterial clamp is removed, and the kidney is reperfused with oxygenated blood once again. Ironically this essential reperfusion with oxygenated blood brings with it further injury. Together they are termed IRI. The pathophysiology of IRI (described in chapter one) involves hundreds of interconnected processes that alter cellular biology and physiology, which can ultimately lead to a permanent change in form and function.

Improving Outcomes After Ischaemia Reperfusion Injury

Historically as there was no clinically proven method of boosting the regenerative capacity of the kidney, most therapies targeting IRI have focused on reducing the extent of the injury. Streamlining the retrieval and transportation process, allocation tactics and implantation techniques have all helped reduce the CIT, and in return, the extent of the IRI. Other logistical techniques such as the development of rigs that allow the organ to be perfused during transportation or before implantation have become increasingly popular. Initially used in liver and thoracic organs they have recently seen increasing popularity in renal transplantation. They have the added advantage of allowing pre-implantation evaluation of perfusion and urine output. Perfusion rigs also offer the opportunity to administer therapies ex vivo. Techniques such as those described have certainly improved outcomes, but complexity and severity of IRI have so far defeated therapeutic strategies.

Many therapies have been studied in the animal model of renal IRI, but only a minority of them have made it to clinical trials. Therapies showing promise in animal models include

hormonal therapies, such as oestrogen and beta-human chorionic gonadotropin and complement targeting therapies. Zheng et al. demonstration of improved renal function after the administration of an siRNA cocktail solution targeting complement 3, transcription factor RelB and apoptosis antigen 1 (Gueler et al. 2015; Zheng et al. 2016; Z. Feng et al. 2010). Studies have also targeted the cell death pathways in renal IRI, including apoptosis, necroptosis, ferroptosis and MPT-driven necrosis. Lau et al. work that has shown mice receiving receptor-interacting serine/threonine kinase 3 (RIPK3) -/- kidney in a rat model of transplantation had better function and survival. They suggested this was due to the necroptosis pathway dependence on the RIPK1-RIPK3 complex and proposed inhibition of the cell death pathways could provide clinical benefit (Lau et al. 2013).

Research has also focused on the immune system's response to IRI including the innate, adaptive and complement system. Reducing an exaggerated innate response, such as TLR inhibition or interleukin therapy or adenosine A2A receptor (A2AR) agonists therapy significantly reduces renal injury and improves function. All of which is promising, but these have not been successfully translated in clinical trials (Huang et al. 2015; Farrar et al. 2012).

Despite all previous therapeutic interventions however, stem cells and their paracrine function demonstrate the greatest potential. They have been extensively researched in the battle against IRI for over 20 years.

Stem Cells to Ameliorate Ischaemia Reperfusion Injury

The definition, classification and terminology of stem cells are complex, disputed and evolving and is discussed in more details in chapter three. In brief, they can be classified based on their differentiation potential or their origin (Barzegar et al. 2019). Different sources, harvesting techniques, preparations such as cultured or uncultured, associated stem cell populations and extracellular vesicles, modifications and routes of administration make for thousands of combinations when it comes to stem cell therapy. That is one of the reasons that getting an exact mechanism of actions can be difficult. Also, stem cells have multiple mechanisms of action. They have shown to reduce cell damage and death and at the same time, increase proliferation and restore renal function after IRI.

Chen et al. are one of many groups who have proposed that mesenchymal stem cells increase growth factors such as hepatocyte growth factor (HGF), IGF-1, TGF and VEGF improve

renal function after IRI (Xiaopeng Yuan et al. 2017). Reduction of pro-inflammatory cytokines such as CXCL12, IL- 6, TNF-α, IL-1β, IFN-γ, TNF, IFN-γ, TGF-β and increase of anti-inflammatory factors IL-10, fibroblast growth factor (FGF) have also been demonstrated (Sheashaa et al. 2016; Toyohara et al. 2015; J.-B. Zhang et al. 2017). It should be noted that the role of cytokines is dynamic; for example, CXCL12 increases after the injury to promote repair, but paradoxically can then become pro-inflammatory.

Counteracting the injurious reperfusion aspect of IRI, stem cells in renal IRI have demonstrated properties that reduce oxidative stress by methods such as increasing the ROS scavenger glutothionine transferase and superoxide dismutase (Fahmy et al. 2017; Zhuo et al. 2013), reducing ROS production (Tarng et al. 2016) and preserving normal levels of electron fluxes in ATP synthesis (Lindoso et al. 2014). Paracrine effects are thought to be the mainstay of stem cell therapy in renal IRI. The old dogma that stem cells home to the area of injury, infiltrate and differentiate into renal cells has not been convincingly defined and is unlikely to play a significant role in the recovery after IRI. It is, however, likely that the stem cells encourage resident tubular cells to regenerate and to become more resistant to programmed cell death and injury.

Of the stem cell sources, uncultured adult ASC could be considered one of the more easily accessible and abundant sources, especially intraoperatively at the time of transplantation. Besides, unlike other sources that require reprogramming and extensive lab preparation, this stem cell population can quickly be isolated from adipose tissue as part of the stromal vascular fraction (40 minutes using Cytori Celution CRS system, Cytori Therapeutics, San Diego, USA). They are safe for therapeutic use immediately or can be frozen for later use. The abundant supply reduces the need for culturing, but the option is available if desired.

ASC and other components in the stromal vascular fraction have been used in numerous animal models of IRI. Sheashaa et al. found a significant reduction in serum creatinine, malondialdehyde and histological injury score in rats that received cultured adipose-derived mesenchymal cells (Sheashaa et al. 2016). They proposed that the stem cells, among other actions, ameliorated the oxidative stress and lipid peroxidation. A theory that was similarly demonstrated by Chen et al. (Yen-Ta Chen et al. 2011). The dampened ROS insult resulted in reduced cell death.

Similarly, Zhang et al. demonstrated anti-apoptotic effects potentially due to a reduction in the anti-apoptotic regulator, B-cell lymphoma 2 (J.-B. Zhang et al. 2017). Also, they found

a significant decrease in pro-inflammatory cytokines (such as IL-6, IFN-y) and inflammation associated proteins (HGF and CXCL12) adding anti-inflammatory properties to the repertoire of adipose-derived mesenchymal stem cells. Moreover, many other studies can be found demonstrating the ameliorative effects ASC in renal IRI with anti-inflammatory, anti-oxidant, and anti-apoptotic effects being the common demonstrated mechanisms (Yen-Ta Chen et al. 2011; Shih et al. 2013; K. Li et al. 2010; X. Zhao et al. 2016). There has been less evidence, however, to support the notion that adipose-derived mesenchymal stem cells home to the area of renal injury and differentiate into renal tubular like cells as suggested by the work of Li et al. (K. Li et al. 2010).

However, most of these studies are looking at cultured ASC in animal models of IRI that are not as severe as the IRI sustained by the human kidney at the time of transplant. We envisage uncultured ADSVF directly injected into the renal artery at the time of transplantation as the artery is easily accessible. ADSVF can be processed from adipose tissue in less than 40mins therefore fat retrieval, processing, and subsequent stromal vascular fraction injection can all be achieved at the time of transplantation. Liuhua Zhou et al. have compared the efficacy of ADSVF and ASC and found the ADSVF to be just as effective at reducing inflammatory cytokines, promoting cell proliferation and reducing cell apoptosis resulting in reduced tubular injury score and improved renal function. ADSVF has been shown to ameliorate renal IRI in several further studies which attributed it to their paracrine effect (Z. Feng et al. 2010; Yasuda et al. 2012; Zhou et al. 2016). In some studies, ADSVF has shown to be more effective than ASC alone (Sheu et al. 2019). However, more needs to be done to study the mechanism of action of ADSVF as it has not been as thoroughly researched compared to other stem cell sources and stromal fractions (Zhou et al. 2017).

Despite studies showing the safe and effective use of xenotransplantation of human ASC in animal models, human clinical trials of ADSVF or ASC (have fallen behind those looking at other stem cell sources. However, clinical translation has started to pick up the pace. Clinical trials using ADSVF in osteoarthritis, soft tissue and gastrointestinal disorders seem to have advanced the most and a review by Toyserkani et al. looking at the safety of adipose-derived cell therapy found them to show a favourable safety profile so far. Nevertheless, they cautioned that in a large proportion of the studies, safety assessment methods used were of subpar quality. (Toyserkani et al. 2017) A stand out observation and potentially fatal danger of ASC is the thromboembolic potential. Studies have reported thromboembolic events after administration such as myocardial infarction, transient ischaemic attack of the brain, and pulmonary embolism, but these were few and in a high-risk population (Comella

et al. 2016; Perin et al. 2014; Henry et al. 2017). Therefore, dosing is of extreme importance, especially as there needs to be a balance getting a high enough therapeutic dose but not too much that the risk of a thromboembolic event becomes unacceptable. In animal models, the lungs seem particularly vulnerable to thromboembolic events due to the pulmonary microvasculature being one of the first pass organs when injected intravenously. Oncological safety and immunological safety remain the other two main areas which require close observation when looking at ASC and ADSV. However, with the limited studies so far, that does not seem to be a concern with uncultured ADSVF

Previously, our group demonstrated the efficacy of ADSVF at ameliorating kidney IRI in an animal model of severe renal IRI (Fig. 5.5). The abundant source of adipose tissue during transplantation, the quick processing of ADSVF from adipose tissue and the easy accessibility of the renal artery make the concept of delivering uncultured ADSVF directly into the kidney graft at the time of transplant attractive and easily translatable to clinical practice. However, before considering human trials further research on the mechanism, specific to this method, is required. As far as our knowledge there has been no study using uncultured ADSVF in an animal model of renal IRI as severe as ours in which the cell therapy is injected directly into the renal artery just before reperfusion. We hypothesise the mechanisms of action in ameliorating IRI in this model will be like those already described for adipose-derived stem cells therapies in other models of renal IRI.

6.2 HYPOTHESIS

Uncultured adipose-derived stromal vascular fraction administered directly via the renal artery ameliorates the effect of ischaemia reperfusion injury by protecting the kidney, reducing the inflammatory response and retarding the progression to renal fibrosis.

6.3 METHODS

6.3.1 ANIMAL HOUSING AND HUSBANDRY

Animal housing and husbandry were standard throughout all procedures, as described in section 2.1.

6.3.2 RETRIEVAL OF RAT ADIPOSE TISSUE AND ISOLATION OF ADSVF

Adipose tissue was obtained from the inguinal region of adult Fischer 344 rats. The retrieval of rat adipose tissue is described in chapter 2.2. Isolation and storage of adipose-derived stromal vascular fraction were conducted in a standard fashion, as previously described in section 2.4 and 2.5.

6.3.3 QUANTIFICATION, STORAGE AND PREPARATION OF ADSVF FOR ADMINISTRATION

Quantification, storage, and then subsequent preparation of ADSVF for administration was conducted in standard fashion, as previously described in section 2.5.

6.3.4 RENAL ISCHAEMIA REPERFUSION INJURY MODEL, ADMINISTRATION OF CELLS AND PERIOPERATIVE CARE

The ischaemia reperfusion injury model is described in detail in chapter four. In brief, male adult Fischer 344 rats undergo a 2/3 nephrectomy of the right kidney. The rat is recovered for at least two weeks before undergoing surgery in which the left renal artery is clamped for 120 minutes. Before releasing the clamp, the ADSVF or vehicle control is administered via the left renal artery, and the renal artery is repaired. At 120 minutes the clamp is removed, and reperfusion of the left kidney ensues. The animal is then recovered, and its post-operative care is described in chapter 4.3.6. Rats will then be housed as described in section 2.1 until it reaches a particular timepoint (depending on which experimental group it is in) when it will be terminated by carbon dioxide euthanasia.

6.3.5 ORGAN RETRIEVAL AND PROCESSING

Organ retrieval and processing was conducted in a standard fashion as described in chapter 2.6. After the organs were harvested a section of each organ was flash-frozen in liquid nitrogen and then stored in -80C freezer until required for further analysis later. Another section was placed in 20mM HEPES PBS (Sigma Aldrich) at 4ºC and taken for flow cytometric analysis. The remaining tissue was placed in 10% formalin for histological analysis.

6.3.6 SERUM MICROPARTICLE MEASUREMENT

Serum from control and ADSVF injected rats are allowed to thaw then stored in -20C. Samples were diluted to 1:10000 with PBS. Samples were then run in the NanoSight LM10-HS (NanoSight, Salsbury, UK) for size exclusion measurements (exosomal: 30-100 nm and microparticle: 100-1000nm) as per manufacturer instructions and with 70% ethanol cleaning between samples. Five sixty-second videos were taken per sample to determine particle concentration.

6.3.7 QUANTITATIVE REAL-TIME PCR ARRAY

Organs are taken from -80 freezer and homogenised in liquid nitrogen with mortar and pestle. 50-100mg of homogenised organ tissue was placed in 1ml of TRIzol (Thermofischer). Centrifugation and chloroform were used to separate the aqueous and organic phases. The RNA was recovered from the aqueous phase by precipitation with isopropyl alcohol and resuspended in nuclease-free water (QIAGEN, Hilden, Germany). RNA was counted using a Nanodrop (Thermofischer), and RNA was purified by removing DNA with DNAse I, Amplification Grade (Thermofischer). Reverse transcriptase (Thermofischer) was used, following its protocol to create complement DNA (cDNA) from the RNA. The cDNA and fast master mix (Thermofisher) were then prepared for the Taqman Array card and added to the custom Taqman array plates as per instructions. The custom made Taqman array plates assay 47 candidate genes and housekeeping controls (Table 3.2) and was ran on a QuantStudio PCR cycler (Applied Biosystems, Foster City, CA, USA). Relative Ct levels were normalised by housekeeping controls (average of the same three housekeeping genes) and represented as dCt. Data are represented as mean ± SEM.

Differences in average means between two groups determined by Mann-Whitney U test, differences between three groups by One-way ANOVA. *p<0.05, **p < 0.01.

6.3.8 WESTER BLOTS AND PROTEIN ARRAYS

A section from the kidneys retrieved from the terminated rats was immediately placed in protein lysis buffer. It was then homogenised and stored back in protein lysis buffer. Protein concentrations were determined using a Bradford assay. The proteins of homogenised kidneys sample were then separated on a voltage gradient through an acrylamide gel. Protein was transferred onto a nitrocellulose membrane and interrogated for protein detection by antibody reaction and using LI-COR Odyssey CLx fluorescent imager (Licor Biosciences, Nebraska, USA). Col1a2, Nox-1, and Nox-4 (Abcam) were measured and normalised to beta-actin controls. A 27-rat cytokine profiler array was assayed on the whole homogenised kidney of treated and untreated kidneys for cytokines related to inflammation and growth factors per Applied Biosystems protocol.

6.3.9 FLOW CYTOMETRY

Flow cytometric analysis was described in section 5.3.11.

6.3.10 HISTOLOGICAL ANALYSIS

After three to seven days of being fixed in 10% formalin, the organs were then transferred to 70% ethanol for a further 48 hours before being subjected to tissue dehydration and paraffin embedding process. All tissues were then sectioned at 5 micrometres and underwent staining with either haematoxylin and eosin (H&E) or Masson Trichrome for histological assessment.

Histopathological scoring of kidneys was given based on 2-3 sections. A tubular injury score was given between zero and five. Three observers assessed the kidney injury score independently.

Statistics. A 2-way student's t-test was carried out to determine the differences in the mean average for sample sizes >5 of equal variance. Mann-Whitney U test was used to analyse smaller sample sizes. A two-way ANOVA was used to evaluate changes over time. Analyses was performed with Prism 6.02 (GraphPad, San Diego, CA). Mean and standard error of mean (SEM) are displayed unless otherwise stated. Error bars on graphs represent SEM unless otherwise stated. Significance was considered for p values <0.05 (*) but included   p values <0.01 (**), and <0.001 (***) as indicated.

6.4 RESULTS

6.4.1 ADSVF PROVIDE SOME PROTECTION FROM ISCHAEMIA REPERFUSION INJURY

Real-time PCR was performed on the samples of the left kidney, which underwent severe IRI, at different timepoints looking at an array of genes associated with kidney injury and repair. Although the trend was the same for Kidney Injury Molecule-1 (KIM-1) and neutrophil gelatinase-associated Lipocalin (NGAL), there were significant differences with hypoxia-inducible factor 1 subunit alfa (HIF1A) between groups at one week suggesting increased kidney injury in the vehicle control group (Fig. 6.1a). IL-18 was raised after 48hours in the ADSVF treated group, but this marker of increased injury settled by one week. The significantly lower detection of microparticles indicates lower levels of systemic injury in the sera of ADSVF treated rats (Fig. 6.1b).

Tubular injury score by 48 hours already seems reduced in the ADSVF treated group, and this becomes significant by one week (Fig. 6.2). Rat weights for both groups follow the same trend with a dip of weight after surgery then a gradual increase however the ADSVF treated group lost less body weight and by day four are significantly heavier (Fig. 6.3)

Renal function measured previously by our group, using inulin clearance studies, revealed rats treated with $7x10^5$ ADSVF cells have a higher glomerular filtration rate (Fig. 1.5). $7x10^5$ ADSVF resulted in a significant improvement of renal function compared to all other dosages and vehicle control. Higher dosages result in reduced response. Renal function in rats treated with this optimal dose of ADSVF was comparable to sham-operated rats by week 6. Non-invasive renal function measurement in the modified severe IRI model, as described in chapter 2, demonstrates at 48 hours, the ADSVF treated rats have improved residual renal function (Fig. 6.4b).

A
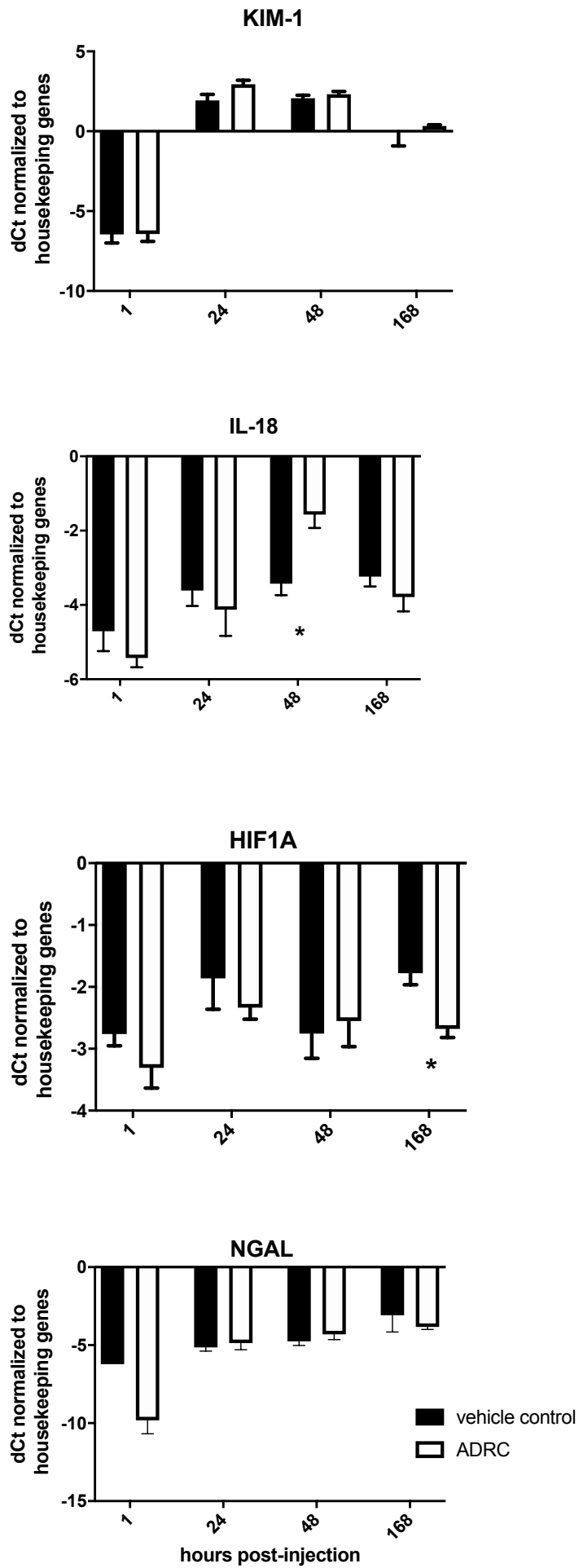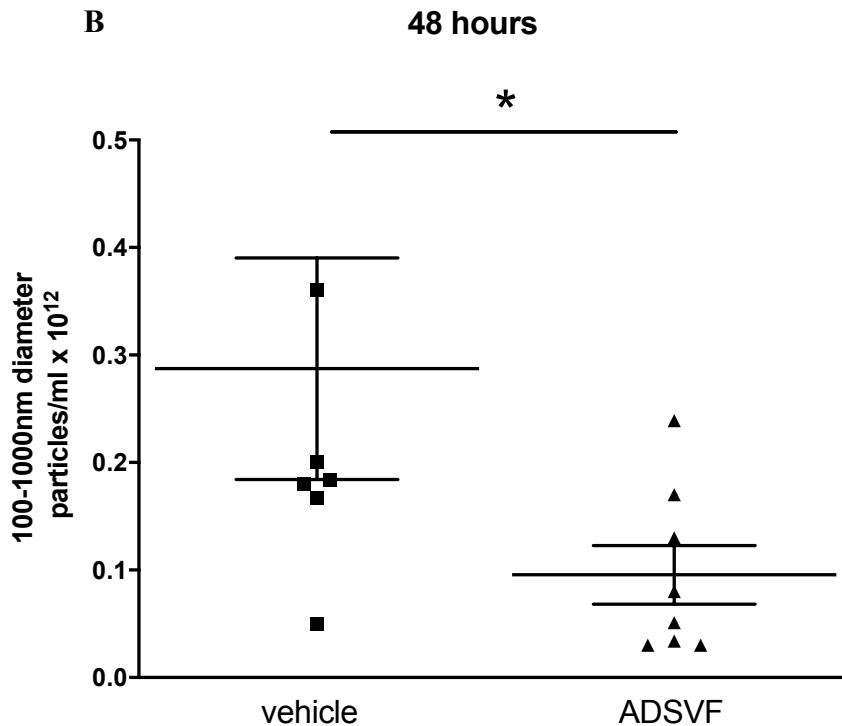
Figure 6.1 ADSVF treated rats have reduced kidney injury and lower levels of systemic injury after IRI. RT-PCR analysis of kidneys which have sustained a renal IRI and then treated with ADSVF or vehicle control via the renal artery. Represented as their delta CT (housekeeping genes Ct minus gene of interest Ct) after 40 cycles. Kidneys retrieved at 1hour (n=4), 24hours (n=5), 48hours (n=8) and 1 week (n=4) post IRI and administration of ADSVF. (A) HIF1A is significantly higher in the vehicle control group but NGAL and KIM-1 follow a similar trend. IL-18 is raised in the ADSVF group at 48 hours before returning to similar levels by 1 week. (B) Microparticle analysis of the sera from ADSVF treated (n=8) and vehicle control (n=6) treated rats shows a significantly higher count of microparticles in the vehicle control group. Exosomal material defined as 30-100 nm and microparticles as 100-1000nm. Represented as the mean and standard error of the mean. Significance was considered for p values <0.05 (*) but included p values <0.01 (**), and <0.001 (***) as indicated.

48 hours

p<0.1

1 week

*

1 week

*
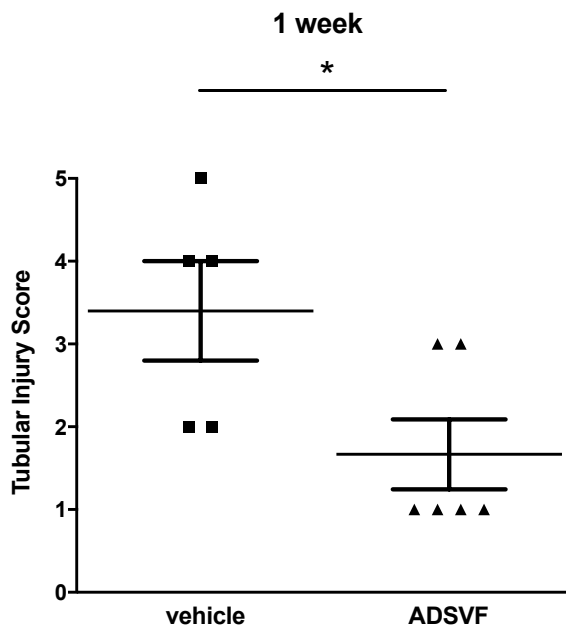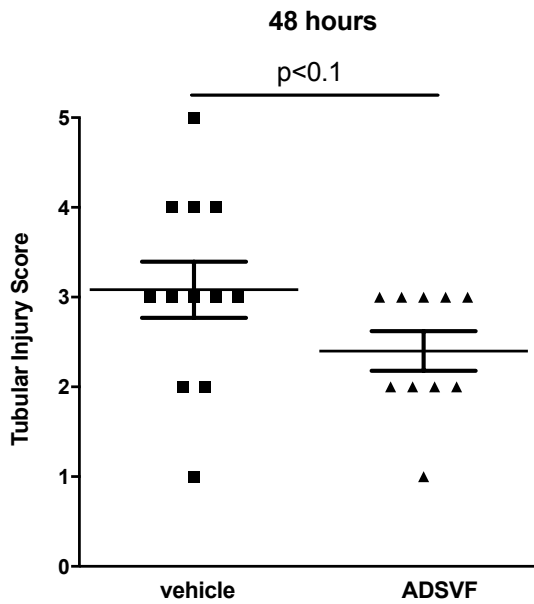
Tubular Injury scoring	
0	Normal
1	Loss of brush border <25% ,mild blebbing, basal membrane integrity
2	Loss of brush border >25%, thick basal membrane, intensive blebbing, mild vacuolization
3	shrunken nuclei, intensive vacuolization
4	(plus) inflammation, cast formation, necrotic/apoptotic cell up to 60%
5	Total/severe necrotic damage >60%

172

Figure 6.2 ADSVF treated rats have reduced renal tubular injury after renal IRI.
Tubular injury score at 48 hours (vehicle n=12, ADSVF n=10) and 1 week (vehicle n=5, ADSVF n=6) of kidneys from rats that underwent renal IRI and where then treated with either ADSVF or vehicle control. Histopathological scoring of kidneys was given based on 3 sections per kidney. A tubular injury score was given between zero and five. Three observers assessed the kidney injury score independently and mean score calculated. After 48 hours there is a trend of increased tubular injury in the vehicle control group and by 1 week there is now a significant increase in injury. Significance was considered for p values <0.05 (*) but included p values <0.01 (**), and <0.001 (***) as indicated.
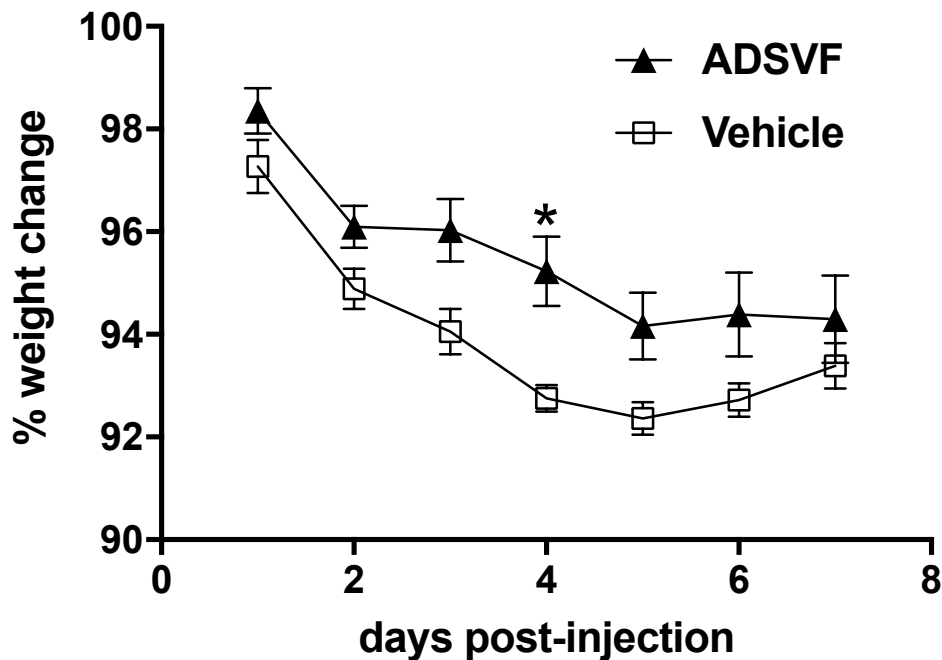
Figure 6.3 Rats treated with ADSVF lose less weight post IRI suggesting reduced post-operative morbidity. Rats were weighed daily post IRI surgery during which they were administered with either ADSVF or vehicle control via the renal artery. The weight change of ADSVF treated rats was less from day one and by day four the difference was statistically significant. Significance was considered for p values <0.05 (*) but included p values <0.01 (**), and <0.001 (***) as indicated.
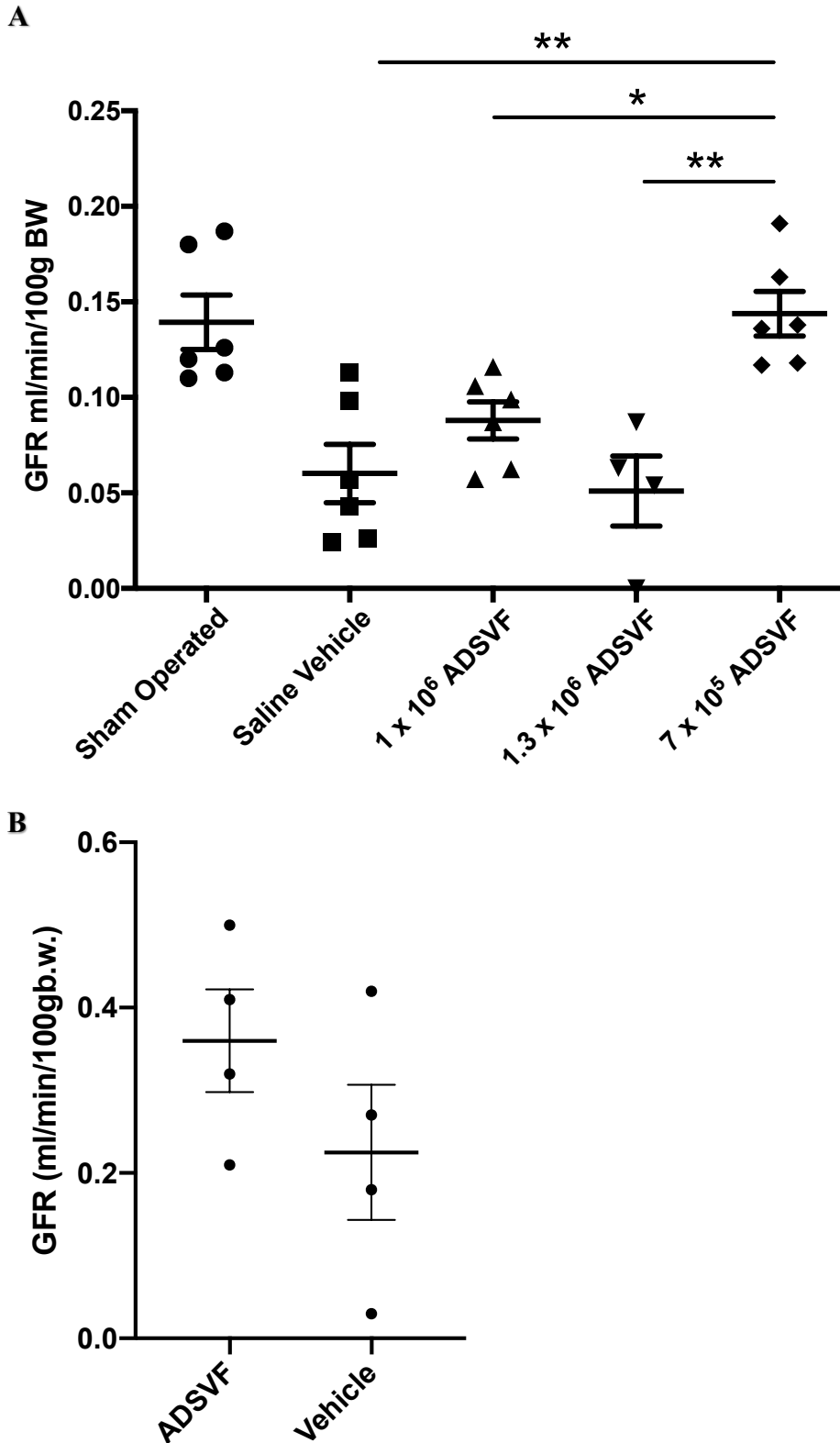
Figure 6.4 ADSVF improve renal function post IRI within a specific concentration range. Rats were subjected to a renal IRI then received ADSVF, at various concentrations, via the renal artery. Sham operated (n=6), vehicle control (n=6), 1×10^6 ADSVF (n=6), 1.3×10^6 ADSVF (n=6) and 7×10^5 ADSVF (n=6). (A) After six weeks, rats that received 7×10^5 ADSVF cells had the most recovered renal function and matched the renal function of

sham operated rats that did not sustain any IRI. Measured using terminal inulin clearance studies performed by group member Dr H. Whalen. (B) Non-invasive measurement of glomerular filtration rate 48 hours post renal IRI and administration of either vehicle control (n=4) and the optimum $7x10^5$ ADSVF cells (n=4) demonstrates at 48hours there is already a trend of improved renal function in the ADSVF treated group.

6.4.2 ADSVF REDUCE PROGRESSION OF FIBROSIS

Gene expression of collagen type IV alpha one chain (COL4A1), HIF1A, tissue inhibitor of metalloproteinases 1 (TIMP 1) and collagen type I alpha 2 chain (COL1A2) were all significantly higher in the vehicle-treated groups at one-week post-IRI (Fig. 6.5). CCL2 was not quite significantly different. VEGF and FGF2 were both greater in the ADSVF treated group by 48 hours, but this did not turn out to be significant by one week.

Protein detection of COL1A2 and VEGF at 48hours suggested the COL1A2 being higher in the vehicle-treated group and VEGF higher in the ADSVF treated group (Fig. 6.6) Histology slides with Masson Trichrome staining, looking at collagenous connective tissue fibres, in rats that were sacrificed at 48 hours, already shows a significant increase in collagen in ADSVF treated rats (Fig.6.7).

TIMP 1

COL1A2

COL4A1

CCL2

176

HIF1A
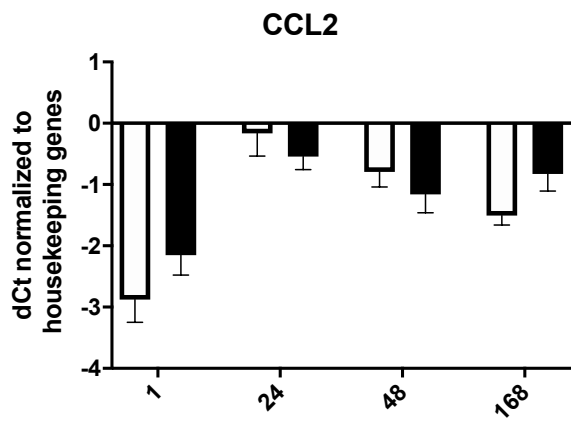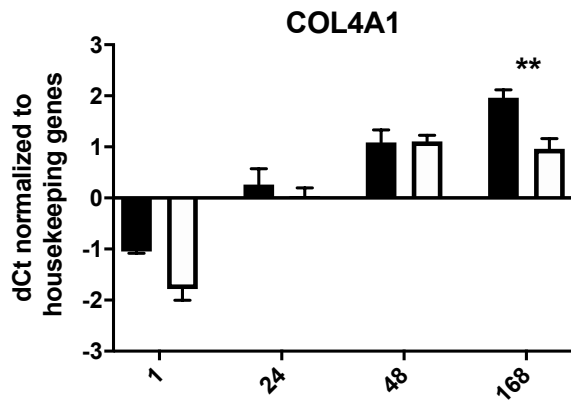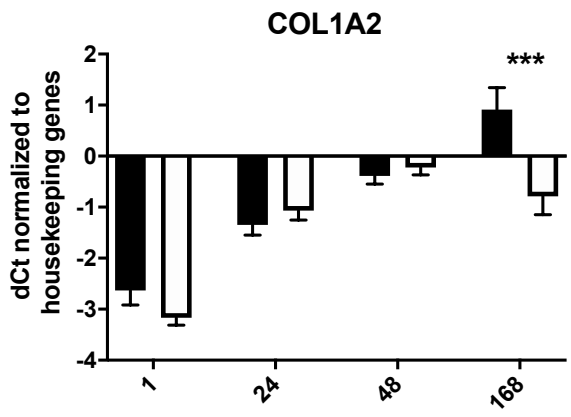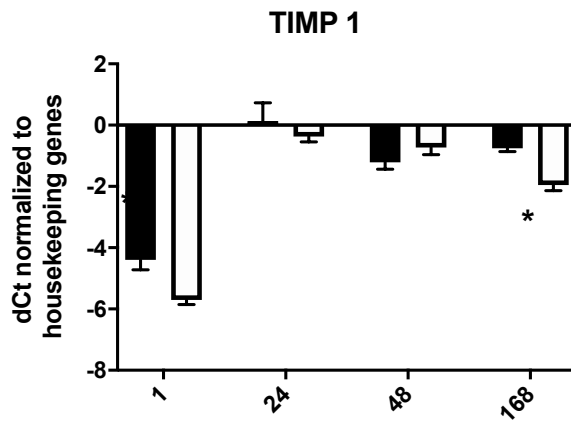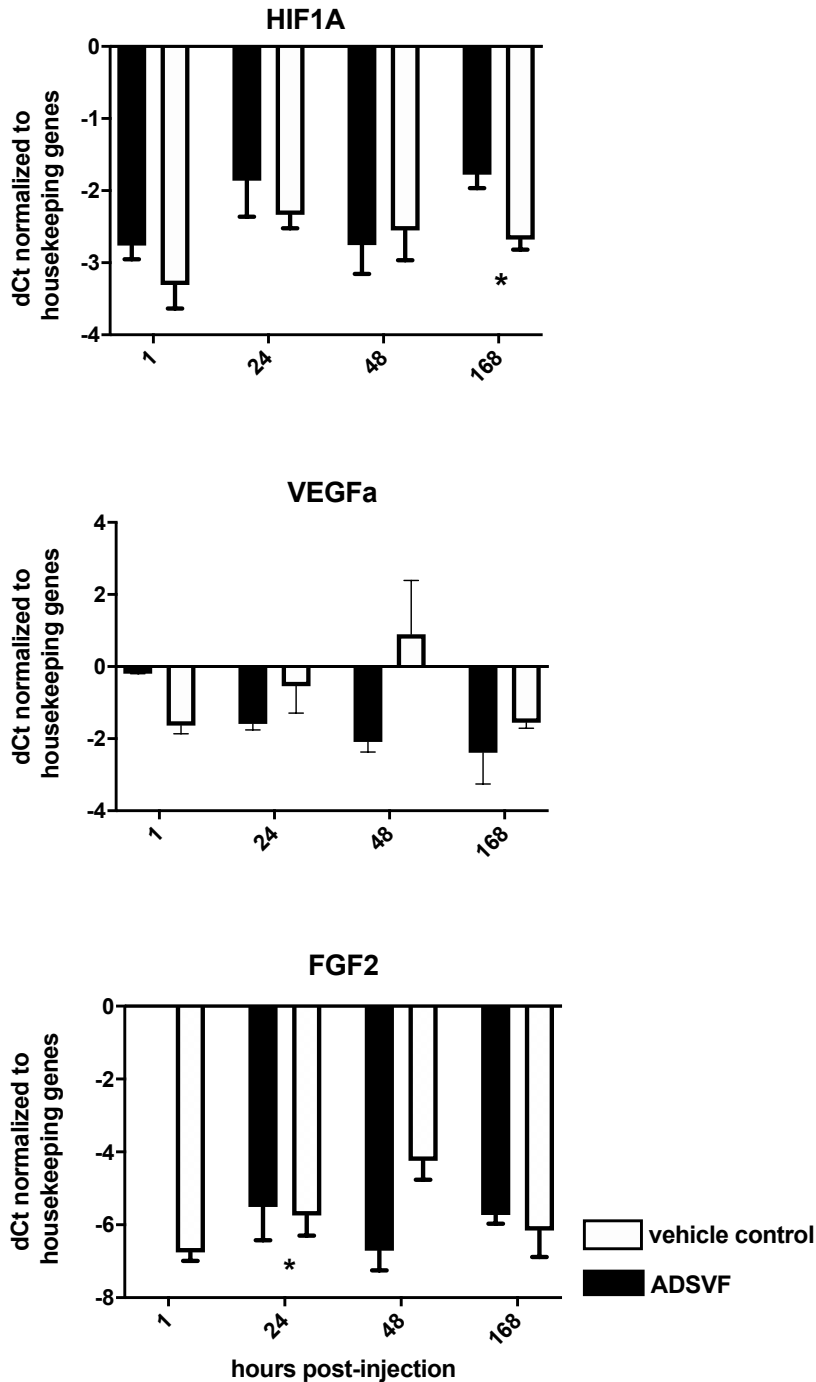
Figure 6.5 Kidneys treated with ADSVF have reduced expression of factors related with fibrosis formation. RT-PCR analysis of kidneys which have sustained a renal IRI and then treated with ADSVF or vehicle control via the renal artery. Represented as their delta CT (housekeeping genes Ct minus gene of interest Ct) after 40 cycles. Kidneys retrieved at 1 hour (n=4) 24hours (n=5), 48hours (n=8) and 1 week (n=4) post IRI/administration of ADSVF. Gene expression of COL4A1, HIF1A, TIMP 1 and

COL1A2 were all significantly higher in the vehicle-treated groups at one-week post-IRI. CCL2 was not quite significantly different but followed a similar trend of being higher in the vehicle treated groups. VEGF and FGF2 were both greater in the ADSVF treated group by 48 hours, then returned to similar levels by one week.

Significance was considered for p values <0.05 (*) but included p values <0.01 (**), and <0.001 (***) as indicated.
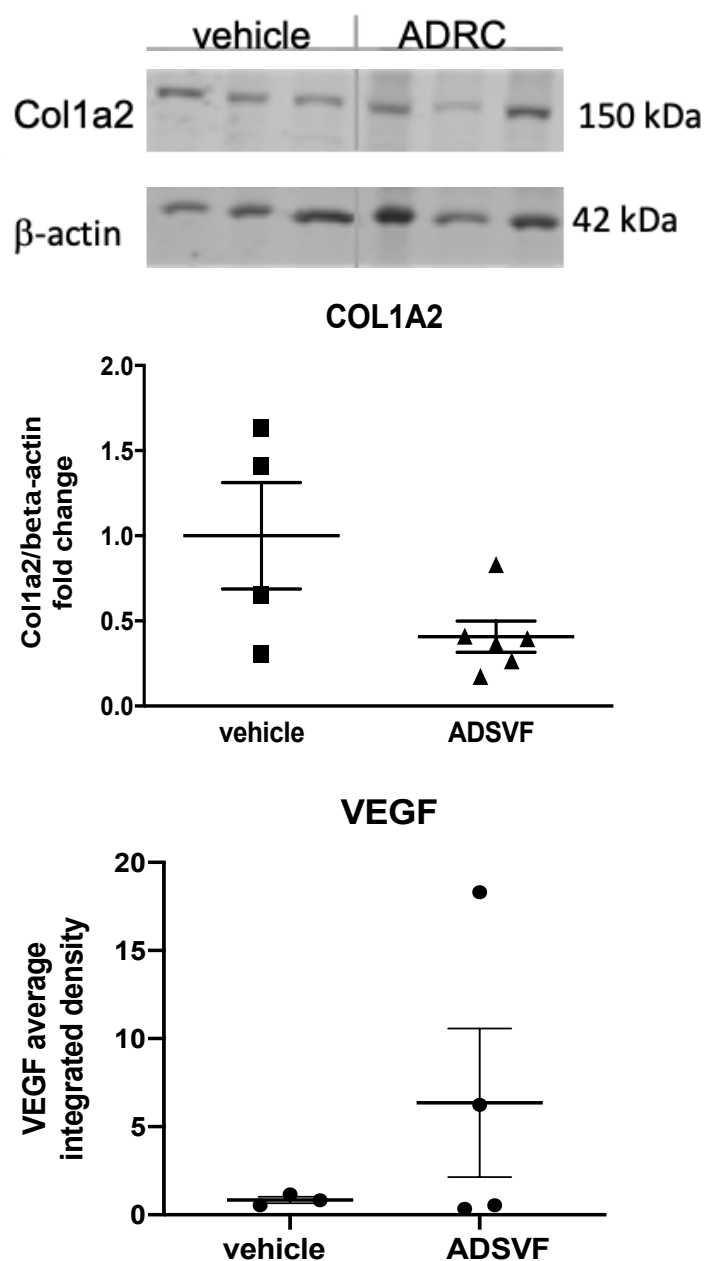
Figure 6.6 Kidneys treated with ADSVF have favourable levels of proteins related to reduced fibrosis formation. Protein analysis of kidneys which have sustained a renal IRI and then treated with ADSVF or vehicle control via the renal artery. Samples taken 48hours post IRI and administration of ADSVF/vehicle control. **(A)** COL1A2 was lower

in the ADSVF treated group using western blot analysis (Vehicle n=4, ADSVF n=6) and (B) VEGF detection was higher in ADSVF group on rat cytokine protein array (vehicle n=3, ADSVF n=4).
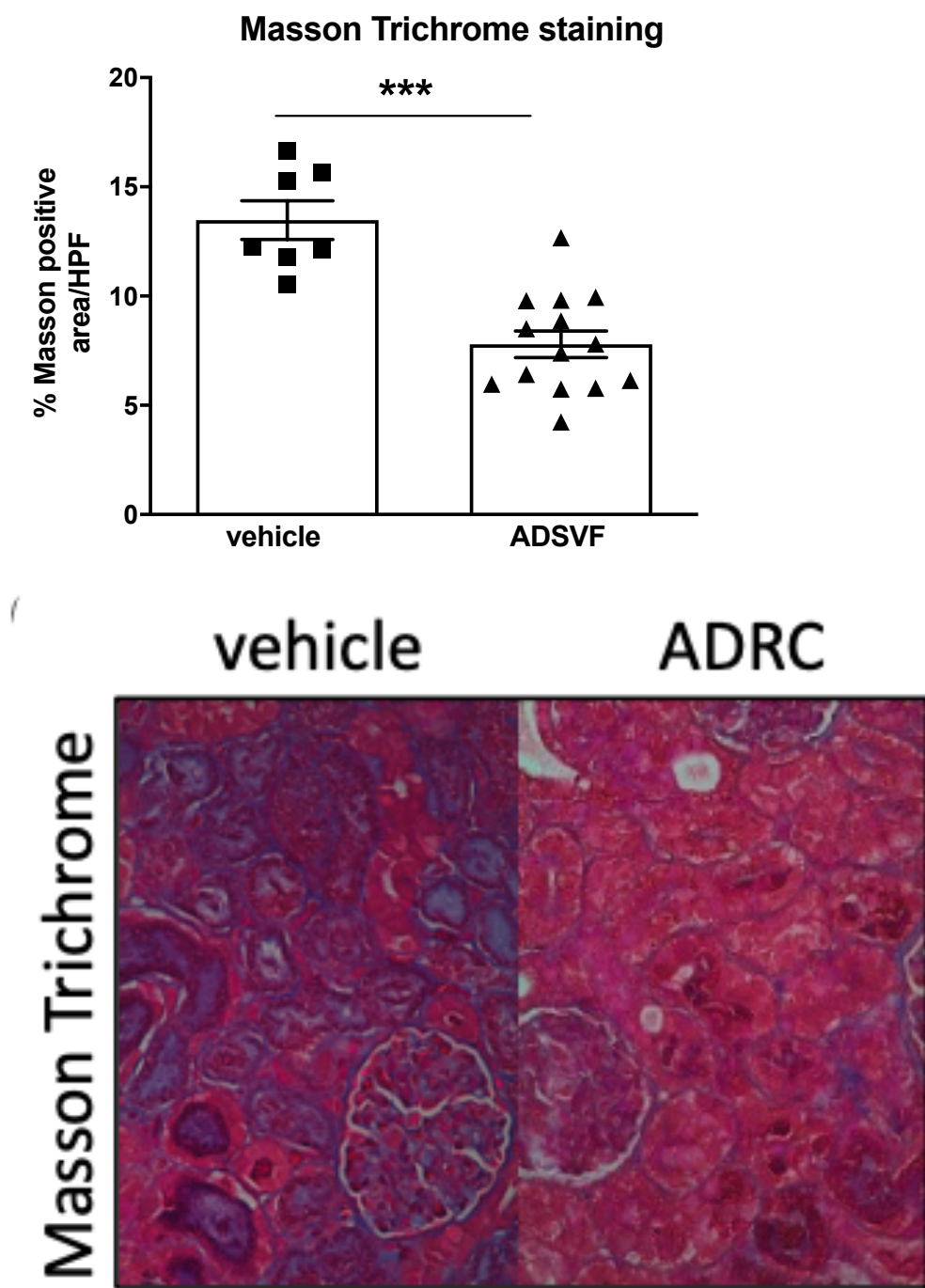
Figure 6.7 Reduced fibrosis in the ADSVF groups seen on histological analysis. Representative Masson's Trichrome staining of kidney tissue which have sustained a renal IRI and then treated with ADSVF or vehicle control via the renal artery. Tissues analysed one week post IRI and administration of ADSVF/vehicle control. Masson Trichrome staining for detection of collagen in F344 rats (vehicle n=7, ADSVF n=14). Representative

image 20x magnification (blue-stained areas expressed as percentage of total surface area) . There was a significant increase of fibrosis in the vehicle treated group. Significance was considered for p values <0.05 (*) but included p values <0.01 (**), and <0.001 (***) as indicated.

6.4.3 ADSVFS REDUCE INFLAMMATION

Pro-inflammatory chemokine CXCL 12 is significantly raised by one week in vehicle control-treated animals. Cytokine colony-stimulating factor 2 (CSF2) which plays a role in the immune / inflammatory cascade, although not quite significant, follows a similar trend in each group (Fig. 6.8). However, when the protein levels of CSF2 are measured, the higher levels in the vehicle group at one week are significant (Fig. 6.9). Cytotoxic T-lymphocyte-associated protein 4 (CTLA 4) which downregulates the immune response, on the other hand, is significantly lower in vehicle groups by one week. The CTLA 4 ligand, CD86, is again significantly lower in the vehicle-treated group (Fig. 6.9)

Flow cytometric analysis of the left kidney looking for leucocytes (CD45+) found a tendency for a higher level in control-treated rats by 48 hours. Histological analysis to assess leukocytes in the form of infiltrates again found higher levels in the control-treated kidney by 48 hours (Fig. 6.10) By one week the infiltrate lesion score was significantly higher in the vehicle control group. Horseshoe nucleated cells, characteristic of neutrophils and monocytes, clustered together, typically near a vessel, was considered a lesion.
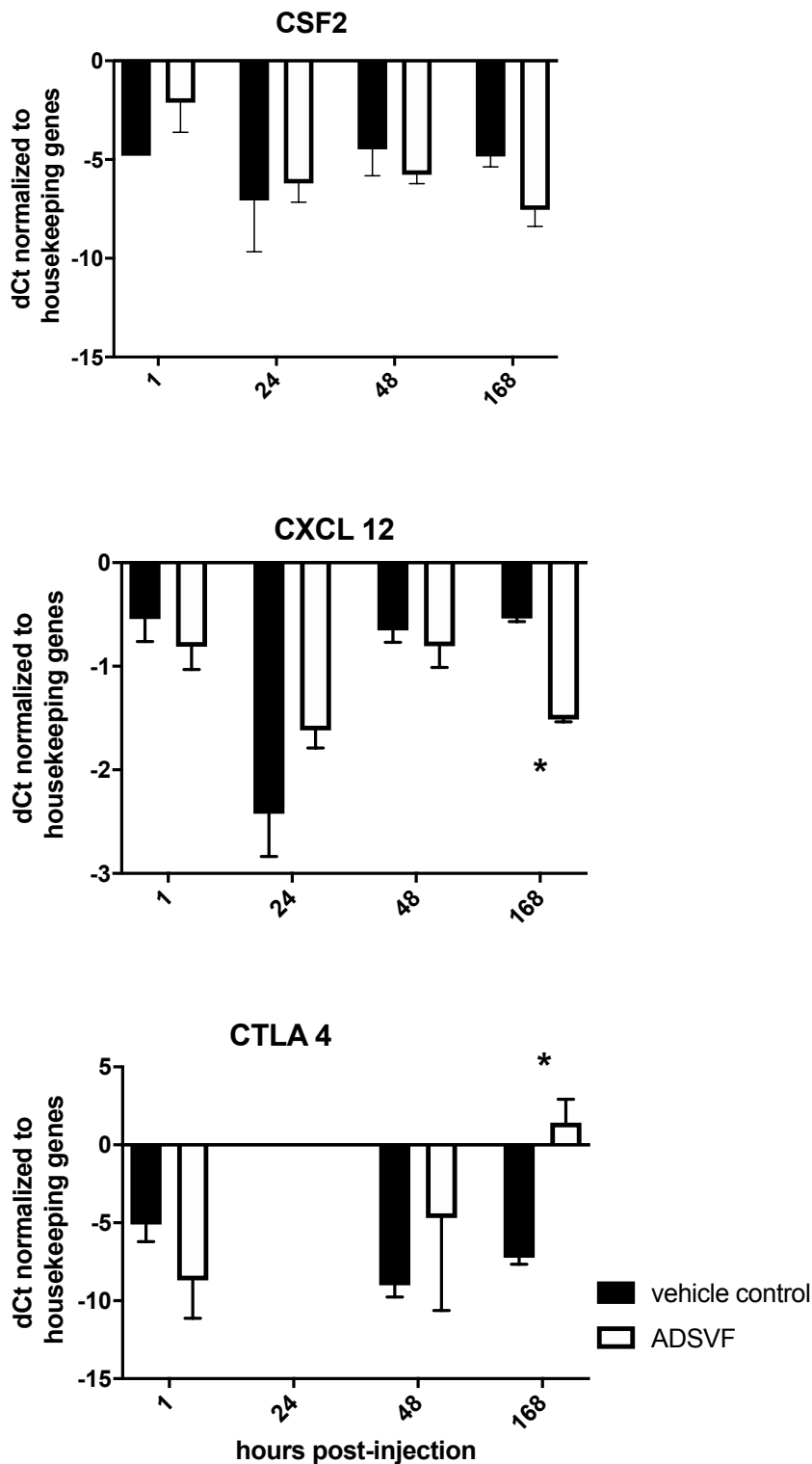
Figure 6.8 Gene expression of pro-inflammatory mediators are reduced in ADSVF treated rats. RT-PCR analysis of kidneys which have sustained a renal IRI and then treated with ADSVF or vehicle control via the renal artery. Represented as their delta CT (housekeeping genes Ct minus gene of interest Ct) after 40 cycles. Kidneys retrieved at 1 hours (n=4), 24hours (n=5), 48hours (n=8) and 1 week (n=4) post IRI/administration of ADSVF. Pro-inflammatory chemokine CXCL 12 is significantly raised by one week in vehicle control-treated animals. CSF2 although not quite significant, follows a similar trend

of being higher in the vehicle treated group between 48 hours and 1 week. CTLA 4 on the other hand, is significantly higher in ADSVF groups by one week. Significance was considered for p values <0.05 (*) but included p values <0.01 (**), and <0.001 (***) as indicated.
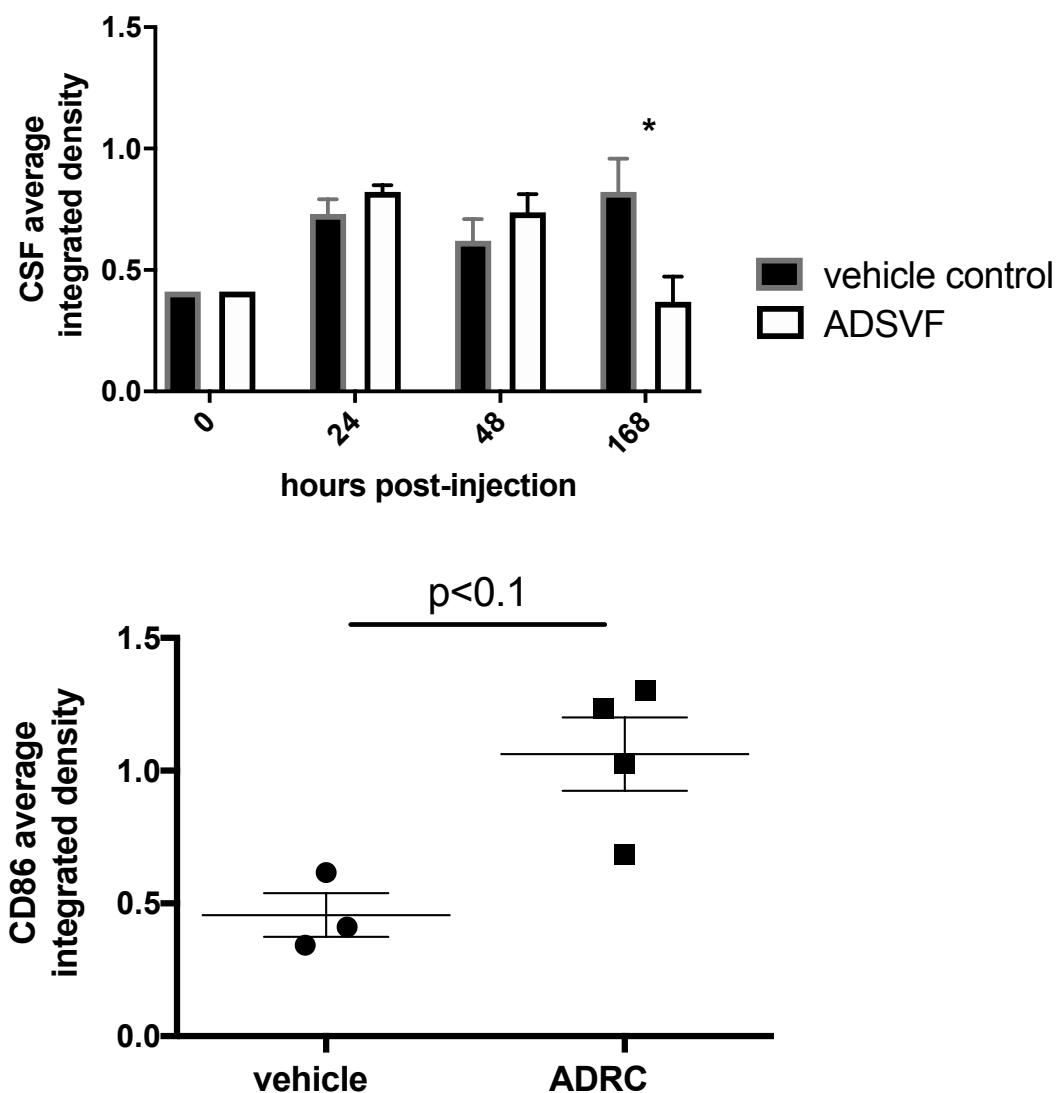
Figure 6.9 Protein levels of inflammatory mediators demonstrate favourable anti-inflammatory trends in ADSVF treated rats. Protein analysis of kidneys which have sustained a renal IRI and then treated with ADSVF or vehicle control via the renal artery. (A) Rat cytokine array panel used to detect CSF at 1 (n=1), 24 (n=4), 48 (n=4) hours and one week (n=3). CSF is significantly lower in the ADSVF treated group by 1 week. (B) Samples taken 48hours demonstrate increased levels of CD86 in the ADRC treated group (vehicle n=3, ADSVF n=4). Significance was considered for p values <0.05 (*) but included p values <0.01 (**), and <0.001 (***) as indicated.

A

B

1 week
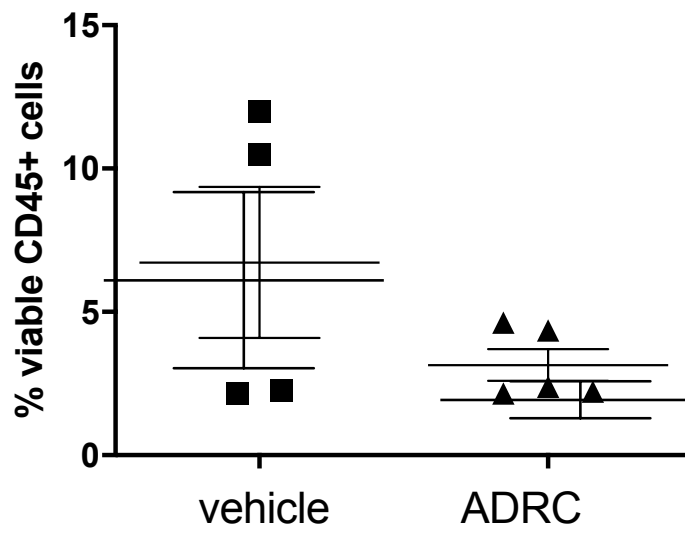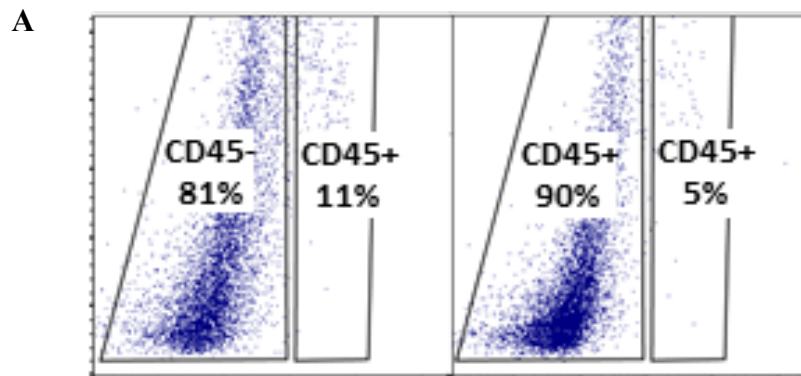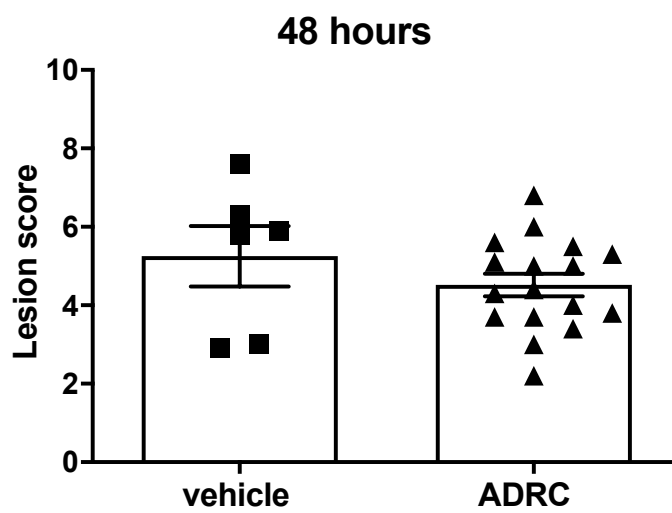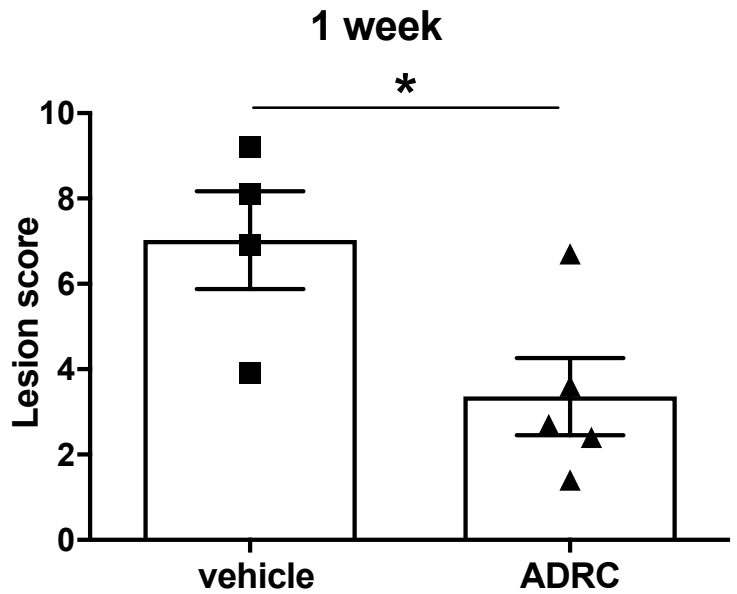
Figure 6.10 ADSVF treated rats have lower levels of immune infiltrates. Flow cytometric and histological analysis was performed on kidneys which have sustained a renal IRI and then treated with ADSVF or vehicle control via the renal artery. (A) Flow cytometric analysis looking for CD45+ leucocyte levels at 48 hours in the left kidney of vehicle control (n=4,) and ADSVF treated (n=5) rats show an increased percentage of leukocytes in the vehicle control group. (B) Infiltrate lesion score at 48 hours (vehicle control n=6, ADSVF n=17) and one week (vehicle control n=4, ADSVF n=5) in vehicle control and ADSVF treated rats was calculated using histology. Horseshoe nucleated cells, characteristic of neutrophils and monocytes, clustered together, typically near a vessel, was considered a lesion, and was blinded analysed by three separate assessors. ADSVF treated rats has a significantly lower infiltrate lesion score. Significance was considered for p values <0.05 (*) but included p values <0.01 (**), and <0.001 (***) as indicated.

6.5 DISCUSSION

Many research groups have demonstrated the ameliorative effects of ADSVF in renal ischaemia reperfusion injury. Although our model is unique in the severity of ischaemia reperfusion it induces, and the route of administration (via the renal artery) differs, the underlying mechanisms are likely to be similar. ADSVFs have proven regenerative, anti-inflammatory, antioxidant, immune-modulatory properties, as demonstrated in a variety of bodily systems and diseases. In our research, an improvement in renal function can be seen within the first few days. In this short timeframe, it is unlikely the kidney has had an opportunity to regenerate the damaged tissue into functionally active tissue, although they may exert this regenerative effect in the long-term. Most likely, ADSVF can dampen the damaging factors associated with IRI or protect the kidney in some way, therefore, retaining a higher degree of renal function.

HIF1A, a marker for injury and antioxidant, was significantly raised in the vehicle-treated group suggesting increased hypoxic injury. However, KIM -1, which is a marker for proximal tubule injury, and NGAL, which rises during renal ischaemia and excreted by the renal tubular cells, followed a similar trend in both groups. Perhaps the ADSVF have varying degrees of efficacy within the kidney and are more effective at reducing injury on other kidney structures, like the glomerulus. The reduced injury implied by HIF1A is further supported by the significant reduction in microparticles in the sera at just 48 hours, a significantly lower tubular injury score by one week and overall improved well-being (measured in rat weight) by as early as day four. This reduction in injury secondary to the severe IRI translates to improved renal function in the long-term as there is reduced nephron loss and therefore, a higher baseline for recovery. However, it is unclear if this protection or another mechanism provides most of the initial amelioration against the IRI.

Kidney repair after an injury is a complex finely balanced process of formation and degradation. An exaggerated uncontrolled response to significant injury leads to renal fibrosis characterised as glomerulosclerosis, tubule-interstitial fibrosis (pathological deposits of extracellular matrix), inflammatory infiltrate and loss of renal parenchyma (Y. Liu 2011). The extracellular matrix (ECM) is in a constant dynamic state of remodelling. Many cell types and signalling mediators are involved in the development of fibrosis such as the activation of mesangial cells, fibroblasts and tubular epithelial cells that produce extracellular matrix components (Eddy 2000). TGF-b and its downstream Smad signalling

pathway is one of the most popular and studied pathways involved in cellular activation in renal fibrosis.

Although we did not find any significant differences in TGF-b, there was a significant rise of COL4A1 and COL4A2 which is stimulated by TGF-b. Along with collagen type IV, there is a significant increase collagen type I expression and increased collagen type I and IV in the ECM of the kidney are cardinal features of renal fibrosis. MMPs have a complex role in renal fibrosis and not just in ECM degradation which was traditionally thought (Boor et al. 2007; Catania et al. 2007; Pardo & Selman 2006). Although the major role of MMPs seems to be in ECM degradation, this process can be temporarily inhibited by TIMPs (Catania et al. 2007). TIMP 1, which was increased in the vehicle control group, has been associated with early events of renal disease progression in human and rodent models (Catania et al. 2007; T. S. Johnson et al. 2002; Eddy 2000).

Interestingly FGF-2 was significantly higher in the ADSVFs treated group at 48hours. However, excessive FGF-2 may play a role in the development of kidney fibrosis despite being necessary for the initial repair (Z. Xu & Dai 2017). Also, FGF2 protects against renal IRI by attenuating the inflammatory response (X.-H. Tan et al. 2017).

VEGF is also significantly increased in the ADSVF group and may have a role in promoting endothelial survival and proliferation (Kanellis et al. 2002). A VEGF-A increase is not routinely seen after renal IRI and reducing it is associated with tubulointerstitial fibrosis. Increased expression is detrimental in various renal diseases and is likely dependent on the degree and timing of expression. Therefore, like many processes in kidney recovery, a delicate balance is fundamental. The VEGF-A may be induced by the increased of HIF1A, but as the expression of HIF1A did not significantly rise in the vehicle control group until five days after VEGF increase, this is not actively supported. HIF1A has, however, been linked with the development of fibrogenesis by increasing matrix modifying factors and facilitating epithelial to mesenchymal transition (Higgins et al. 2007).

Masson Trichrome staining of ADSVF treated kidney sections demonstrated decreased expression of interstitial factors correlating with lower levels of fibrosis. Cumulatively this evidence may suggest that along with reducing the initial insult, ADSVFs decrease the progression to renal fibrosis by favourably altering the balancing of some of the key mediators involved in repair and fibrosis.

As seen in other bodily systems, it appears the ADSVFs have an immunomodulatory effect post renal IRI. Proinflammatory mediators like CXCL12 and CSF2 1-week post-administration are reduced in the ADSVF treated groups while immunomodulatory receptors like CTLA4 are increased. Cumulatively this could result in a reduced inflammatory response involving a host of immune cells. T cells upregulate CTLA4 expression and when bound to its ligand CD86, which is raised in ADSVF treated groups, it puts the brakes on T cells function. CTLA4 influence specifically on Treg function is particularly well studied, and although complex, the raised CTLA4 could exert an anti-inflammatory influence in part through the Tregs as we know the Tregs rely heavily on CTLA4 (Walker 2013). As a result of these immunomodulatory actions, you would expect reduced infiltration of leukocytes into the injured kidney, and this was demonstrated by the reduced number of CD45+ cells, detected by flow cytometry, and lesion counts in histology. However, we do appreciate that it is difficult to get accurate quantitative data from histology.

With all the RT PCR data, we must be cautious that there is not always a direct correlation to human pathophysiology. CXCL12 (SDF1) and its primary receptor, CXCR4, for example, have a higher expression in humans compared to rodents and humans have more splice variants compared to rodents, but compared to other cytokines there are high homology between human and rodents (Janssens et al. 2018). These differences, in all cytokines, can affect the activities they show in various processes and therefore will not necessarily be replicated in human trials. A further limitation of the RT PCR was the homogenate used. Using the whole kidney, and not focussing on a micro-section, dilutes the signal. Most of the interventions seem to be taking place around the glomerulus, or the cortex, and perhaps resecting the cortex and homogenising that instead of the whole kidney would be a more refined method. Also, with gene expression studies cytokines and proteins can be anti-inflammatory in one state or environment and the opposite in another. RNA analysis alone does not explain the full picture and further investigation into these pathways is necessary if we are to get a deeper understanding of how ADSVF ameliorates IRI. A final consideration is that these mechanistic studies did not investigate the differentiation potential of ADSVF. It is difficult to prove that ADSVF, in particular the ASC, integrate into the kidney and divide and develop into functional kidney cells. Attempting to reveal an increased proliferation of resident renal cells, due to the paracrine effect of administered ADSVF in the kidney could be considered in the future. However, tracing ADSVF to show that they are proliferating and differentiating into kidney parenchyma would be more challenging to demonstrate.

In summary, maintaining balance is essential to well-being. ADSVF does not stop the necessary repair and regeneration of the kidney but may regulate its response to reduce fibrosis and detrimental inflammation. The diverse ADSVF population contain a variety of mediators in the form of cytokines, chemokines, exosomes and undoubtedly have thousands of effects on the injured kidney. Not all these effects will be advantageous, but the overall impact of ADSVF results in improved renal function. Added to the notion that the presence of the ADSVF reduces the degree of IRI, they show high potential for clinical translation in the transplant setting. It is not possible to conclude whether it is the ability to reduce the injury or the ability to balance the response, which has the most significant effect on the long-term renal function. The necessity to determine this answer depends on the proposed timing of ADSVF administration in the clinical setting. The regenerative and reparative effect of ADSVF could also be used in other renal pathologies and interventional radiology could be utilised to administer them directly into the renal artery.

CHAPTER 7:

GENERAL DISCUSSION

7.1.1 SUMMARY OF KEY FINDINGS

This thesis had a particular remit; to investigate how non-cultured regenerative cell therapy could be implemented with a single dose at the time of kidney transplantation in a bid to ameliorate IRI. The introduction chapter justified why we chose fresh uncultured ADSVF and our proposed clinical model of implementing stem cell therapy to ameliorate transplant related IRI. In brief, cellular therapies have been used in many clinical trials, and ASC so far have demonstrated a promising safety profile. ADSVF was chosen as the regenerative cellular therapy of choice due to the high concentration of stem cells, ease of accessibility to adipose tissue and a reasonably simple extraction process. Cytori Therapeutics (San Diego, USA) has developed a machine that can process adipose tissue into ADSVF, in the clinical setting, within 60 minutes with minimal expertise required: yielding fresh uncultured cells quickly and reproducibly.

To the best of our knowledge, no group has administered fresh, uncultured, ADSVF via the renal artery peri-transplant, in humans or in human kidneys ex vivo, in a bid to ameliorate IRI. Data exists on ADSVF use in renal IRI and the use of cellular therapies via the renal artery of a graft but not in the combination we propose. Before considering clinical trials, basic science specific to this methodology is required, to build on current related and generic data. Outcomes of this thesis will build on the animal model functional data that already exists, add to the safety profile of using ADSVF and form the foundations of future planning, clinical study design and ethics approval.

Aims 1 & 2: Characterisation of ADSVF

The aim of this chapter is twofold. Firstly, to add data on fresh ADSVF obtained from the rat inguinal fat depot as this is what our group has demonstrated to have ameliorative properties in renal IRI. This knowledge is essential if we are to determine the mechanism of action, and later the safety profile. Secondly, very little data exist on the peri-renal depot as a source of ADSVF. It is essential to determine any potential difference between inguinal and peri-renal adipose tissue, especially as our clinical model could utilise peri-renal adipose

189

tissue as a source of ADSVF. We also wanted to compare rat adipose tissue used in our animal models with human adipose tissue which will be used in the clinical setting to ensure there are no concerning major differences.

The analysis of this chapter confirmed a viable cell population from both adipose depots even after storage in liquid nitrogen and subsequent thawing. The cell populations were similar between inguinal and peri-renal sources but demonstrated a significantly higher leucocyte population in the inguinal depot – the clinical relevance when administering inguinal ADSVF via the renal artery is unknown.

Due to the lower amount of adipose tissue stored in peri-renal tissue (and therefore reduced ADSVF yield), we did not use peri-renal-derived ADSVF in our animal model of renal IRI. However, humans store considerably more peri-renal adipose tissue (enough to obtain a therapeutic volume of ADSVF) therefore this would be less of an issue in clinical translation. The similar viability and heterogenicity of the peri-renal ADSVF, from both human and rats, is reassuring for moving to clinical translation as there is a high probability of using peri-renal ADSVF in the clinical settings.

The gene expression analysis results from the ADSVF were as expected with the expression of factors related to repair and regeneration.

Future research in this topic could focus on adipose tissue from patients with ESRF; as the transplant recipient is an attractive source of adipose tissue. We know different donor pathologies can alter properties of ADSVF. For example, Markus et al. found T-reg cells are significantly reduced in the ADSVF in the fat of obese rats compared to normal rats which had an effect of their ability to produce anti-inflammatory mediators (Feuerer et al. 2009). Further research could also be performed on peri-renal adipose tissue that has been stored on ice for 10 hours or so to better represent the peri-renal adipose tissue that comes with the donated kidney graft.

In conclusion, this chapter has revealed that rat inguinal ADSVF varies slightly in its proportions of cell subsets compared to rat peri renal ADSVF and human peri renal ADSVF. But overall, the cell populations are similar between all sources. Rat inguinal ADSVF has proven its efficacy in ameliorating renal IRI therefore, the similar rat peri-renal and human peri renal ADSVF will likely have the same potential. Furthermore, a similar population is unlikely to have any additional risks associated with it.

Aim 3: The animal model

To investigate the potential mechanism of action and biodistribution of the ADSVF, an animal model had to be chosen that could closely replicate the transplant patient. A new animal licence application was created specifically for this thesis with three severe animal protocols included in it. Over 200 microsurgical procedures were performed during this period of research. Samples in the form of tissue, RNA, serum, and histology from over 90 rats have been studied and stored. A large proportion of which is not included in this thesis and is the subject of ongoing research. The animal licence created for this thesis has been adopted by other researchers studying renal IRI.

Multiple rodent models exist which replicate acute kidney injury and renal IRI. The closest imitation would be to perform kidney transplants in rodents. However, despite being a powerful research tool, there are significant drawbacks to performing this model. Firstly, it is technically challenging, and experienced microsurgeons may find it difficult to anastomose the vessels repetitively and successfully. Consistent evolution of the technique has improved outcomes but the potential of complications, which would be terminal, remains high. (Plenter et al. 2015). Secondly, the surgery itself is lengthy with three anastomoses to be performed once adequate exposure is achieved. Finally, there is an additional procedure and animal sacrifice required to retrieve a kidney graft. Overall, a time consuming, technically challenging, high-risk model with a long learning curve. Also, depending on the research, a contralateral nephrectomy is often performed a few days post-transplant. For those reasons, a transplant animal model as the foundations of this research would not be acceptable, especially when large numbers are planned. The unilateral IRI model, which was modified by Whalen et al. creates a significant permanent IRI with representative histological damage comparative to transplant related IRI. However, in a bid to better represent the transplant patients, reduce animal numbers and make it simpler, a further evolution of this model was created.

Chapter four demonstrated that 2/3 nephrectomy of the contralateral untouched kidney is feasible with no increase in morbidity and mortality. The additional procedure, once experienced, takes the surgeon 15 minutes and the rat makes a full recovery. By performing this 2/3 nephrectomy of the right kidney, the left IRI kidney is now recovering in an environment of reduced renal function and associated metabolic imbalances – similar to the dialysis patient receiving a kidney transplant. As rodent dialysis does not exist this is

probably the furthest the animal model can be taken with regards to representing the transplant scenario.

Non-invasive renal function monitoring further enhances the model as it allows for a longitudinal measurement of renal function. Also, it reduces the number of animals required, which is an important addition welcomed by the animal licence ethics boards.

The minor technical improvements, described in chapter four, help streamline the surgical procedure without compromising animal welfare. In addition to being quicker, it also makes teaching the model easier to learn.

As it stands, the model seems to have been optimised as much as possible. Future techniques and devices will no doubt allow it to continue to develop. It is an effective and acceptable means of testing therapies targeting renal transplant related IRI. The addition of immunosuppression would take the model one step closer to mimicking the renal transplant patient.

Organoids may further reduce the need for animal testing. Kidney organoids have already been used to investigate some renal conditions such as polycystic kidney disease. Organoids that investigate IRI are however more challenging as the pathology of IRI is the result of a cessation of blood then restoration of blood. Complex kidney organoids with a representative vasculature to test IRI does not exist, but they may in the future have role to play in some specific aspects of IRI such as fibrosis formation.

Aim 4: Biodistribution

Few groups have used direct renal artery administration in their animal models to avoid non-targeted biodistribution of the administered therapy. There have been no clinical studies in which stem cells or other types of cellular therapy have been injected into the renal artery. In most incidents of renal disease or injury the renal artery is not accessible. However, at the time of renal transplant the surgeon has easy access to the renal artery and veins. Therefore, administering therapy through this route could be considered a niche technique and only viable in the transplant setting. If renal artery administration of regenerative cells were found to be advantageous, the rapidly expanding field of interventional radiology would allow administration of regenerative cellular therapies for non-transplant related kidney injury

such as drug-induced, post heart transplant, post sepsis. Potentially even as a route for directed treatment for graft rejection.

The aim of chapter five was to investigate if administration of ADSVF via the renal artery reduced off-target biodistribution. Through two modalities, DiR labelled cells, PKH26 labelled cells, it was convincing that ADSVF remained in the kidney for at least 48 hours. Reducing the time for homing and ensuring maximum concentration possible of cells within the kidney for them to effectuate potential therapeutic paracrine action. No significant increase in signal was seen in any other organ.

The liver and lungs seem to be where most labelled regenerative cells collected after systemic administration in published studies. Also, in our work, the liver had increased signal in IVIS scanning and in sectioned fluorescent imaging, however, the diffuse quality of the fluorescence suggested degradation of the dyed ADSVF cellular membrane. For confirmation, studies through flow cytometry and immunohistochemistry of the liver and lungs, demonstrating minimal viable cells, would help further support the use of renal artery administration.

Histological sections indicated that the majority of retained cells within the kidney resided within the cortex of the kidney. Interestingly research published this year found labelled ASC in both the cortex and the medulla (Zaw Thin et al. 2020). The experiments involved administering the cells via the renal artery under ultrasound guidance in healthy mice. One explanation could be that the injured vasculature in the kidneys in our model traps the cells, or the cells are attracted to the injured microvasculature and surrounding cells due to chemoattractants. To further investigate the micro localisation of labelled cells, the sections could be examined using immunohistochemistry and confocal microscopy. Imaging using higher magnification has since been performed by our group and confirms the presence of the ADSVF within the glomerulus. Recent studies using in vivo porcine renal artery administration and ex-vivo human kidney graft renal artery administration of labelled MSCs both confirmed the localisation of MSC within the cortex of the kidney (Sierra-Parraga et al. 2019; Thompson et al. 2020). Interestingly the porcine model was attempted again with deactivated MSC and biodistribution was unchanged so perhaps the chemoattractant effect of the injured kidney cells does not play such a significant role in biodistribution when administered via the renal artery (Sierra-Parraga et al. 2019).

Overall administration of ADSVF via the renal artery is an effective means of delivering the cells directly to an injured kidney. Unwanted non-target distribution appears to be reduced. Using the renal artery may allow for higher concentrations of ADSVF to be administered as there is less worry of systemic interference or conversely lower concentrations since more potentially therapeutic cells will be delivered locally. However, one major limitation of research from a clinical standpoint is the discrepancies of the rat microvasculature and human microvasculature and the concentration of ADSVF required. Encouraging as the results are as a means of administrating the cells, further research is required to address those points. One option would be to perform similar research on a porcine model. That way dosage titrations can be performed to find a therapeutic range and help determine the maximum dosage before deleterious clogging of the vessels occur. Another option, potentially more favourable, would be to administer the ADSVF in discarded organs (retrieved but rejected for implantation). Ex vivo kidney perfusion rigs would allow for functional analysis, and then once the observation period is finished, the kidneys could undergo analysis for thromboembolic events. This route would be more representative and would avoid a laborious large animal model.

Aim 5: Mechanisms of action

Chapter six set out to define potential mechanisms of ADSVF therapeutic action. We know from published research, MSC have an array of functions and to thoroughly investigate even several of these pathways would require extensive research. More specifically, this chapter aimed to confirm if uncultured ADSVF administered into a severe model of renal IRI implement some of the mechanisms described in existing research on MSC from adipose tissue and other origins. Through gene expression, protein detection and histology, we were able to highlight protective and anti-inflammatory properties along with reduced kidney fibrosis. These properties have all been revealed in other stem cell sources used to treat various diseases. As they act similarly, the risks of using ADSVF to treat renal IRI is unlikely to be hugely different from the clinical trial that has already taken place using ADSVF in various pathologies. Also, a lower concentration of ADSVF may be required compared to systemic administration as the full administered therapy is straight into the kidneys. Lower dosages will minimise the thrombotic risk of ADSVF.

In summary, ADSVF has a repertoire of paracrine actions. The gene expression analysis results from this chapter were as expected with expression of factors related to repair and

regeneration. These results will not only add to the safety profile but may aid in discovery of optimal timing of administration. It seems likely that ADSVF provide a degree of protection from ischaemia reperfusion injury as kidney function, tubular injury score, sera microparticles levels are improved within 48 hours. The presence of ADSVF at the time of reperfusion dampens the harmful effects and aids in the maintenance of higher residual function and structure. It is unlikely these changes are due to regeneration so early on. Therefore, to ameliorate IRI, data indicate ADSVF should be administered peri- IRI. Pre IRI may provide even more benefits.

Future studies could focus on and define some of these pathways in more details. Gene knock out techniques, single-cell sequencing and kidney organoids could all be considered. As exciting and useful to other research groups as this would be, further knowledge of specific pathways may not be required to move forward to clinical trials. If a particular pathway was identified, it might be a potential target for future therapies, but in our envisaged point of care extraction and administration clinical model, the therapy (ADSVF) is relatively fixed.

7.2 MOVING FORWARD WITH ADSVF IN RENAL TRANSPLANTATION

Two routes can be embarked upon moving forward from the work presented. One takes the use of ADSVF a step closer to clinical translation. The other builds on the basic science of ADSVF to look at the therapeutic potentiators of ADSVF.

Moving forward with the basic science could take multiple routes. Useful work would include delving further into mechanisms of actions of the ADSVF and, defining the role of the subpopulations of the ADSVF and the interactions between them. Creating a 3D environment (organoids) of the renal cortex and recreating IRI microenvironment would enable more focused, less diluted, analysis of gene expression and mechanistic studies. It would also reduce the need for animal use. Functional analysis may not be possible, but inflammation, fibrosis, angiogenesis pathways could be delineated in more detail. Identifying the most therapeutic subpopulations of the ADSVF would mean creating therapies which are more potent and could help avoid the thromboembolic risks of ADSVF – but could also introduce new risks such as the introduction of microbes during the processing.

There is enough basic science knowledge on MSC, ADSVF and ASC to move into translational research. This thesis builds on this knowledge specific to the clinical translation of ADSVF as a point-of-care intervention in the renal transplant setting. A few years ago, use of ADSVF in kidney grafts would have been an ambitious proposal, but two things have changed since. Firstly, more clinical studies have since been completed using stem cells for a various pathology which has led to feasibility and safety becoming more widely accepted. Secondly, the increased use of ex vivo perfusion rigs provide a means of administering ADSVF to the kidney before direct exposure to patients; a middle ground to injecting the ADSVF into a kidney graft in vivo.

Progressing to a Clinical Trial

For over ten years there have been many clinical trials of MSC in solid organ transplantation. Most of the research has been used as an induction therapy to prevent both delayed graft function and acute rejection. Safety, feasibility, and efficacy have been demonstrated, but these studies are highly variability and do not provide a blanket assurance of safety and efficacy of all cellular therapies. The condition being treated, the cell source, preparation technique, administration route and timing could all alter the outcome.

The number of completed clinical studies specifically focusing on MSC used to combat renal transplant associated IRI is very low. Of the few studies that are published, they have shown the safety and feasibility of MSCs in kidney transplant, but again none were uncultured ADSVF or via the renal artery. At least it is reassuring that systemic administration via a central vessel does not cause any first-pass organ injury (Pileggi et al. 2013). In theory, targeted administration via the renal artery will be even safer at reducing non-targeted engraftment.

Currently 71 (10 recruiting, three not recruiting yet, and 32 completed) studies are registered on clinicaltrials.gov aimed at renal IRI specifically. Of those, three are using cellular therapies: Jarmi et al. from the Mayo Clinic in Florida are performing a feasibility and safety study of using ASC in DCD donors (Jarmi 2020). The 15 patients will be split into three groups of administrations: intraarterial, intravenous and intra-parenchymal. It is not known if these are uncultured ASC, and if the artery of administration will be the renal artery. The other two studies are looking at the intravenous administration of BM MSC after reperfusion.

Parraga et al. have administered MSC directly into the renal artery but this was in a porcine model of IRI (Sierra-Parraga et al. 2019). They report similar results to our biodistribution studies in which there is minimal off-target engraftment and retention was mainly seen within the renal cortex. This is reassuring as porcine kidneys better represent the size of human kidneys. With the cumulative knowledge, it does not seem unreasonable to establish a safety, feasibility clinical trial using ADSVF via the renal artery at the time of transplantation. There has been no research published of clinical trials looking at fresh uncultured ADSVF administered via the renal artery at the time of transplantation.

When it comes to looking at the administration of cellular therapies on machine organ perfusion rigs, there has been much more progress compared to direct human studies. Again, no groups have used ADSVF as their cellular therapy of choice. Earlier this year a group from the United Kingdom published in the American Journal of Transplant their work administering cellular therapeutics directly into the renal artery of human kidneys in a normothermic machine perfusion rig (Thompson et al. 2020). They claim this was the first time multipotent adult progenitor cells have successfully been administered into human kidneys during normothermic machine perfusion (NMP). After 7 hours of NRP with MSC, they measured functional parameters, biodistribution, injury markers and cytokine profile. They concluded the MSC treated kidneys had improved urine output and microvasculature perfusion plus reduced markers of injury. Interestingly, they again found most of the labelled cells to be in the glomeruli, within the cortex, in keeping with our biodistribution studies.

The significant difference in their study, compared to a study proposal building on the findings of this thesis, is the use of cultured BM MSC. The BM MSC NM P study was well designed and having a similar study design, to one that has been approved by a British ethics committee, would make obtaining approval to test ADSVF less arduous. Ethics approval will be one of the main hurdles to address when setting up a study using the ADSVF in ex vivo perfusion. Initially, it was presumed using ADSVF from the peri-renal adipose tissue of the donated kidney grafts would bypass some of the regulatory requirements. However, this is not going to be the case. The use of collagenases on adipose tissue to extract the ADSVF was considered a "significant manipulation" of the tissue and can no longer be considered homologous (Raposio & Ciliberti 2017).

Another factor to consider is the concentration of cells to administer. The BM NMP study used 50 million cells which were proved safe and effective. Porcine studies have used around 10 million cells. As thromboembolic events are the main concern, utilizing 50 million cells

makes sense as it has already proven safe and effective. Future studies could then look at titration dosage regimes and timings.

The methods used within this thesis could be integrated into a clinical ex vivo perfusion study (Fig 7.1). Gene expression and biodistribution could be added to the outcomes as would functional analysis in the form of urine output, serum electrolytes, and injury markers such as NGAL. Applying to NHS Blood and Transplant regulatory body to receive paired kidneys which have been declined for transplantation would reduce some of the variables.
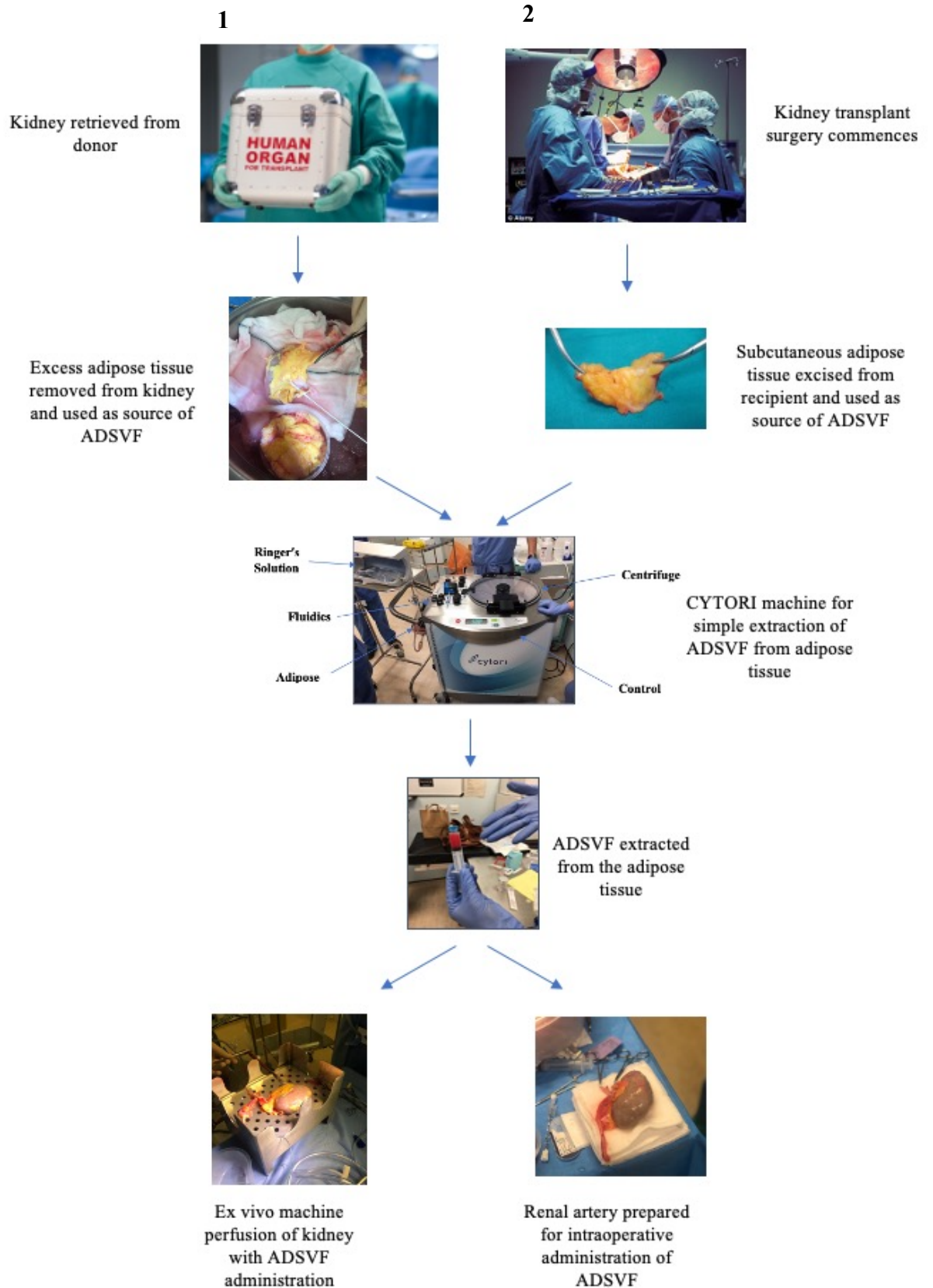
Figure 7.1 Two potential methods for delivering ADSVF in a clinical study using human kidneys. (1) The kidney is retrieved from donor as normal. The implanting centre removes the peri-renal adipose tissue, but instead of discarding it, the adipose tissue is processed on-site to extract the ADSVF using the Cytori therapeutics machine. The ADSVF is then either injected into the renal artery in a normothermic perfusion rig which recirculates

any cells that pass out the renal vein and after a period of perfusion on the rig the kidney is then implanted in the recipient in the usual manner. Or the ADSVF is administered via the renal artery of the kidney at the time of transplantation surgery. (2) Kidney arrives at the implanting centre and is prepared for implantation as usual. Implantation surgery proceeds. Once skin incision is performed, subcutaneous adipose tissue is taken from the recipient and processed in theatre, using the Cytori machine, to extract ADSVF. The operation then continues as normal. When the ADSVF are ready they are administered via the renal artery of the kidney during the transplantation surgery.

7.3 FUTURE OF CELLULAR THERAPIES IN KIDNEY TRANSPLANTATION

The field of transplantation has come a long way since the first kidney transplant in 1954 by Joseph Murray in Boston. The transplant between identical twins was the first of hundreds of thousands of transplants which have since taken place. The most seismic shift in the practice of transplantation since then has been the advent of immunosuppression. Refinement of retrieval, preservation during transportation, surgery, immunosuppression, and post-transplant follow up ensured a steady improvement in transplant outcomes over the last 50 years. With demand for organs increasing and outstripping supply all around the world, we now more than ever need a solution to organ shortages.

Increasing the number of organ donors will only take us so far, and in some societies, we are near fully maximising the donor pool. We need to make discarded kidneys useable; transplants that last longer and find a way to create more organs. For all these options, cellular medicine is the likely answer with both their regenerative cells subsets and immunoregulatory cell subsets playing a role.

The road in which cellular medicine changes transplantation undoubtedly will pass several breakthroughs.

SHORT TERM

Cellular Therapies to Induce Immunotolerance

For several years now, clinical trials have been investigating the use of cellular therapies in inducing immunotolerance. Last month in May of 2020 The ONE Study was published in the Lancet (Sawitzki et al. 2020). It analysed seven non-randomised phase 1 and 2A trails looking at the use of cell-based medical products in reducing immunosuppression in organ transplantation. Cells included T cell, dendritic cells and macrophages. There was also a reference control group. They concluded that the use of cellular therapy was safe and feasible and reported fewer infections in the early phase trials. The group have now moved onto the TWO Study which focusses on regulatory T cells. The door is open for more advanced clinical trials with dosages, timings, targeted, combination or altered cellular therapies. Successful regimes could be used in the general population soon, but whether immunotolerance lasts with reduced chronic rejection and more prolonged graft survival will take years to establish.

Cellular Therapies to Ameliorate IRI

The basis of this thesis was on cellular therapies used for their protective and regenerative potential against IRI. As previously discussed early in this chapter, the increasing popularity of perfusion rigs has allowed cellular therapies to be administered to organs with a safety net that avoids direct administration into transplant recipients. The vast combination of sources, preparations, additives, timing, and dosages means outcomes will undoubtedly improve. Also, as discussed in chapter one, there are now techniques which can boost the regenerative capacity of cellular therapies. Unlike the immunomodulatory cellular therapies, the effectiveness of regenerative cellular therapies, such as ADSVF, to ameliorate IRI, will be known immediately after implementation. Therefore, there will be a higher chance that effective regimes will be discovered sooner – compared to waiting years to see if immunotolerance last. However longitudinal studies for both immunotolerance and regenerative cellular therapies will still be required. Regenerative cellular therapies will open the door to discarded kidneys and could also increase graft survival: as IRI and graft survival have a strong correlation. The use of regenerative cells is unlikely to solve the demand for organs completely but will play a significant role and act as a steppingstone for upcoming advancements.

MEDIUM TERM

Cellular Therapies in Xenotransplantation

Xenotransplantation of a kidney was first performed over 100 years ago, and multiple attempts have been performed since. Nevertheless, even from non-human primates, the kidneys succumb to the hosts' immune defences. Nowadays, non-human primates are not the most likely source of xenotransplantation due to ethical reasons, high risk of infection transmission and organ size (Lu et al. 2019). Pig kidneys, however, address many of these issues and have a reduced size discrepancy. Also, porcine heart valves have been commercially available since the 1970s.

The rejection faced by xenotransplantation is also much greater than unmatched human transplant due to the great genetic distances between primates and humans (Lu et al. 2019). Hyperacute rejection, acute humoral xenograft rejection, cellular rejection (NK, T cells, macrophages) then coagulation dysregulation all must be overcome for the xenograft to survive long-term. Gene modification of the pigs through techniques such as clustered regularly interspaced short palindromic repeats (CRISPR) to address the multiple antigens has been performed with varying degrees of success. Newer gene modifying techniques like CRISPR has speeded up the rate of progress. Gene modified pigs have been created, such as galactosyltransferase gene knockout pigs. Galactosyltransferase is the major hyperacute rejection xenoantigen of pigs (Kobayashi & Cooper 1999). In another study, pigs which express human complement regulatory proteins have reduced complement-mediated graft injury but fail to last long term (Burdorf et al. 2014). The longest graft survival to date, from pig to non-human primate, is 499 days (S. C. Kim et al. 2019). It is inevitable in the not-so-distant future a genetically modified pig will be the source of a kidney graft for humans. However, using the strategies described so far, human recipients will still require immunosuppression.

Cellular therapies could role to play in the immunosuppressive regimes for xenotransplantation. Another central role in this field is the creation of human-animal chimaeras. With the discovery of induced pluripotent stem cells, there has been renewed interest in interspecies chimaeras and their potential in organ supply for transplantation. Two approaches include blastocyte complementation or targeted organ complementation. The latter being more favourable. Targeted organ complementation uses modified stem cells (modified by procedures such as gene editing) that are restricted to differentiating into the

organ of interest or by using lineage-committed progenitor cells. They are then implanted in zygotes, blastocysts or embryos of the host animal which has been genetically modified to be an organ-knockout.

In 2017, there was the first proof of concept that an interspecies organ transplant can treat a medical condition (Yamaguchi et al. 2017). Then in the same year, a group from the Salk in San Diego were able to successfully inject pig embryos with human stem cells and maintain survival for almost one month (Jun Wu et al. 2017). To date, there has been no human chimerism that has developed long enough to create a functioning organ, but with growing understanding, it will undoubtedly happen in the near future. Using induced pluripotent stem cells or lineage-committed progenitor cells from the human requiring the organ could mean patient-specific and immune matched organs. Significant challenges will be the timing of the introduced stem cells to the embryo, especially before the immune system develops. In theory, it seems it will be a matter of when and not if human-pig chimerism for transplantation is achieved. However ethically this may be too much for society. Humanised pigs with human-like cognitive abilities or even looks will unlikely be an eventuality, especially with targeted organ approach, but it was enough for the United States of America to ban public funding of human-animal hybrids. However, there are calls for these laws to change.

Artificial Organs

Not a cellular therapy but worth mentioning are artificial. In 2011 surgeons in Iceland transplanted a completely synthetic lab-grown trachea, made from a non-composite polymer seeded with stem cells, in a young patient with cancer (Jungebluth et al. 2011). Since then, artificial organs have developed to perform more complex functions. SynCardia, a company from Arizona, USA have created an artificial heart which can provide in vivo cardiac function until a heart transplant becomes available (Morshuis et al. 2020). Creating more complex organs that can replace the need for liver or kidneys transplants have not been invented. It is unlikely that artificial organs will be able to perform all the functions of complex organs. The kidney for examples not only "filters" the blood but maintains water balance, blood pressure, acid-base balance, vitamin D homeostasis and the creation of red blood cells. However, they may be able to soon develop an artificial organ that perform essential functions such as the filtering and removal of excess fluids. The other functions could be managed pharmacologically. Such an organ is being developed by The Kidney Project, which is creating a bioartificial kidney at the University of California. They are

unlikely to be in widespread clinical use any time soon as it has never been implanted in humans. If successfully developed, they may prevent the need of a patient going on dialysis. However, whether they can be a long-term alternative to organ transplantation is unlikely as the outcomes of a transplant that performs all functions compared to an artificial organ that performs some essential functions is going to be preferred. Nevertheless, they could provide a valuable bridge for patients waiting for a transplant. If they are easier to implant, it could be used on patients not fit enough to undergo full transplant surgery or for those unable to take immunosuppression due to recent malignancy.

LONG TERM

Cellular Therapies in Bioengineering of Organs

The holy grail for transplantation is the ability to create organs in the laboratory for implantation. Using recipient stem cells, the recipient will not require lifelong immunosuppression and will not suffer the failure of their graft due to chronic low-grade rejection. There are many methods currently being researched to overcome the challenges. Inducing stem cells to follow a particular organ differentiation has been achieved including the ability to create kidney tubular epithelial organoids. However, one of the more significant challenges is creating the complex structure of a functioning organ and in particular the vasculature. The kidney also requires a collecting system for urine which must be integrated with the functional tubules. Basic organs such as outer ear and oesophagus have been successfully created and implanted. In 2018 MacQueen et al. created a small heart beating ventricle complete with blood supply, but complex functioning structures suitable for implantation such as liver and kidneys are not likely to be bioengineered any time soon (MacQueen et al. 2018).

There are multiple approaches taken to bioengineer organs. 3D scaffolds seeded with stem cells was the first tactic. Then 3D printing using a "bio-ink" of induced pluripotent cells allowed for more accurate structural design and has been successful in the simple organ structures. However, integrating the vasculature has not been possible with standard 3D printing. The induced pluripotent cells used in the bio-ink are reprogrammed into the functional cell required once they have been printed. Advances in 3D printing have resulted in the creation of functional tissues complexes with integrated vasculature but nowhere near

as complex as the vasculature required for each cell to be in close enough proximity to a blood vessel.

Another technique involves taking an organ and removing all cellular material leaving the extracellular matrix. This process is called organ decellularisation. The extracellular matrix of the vasculature is remarkably mostly intact. In theory, the decellularised kidney can then be repopulated with stem cells to grow back into a functioning organ. Bombelli et al. demonstrated that renal stem/progenitor cells were able to populate the scaffold of a decellularised kidney slice and form proximal tubules, distal tubules and endothelium (Bombelli et al. 2018). Undeniably a massive feat but creating the right environment and developing a recellularisation technique to create a fully functioning kidney will be a significant challenge.

To conclude, ADSVF from rat peri-renal and inguinal adipose depots share similar subpopulation but vary in the proportions of each subpopulation. These subpopulations are also found in human adipose depots. Administration of ADSVDF via the renal artery likely ameliorate IRI through similar mechanisms demonstrated when MSCs are administered via other routes. Renal artery administration of ADSVF is feasible and safe in animal models and reduces non-target distribution.

The next step would be to study the use of ADSVF, via the renal artery in ex vivo organ perfusion, on kidneys rejected for transplantation. Cellular medicine is undoubtedly the future of solid organ transplantation and the transplant community has started to accept their role. Immune cellular therapies to induce immunotolerance and regenerative cellular therapies (stem cells and their associated stromal fraction) to ameliorate IRI has already started to see clinical translation. Organs from human-pig chimaeras will likely be available for human transplantation in the not-so-distant future but maybe deemed morally objectionable for many and therefore may not be adopted by all societies. Eventually, donor specific bioengineered kidneys will seismically transform the field of transplantation.

BIBLIOGRAPHY

Acosta, J.R. et al., 2016. Increased fat cell size: a major phenotype of subcutaneous white adipose tissue in non-obese individuals with type 2 diabetes. *Diabetologia*, 59(3), pp.560–570.

Adams, P.L., 2006. Long-term patient survival: strategies to improve overall health. *American journal of kidney diseases : the official journal of the National Kidney Foundation*, 47(4 Suppl 2), pp.S65–85.

Alessandrini, A. & Turka, L.A., 2017. FOXP3-Positive Regulatory T Cells and Kidney Allograft Tolerance. *American journal of kidney diseases : the official journal of the National Kidney Foundation*, 69(5), pp.667–674.

Angelotti, M.L. et al., 2012. Characterization of renal progenitors committed toward tubular lineage and their regenerative potential in renal tubular injury. *Stem cells (Dayton, Ohio)*, 30(8), pp.1714–1725.

Annabi, B. et al., 2003. Hypoxia promotes murine bone-marrow-derived stromal cell migration and tube formation. *Stem cells (Dayton, Ohio)*, 21(3), pp.337–347.

Anon, Nature Metabolism.

Asahara, T. et al., 1996. Accelerated Restitution of Endothelial Integrity and Endothelium-Dependent Function After phVEGF165 Gene Transfer. *Circulation*, 94(12), pp.3291–3302.

Attallah, N. et al., 2004. The potential role of statins in contrast nephropathy. *Clinical nephrology*, 62(4), pp.273–278.

Aurell, M., 1994. Accurate and feasible measurements of GFR--is the iohexol clearance the answer? *Nephrology, dialysis, transplantation : official publication of the European Dialysis and Transplant Association - European Renal Association*, 9(9), pp.1222–1224.

Awad, A.S. et al., 2009. Compartmentalization of neutrophils in the kidney and lung following acute ischemic kidney injury. *Kidney international*, 75(7), pp.689–698.

Baer, P.C. et al., 2019. Isolation, Characterization, Differentiation and Immunomodulatory Capacity of Mesenchymal Stromal/Stem Cells from Human Perirenal Adipose Tissue. *Cells*, 8(11), p.1346.

Bai, M. et al., 2018. IL-17A improves the efficacy of mesenchymal stem cells in ischemic-reperfusion renal injury by increasing Treg percentages by the COX-2/PGE2 pathway. *Kidney international*, 93(4), pp.814–825.

Baines, C.P., 2009. The mitochondrial permeability transition pore and ischemia-reperfusion injury. *Basic research in cardiology*, 104(2), pp.181–188.

Bajwa, A., Kinsey, G.R. & Okusa, M.D., 2009. Immune mechanisms and novel pharmacological therapies of acute kidney injury. *Current drug targets*, 10(12), pp.1196–1204.

Balducci, L. et al., 2014. Immortalization of human adipose-derived stromal cells: production of cell lines with high growth rate, mesenchymal marker expression and capability to secrete high levels of angiogenic factors. *Stem cell research & therapy*, 5(3), pp.63–15.

Bang, O.Y. & Kim, E.H., 2019. Mesenchymal Stem Cell-Derived Extracellular Vesicle Therapy for Stroke: Challenges and Progress. *Frontiers in neurology*, 10, p.211.

Bantounas, I. et al., 2018. Generation of Functioning Nephrons by Implanting Human Pluripotent Stem Cell-Derived Kidney Progenitors. *Stem cell reports*, 10(3), pp.766–779.

Baracho, N.C.D.V. et al., 2016. Characterization of an experimental model of progressive renal disease in rats. *Acta cirurgica brasileira*, 31(11), pp.744–752.

Baratelli, F. et al., 2005. Prostaglandin E2 induces FOXP3 gene expression and T regulatory cell function in human CD4+ T cells. *The Journal of Immunology*, 175(3), pp.1483–1490.

Barba, J. et al., 2011. [Is there a safe cold ischemia time interval for the renal graft?]. *Actas urologicas espanolas*, 35(8), pp.475–480.

Barbash, I.M. et al., 2003. Systemic delivery of bone marrow-derived mesenchymal stem cells to the infarcted myocardium: feasibility, cell migration, and body distribution. *Circulation*, 108(7), pp.863–868.

Barzegar, M. et al., 2019. Potential therapeutic roles of stem cells in ischemia-reperfusion injury. *Stem cell research*, 37, p.101421.

Basile, D.P. et al., 2001. Renal ischemic injury results in permanent damage to peritubular capillaries and influences long-term function. *American journal of physiology. Renal physiology*, 281(5), pp.F887–99.

Beg, A.A., 2002. Endogenous ligands of Toll-like receptors: implications for regulating inflammatory and immune responses. *Trends in immunology*, 23(11), pp.509–512.

Belizário, J., Vieira-Cordeiro, L. & Enns, S., 2015. Necroptotic Cell Death Signaling and Execution Pathway: Lessons from Knockout Mice. *Mediators of inflammation*, 2015(24), pp.128076–15.

Bennett, M.R. et al., 2007. Laser capture microdissection-microarray analysis of focal segmental glomerulosclerosis glomeruli. *Nephron. Experimental nephrology*, 107(1), pp.e30–40.

Bennett, W.M. et al., 2011. Kidney transplantation in the morbidly obese: complicated but still better than dialysis. *Clinical Transplantation*, 25(3), pp.401–405.

Bi, L.Y. et al., 2015. Effects of autologous SCF- and G-CSF-mobilized bone marrow stem cells on hypoxia-inducible factor-1 in rats with ischemia-reperfusion renal injury. *Genetics and molecular research : GMR*, 14(2), pp.4102–4112.

Blanpain, C. et al., 2004. Self-renewal, multipotency, and the existence of two cell populations within an epithelial stem cell niche. *Cell*, 118(5), pp.635–648.

Blanpain, C., Horsley, V. & Fuchs, E., 2007. Epithelial stem cells: turning over new leaves. *Cell*, 128(3), pp.445–458.

Bombelli, S. et al., 2018. Nephrosphere-Derived Cells Are Induced to Multilineage Differentiation when Cultured on Human Decellularized Kidney Scaffolds. *The American journal of pathology*, 188(1), pp.184–195.

Boor, P. et al., 2007. Treatment targets in renal fibrosis. *Nephrology, dialysis, transplantation : official publication of the European Dialysis and Transplant Association - European Renal Association*, 22(12), pp.3391–3407.

Bourin, P. et al., 2013. Stromal cells from the adipose tissue-derived stromal vascular fraction and culture expanded adipose tissue-derived stromal/stem cells: a joint statement of the International Federation for Adipose Therapeutics and Science (IFATS) and the International Society for Cellular Therapy (ISCT). *Cytotherapy*, 15(6), pp.641–648.

Braun, H. et al., 2012. Cellular senescence limits regenerative capacity and allograft survival. *Journal of the American Society of Nephrology : JASN*, 23(9), pp.1467–1473.

Brehm, M. & Strauer, B.E., 2006. Stem cell therapy in postinfarction chronic coronary heart disease. *Nature clinical practice. Cardiovascular medicine*, 3 Suppl 1(S1), pp.S101–4.

Brennan, T.V. et al., 2004. Early graft function after living donor kidney transplantation predicts rejection but not outcomes. *Am J Transplant*, 4(6), pp.971–979.

Bronte, V. & Pittet, M.J., 2013. The spleen in local and systemic regulation of immunity. *Immunity*, 39(5), pp.806–818.

Burdorf, L. et al., 2014. Expression of human CD46 modulates inflammation associated with GalTKO lung xenograft injury. *Am J Transplant*, 14(5), pp.1084–1095.

Burne, M.J. et al., 2001. Identification of the CD4(+) T cell as a major pathogenic factor in ischemic acute renal failure. *J Clin Invest*, 108(9), pp.1283–1290.

Burns, A.T. et al., 1998. Apoptosis in ischemia/reperfusion injury of human renal allografts. *Transplantation*, 66(7), pp.872–876.

Cai, J. et al., 2014. Maximum efficacy of mesenchymal stem cells in rat model of renal ischemia-reperfusion injury: renal artery administration with optimal numbers. P. Fiorina, ed. *PloS one*, 9(3), p.e92347.

Campbell, K.H. et al., 1996. Sheep cloned by nuclear transfer from a cultured cell line. *Nature*, 380(6569), pp.64–66.

Caplan, A.I., 2009. Why are MSCs therapeutic? New data: new insight M. R. Alison, ed. *The Journal of Pathology*, 217(2), pp.318–324.

Carragee, E.J., Hurwitz, E.L. & Weiner, B.K., 2011. A critical review of recombinant human bone morphogenetic protein-2 trials in spinal surgery: emerging safety concerns and lessons learned. *The spine journal : official journal of the North American Spine Society*, 11(6), pp.471–491.

Catania, J.M., Chen, G. & Parrish, A.R., 2007. Role of matrix metalloproteinases in renal pathophysiologies. *American journal of physiology. Renal physiology*, 292(3), pp.F905–11.

Ceradini, D.J. et al., 2004. Progenitor cell trafficking is regulated by hypoxic gradients through HIF-1 induction of SDF-1. *Nature medicine*, 10(8), pp.858–864.

Chanutin, a. & ferris, e.b., 1932. Experimental renal insufficiency produced by partial nephrectomy: i. Control diet. *Archives of internal medicine*, 49(5), pp.767–787.

Chen, Yeling et al., 2013. Remote ischemic preconditioning fails to improve early renal function of patients undergoing living-donor renal transplantation: a randomized controlled trial. *Transplantation*, 95(2), pp.e4–6.

Chen, Yen-Ta et al., 2011. Adipose-derived mesenchymal stem cell protects kidneys against ischemia-reperfusion injury through suppressing oxidative stress and inflammatory reaction. *Journal of translational medicine*, 9(1), p.51.

Chen, Yimeng et al., 2019. Preservation Solutions for Kidney Transplantation: History, Advances and Mechanisms. *Cell transplantation*, 28(12), pp.1472–1489.

Choi, Y.S. et al., 2012. Mechanical derivation of functional myotubes from adipose-derived stem cells. *Biomaterials*, 33(8), pp.2482–2491.

Chouchani, E.T. et al., 2014. Ischaemic accumulation of succinate controls reperfusion injury through mitochondrial ROS. *Nature*, 515(7527), pp.431–435.

Comella, K. et al., 2016. Effects of the intramyocardial implantation of stromal vascular fraction in patients with chronic ischemic cardiomyopathy. *Journal of translational medicine*, 14(1), pp.158–7.

Craddock, G.N., 1976. Species differences in response to renal ischemia. *Archives of surgery (Chicago, Ill. : 1960)*, 111(5), pp.582–584.

Croall, D.E. & Ersfeld, K., 2007. The calpains: modular designs and functional diversity. *Genome biology*, 8(6), pp.218–11.

Cui, L.-L. et al., 2015. The cerebral embolism evoked by intra-arterial delivery of allogeneic bone marrow mesenchymal stem cells in rats is related to cell dose and infusion velocity. *Stem cell research & therapy*, 6(1), p.11.

De Deken, J., Kocabayoglu, P. & Moers, C., 2016. Hypothermic machine perfusion in kidney transplantation. *Current opinion in organ transplantation*, 21(3), pp.294–300.

De Filippo, R.E. et al., 2015. Penile urethra replacement with autologous cell-seeded tubularized collagen matrices. *J Tissue Eng Regen Med*, 9(3), pp.257–264.

De Ugarte, D.A. et al., 2003. Differential expression of stem cell mobilization-associated molecules on multi-lineage cells from adipose tissue and bone marrow. *Immunology letters*, 89(2-3), pp.267–270.

delaRosa, O. et al., 2012. Human adipose-derived stem cells impair natural killer cell function and exhibit low susceptibility to natural killer-mediated lysis. *Stem cells and development*, 21(8), pp.1333–1343.

Denhaerynck, K. et al., 2005. Prevalence, consequences, and determinants of nonadherence in adult renal transplant patients: a literature review. *Transplant international : official journal of the European Society for Organ Transplantation*, 18(10), pp.1121–1133.

DiRito, J.R. et al., 2018. The future of marginal kidney repair in the context of normothermic machine perfusion. *Am J Transplant*, 18(10), pp.2400–2408.

Dong, X. et al., 2007. Resident dendritic cells are the predominant TNF-secreting cell in early renal ischemia-reperfusion injury. *Kidney international*, 71(7), pp.619–628. Available at: http://eutils.ncbi.nlm.nih.gov/entrez/eutils/elink.fcgi?dbfrom=pubmed&id=17311071&retmode=ref&cmd=prlinks.

Dorweiler, B. et al., 2007. Ischemia-Reperfusion Injury. *European Journal of Trauma and Emergency Surgery*, 33(6), pp.600–612. Available at: http://link.springer.com/article/10.1007/s00068-007-7152-z.

Dousdampanis, P. et al., 2014. Hyperuricemia and chronic kidney disease: an enigma yet to be solved. *Renal failure*, 36(9), pp.1351–1359.

Duranton, F. et al., 2012. Normal and pathologic concentrations of uremic toxins. *Journal of the American Society of Nephrology : JASN*, 23(7), pp.1258–1270.

Eddy, A.A., 2000. Molecular basis of renal fibrosis. *Pediatr Nephrology*, (15), pp.290–301.

Eggenhofer, E. et al., 2012. Mesenchymal stem cells are short-lived and do not migrate beyond the lungs after intravenous infusion. *Frontiers in immunology*, 3, p.297.

Eggenhofer, E., Benseler, V. & Kroemer, A., 2013. Mesenchymal stem cells are short-lived and do not migrate beyond the lungs after intravenous infusion. *stem cells in*.

Eltzschig, H.K. & Eckle, T., 2011. Ischemia and reperfusion--from mechanism to translation. *Nature medicine*, 17(11), pp.1391–1401.

Esteves, C.L. et al., 2017. Isolation and characterization of equine native MSC populations. *Stem cell research & therapy*, 8(1), pp.80–12.

Fahmy, S.R. et al., 2017. Therapeutic efficacy of human umbilical cord mesenchymal stem cells transplantation against renal ischemia/reperfusion injury in rats. *Tissue & cell*, 49(3), pp.369–375.

Farrar, C.A. et al., 2012. Inhibition of TLR2 promotes graft function in a murine model of renal transplant ischemia-reperfusion injury. *FASEB journal : official publication of the Federation of American Societies for Experimental Biology*, 26(2), pp.799–807.

Feng, J. et al., 2018. Intravenous Anesthetics Enhance the Ability of Human Bone Marrow-Derived Mesenchymal Stem Cells to Alleviate Hepatic Ischemia-Reperfusion Injury in a Receptor-Dependent Manner. *Cellular physiology and biochemistry : international journal of experimental cellular physiology, biochemistry, and pharmacology*, 47(2), pp.556–566.

Feng, Z. et al., 2010. Fresh and cryopreserved, uncultured adipose tissue-derived stem and regenerative cells ameliorate ischemia-reperfusion-induced acute kidney injury.

Nephrology, dialysis, transplantation : official publication of the European Dialysis and Transplant Association - European Renal Association, 25(12), pp.3874–3884.

Feuerer, M. et al., 2009. Lean, but not obese, fat is enriched for a unique population of regulatory T cells that affect metabolic parameters. *Nature medicine*, 15(8), pp.930–939.

Finco, D.R. & Duncan, J.R., 1976. Evaluation of blood urea nitrogen and serum creatinine concentrations as indicators of renal dysfunction: a study of 111 cases and a review of related literature. *Journal of the American Veterinary Medical Association*, 168(7), pp.593–601.

Fischer, U.M. et al., 2009. Pulmonary passage is a major obstacle for intravenous stem cell delivery: the pulmonary first-pass effect. *Stem cells and development*, 18(5), pp.683–692.

Flores, J. et al., 1972. The role of cell swelling in ischemic renal damage and the protective effect of hypertonic solute. *J Clin Invest*, 51(1), pp.118–126.

Forbes, J.M. et al., 2000. Ischemic acute renal failure: long-term histology of cell and matrix changes in the rat. *Kidney international*, 57(6), pp.2375–2385.

Fraser, J.K. et al., 2007. Differences in stem and progenitor cell yield in different subcutaneous adipose tissue depots. *Cytotherapy*, 9(5), pp.459–467.

Friedenstein, A.J., Chailakhjan, R.K. & Lalykina, K.S., 1970. The development of fibroblast colonies in monolayer cultures of guinea-pig bone marrow and spleen cells. *Cell and tissue kinetics*, 3(4), pp.393–403.

Gao, J. et al., 2001. The dynamic in vivo distribution of bone marrow-derived mesenchymal stem cells after infusion. *Cells Tissues Organs*, 169(1), pp.12–20.

Ghadge, S.K. et al., 2011. SDF-1α as a therapeutic stem cell homing factor in myocardial infarction. *Pharmacology & therapeutics*, 129(1), pp.97–108.

Gill, J.S. et al., 2013. The survival benefit of kidney transplantation in obese patients. *Am J Transplant*, 13(8), pp.2083–2090.

Giordano, A., Galderisi, U. & Marino, I.R., 2007. From the laboratory bench to the patient's bedside: an update on clinical trials with mesenchymal stem cells. *J Cell Physiol*, 211(1), pp.27–35.

Gonzalez-Rey, E. et al., 2010. Human adipose-derived mesenchymal stem cells reduce inflammatory and T cell responses and induce regulatory T cells in vitro in rheumatoid arthritis. *Annals of the rheumatic diseases*, 69(1), pp.241–248.

Grassi, D. et al., 2013. Chronic hyperuricemia, uric acid deposit and cardiovascular risk. *Current pharmaceutical design*, 19(13), pp.2432–2438.

Gu, M. et al., 2012. Microfluidic single-cell analysis shows that porcine induced pluripotent stem cell-derived endothelial cells improve myocardial function by paracrine activation. *Circ Res*, 111(7), pp.882–893.

Gueler, F. et al., 2015. A novel therapy to attenuate acute kidney injury and ischemic allograft damage after allogenic kidney transplantation in mice. *PloS one*, 10(1), p.e0115709.

Gutierrez-Aranda, I. et al., 2010. Human induced pluripotent stem cells develop teratoma more efficiently and faster than human embryonic stem cells regardless the site of injection. *Stem cells (Dayton, Ohio)*, 28(9), pp.1568–1570.

Halestrap, A.P., 2010. A pore way to die: the role of mitochondria in reperfusion injury and cardioprotection. *Biochemical Society transactions*, 38(4), pp.841–860.

Han, Z. et al., 2012. The role of immunosuppression of mesenchymal stem cells in tissue repair and tumor growth. *Cell & bioscience*, 2(1), p.8.

Hanifa, M.A. et al., 2019. Tissue, urine and blood metabolite signatures of chronic kidney disease in the 5/6 nephrectomy rat model. *Metabolomics : Official journal of the Metabolomic Society*, 15(8), pp.112–16.

Hardy, W.R. et al., 2017. Transcriptional Networks in Single Perivascular Cells Sorted from Human Adipose Tissue Reveal a Hierarchy of Mesenchymal Stem Cells. *Stem cells (Dayton, Ohio)*, 35(5), pp.1273–1289.

Harn, H.-J. et al., 2012. Adipose-derived stem cells can abrogate chemical-induced liver fibrosis and facilitate recovery of liver function. *Cell transplantation*, 21(12), pp.2753–2764.

Henry, T.D. et al., 2017. The Athena trials: Autologous adipose-derived regenerative cells for refractory chronic myocardial ischemia with left ventricular dysfunction. *Catheterization and cardiovascular interventions : official journal of the Society for Cardiac Angiography & Interventions*, 89(2), pp.169–177.

Higgins, D.F. et al., 2007. Hypoxia promotes fibrogenesis in vivo via HIF-1 stimulation of epithelial-to-mesenchymal transition. *J Clin Invest*, 117(12), pp.3810–3820.

Honczarenko, M. et al., 2006. Human bone marrow stromal cells express a distinct set of biologically functional chemokine receptors. *Stem cells (Dayton, Ohio)*, 24(4), pp.1030–1041.

Horwitz, E.M. et al., 2005. Clarification of the nomenclature for MSC: The International Society for Cellular Therapy position statement. *Cytotherapy*, 7(5), pp.393–395.

Hosgood, S.A. & Nicholson, M.L., 2011. First in man renal transplantation after ex vivo normothermic perfusion. *Transplantation*, 92(7), pp.735–738.

Hosgood, S.A. et al., 2017. Protocol of a randomised controlled, open-label trial of ex vivo normothermic perfusion versus static cold storage in donation after circulatory death renal transplantation. *BMJ open*, 7(1), p.e012237.

Hörbelt, M. et al., 2007. Acute and chronic microvascular alterations in a mouse model of ischemic acute kidney injury. *American journal of physiology. Renal physiology*, 293(3), pp.F688–95.

Hu, J. et al., 2016. [Mesenchymal stem cells attenuate acute kidney injury via regulation of natural immune system]. *Zhonghua wei zhong bing ji jiu yi xue*, 28(3), pp.235–240.

Huang, Q. et al., 2015. IL-25 Elicits Innate Lymphoid Cells and Multipotent Progenitor Type 2 Cells That Reduce Renal Ischemic/Reperfusion Injury. *Journal of the American Society of Nephrology : JASN*, 26(9), pp.2199–2211.

Hunter, J.P. et al., 2012. Effects of hydrogen sulphide in an experimental model of renal ischaemia-reperfusion injury. *The British journal of surgery*, 99(12), pp.1665–1671.

Huynh, M.J. et al., 2015. Donation after Circulatory Death Renal Allografts--Does Donor Age Greater than 50 Years Affect Recipient Outcomes? *The Journal of urology*, 194(4), pp.1057–1061.

Im, G.-I., Shin, Y.-W. & Lee, K.-B., 2005. Do adipose tissue-derived mesenchymal stem cells have the same osteogenic and chondrogenic potential as bone marrow-derived cells? *Osteoarthritis and cartilage*, 13(10), pp.845–853.

Jablonski, P. et al., 1983. An experimental model for assessment of renal recovery from warm ischemia. *Transplantation*, 35(3), pp.198–204.

Janssens, R., Struyf, S. & Proost, P., 2018. The unique structural and functional features of CXCL12. *Cellular & molecular immunology*, 15(4), pp.299–311.

Jarmi, T., 2020. *Feasibility and Safety of Allogeneic Adipose Mesenchymal Stem Cells (aMSCs) Delivery Into Kidney Allografts Procured From Deceased Donors With High Kidney Donor Profile Index (KDPI),*

Jiang, H. et al., 2015. Protective effects of three remote ischemic conditioning procedures against renal ischemic/reperfusion injury in rat kidneys: a comparative study. *Irish journal of medical science*, 184(3), pp.647–653.

Jin, Z.Q., Karliner, J.S. & Vessey, D.A., 2008. Ischaemic postconditioning protects isolated mouse hearts against ischaemia/reperfusion injury via sphingosine kinase isoform-1 activation. *Cardiovascular research*, 79(1), pp.134–140.

Jo, A. et al., 2014. The versatile functions of Sox9 in development, stem cells, and human diseases. *Genes & Diseases*, 1(2), pp.149–161.

Jo, S.-H. et al., 2008. Prevention of radiocontrast medium-induced nephropathy using short-term high-dose simvastatin in patients with renal insufficiency undergoing coronary angiography (PROMISS) trial--a randomized controlled study. *American heart journal*, 155(3), pp.499.e1–8.

Johnson, D.W. et al., 2002. The effect of obesity on renal transplant outcomes. *Transplantation*, 74(5), pp.675–681.

Johnson, R.J. et al., 2013. Uric acid and chronic kidney disease: which is chasing which? *Nephrology, dialysis, transplantation : official publication of the European Dialysis and Transplant Association - European Renal Association*, 28(9), pp.2221–2228.

Johnson, T.S. et al., 2002. Matrix metalloproteinases and their inhibitions in experimental renal scarring. *Experimental nephrology*, 10(3), pp.182–195.

Jungebluth, P. et al., 2011. Tracheobronchial transplantation with a stem-cell-seeded bioartificial nanocomposite: a proof-of-concept study. *Lancet (London, England)*, 378(9808), pp.1997–2004.

Kadkhodaee, M. et al., 2011. First report of the protective effects of remote per- and postconditioning on ischemia/reperfusion-induced renal injury. *Transplantation*, 92(10), p.e55.

Kalogeris, T. et al., 2012. Cell Biology of Ischemia/Reperfusion Injury. *International review of cell and molecular biology*, 298, pp.229–317.

KANELLIS, J. et al., 2002. Renal ischemia-reperfusion increases endothelial VEGFR-2 without increasing VEGF or VEGFR-1 expression. *Kidney international*, 61(5), pp.1696–1706.

Katayama, R. et al., 2010. Calculation of glomerular filtration rate in conscious rats by the use of a bolus injection of iodixanol and a single blood sample. *Journal of pharmacological and toxicological methods*, 61(1), pp.59–64.

Kelly, K.J. et al., 1996. Intercellular adhesion molecule-1-deficient mice are protected against ischemic renal injury. *J Clin Invest*, 97(4), pp.1056–1063.

Khanal, S. et al., 2005. Statin therapy reduces contrast-induced nephropathy: an analysis of contemporary percutaneous interventions. *The American journal of medicine*, 118(8), pp.843–849.

Kim, S.C. et al., 2019. Long-term survival of pig-to-rhesus macaque renal xenografts is dependent on CD4 T cell depletion. *Am J Transplant*, 19(8), pp.2174–2185.

Ko, I.K. et al., 2013. In situ tissue regeneration through host stem cell recruitment. *Experimental & molecular medicine*, 45(11), pp.e57–e57.

Kobayashi, T. & Cooper, D.K., 1999. Anti-Gal, alpha-Gal epitopes, and xenotransplantation. *Sub-cellular biochemistry*, 32(Chapter 10), pp.229–257.

Kontodimopoulos, N. & Niakas, D., 2008. An estimate of lifelong costs and QALYs in renal replacement therapy based on patients' life expectancy. *Health policy (Amsterdam, Netherlands)*, 86(1), pp.85–96.

Kurtz A. Mesenchymal stem cell delivery routes and fate. Int J Stem Cells. 2008;1:1–7.

Kroemer, G., Galluzzi, L. & Brenner, C., 2007. Mitochondrial membrane permeabilization in cell death. *Physiological reviews*, 87(1), pp.99–163.

Krogstrup, N.V. et al., 2017. Remote Ischemic Conditioning on Recipients of Deceased Renal Transplants Does Not Improve Early Graft Function: A Multicenter Randomized, Controlled Clinical Trial. *Am J Transplant*, 17(4), pp.1042–1049.

Kronenwett, R., Martin, S. & Haas, R., 2000. The role of cytokines and adhesion molecules for mobilization of peripheral blood stem cells. *Stem cells (Dayton, Ohio)*, 18(5), pp.320–330.

Kvietys, P.R. & Granger, D.N., 2012. Role of reactive oxygen and nitrogen species in the vascular responses to inflammation. *Free Radical Biology and Medicine*, 52(3), pp.556–592.

Kwon, T.H. et al., 1998. Reduced AQP1, -2, and -3 levels in kidneys of rats with CRF induced by surgical reduction in renal mass. *The American journal of physiology*, 275(5), pp.F724–41.

Lam, P.K. et al., 2017. Topical Application of Mesenchymal Stromal Cells Ameliorated Liver Parenchyma Damage After Ischemia-Reperfusion Injury in an Animal Model. *Transplantation direct*, 3(6), p.e160.

Lange, C. et al., 2005. Administered mesenchymal stem cells enhance recovery from ischemia/reperfusion-induced acute renal failure in rats. *Kidney international*, 68(4), pp.1613–1617.

Lassailly, F., Griessinger, E. & Bonnet, D., 2010. "Microenvironmental contaminations" induced by fluorescent lipophilic dyes used for noninvasive in vitro and in vivo cell tracking. *Blood*, 115(26), pp.5347–5354.

Lau, A. et al., 2013. RIPK3-mediated necroptosis promotes donor kidney inflammatory injury and reduces allograft survival. *Am J Transplant*, 13(11), pp.2805–2818.

Laupacis, A. et al., 1996. A study of the quality of life and cost-utility of renal transplantation. *Kidney international*, 50(1), pp.235–242.

Lee, A.S. et al., 2011. Preclinical derivation and imaging of autologously transplanted canine induced pluripotent stem cells. *Journal of Biological Chemistry*, 286(37), pp.32697–32704.

Lee, S. et al., 2011. Distinct macrophage phenotypes contribute to kidney injury and repair. *Journal of the American Society of Nephrology : JASN*, 22(2), pp.317–326.

Lee NE, Kim SJ, Yang SJ, Joo SY, Park H, Lee KW, Yang HM, Park JB. Comparative characterization of mesenchymal stromal cells from multiple abdominal adipose tissues and enrichment of angiogenic ability via CD146 molecule. Cytotherapy. 2017 Feb;19(2):170-180. doi: 10.1016/j.jcyt.2016.11.002. Epub 2016 Dec 23. PMID: 28024875.

Leemans, J.C. et al., 2005. Renal-associated TLR2 mediates ischemia/reperfusion injury in the kidney. *J Clin Invest*, 115(10), pp.2894–2903.

Leibacher, J. & Henschler, R., 2016. Biodistribution, migration and homing of systemically applied mesenchymal stem/stromal cells. *Stem cell research & therapy*, 7(1), p.7.

Levitt, M., 2015. Could the organ shortage ever be met? *Life Sci Soc Policy*, 11, p.6.

Li, K. et al., 2010. Not a process of simple vicariousness, the differentiation of human adipose-derived mesenchymal stem cells to renal tubular epithelial cells plays an important role in acute kidney injury repairing. *Stem cells and development*, 19(8), pp.1267–1275.

Li, L. et al., 2008. The chemokine receptors CCR2 and CX3CR1 mediate monocyte/macrophage trafficking in kidney ischemia-reperfusion injury. *Kidney international*, 74(12), pp.1526–1537.

Li, P. et al., 2013. PKH26 can transfer to host cells in vitro and vivo. *Stem cells and development*, 22(2), pp.340–344.

Lim, M. et al., 2018. Intravenous injection of allogeneic umbilical cord-derived multipotent mesenchymal stromal cells reduces the infarct area and ameliorates

cardiac function in a porcine model of acute myocardial infarction. *Stem cell research & therapy*, 9(1), pp.129–17.

Lin, C.-S., Lin, G. & Lue, T.F., 2012. Allogeneic and xenogeneic transplantation of adipose-derived stem cells in immunocompetent recipients without immunosuppressants. *Stem cells and development*, 21(15), pp.2770–2778.

Lindoso, R.S. et al., 2014. Extracellular vesicles released from mesenchymal stromal cells modulate miRNA in renal tubular cells and inhibit ATP depletion injury. *Stem cells and development*, 23(15), pp.1809–1819.

Liu, L. et al., 2011. Hypoxia-Inducible Factor-1α Is Essential for Hypoxia-Induced Mesenchymal Stem Cell Mobilization into the Peripheral Blood. *Stem cells and development*, 20(11), pp.1961–1971.

Liu, N. et al., 2018. Enhanced proliferation and differentiation of HO-1 gene-modified bone marrow-derived mesenchymal stem cells in the acute injured kidney. *International journal of molecular medicine*, 42(2), pp.946–956.

Liu, Y., 2011. Cellular and molecular mechanisms of renal fibrosis. *Nature Reviews Nephrology*, 7, p.684.

Liu, Z.C., Chow, K.M. & Chang, T.M.-S., 2003. Evaluation of two protocols of uremic rat model: partial nephrectomy and infarction. *Renal failure*, 25(6), pp.935–943.

Lobb, I. et al., 2014. Hydrogen sulfide treatment ameliorates long-term renal dysfunction resulting from prolonged warm renal ischemia-reperfusion injury. *Canadian Urological Association journal = Journal de l'Association des urologues du Canada*, 8(5-6), pp.E413–8.

Lobb, I. et al., 2015. Hydrogen Sulfide Treatment Mitigates Renal Allograft Ischemia-Reperfusion Injury during Cold Storage and Improves Early Transplant Kidney Function and Survival Following Allogeneic Renal Transplantation. *The Journal of urology*, 194(6), pp.1806–1815.

Lombardi, D., Becherucci, F. & Romagnani, P., 2016. How much can the tubule regenerate and who does it? An open question. *Nephrology, dialysis, transplantation : official publication of the European Dialysis and Transplant Association - European Renal Association*, 31(8), pp.1243–1250.

Lu, T. et al., 2019. Xenotransplantation: Current Status in Preclinical Research. *Frontiers in immunology*, 10, p.3060.

Luan, F.L., 2002. Kidney transplantation from donors without a heartbeat. *The New England journal of medicine*, 347(22), pp.1799–801– author reply 1799–801.

Lüttichau, Von, I. et al., 2005. Human adult CD34- progenitor cells functionally express the chemokine receptors CCR1, CCR4, CCR7, CXCR5, and CCR10 but not CXCR4. *Stem cells and development*, 14(3), pp.329–336.

M, C. et al., 2010. *Diannexin, a Novel Ischemia/Reperfusion Therapeutic Agent, Reduces Delayed Graft Function (DGF) in Renal Transplant Recipients from Marginal Donors. Oral Presentation,*

MacAllister, R. et al., 2015. REmote preconditioning for Protection Against Ischaemia–Reperfusion in renal transplantation (REPAIR): a multicentre, multinational, double-blind, factorial designed randomised controlled trial. *Efficacy and Mechanism Evaluation*, 2(3), pp.1–60.

Maceyka, M. et al., 2012. Sphingosine-1-phosphate signaling and its role in disease. *Trends in Cell Biology*, 22(1), pp.50–60.

MacQueen, L.A. et al., 2018. A tissue-engineered scale model of the heart ventricle. *Nature biomedical engineering*, 2(12), pp.930–941.

Man, K. et al., 2005. FTY720 attenuates hepatic ischemia-reperfusion injury in normal and cirrhotic livers. *Am J Transplant*, 5(1), pp.40–49.

Mannon, R.B., 2006. Therapeutic targets in the treatment of allograft fibrosis. *Am J Transplant*, 6(5 Pt 1), pp.867–875.

Mäkelä, T. et al., 2015. Safety and biodistribution study of bone marrow-derived mesenchymal stromal cells and mononuclear cells and the impact of the administration route in an intact porcine model. *Cytotherapy*, 17(4), pp.392–402.

McAnulty, J.F. et al., 2002. Successful six-day kidney preservation using trophic factor supplemented media and simple cold storage. *Am J Transplant*, 2(8), pp.712–718.

McCully, J.D. et al., 2004. Differential contribution of necrosis and apoptosis in myocardial ischemia-reperfusion injury. *American Journal of Physiology - Heart and Circulatory Physiology*, 286(5), pp.H1923–H1935.

Meier-Kriesche, H.-U. & Kaplan, B., 2002. Waiting time on dialysis as the strongest modifiable risk factor for renal transplant outcomes: a paired donor kidney analysis. *Transplantation*, 74(10), pp.1377–1381.

Meier-Kriesche, H.U. et al., 2001. Survival improvement among patients with end-stage renal disease: trends over time for transplant recipients and wait-listed patients. *Journal of the American Society of Nephrology*, 12(6), pp.1293–1296.

Meng, X.-M., Nikolic-Paterson, D.J. & Lan, H.Y., 2014. Inflammatory processes in renal fibrosis. *Nature Reviews Nephrology*, 10(9), pp.493–503.

Meng, X.-M., Nikolic-Paterson, D.J. & Lan, H.Y., 2016. TGF-β: the master regulator of fibrosis. *Nature Reviews Nephrology*, 12(6), pp.325–338.

Mills, K.T. et al., 2016. Global Disparities of Hypertension Prevalence and Control: A Systematic Analysis of Population-Based Studies From 90 Countries. *Circulation*, 134(6), pp.441–450.

Mitchell, J.R. et al., 2010. Short-term dietary restriction and fasting precondition against ischemia reperfusion injury in mice. *Aging cell*, 9(1), pp.40–53.

Mori da Cunha, M.G.M.C. et al., 2017. Vascular Endothelial Growth Factor Up-regulation in Human Amniotic Fluid Stem Cell Enhances Nephroprotection After Ischemia-Reperfusion Injury in the Rat. *Critical care medicine*, 45(1), pp.e86–e96.

Morigi, M. et al., 2008. Human Bone Marrow Mesenchymal Stem Cells Accelerate Recovery of Acute Renal Injury and Prolong Survival in Mice. *Stem cells (Dayton, Ohio)*, 26(8), pp.2075–2082.

Morigi, M. et al., 2004. Mesenchymal stem cells are renotropic, helping to repair the kidney and improve function in acute renal failure. *Journal of the American Society of Nephrology*, 15(7), pp.1794–1804.

Morshuis, M. et al., 2020. Heart transplantation after SynCardia® total artificial heart implantation. *Annals of cardiothoracic surgery*, 9(2), pp.98–103.

Mueller, T.F., Solez, K. & Mas, V., 2011. Assessment of kidney organ quality and prediction of outcome at time of transplantation. *Seminars in immunopathology*, 33(2), pp.185–199.

Murphy, E. & Steenbergen, C., 2008. Ion transport and energetics during cell death and protection. *Physiology (Bethesda, Md.)*, 23(2), pp.115–123.

Nagahama, H. et al., 2018. Preservation of interhemispheric cortical connections through corpus callosum following intravenous infusion of mesenchymal stem cells in a rat model of cerebral infarction. *Brain research*, 1695, pp.37–44.

Nakao, A. et al., 2008. Ex vivo carbon monoxide prevents cytochrome P450 degradation and ischemia/reperfusion injury of kidney grafts. *Kidney international*, 74(8), pp.1009–1016.

Nasralla, D. et al., 2018. A randomized trial of normothermic preservation in liver transplantation. *Nature*, 557(7703), pp.50–56.

Nauta, A.J. & Fibbe, W.E., 2007. Immunomodulatory properties of mesenchymal stromal cells. *Blood*, 110(10), pp.3499–3506.

Nevins, T.E., Nickerson, P.W. & Dew, M.A., 2017. Understanding Medication Nonadherence after Kidney Transplant. *Journal of the American Society of Nephrology : JASN*, 28(8), pp.2290–2301.

NHS Blood and Transplant, N.B.A.T., 2019. *NHS Blood and Transplant Annual Activity Report 2018-2019, UK*, Available at: https://nhsbtdbe.blob.core.windows.net/umbraco-assets-corp/16418/section-5-kidney-activity.pdf.

NHS Blood and Transplant, N.B.A.T., *Taking organ utilisation to 2020*,

Nicholson, M.L. et al., 2015. A Double Blind Randomized Clinical Trial of Remote Ischemic Conditioning in Live Donor Renal Transplantation. *Medicine*, 94(31), p.e1316.

Nicoletto, B.B. et al., 2014. Effects of obesity on kidney transplantation outcomes: a systematic review and meta-analysis. *Transplantation*, 98(2), pp.167–176.

Qi S, Wu D. Bone marrow-derived mesenchymal stem cells protect against cisplatin-induced acute kidney injury in rats by inhibiting cell apoptosis. Int J Mol Med. 2013;32:1262–72.

Oh, D.-J. et al., 2008. Fractalkine receptor (CX3CR1) inhibition is protective against ischemic acute renal failure in mice. *American journal of physiology. Renal physiology*, 294(1), pp.F264–71.

Olivetti, G. et al., 1977. Morphometry of the renal corpuscle during normal postnatal growth and compensatory hypertrophy. A light microscope study. *The Journal of cell biology*, 75(2 Pt 1), pp.573–585.

Olson, J.L. et al., 1982. Altered glomerular permselectivity and progressive sclerosis following extreme ablation of renal mass. *Kidney international*, 22(2), pp.112–126.

Ong, S.-B. et al., 2010. Inhibiting mitochondrial fission protects the heart against ischemia/reperfusion injury. *Circulation*, 121(18), pp.2012–2022.

Oron, U. et al., 2014. Autologous bone-marrow stem cells stimulation reverses post-ischemic-reperfusion kidney injury in rats. *American journal of nephrology*, 40(5), pp.425–433.

Pardo, A. & Selman, M., 2006. Matrix metalloproteases in aberrant fibrotic tissue remodeling. *Proceedings of the American Thoracic Society*, 3(4), pp.383–388.

Parekkadan, B. et al., 2011. Bone marrow stromal cell transplants prevent experimental enterocolitis and require host CD11b+ splenocytes. *Gastroenterology*, 140(3), pp.966–975.

Pasparakis, M. & Vandenabeele, P., 2015. Necroptosis and its role in inflammation. *Nature*, 517(7534), pp.311–320.

Perin, E.C. et al., 2014. Adipose-derived regenerative cells in patients with ischemic cardiomyopathy: The PRECISE Trial. *American heart journal*, 168(1), pp.88–95.e2.

Pileggi, A. et al., 2013. Mesenchymal stromal (stem) cells to improve solid organ transplant outcome: lessons from the initial clinical trials. *Current opinion in organ transplantation*, 18(6), pp.672–681.

Pill, J. et al., 2005. Fluorescein-labeled sinistrin as marker of glomerular filtration rate. *European journal of medicinal chemistry*, 40(10), pp.1056–1061.

Pill, J. et al., 2006. Pharmacological profile and toxicity of fluorescein-labelled sinistrin, a novel marker for GFR measurements. *Naunyn-Schmiedeberg's archives of pharmacology*, 373(3), pp.204–211.

PLATT, R., 1952. Structural and functional adaptation in renal failure. *British medical journal*, 1(4773), pp.1372–7– concl.

Plenter, R. et al., 2015. Murine Kidney Transplant Technique. *Journal of visualized experiments : JoVE*, (105), p.e52848.

Polyak, M.M. et al., 1999. Prostaglandin E1 influences pulsatile preservation characteristics and early graft function in expanded criteria donor kidneys. *The Journal of surgical research*, 85(1), pp.17–25.

Ponticelli, C.E., 2015. The impact of cold ischemia time on renal transplant outcome. *Kidney international*, 87(2), pp.272–275.

Port FK, Bragg-Gresham JL, Metzger RA, Dykstra DM, Gillespie BW, Young EW, et al. Donor characteristics associated with re- duced graft survival: an approach to expanding the pool of kidney donors. Transplantation. 2002;74:1281–6.

Pruthi, R., Steenkamp, R. & Feest, T., 2013. UK Renal Registry 16th annual report: chapter 8 survival and cause of death of UK adult patients on renal replacement therapy in 2012: national and centre-specific analyses. *Nephron. Clinical practice*, 125(1-4), pp.139–169.

Puelles, V.G. et al., 2011. Glomerular number and size variability and risk for kidney disease. *Current opinion in nephrology and hypertension*, 20(1), pp.7–15.

Purkerson, M.L., Hoffsten, P.E. & Klahr, S., 1976. Pathogenesis of the glomerulopathy associated with renal infarction in rats. *Kidney international*, 9(5), pp.407–417.

Qi, S. & Wu, Dongcheng, 2013. Bone marrow-derived mesenchymal stem cells protect against cisplatin-induced acute kidney injury in rats by inhibiting cell apoptosis. *International journal of molecular medicine*, 32(6), pp.1262–1272.

Qiao, P.-F. et al., 2015. Heat shock pretreatment improves stem cell repair following ischemia-reperfusion injury via autophagy. *World journal of gastroenterology*, 21(45), pp.12822–12834.

Quiroga, I. et al., 2006. Major effects of delayed graft function and cold ischaemia time on renal allograft survival. *Nephrology, dialysis, transplantation : official publication of the European Dialysis and Transplant Association - European Renal Association*, 21(6), pp.1689–1696.

Raposio, E. & Ciliberti, R., 2017. Clinical use of adipose-derived stem cells: European legislative issues. *Annals of medicine and surgery (2012)*, 24, pp.61–64.

Raven, A. et al., 2017. Cholangiocytes act as facultative liver stem cells during impaired hepatocyte regeneration. *Nature*, 547(7663), pp.350–354.

Ray, C., Sohrabi, S. & Talbot, D., 2009. Machine perfusion or cold storage in deceased-donor kidney transplantation. *The New England journal of medicine*, 360(14), pp.1460–author reply 1461.

Reese, P.P., Boudville, N. & Garg, A.X., 2015. Living kidney donation: outcomes, ethics, and uncertainty. *Lancet (London, England)*, 385(9981), pp.2003–2013.

Renkens, J.J.M. et al., 2005. Outcome of nonheart-beating donor kidneys with prolonged delayed graft function after transplantation. *Am J Transplant*, 5(11), pp.2704–2709.

Rennert, R.C. et al., 2012. Stem cell recruitment after injury: lessons for regenerative medicine. *Regenerative medicine*, 7(6), pp.833–850.

Rhee, C.M., Ahmadi, S.-F. & Kalantar-Zadeh, K., 2016. The dual roles of obesity in chronic kidney disease: a review of the current literature. *Current opinion in nephrology and hypertension*, 25(3), pp.208–216.

Ries, C. et al., 2007. MMP-2, MT1-MMP, and TIMP-2 are essential for the invasive capacity of human mesenchymal stem cells: differential regulation by inflammatory cytokines. *Blood*, 109(9), pp.4055–4063.

Rinkevich, Y. et al., 2014. In vivo clonal analysis reveals lineage-restricted progenitor characteristics in mammalian kidney development, maintenance, and regeneration. *Cell reports*, 7(4), pp.1270–1283.

Rogers, N.M., Thomson, A.W. & Isenberg, J.S., 2012. Activation of parenchymal CD47 promotes renal ischemia-reperfusion injury. *Journal of the American Society of Nephrology : JASN*, 23(9), pp.1538–1550.

Romano, M. et al., 2019. Past, Present, and Future of Regulatory T Cell Therapy in Transplantation and Autoimmunity. *Frontiers in immunology*, 10, p.43.

Romano, M. et al., 2017. Treg therapy in transplantation: a general overview. *Transplant international : official journal of the European Society for Organ Transplantation*, 30(8), pp.745–753.

Rombouts, W.J.C. & Ploemacher, R.E., 2003. Primary murine MSC show highly efficient homing to the bone marrow but lose homing ability following culture. *Leukemia*, 17(1), pp.160–170.

Rüster, B. et al., 2006. Mesenchymal stem cells display coordinated rolling and adhesion behavior on endothelial cells. *Blood*, 108(12), pp.3938–3944.

Ryan, D. et al., 2018. Development of the Human Fetal Kidney from Mid to Late Gestation in Male and Female Infants. *EBioMedicine*, 27, pp.275–283.

Sadek E, Afifi NM, Elfattah L, Mohsen MAA. Histological study on effect of mesenchymal stem cell therapy on experimental renal injury induced by ischemia/reperfusion in male albino rat. Int J Stem Cells. 2013;6:55–66.

Saeedi, P. et al., 2019. Global and regional diabetes prevalence estimates for 2019 and projections for 2030 and 2045: Results from the International Diabetes Federation Diabetes Atlas, 9th edition. *Diabetes research and clinical practice*, 157, p.107843.

Saidi, R.F. et al., 2014. Human adipose-derived mesenchymal stem cells attenuate liver ischemia-reperfusion injury and promote liver regeneration. *Surgery*, 156(5), pp.1225–1231.

Salahudeen, A.K., 2004. Cold ischemic injury of transplanted kidneys: new insights from experimental studies. *American journal of physiology. Renal physiology*, 287(2), pp.F181–7.

Salahudeen, A.K., Joshi, M. & Jenkins, J.K., 2001. Apoptosis versus necrosis during cold storage and rewarming of human renal proximal tubular cells. *Transplantation*, 72(5), pp.798–804.

Sanada, S., Komuro, I. & Kitakaze, M., 2011. Pathophysiology of myocardial reperfusion injury: preconditioning, postconditioning, and translational aspects of protective measures. *American Journal of Physiology - Heart and Circulatory Physiology*, 301(5), pp.H1723–41.

Sawitzki, B. et al., 2020. Regulatory cell therapy in kidney transplantation (The ONE Study): a harmonised design and analysis of seven non-randomised, single-arm, phase 1/2A trials. *Lancet (London, England)*, 395(10237), pp.1627–1639.

Schaapherder, A. et al., 2018. Equivalent Long-term Transplantation Outcomes for Kidneys Donated After Brain Death and Cardiac Death: Conclusions From a Nationwide Evaluation. *EClinicalMedicine*, 4-5, pp.25–31.

Schenk, S. et al., 2007. Monocyte chemotactic protein-3 is a myocardial mesenchymal stem cell homing factor. *Stem cells (Dayton, Ohio)*, 25(1), pp.245–251.

Schmidt, D. & Salahudeen, A., 2007. The obesity-survival paradox in hemodialysis patients: why do overweight hemodialysis patients live longer? *Nutrition in clinical practice : official publication of the American Society for Parenteral and Enteral Nutrition*, 22(1), pp.11–15.

Schmuck, E.G. et al., 2016. Biodistribution and Clearance of Human Mesenchymal Stem Cells by Quantitative Three-Dimensional Cryo-Imaging After Intravenous Infusion in a Rat Lung Injury Model. *Stem Cells Translational Medicine*, 5(12), pp.1668–1675.

Schock-Kusch, D. et al., 2011. Transcutaneous assessment of renal function in conscious rats with a device for measuring FITC-sinistrin disappearance curves. *Kidney international*, 79(11), pp.1254–1258.

Schock-Kusch, D. et al., 2009. Transcutaneous measurement of glomerular filtration rate using FITC-sinistrin in rats. *Nephrology, dialysis, transplantation : official publication of the European Dialysis and Transplant Association - European Renal Association*, 24(10), pp.2997–3001.

Schrepfer, S. et al., 2007. Stem cell transplantation: the lung barrier. *Transplantation Proceedings*, 39(2), pp.573–576.

Sert, I. et al., 2014. The effect of cold ischemia time on delayed graft function and acute rejection in kidney transplantation. *Saudi journal of kidney diseases and transplantation : an official publication of the Saudi Center for Organ Transplantation, Saudi Arabia*, 25(5), pp.960–966.

Shea, S.M., Raskova, J. & Morrison, A.B., 1978. A stereologic study of glomerular hypertrophy in the subtotally nephrectomized rat. *The American journal of pathology*, 90(1), pp.201–210.

Sheashaa, H. et al., 2016. Protective effect of adipose-derived mesenchymal stem cells against acute kidney injury induced by ischemia-reperfusion in Sprague-Dawley rats. *Experimental and therapeutic medicine*, 11(5), pp.1573–1580.

Shen, B. et al., 2016. CCR2 Positive Exosome Released by Mesenchymal Stem Cells Suppresses Macrophage Functions and Alleviates Ischemia/Reperfusion-Induced Renal Injury. *Stem cells international*, 2016(1, article 111), pp.1240301–9.

Sheu, J.-J. et al., 2019. Therapeutic effects of adipose derived fresh stromal vascular fraction-containing stem cells versus cultured adipose derived mesenchymal stem cells on rescuing heart function in rat after acute myocardial infarction. *American journal of translational research*, 11(1), pp.67–86.

Shi, M. et al., 2007. Regulation of CXCR4 expression in human mesenchymal stem cells by cytokine treatment: role in homing efficiency in NOD/SCID mice. *Haematologica*, 92(7), pp.897–904.

Shih, Y.-C. et al., 2013. Adipose-Derived Stem Cells Exhibit Antioxidative and Antiapoptotic Properties to Rescue Ischemic Acute Kidney Injury in Rats. *Plastic and Reconstructive Surgery*, 132(6), pp.940e–951e.

Shimamura, T. & Morrison, A.B., 1975. A progressive glomerulosclerosis occurring in partial five-sixths nephrectomized rats. *The American journal of pathology*, 79(1), pp.95–106.

Sierra-Parraga, J.M. et al., 2019. Mesenchymal Stromal Cells Are Retained in the Porcine Renal Cortex Independently of Their Metabolic State After Renal Intra-Arterial Infusion. *Stem cells and development*, 28(18), pp.1224–1235.

Simmons, R.G., Anderson, C.R. & Abress, L.K., 1990. Quality of life and rehabilitation differences among four end-stage renal disease therapy groups. *Scandinavian journal of urology and nephrology. Supplementum*, 131, pp.7–22.

Singh, R.P. et al., 2011. Kidney transplantation from donation after cardiac death donors: lack of impact of delayed graft function on post-transplant outcomes. *Clinical Transplantation*, 25(2), pp.255–264.

Sivanathan, K.N. et al., 2015. Interleukin-17A-Induced Human Mesenchymal Stem Cells Are Superior Modulators of Immunological Function. *Stem cells (Dayton, Ohio)*, 33(9), pp.2850–2863.

Snoeijs, M.G. et al., 2010. Kidneys from donors after cardiac death provide survival benefit. *Journal of the American Society of Nephrology : JASN*, 21(6), pp.1015–1021.

Sosa, R.A. et al., 2016. Early cytokine signatures of ischemia/reperfusion injury in human orthotopic liver transplantation. *JCI Insight*, 1(20), p.e89679.

Strauer, B.E. et al., 2005. Regeneration of human infarcted heart muscle by intracoronary autologous bone marrow cell transplantation in chronic coronary artery disease: the IACT Study. *J Am Coll Cardiol*, 46(9), pp.1651–1658.

Sun, P. et al., 2016. Human endometrial regenerative cells attenuate renal ischemia reperfusion injury in mice. *Journal of translational medicine*, 14(1), p.28.

Sun, Q. et al., 2017. Allogeneic mesenchymal stem cell as induction therapy to prevent both delayed graft function and acute rejection in deceased donor renal transplantation: study protocol for a randomized controlled trial. *Trials*, 18(1), p.545.

Sutton, T.A., 2009. Alteration of microvascular permeability in acute kidney injury. *Microvascular research*, 77(1), pp.4–7.

Sutton, T.A., Fisher, C.J. & Molitoris, B.A., 2002. Microvascular endothelial injury and dysfunction during ischemic acute renal failure. *Kidney international*, 62(5), pp.1539–1549.

Szydlowska, K. & Tymianski, M., 2010. Calcium, ischemia and excitotoxicity. *Cell calcium*, 47(2), pp.122–129.

Takahashi, K. et al., 2007. Induction of pluripotent stem cells from adult human fibroblasts by defined factors. *Cell*, 131(5), pp.861–872.

Talukder, M.A.H., Zweier, J.L. & Periasamy, M., 2009. Targeting calcium transport in ischaemic heart disease. *Cardiovascular research*, 84(3), pp.345–352.

Tan, R.-Z. et al., 2019. An optimized 5/6 nephrectomy mouse model based on unilateral kidney ligation and its application in renal fibrosis research. *Renal failure*, 41(1), pp.555–566.

Tan, X. et al., 2015. Postconditioning attenuates renal ischemia-reperfusion injury by mobilization of stem cells. *Journal of nephrology*, 28(3), pp.289–298.

Tan, X.-H. et al., 2017. Fibroblast growth factor 2 protects against renal ischaemia/reperfusion injury by attenuating mitochondrial damage and proinflammatory signalling. *Journal of cellular and molecular medicine*, 21(11), pp.2909–2925.

Taner, T. et al., 2015. Compensatory hypertrophy of the remaining kidney in medically complex living kidney donors over the long term. *Transplantation*, 99(3), pp.555–559.

Tang, M. et al., 2018. Mesenchymal stem cells alleviate acute kidney injury by down-regulating C5a/C5aR pathway activation. *International urology and nephrology*, 87(5), p.918.

Tarng, D.-C. et al., 2016. Induced Pluripotent Stem Cell-Derived Conditioned Medium Attenuates Acute Kidney Injury by Downregulating the Oxidative Stress-Related Pathway in Ischemia-Reperfusion Rats. *Cell transplantation*, 25(3), pp.517–530.

Tat, P.A. et al., 2010. The efficient generation of induced pluripotent stem (iPS) cells from adult mouse adipose tissue-derived and neural stem cells. *Cell transplantation*, 19(5), pp.525–536.

Taylor, D.A. et al., 2018. Building a Total Bioartificial Heart: Harnessing Nature to Overcome the Current Hurdles. M. Slepian, ed. *Artificial organs*, 42(10), pp.970–982.

Thompson, E.R. et al., 2020. Novel delivery of cellular therapy to reduce ischaemia reperfusion injury in kidney transplantation. *Am J Transplant*, p.ajt.16100.

Thomson, J.A. et al., 1998. Embryonic stem cell lines derived from human blastocysts. *Science (New York, N.Y.)*, 282(5391), pp.1145–1147.

Thurman, J.M. et al., 2006. Treatment with an inhibitory monoclonal antibody to mouse factor B protects mice from induction of apoptosis and renal ischemia/reperfusion injury. *Journal of the American Society of Nephrology*, 17(3), pp.707–715.

Tiemessen, M.M. et al., 2007. CD4+CD25+Foxp3+ regulatory T cells induce alternative activation of human monocytes/macrophages. *Proceedings of the National Academy of Sciences of the United States of America*, 104(49), pp.19446–19451.

Tingle, S.J. et al., 2020. Hypothermic machine perfusion is superior to static cold storage in deceased donor kidney transplantation: A meta-analysis. *Clinical Transplantation*, 34(4), p.e13814.

Tonelli, M. et al., 2011. Systematic review: kidney transplantation compared with dialysis in clinically relevant outcomes. *Am J Transplant*, 11(10), pp.2093–2109.

Torres Crigna, A. et al., 2018. Stem/Stromal Cells for Treatment of Kidney Injuries With Focus on Preclinical Models. *Front Med (Lausanne)*, 5, p.179.

Toupet, K. et al., 2015. Survival and biodistribution of xenogenic adipose mesenchymal stem cells is not affected by the degree of inflammation in arthritis. X.-M. Shi, ed. *PloS one*, 10(1), p.e0114962.

Toyohara, T. et al., 2015. Cell Therapy Using Human Induced Pluripotent Stem Cell-Derived Renal Progenitors Ameliorates Acute Kidney Injury in Mice. *Stem Cells Translational Medicine*, 4(9), pp.980–992.

Toyserkani, N.M. et al., 2017. Concise Review: A Safety Assessment of Adipose-Derived Cell Therapy in Clinical Trials: A Systematic Review of Reported Adverse Events. *Stem Cells Translational Medicine*, 6(9), pp.1786–1794.

Tögel, F. et al., 2005. Administered mesenchymal stem cells protect against ischemic acute renal failure through differentiation-independent mechanisms. *American journal of physiology. Renal physiology*, 289(1), pp.F31–42.

Treckmann, J. et al., 2011. Machine perfusion versus cold storage for preservation of kidneys from expanded criteria donors after brain death. *Transplant international : official journal of the European Society for Organ Transplantation*, 24(6), pp.548–554.

van den Akker, E.K. et al., 2014. Ischemic postconditioning in human DCD kidney transplantation is feasible and appears safe. *Transplant international : official journal of the European Society for Organ Transplantation*, 27(2), pp.226–234.

van den Akker, E.K. et al., 2013. Protection against renal ischemia-reperfusion injury by ischemic postconditioning. *Transplantation*, 95(11), pp.1299–1305.

van der Veeken, J. et al., 2016. Memory of Inflammation in Regulatory T Cells. *Cell*, 166(4), pp.977–990.

Via, A.G., Frizziero, A. & Oliva, F., 2012. Biological properties of mesenchymal Stem Cells from different sources. *Muscles, ligaments and tendons journal*, 2(3), pp.154–162.

Vignali, D.A.A., Collison, L.W. & Workman, C.J., 2008. How regulatory T cells work. *Nature reviews. Immunology*, 8(7), pp.523–532.

Vijay, J. et al., 2020. Single-cell analysis of human adipose tissue identifies depot and disease specific cell types. *Nature metabolism*, 2(1), pp.97–109.

Viswanathan, S. et al., 2019. Mesenchymal stem versus stromal cells: International Society for Cell & Gene Therapy (ISCT®) Mesenchymal Stromal Cell committee position statement on nomenclature. *Cytotherapy*, 21(10), pp.1019–1024.

Vlachopanos, G., Kassimatis, T.I. & Agrafiotis, A., 2015. Perioperative administration of high-dose recombinant human erythropoietin for delayed graft function prevention in kidney transplantation: a meta-analysis. *Transplant international : official journal of the European Society for Organ Transplantation*, 28(3), pp.330–340.

Walker, L.S.K., 2013. Treg and CTLA-4: two intertwining pathways to immune tolerance. *Journal of autoimmunity*, 45, pp.49–57.

Wang, J.-L., Zhou, Y. & Yuan, W.-J., 2012. [Relationship between body mass index and all-cause mortality in hemodialysis patients: a meta-analysis]. *Zhonghua nei ke za zhi*, 51(9), pp.702–707.

Wang, K. & Kestenbaum, B., 2018. Proximal Tubular Secretory Clearance: A Neglected Partner of Kidney Function. *Clinical journal of the American Society of Nephrology : CJASN*, 13(8), pp.1291–1296.

Wang, L.-J. et al., 2019. Efficacy Evaluation and Tracking of Bone Marrow Stromal Stem Cells in a Rat Model of Renal Ischemia-Reperfusion Injury. *BioMed research international*, 2019(6), pp.9105768–11.

Wang, W. et al., 2014. Mesenchymal stem cells promote liver regeneration and prolong survival in small-for-size liver grafts: involvement of C-Jun N-terminal kinase, cyclin D1, and NF-kappaB. M. Wang, ed. *PloS one*, 9(12), p.e112532.

Wang, X. et al., 2018. BMMSCs protect against liver ischemia/reperfusion injury via HO1 mediated autophagy. *Molecular medicine reports*, 18(2), pp.2253–2262.

Wang, Y. et al., 2007. Ex vivo programmed macrophages ameliorate experimental chronic inflammatory renal disease. *Kidney international*, 72(3), pp.290–299.

Wei, Q. & Dong, Z., 2012. Mouse model of ischemic acute kidney injury: technical notes and tricks. *American journal of physiology. Renal physiology*, 303(11), pp.F1487–94.

Whalen, H. et al., 2016. A novel rodent model of severe renal ischemia reperfusion injury. *Renal failure*, 38(10), pp.1694–1701.

Wolfe, R.A. et al., 1999. Comparison of mortality in all patients on dialysis, patients on dialysis awaiting transplantation, and recipients of a first cadaveric transplant. *The New England journal of medicine*, 341(23), pp.1725–1730.

Wolfs, T.G.A.M. et al., 2002. In Vivo Expression of Toll-Like Receptor 2 and 4 by Renal Epithelial Cells: IFN-γ and TNF-α Mediated Up-Regulation During Inflammation. *The Journal of Immunology*, 168(3), pp.1286–1293.

Woolthuis, C.M. et al., 2014. Aging impairs long-term hematopoietic regeneration after autologous stem cell transplantation. *Biology of blood and marrow transplantation : journal of the American Society for Blood and Marrow Transplantation*, 20(6), pp.865–871.

Wszola, M. et al., 2014. Preservation of kidneys by machine perfusion influences gene expression and may limit ischemia/reperfusion injury. *Progress in transplantation (Aliso Viejo, Calif.)*, 24(1), pp.19–26.

Wu, Huiling et al., 2007. TLR4 activation mediates kidney ischemia/reperfusion injury. *J Clin Invest*, 117(10), pp.2847–2859.

Wu, Jiang et al., 2007. Intravenously Administered Bone Marrow Cells Migrate to Damaged Brain Tissue and Improve Neural Function in Ischemic Rats. *Cell transplantation*, 16(10), pp.993–1005.

Wu, Jianyong et al., 2014. Remote ischemic conditioning enhanced the early recovery of renal function in recipients after kidney transplantation: a randomized controlled trial. *The Journal of surgical research*, 188(1), pp.303–308.

Wu, Jun et al., 2017. Interspecies Chimerism with Mammalian Pluripotent Stem Cells. *Cell*, 168(3), pp.473–486.e15.

Wu, Yaojiong & Zhao, R.C.H., 2012. The role of chemokines in mesenchymal stem cell homing to myocardium. *Stem cell reviews*, 8(1), pp.243–250.

Wynn, R.F. et al., 2004. A small proportion of mesenchymal stem cells strongly expresses functionally active CXCR4 receptor capable of promoting migration to bone marrow. *Blood*, 104(9), pp.2643–2645.

Xin, H. et al., 2015. Effect of high-dose erythropoietin on graft function after kidney transplantation: a meta-analysis of randomized controlled trials. *Biomedicine & pharmacotherapy = Biomedecine & pharmacotherapie*, 69, pp.29–33.

Xu, Y. et al., 2016. 3D spheroid culture enhances survival and therapeutic capacities of MSCs injected into ischemic kidney. *Journal of cellular and molecular medicine*, 20(7), pp.1203–1213.

Xu, Z. & Dai, C., 2017. Ablation of FGFR2 in Fibroblasts Ameliorates Kidney Fibrosis after Ischemia/Reperfusion Injury in Mice. *Kidney diseases (Basel, Switzerland)*, 3(4), pp.160–170.

Yamaguchi, T. et al., 2017. Interspecies organogenesis generates autologous functional islets. *Nature*, 542(7640), pp.191–196.

Yang, C. et al., 2014. A novel proteolysis-resistant cyclic helix B peptide ameliorates kidney ischemia reperfusion injury. *Biochimica et biophysica acta*, 1842(11), pp.2306–2317.

Yang, C. et al., 2015. Cyclic Helix B Peptide in Preservation Solution and Autologous Blood Perfusate Ameliorates Ischemia-Reperfusion Injury in Isolated Porcine Kidneys. *Transplantation direct*, 1(2), pp.e6–9.

Yasuda, K. et al., 2012. Autologous cell therapy for cisplatin-induced acute kidney injury by using non-expanded adipose tissue-derived cells. *Cytotherapy*, 14(9), pp.1089–1100.

Ysebaert, D.K. et al., 2000. Identification and kinetics of leukocytes after severe ischaemia/reperfusion renal injury. *Nephrology, dialysis, transplantation : official publication of the European Dialysis and Transplant Association - European Renal Association*, 15(10), pp.1562–1574.

Yuan, Xiaodong et al., 2017. Extracellular vesicles from human-induced pluripotent stem cell-derived mesenchymal stromal cells (hiPSC-MSCs) protect against renal ischemia/reperfusion injury via delivering specificity protein (SP1) and transcriptional activating of sphingosine kinase 1 and inhibiting necroptosis. *Cell death & disease*, 8(12), p.3200.

Yuan, Xiaopeng et al., 2017. Bone mesenchymal stem cells ameliorate ischemia/reperfusion-induced damage in renal epithelial cells via microRNA-223. *Stem cell research & therapy*, 8(1), p.146.

Zager, R.A., 1991. Adenine nucleotide changes in kidney, liver, and small intestine during different forms of ischemic injury. *Circulation Research*, 68(1), pp.185–196.

Zager, R.A., 1987. Partial aortic ligation: a hypoperfusion model of ischemic acute renal failure and a comparison with renal artery occlusion. *The Journal of laboratory and clinical medicine*, 110(4), pp.396–405.

Zager, R.A., Johnson, A.C.M. & Becker, K., 2011. Acute unilateral ischemic renal injury induces progressive renal inflammation, lipid accumulation, histone modification, and "end-stage" kidney disease. *American journal of physiology. Renal physiology*, 301(6), pp.F1334–45.

Zaw Thin, M. et al., 2020. Stem cell delivery to kidney via minimally invasive ultrasound-guided renal artery injection in mice. *Scientific reports*, 10(1), pp.7514–12.

Zhang, J.-B. et al., 2017. Adipose-derived mesenchymal stem cells therapy for acute kidney injury induced by ischemia-reperfusion in a rat model. *Clinical and experimental pharmacology & physiology*, 44(12), pp.1232–1240.

Zhang, L.-M. et al., 2016. Pharmacological inhibition of MyD88 homodimerization counteracts renal ischemia reperfusion-induced progressive renal injury in vivo and in vitro. *Scientific reports*, 6(1), pp.26954–14.

Zhang, R. et al., 2015. In vivo magnetic resonance imaging of iron oxide-labeled, intravenous-injected mesenchymal stem cells in kidneys of rabbits with acute ischemic kidney injury: detection and monitoring at 1.5 T. *Renal failure*, 37(8), pp.1363–1369.

Zhang, S. et al., 2015. Corticosterone mediates the inhibitory effect of restraint stress on the migration of mesenchymal stem cell to carbon tetrachloride-induced fibrotic liver by downregulating CXCR4/7 expression. *Stem cells and development*, 24(5), pp.587–596.

Zhang, Z.-X. et al., 2008. NK cells induce apoptosis in tubular epithelial cells and contribute to renal ischemia-reperfusion injury. *Journal of immunology (Baltimore, Md. : 1950)*, 181(11), pp.7489–7498.

Zhao, H. et al., 2018. Ischemia-Reperfusion Injury Reduces Long Term Renal Graft Survival: Mechanism and Beyond. *EBioMedicine*, 28, pp.31–42.

Zhao, X. et al., 2016. Three-Dimensional Aggregates Enhance the Therapeutic Effects of Adipose Mesenchymal Stem Cells for Ischemia-Reperfusion Induced Kidney Injury in Rats. *Stem cells international*, 2016, pp.9062638–11.

Zhao, Y.-Y., 2013. Metabolomics in chronic kidney disease. *Clinica chimica acta; international journal of clinical chemistry*, 422, pp.59–69.

Zheng, X. et al., 2016. Attenuating Ischemia-Reperfusion Injury in Kidney Transplantation by Perfusing Donor Organs With siRNA Cocktail Solution. *Transplantation*, 100(4), pp.743–752.

Zhou, L. et al., 2017. Comparison of human adipose stromal vascular fraction and adipose-derived mesenchymal stem cells for the attenuation of acute renal ischemia/reperfusion injury. *Scientific reports*, 7(1), p.44058.

Zhou, L. et al., 2016. Preischemic Administration of Nonexpanded Adipose Stromal Vascular Fraction Attenuates Acute Renal Ischemia/Reperfusion Injury and Fibrosis. *Stem Cells Translational Medicine*, 5(9), pp.1277–1288.

Zhu, F. et al., 2017. Adipose-derived mesenchymal stem cells employed exosomes to attenuate AKI-CKD transition through tubular epithelial cell dependent Sox9 activation. *Oncotarget*, 8(41), pp.70707–70726.

Zhu, X. et al., 2012. The comparition of biological characteristics and multilineage differentiation of bone marrow and adipose derived Mesenchymal stem cells. *Cell Tissue Res*, 350(2), pp.277–287.

Zhuo, W. et al., 2013. Efficiency of Endovenous Versus Arterial Administration of Mesenchymal Stem Cells for Ischemia-Reperfusion–Induced Renal Dysfunction in Rats. *Transplantation Proceedings*, 45(2), pp.503–510.

Zuk, P., 2013. Adipose-derived stem cells in tissue regeneration: a review. *ISRN Stem Cells*.

APPENDICIES:

Appendix 1

ISOLATION OF ADIPOSE DERIVED STROMAL VASCULAR FRACTION

A biological safety cabinet (BSC), scissors and forceps were cleaned with 70% ETOH before use. For extraction of the ADSVF, from the rat and human adipose tissue, the following steps were taken:

1. Adipose tissue was transferred to a sterile 10cm Petri dish

2. Scissors are used to mince the tissue down to small pieces of no more than 4mm in diameter. Initially, electronic homogenisation was attempted using the Gentle Macs (Miltenyi Biotec. Bergisch Gladbach, Germany) but final ADSVF quantities were inadequate.

3. Homogenised tissue was then transferred to a 50ml conical tube, and 25ml of PBS was added - 5x the volume of adipose tissue. From our rats both inguinal regions would produce around 5ml of homogenised tissue

4. 0.5ml Celase (Cytori Therapeutics Inc., San Diego, USA), which equates to 3.5mg of Celase, was added to each conical tube containing 30ml of homogenised tissue and PBS.

5. The tube was briefly vortexed and then put into an incubator with shaker for constant agitation for 30 minutes

6. After the 30 minutes, the tube was shaken to break up any larger chunks and put back in the incubator for a further 15 minutes.

7. The tube was then centrifuged for 5 minutes (600x g at room temperature with low brake speed)

8. In the BSC, the supernatant was aspirated off, and 5ml of PBS was added using a new pipette to resuspend the cells. At this point, up to 4 tubes can be combined if processing multiple samples at the same time. The volume was then adjusted up to 25ml with PBS

9. Centrifuge a second time for 5 minutes (400x g at room temp with low brake speed)

10. Supernatant aspirated without disturbing the cell pellet

11. 25ml added to the tube and centrifuged a third time for 5 minutes (400x g at room temp with low brake speed)

12. Supernatant aspirated without disturbing the cell pellet and the pellet resuspended with 25ml PBS

13. 250ul of IntravaseTM (Cytori Therapeutics Inc., San Diego, USA) was added to the conical tube (250ul IntravaseTM for every 25ml of PBS)

14. The tube was left to incubate at room temperature for 10 minutes on a shaker.

15. Centrifuge a fourth time for 5 minutes (400x g at room temp with low brake speed)

16. Supernatant aspirated and using a pipette and the pellet was resuspended with 5ml PBS

17. The cell suspension was passed through a 100um cell strainer and collected in a new sterile 50ml conical tube. The strainer was rinsed with 5ml of PBS to ensure maximum recovery of cells.

18. The strained cell suspension was then passed through a 40ul cell strainer and collected in a new 50ml conical tube. Again, the strainer was rinsed with 5ml PBS to ensure maximum recovery of cells. This cell suspension is now considered the ADSVF

Conical tubes containing cell suspension was put on ice while cell counting was performed. 0.5ml of ADSVF was taken and put into a 1.5ml tube for cell counting.

Appendix 2

QUANTIFICATION, STORAGE AND PREPARATION OF ADSVF FOR ANALYSIS

Cells were counted using the ChemoMetec NC-100 Mamillian NucleoCounter (Allerod, Denmark, Product number 900-0004) and its associated Reagent A100 (lysis buffer) & Reagent B (stabilizing buffer) and Nucleocounter cassettes. The cassettes are coated with immobilized propidium iodine, a fluorescent intercalating agent that binds to the DNA. Propidium iodine cannot pass an intact cell membrane; therefore attaches to the nucleus of dead cells and the Nucleocounter can then count the non-viable cells using fluorescent microscopy. Then a new cell suspension sample is mixed with lysis buffer and then the stabilizing buffer to allow counting of the total concentration of cells. Through simple calculation, using the cell concentrations, the total viable cell population can be determined from subtracting the non-viable population from the total population concentration.

$$\%viability = \frac{C_t \cdot M_t - C_{nv} \cdot M_{nv}}{C_t \cdot M_t} \cdot 100\%$$

% viability	The percentage of viable cells in the original cell suspension.
C_t	The total concentration of cells in the NucleoCassette (the displayed result of the total cell count).
C_{nv}	The concentration of non-viable cells in the NucleoCassette (the result displayed when counting the non-viable cells).
M_t	The multiplication factor used for the total cell count (most often 3).
M_{nv}	The multiplication factor used for the non-viable cell count (most often 1).

Storage

Once counted, the ADSCF was then prepared for storage if they were not going to be used or analysed immediately:

1. The remaining cell suspension or ADSVF was centrifuged for 5 minutes (400x g at room temp with low brake speed). The supernatant was then aspirated.
2. The cell pellet was resuspended with PBS. 0.5ml PBS is added for every 1 million cells in the cell pellet (as determined by the sample taken for cell counting). Therefore, if there were 3 million cells in the pellet 1.5ml of PBS would be added to resuspend the pellet.

3. A 1.5ml cryogenic tube was labelled and 700ul of Dulbecco's Modified Eagle Medium (DMEM) (Life Technologies Corporation. Paisley, UK) was added to each cryogenic tube.

4. 1million cells (or 0.5ml) was taken from the cell suspension and put into the cryogenic tube containing the DMEM. 100ul of Dimethyl sulfoxide (Fisher Scientific UK Ltd. Loughborough, UK) and 200ul of rat serum is then added to the cryogenic tubes taking the total volume to 1.5ml.

5. The Cryogenic tubes are then put into a cryogenic freezing container and placed in the –80°C freezer for 12 hours. Afterwards they are transferred to the liquid nitrogen for storage until required.

Preparation for use

When the ADSVF is required for analysis or use within the animal model the following steps were taken:

1. Cryogenic tubes containing ADSVF are taken from the liquid nitrogen and allowed to thaw.

2. The sample is then spun down using a mini centrifuge (Sprout. Heathrow Scientific, Illinois, USA) for at least 20 seconds and a visible pellet is formed

3. The supernatant is decanted and 200micro litres of PBS added to re suspend the cells.

4. Samples are spun again using the mini centrifuge for at least 20 seconds and a visible pellet is formed

5. Steps 3 and 4 are repeated

6. Once the wash is completed the pellet is resuspended with 200microliters of PBS using a pipette

7. 20microliters of this solution was taken and added to another Eppendorf containing 180microlitres of PBS. This 200microliters is used for calculating the viable cell population as described above using the NucleoCounter.

8. If a specific number of cells are required, the volume is calculated, and excess cells are aspirated from the Eppendorf containing then thawed ADSVF

9. 300micorliters of 10% rat serum is then added cell suspension. The total volume of cell suspension and rat serum is usually between 400 and 450 microliters depending on the degree of cell death from the freezing and thawing process and the number of cells required.

Appendix 3

RODENT MODEL OF RENAL TRANSPLANT ISCHAEMIA REPERFUSION INJURY – STANDARD OPERATING PROCEDURE

Equipment

Microsurgical equipment:

- Wild Heerbrugg Ltd operating microscope – zoom 10-30x 60mm LED light ring (Microscope Systems Scotland)
- Far infrared heating pad and infrared thermometer (Kent Scientific: DCT-15)
- Operating board (30x30cm). Covered with disposable plastic sheeting, held in place with adhesive tape.
- The following microsurgical instruments were obtained from Mercian® (Mercian Surgical Supply Co Ltd, Worcestershire, United Kingdom)
  - – Microsurgical vessel dilators with 0.1mm tips. (D-5a.1)
  - – Microsurgical vessel dilators with 0.2mm tips. (D-5a.2)
  - – Microsurgical vessel dilators with 0.3mm tips. (D-5a.3)
  - – Angulated forceps with 0.3mm tips. (JFA-5b)
  - – Dissecting microsurgical scissors with curved tips (SDC-15)
  - – Adventitia microsurgical scissors with sharp tips (SAS-15)
  - – Microsurgical needle holder without a lock, curved tips 0.4mm. (B-15-8)
  - – Tubing introducing forceps, tips 0.35mm. (TIF02)
  - – Clamp applying forceps. (CAF-4)
  - – Atraumatic vascular clamps. (B1-V and B2-V))
- Electric hair clippers
- 15G Scalpel
- Sterile Dressing packs (Nu-care Products Ltd, Bedfordshire, United Kingdom: DP10025)
- Sterile Cautery (John Weiss & Son Ltd, Milton Keynes, United Kingdom: 0111122)
- 30G Rycroft Cannula (0108003)
- Blunt retractors (18200-12) and elastomers (18200-07) (Fine Science Tools, Heidelberg)
- Sterile cotton tip applicators (Nu-care Products Ltd, Bedfordshire, United Kingdom: M982S)

- 10/0 nylon sutures. (Schuco Ltd, ZX-AK-0105, DR4 needle) or Ethilon® Suture, 10/0 non absorbable, monofilament, 13cm, 3.8mm, 3/8 circle taper point needle (Ethicon, Inc. W2870)
- Vicryl® Suture, 4/0 undyed, 19mm, 45cm, circle reverse cutting (Ethicon, Inc. W9925)
- Prestige Latex Sterile Gloves (Nu-care Products Ltd, Bedfordshire, United Kingdom: GS33LE)
- 365 Standard Sterile Gowns (Nu-care Products Ltd, Bedfordshire, United Kingdom: D20304)

Stage 1 – 2/3 nephrectomy of right kidney

Young adult male Fisher 344 rats were anaesthetised with isoflurane. Abdominal hair is shaved, and the rat is placed on a heating mat. The skin is prepped with chlorhexidine and draped to obtain a sterile field. A two-centimetre upper midline incision is made using a fully aseptic technique. Using scissors, the peritoneum is opened. Bowel contents are gently retracted to the left to reveal the right kidney. The fascia surrounding the renal hilum are opened and the renal artery identified. Due to varying anatomy, non-traumatic micro-forceps are used to briefly (3 seconds) clamp branches of the renal artery in order to determine blood distribution form that particular artery. Using 10-0 Nylon one or two or three branches of the renal artery are ligated to leave only 1/3 of the kidney perfused with arterial blood. Bowel retraction was then removed to return the normal positioning of the bowel. Peritoneum and skin are closed individually using a continuous 4-0 polyglactin suture (Vicryl®). Total surgical time ranged from 15-30minutes. Post-surgical care: The animal is injected with 4ml of subcutaneous 0.9% saline postoperatively and placed alone in the warmed recovery cage with free access to food and water. Buprenorphine analgesia was injected subcutaneously, at 0.005mg per 100g of body weight. The animal is returned to its home cage once fully recovered from the anaesthesia.

Stage 2 – ischaemia reperfusion injury of left kidney and cannulation of renal artery

Once recovered from the right partial nephrectomy procedure for at least two weeks the rat is anaesthetised with isoflurane. Abdominal hair is shaved, and the rat is placed on a heating

mat. The temperature is adjusted to maintain the core temperature of 36.5-37°C. The skin is prepped with chlorhexidine and draped to obtain a sterile field. Using a fully aseptic technique, the previous midline incision is reopened and extended to around five centimetres. Bowels are gently retracted to expose the left kidney. The fascia surrounding the renal hilum is opened, and the left renal artery is identified. A segment of the renal artery is carefully cleared of fascia and its attachment to the renal vein with blunt dissection using cotton tips and forceps. Two non-traumatic vascular micro clamps are placed on the renal artery to induce renal ischaemia and the time noted. The kidney is inspected to make sure the clamps have entirely occluded perfusion. If the animal is to receive an intervention via the renal artery then 20 minutes before the end of the ischaemia (minute 100) an incision large enough to fit a 30-gauge catheter is made to the anterior wall of the renal artery between the clamps. 7x105 ADSVF cells in 0.3ml PBS is administered with a 1ml syringe and a 30-gauge catheter through the incision. The distal clamp is momentarily released to allow the infusion to travel through the renal artery and into the kidney. Perfusion of the kidney with the ADSVF/PBS is confirmed by the visualisation of the kidney changing colour. The distal clamp is re-applied to prevent back bleeding from the kidney. The renal artery incision is repaired longitudinally with interrupted 10-0 Nylon. Clamps are removed after 120 minutes of warm ischaemia. Bowel retraction is removed to allow the normal positioning of the bowel. Peritoneum and skin are closed individually using a continuous 4-0 polyglactin suture (Vicryl®). Total surgical time ranges from 140-160minutes. Post-surgical care: The animal is injected with 2.5ml of subcutaneous 0.9% saline postoperatively and placed alone in the warmed recovery cage with free access to food and water. Buprenorphine analgesia is injected subcutaneously, at 0.005mg per 100g of body weight. The animal is returned to its home cage once fully recovered from the anaesthesia.

Training schedule

When learning either the 2/3 nephrectomy procedure or the IRI with renal artery cannulation procedure, there is initially a period of training on humanely killed rats. The number varies as per trainee but is approximately five. Then, under supervision, the trainee will commence a period of training on several live animals which will be humanely killed before recovery (5 to 10 depending on trainee progress). The trainee will commence to operate, supervised, on experimental rats that will be recovered. Once a success rate of >80% is achieved, then they are approved for independent practice.

To reduce animal numbers during training, the 2/3 nephrectomy procedure can be performed on both the left and right kidneys of the cadaveric and non-recovered rats. Similarly, the IR with renal artery cannulation training can be performed on both the right and left kidney of the cadaveric and non-recovered rats.

Developed surgical guidelines

After performing over 200 microsurgical procedures, we have found the following tips to be helpful:

- 10-0 monofilament suture is expensive and was not always straightforward to source. After using it use the remaining suture was soaked in chlorhexidine, rinsed and stored. Before the next operation, the suture was then autoclaved in autoclave approved box. The same suture could be used to perform multiple procedures. We had no issue with infection or suture fracture, causing the breakdown of the anastomosis.

- Closing peritoneum with a continuous suture (3-0 Vicryl®), locking it then running the stitch back to close the skin allows for a two-layer closure with one stitch. We had no hernia postoperatively using this method.

- Having two sets of microsurgical instruments makes it possible to perform multiple 2/3 nephrectomy surgeries in a morning session. One set can be sterilised as the other is in use.

- Precise, sharp and undamaged microsurgical scissors are essential to make a small clean hole in the renal artery. We had our scissors refurbished and realigned if they were dropped or not cutting cleanly.

- Surgery should be stopped, and rat terminated if any bowel injury occurs. Suture repair of the bowel, washout of abdomen and antibiotics postoperatively is unlikely to be successful and can lead to unnecessary distress to the rat postoperatively.

- When performing IR surgery, a 1cm x 1cm cutting of a sterile swab rolled up can be placed in the abdomen to gently wedge the spleen up into the left upper quadrant out of the operating field. Good surgical exposure is essential for efficient and safe operation. Make sure to remove at the end of the operation.

- Opening the avascular tissue between the kidney hilum and peri-renal fat and then following this plane up the medial edge of the kidney is a quick route to get behind the fat covering the renal artery. Once making this incision, the fat medial to the kidney can be lifted, and the renal artery can be easily identified and traced back to

the aorta. Not only is this route quick and causes minimal bleeding it also avoids the need to tie off the suprarenal vein.

- During IRI surgery locating the renal artery should be the priority after creating adequate exposure. Once the artery has been located, it should be clamped. This will start the 120 minutes of ischaemia. Then skeletonising the rest of the renal artery can begin, so it is ready for cannulation. Skeletonising the artery may take up to 30 minutes, and if this is done before clamping it is essentially adding 30 minutes on to the operation. From knife to skin to clamping the renal artery takes around 15 minutes. After the 120 minutes ischaemia, it takes around 10 minutes for a final inspection to ensure no bleeding, placement of organs back into their anatomical position and closure of peritoneum and skin. Total operative time can, therefore, be as little as 2hour 30minutes. Two per day is feasible.

- Cannulating the renal artery with the 30G Rycroft cannula in the right hand and using not traumatic forceps in the left hand to gently clamp around the artery cannulated by the catheter allows administration of therapy in a more controlled manner with minimal spillage and minimal damage to the artery.

- Opening the proximal renal artery clamp but leaving the distal clamp can allow testing of renal artery suture repair without reperfusion of the kidneys. Patency and haemostasis of the repair are assessed. Once the repair is proven to be adequate, the distal clamp remains on until the desired 120minutes of ischaemia has been achieved then the distal clamp can be removed at exactly 120minutes.

- Some bleeding after suture closure of the renal artery defect does not necessarily mean a further suture is required. Some very light pressure with a cotton tip applicator (just enough pressure to stop bleeding but not occlude the vessel - often the weight of the applicator alone is enough) for one full minute can often be enough to stop the bleeding. If it is still bleeding, another suture can be added.